



HAL
open science

Drosophila-Lactobacillus plantarum as a model of facultative nutritional mutualism

Théodore Grenier

► **To cite this version:**

Théodore Grenier. Drosophila-Lactobacillus plantarum as a model of facultative nutritional mutualism. Bacteriology. Université de Lyon, 2021. English. NNT : 2021LYSEN048 . tel-03460737

HAL Id: tel-03460737

<https://theses.hal.science/tel-03460737>

Submitted on 1 Dec 2021

HAL is a multi-disciplinary open access archive for the deposit and dissemination of scientific research documents, whether they are published or not. The documents may come from teaching and research institutions in France or abroad, or from public or private research centers.

L'archive ouverte pluridisciplinaire **HAL**, est destinée au dépôt et à la diffusion de documents scientifiques de niveau recherche, publiés ou non, émanant des établissements d'enseignement et de recherche français ou étrangers, des laboratoires publics ou privés.



Numéro National de Thèse : 2021LYSEN048

THESE DE DOCTORAT DE L'UNIVERSITE DE LYON

opérée par

l'Ecole Normale Supérieure de Lyon

Ecole Doctorale N° 340

Biologie Moléculaire, Intégrative et Cellulaire (BMIC)

Discipline : Sciences de la Vie et de la Santé

Soutenue publiquement le 29/09/2021, par :

Théodore GRENIER

Mutualisme nutritionnel facultatif entre animal et bactéries : apport du modèle *Drosophile-Lactobacillus plantarum*

Devant le jury composé de :

MIGUEL-ALIAGA, Irene Professeure, Imperial College of London
GHIGO, Jean-Marc Professeur, Institut Pasteur
ROLHION, Nathalie Chargée de recherche, INSERM
MERABET, Samir Directeur de recherche, CNRS ENS de Lyon
LEULIER, François Directeur de recherche, CNRS ENS de Lyon

Rapporteure
Rapporteur
Examinatrice
Examineur
Directeur de thèse

Index

Remerciements	4
List of Abbreviations	6
Introduction	7
I The gut microbiota	8
1) Origin and diversity	8
2) Influence on host's physiology	9
3) Influence on growth	11
4) Models of host-microbiota research	12
II <i>Drosophila</i> as a model to study host-microbes interactions	13
1) <i>Drosophila</i> and pathogenic microbes	13
2) <i>Drosophila</i> and symbiotic microbes	15
3) Microbiota and behaviour	17
4) Microbiota and energy metabolism	18
5) Microbiota and lifespan	19
6) Microbiota and fecundity	20
7) Microbiota and post-embryonic growth	21
III <i>Drosophila</i> as a model to study growth and nutrition	24
1) <i>Drosophila</i> and growth	24
2) <i>Drosophila</i> and nutrition	30
Objectives	32
References	33
Chapter I: <i>Drosophila</i>-associated bacteria differentially shape the nutritional requirements of their host during juvenile growth	56
Abstract	57
Introduction	57
Results and discussion	60
Conclusion	73
Material and Methods	75
Supporting information	79
References	81
Chapter II: A symbiotic bacterium supports the growth of its host on an unbalanced diet through GCN2 activation in the intestine	88
Abstract	89
Introduction	90
Results	92
Discussion	110
Material and Methods	113
Supporting information	120
References	127
Conclusion and perspectives	136
References	142
Annexes	144

Annex 1: Metabolic cooperation among commensal bacteria supports <i>Drosophila</i> juvenile growth under nutritional stress	145
Annex 2: <i>Drosophila</i> perpetuates nutritional mutualism by promoting the fitness of its intestinal symbiont <i>Lactobacillus plantarum</i>	188
Annex 3: How commensal microbes shape the physiology of <i>Drosophila melanogaster</i>	214

Remerciements

Pendant ces quatre années que j'ai passées à l'IGFL, très souvent, des amis ou des membres de ma famille m'ont posé cette question : « et ta thèse ? comment ça se passe ? » A chaque fois, je répondais « bien ». Ou « très bien ». Ou « super bien ». Et vraiment, je peux le dire maintenant que j'ai fini : ma thèse s'est super bien passée. Bien sûr, il y a eu des moments difficiles, des moments de stress, des moments où ça ne marchait pas comme je voulais. Mais j'ai toujours été heureux de venir au labo le matin, et je n'ai jamais regretté m'être lancé dans cette aventure. Pourquoi ? Qu'est-ce qui fait qu'une thèse se passe bien ou se passe mal ? Pour moi, il y a au moins deux raisons.

La première raison, c'est que j'aimais ce que je faisais. J'ai travaillé sur un sujet qui me passionnait, j'ai eu l'occasion de réfléchir intensément à toutes sortes de problèmes et, parfois, j'ai trouvé des solutions. J'ai pu réaliser toutes sortes d'expériences, et parfois, ces expériences donnaient des résultats intéressants. J'ai pu poser des questions et, parfois, trouver des réponses.

La deuxième raison, qui est peut-être la plus importante, tient aux personnes avec lesquelles j'ai eu la chance de travailler.

Tout d'abord bien sûr, François. Tu as été le directeur de thèse parfait pour moi : tu m'as fait confiance en me laissant l'autonomie que je voulais, et en même temps tu étais toujours là dès que j'avais besoin d'aide. J'ai beaucoup appris de ces quatre années avec toi. De tes qualités de chercheur : ton inventivité, ton exigence pour des manips « claires, carrées, béton », ta compréhension et ta capacité à transformer des résultats intéressants en un bel article scientifique. De tes qualités humaines aussi : ta gestion de ton équipe, ta bienveillance, ta détermination. Et merci pour tous les bons moments qu'on a passés ensemble, les cafés, les déjeuners, les journées de team-building.

Ensuite, mes collègues actuels ou passés. Ça a été un plaisir de passer ces quatre ans avec vous ! Merci Houssam, pour tes manips et pour ta bonne humeur. Merci Renata, pour ton aide avec la génétique (des bactéries) et pour nos bons moments autour d'un café. Merci Dali, pour ton aide avec la génétique (des mouches) et pour nos grandes discussions en fly room. Merci Filipe pour nos discussions et pour ton fil twitter, parfois très drôles, parfois très intéressants scientifiquement, et parfois même les deux (#BluePoopChallenge). Merci Jean-Louis pour avoir été un chef de bureau bienveillant malgré un ton parfois sarcastique. Merci Amélie pour tous les bons moments passés ensemble : tu es à présent la senior PhD student du labo. Je compte sur toi et je suis sûr que toi aussi tu pourras dire bientôt : « ma thèse s'est super bien passée ». Merci Juliette, Anne, Cathy, Stéphanie, Damien, Lucie, Méline, Amandine, Maria-Elena, Loan, Hugo, Anne-Laure et Coralie, pour votre aide et pour votre compagnie. Merci à Vincent et Claire-Emmanuelle : ça fait un moment qu'on n'est plus collègues, mais on est quand même restés amis !

Un remerciement spécial à toi, Jess. On a fait tellement de choses super ensemble : des articles, des congrès, des jeux, et beaucoup, beaucoup de discussions autour d'un déjeuner ou d'un café. Sans toi ma thèse n'aurait pas été la même : elle aurait été plus courte d'un papier et de beaucoup de bonheur.

Merci aussi à tous les autres membres de l'IGFL. Un grand merci en particulier à Rachel, Guillaume, Jonathan et Solène pour les moments partagés en cafet et en dehors du labo. Merci Coco pour tes memes et pour avoir donné un but à mes stocks de carboglace inutilisés. Merci Fabienne, merci Sonia pour votre aide si précieuse. Merci Christian pour les autoclaves et les gâteaux. Merci à toutes celles et ceux avec qui j'ai collaboré pour nos articles : Benjamin, Sandrine, Isabelle, Pedro, Patrice, Nicolas, Hubert, Fédé.

Merci à Stéphane, Anna et Rénaud, les membres de mon comité de suivi de thèse, pour vos conseils et vos retours.

Merci aux organismes qui ont financé ma thèse : l'ENS de Lyon, la FRM, l'ANR.

Merci à toutes celles et tous ceux qui ont été à mes côtés pendant ces quatre années. Merci à ma famille et à mes amis pour avoir patiemment supporté mes longues explications plus ou moins claires sur mon sujet de thèse. Merci de vous y être intéressé ou d'avoir bien fait semblant !

Enfin, un grand merci à Samir Merabet, Irene Miguel-Aliaga, Jean-Marc Ghigo et Nathalie Rolhion pour avoir accepté d'être les membres de mon jury.

List of abbreviations

4E-BP: eIF4E-binding protein
AA: Amino Acid
AMP: Anti-Microbial Peptide or Adult Midgut Precursor
BCAA: Branch-Chained Amino Acid
CFU: Colony Forming Unit
CR: Conventionally-Reared
DAEL: Days After Egg-Laying
DILP: Drosophila Insulin-Like Peptide
D50: median time of pupariation
dsRed: red fluorescence protein
DT: Developmental Timing
EAA: Essential Amino Acid
EE cells: Entero Endocrine cells
FLY AA: AA composition based on Drosophila's exome
Gal4: transcription activator protein
GCN2: General Control Nonderepressible 2
GF: Germ-Free
HD: Holidic Diet
Hh: Hedgehog
HK: Heat-Killed
HPLC-MS: High-Performance Liquid Chromatography coupled with Mass Spectrometry
IMD: Immune Deficiency
InR: Insulin Receptor
IPC: Insulin-Producing Cell
ISC: Intestinal Stem Cells
KD: Knock-Down
KO: Knock-Out
KEGG: Kyoto Encyclopaedia of Genes and Genomes
MM AA: mismatched AA composition
NAL: Nucleic Acids and Lipids Precursors
NEAA: Non-Essential Amino Acid
OD: Optical Density
PG: Peptidoglycan
PGRP: Peptidoglycan Recognition Protein
RNAi: RNA interference
rRNA: ribosomal RNA
ROS: Reactive Oxygen Species
TAG: triglycerides
TOR: Target Of Rapamycin
Tn: transposon
tRNA: transfer RNA
UAS: Upstream Activation Sequence (enhancer activated by a Gal4)
WT: Wild-Type

Introduction

I The gut microbiota

1) Origin and diversity

Microbes are everywhere. Recent estimations propose that the total biomass of bacteria on Earth represents ~70 gigatons of carbon (Gt C) out of a total of ~550 Gt C. Archaea represent ~7 GtC, protists ~4 Gt C, fungi ~12 Gt C and viruses 0,2 Gt C (Bar-On et al., 2018). Microbes can colonize many environments, including extreme environments such as deep-sea hydrothermal vents (Dick, 2019), acidic lakes (Rothschild and Mancinelli, 2001) or hypersaline brines (Uma et al., 2020). Microbes can also colonize multi-cellular organisms, including animals: they engage in a relationship of symbiosis (*i.e.*, two organisms living together). Co-evolution has allowed the symbionts to adapt to their host and benefit from abundant nutrients and shelter. Some microbes have even lost their ability to live outside of their host: they are called obligate symbionts (*e.g.* the pea aphid symbiont *Buchnera aphidicola* (Zientz et al., 2004)). Others are transient: they have a versatile lifestyle that allows them to colonize several environments, including animal hosts (*e.g.* the lactic acid bacterium *Lactiplantibacillus plantarum* that can be found in plants, dairy products and the gut of Mammals and Insects (Duar et al., 2017)).

Some symbiotic microbes are extracellular: they live on the epithelia or in the lumen of organs such as the intestine. Extracellular microbes colonize their host at birth, allowing some vertical transmission (Funkhouser and Bordenstein, 2013), and later through environmental exposure. Intracellular microbes are vertically transmitted. They are very common in Insects: for instance, it is estimated that the intracellular bacterium *Wolbachia pipientis* colonizes 40% to 60% of Insect species (Newton and Rice, 2020).

A community of microbes that colonizes a niche is called a microbiota. Many studies have focused on the human gut microbiota (Gilbert et al., 2018). It is composed of bacteria, archaea, protists and fungi, the former being the most abundant and diverse: each individual harbors on average $3,8 \cdot 10^{13}$ bacteria in its colon (Sender et al., 2016), representing 500 to 1000 bacterial species (Sears, 2005). The composition of the gut microbiota varies greatly between animal species, and is influenced by both the species' diet and the phylogeny (Nishida and Ochman, 2018). It is also highly variable within the human species, within a population (as measured in more than 2000 Belgian and Dutch volunteers (Falony et al., 2016)) and between populations: for instance, hunter-gatherers from Tanzania harbour a greater bacterial diversity than post-industrialized Europeans. This difference is probably due to the diet, with the hunter-gatherers consuming a greater variety of vegetal fibres than the Europeans (Schnorr et al., 2014). Within an individual, the microbiota composition changes through life: the new-born's microbiota exhibits low diversity and is enriched in *Bifidobacteria* (Milani et al., 2017). Its composition is affected by the mode of delivery: vaginally-delivered infants are primarily colonized by bacteria from their mother's vaginal and intestinal microbiota whereas C-section-born infants are first in contact with skin and environmental bacteria, and by the mode of feeding (breastfed or formula-fed)

(Munyaka et al., 2014). The diversity then increases as the children transition to solid food (Yatsuneneko et al., 2012). Adults harbour a stable and resilient gut microbiota, though it can be perturbed by antibiotic treatments (Fassarella et al., 2021).

2) Influence on host's physiology

Symbiosis of host and microbes can be of three sorts, defined by the influence of the microbe on its host: parasitism, commensalism and mutualism (Dimijian, 2000).

A parasite is harmful to its host. Parasitic microbes typically infect host's tissues, use host's resources to multiply and spread to other tissues and/or other hosts. Depending on the immune response and the virulence of the microbe, infections by parasites can lead to disease that range in severity from benign to lethal (Peterson, 1996).

A commensal microbe benefits from its host, without affecting it. Most species of the gut microbiota are labelled as commensals, because there is not report of them being either harmful or beneficial to their host (Cremon et al., 2018). However, definitive classification of a microbe as a commensal is difficult, because it is possible that its harmful or beneficial interactions with its host have not yet been discovered (Storelli, 2015). In particular, some commensal bacteria are opportunistic pathogens, or pathobionts: when the host is healthy, they behave as commensals, but in certain circumstances (for example, weakening of the host's immune system) they become pathogenic. For instance, *Klebsiella pneumoniae* is a member of the healthy gut or nasopharyngeal microbiota of humans. However, it can attack immunocompromised patients in hospitals, which makes it a major cause of nosocomial bacterial infections (Podschun and Ullmann, 1998).

Finally, mutualistic microbes provide a benefit to their host. From Elie Metchnikoff, who observed a correlation between consumption of certain dairy products and longevity of Bulgarian peasants (Anukam and Reid, 2007) to 2021, researchers have described the influence of mutualistic symbionts on a multitude of parameters.

The most straightforward manner to know whether symbiotic microbes have an effect on a trait of the host consists in a "knock-out-like" strategy: removing the symbiotic microbes, and comparing with a control condition. The experimental condition without microbes is called axenic or Germ-Free (GF), the control condition is called conventional or conventionally-reared (CR). Louis Pasteur, when discussing the possibility for an animal to live without symbiotic microbes, had the intuition that "life in these conditions would be impossible". We now know that it is not the case, because it has been possible to rear GF animals since the 1940s (Reyniers, 1946). However, the physiology and development of GF animals and their CR counterparts differ in many ways.

First of all, symbiotic microbes allow the maturation of their host's immune system. GF mice harbour reduced populations of several types of immune cells compared to conventionally-reared (CR) mice: CD4+ T cells (Dobber et al., 1992; Ishikawa et al., 2008) and CD25+ T cells (Ishikawa et al., 2008). Especially, the population of Th17, a subset of CD4+ T cells, is promoted by the presence of Segmented Filamentous

Bacteria, a member of the order Clostridiales in mice (Atarashi et al., 2015; Sczesnak et al., 2011). Gut bacteria are also required for mice to develop intestinal lymphoid tissues that generate IgA-producing B cells (Bouskra et al., 2008), and for the secretion of the antimicrobial peptides Reg3 γ (Cash et al., 2006) and Ang4 (Hooper et al., 2003) by Paneth cells. Symbiotic microbes can also improve their host's immunity through direct competition with pathogens. Infection by *Enterococcus faecium* can be precluded by a consortium of four symbiotic bacteria (Caballero et al., 2017), one of which produces a lantibiotic that inhibits *E. faecium*'s growth (Kim et al., 2019). Fecal Microbiota Transplant, *i.e.* the injection of a donor's fecal microbiota to a patient, is a highly efficient therapy against recurrent *Clostridium difficile* infection (van Nood et al., 2013).

Moreover, symbiotic microbes interact with their host's metabolism. A spectacular proof of concept was brought by the lab of Jeffrey Gordon. They observed differences in composition between gut microbiota of pairs of twins discordant for obesity: in particular, obese people tend to have less microbial diversity than lean people (Turnbaugh et al., 2009). Moreover, when they transferred the microbiota of the volunteers to GF mice, they observed that the mice that received the microbiota of obese volunteers gained more fat mass than the mice that received the microbiota of the lean volunteers. This experiment showed for the first time a causal relationship between microbiota composition and host weight gains (Ridaura et al., 2013). Among the microbes that are underrepresented in obese people, *Akkermensia muciniphila* is of particular interest. Supplementation of *A. muciniphila* to mice fed a high-fat diet reduces the fat mass gain of the mice and improves its insulin sensitivity (Everard et al., 2013). This effect can be partly recapitulated by the pasteurized bacterium, or by the protein Amuc_1100 purified from its membrane (Plovier et al., 2017). Moreover, Short-Chain Fatty Acids (SCFAs), especially succinate produced by gut bacteria such as *Prevotella copri*, can improve glucose tolerance and insulin sensitivity (De Vadder et al., 2016).

Furthermore, gut microbes influence their host's behaviour through the "gut-brain axis" (*i.e.* the connexion between the intestine and the central nervous system) (Mayer et al., 2015) and enteroendocrine cells that secrete hormones in response to intestinal cues. GF mice display more exploratory behaviour than CR mice (Bercik et al., 2011) but engage in less social activity and are more prone to stress (Wu et al., 2021). Moreover, transferring the gut microbiota of patients suffering from depression to GF mice causes the recipient mice to exhibit depressive-like behaviour (Chevalier et al., 2020). Gut microbes may influence mice's behaviour through the secretion of metabolites such as Tryptophan (Trp), the precursor of the neurotransmitter serotonin (Gao et al., 2020) or p-Cresol, which can induce autistic-like behaviours in mice (Bermudez-Martin et al., 2021). However, to what extent gut microbes can influence human behaviour is still unclear. On top of its influence on behaviour through the central nervous system, the gut microbiota interacts with the enteric nervous system (Joly et al., 2020), promoting gut motility (Dimidi et al., 2017).

3) Influence on growth

In my thesis, I focused on the influence of symbiotic microbes on juvenile growth. The first idea of a microbial influence on growth in Mammals was brought by the lab of Jeffrey Gordon on children suffering from stunting (stunting is a growth delay due to chronic undernutrition, characterized by low height-for-age score (Stewart et al., 2013)). Subramanian and colleagues observed important differences in composition between the gut microbiota of healthy children and the gut microbiota of children suffering from stunting. Especially, the microbiota of stunted children appeared “immature”, that is to say enriched in taxa that are usually found in high abundance in younger children (Subramanian et al., 2014). Causality between gut microbiota “immaturity” and stunting was then demonstrated by Blanton and colleagues using an approach similar to the one applied to obesity (see above) (Blanton et al., 2016a): transferring the microbiota of stunted children into GF mice fed a low-nutrient diet caused the mice to gain less weight and less mean mass than their counterparts that received the microbiota of healthy children. Moreover, co-housing mice that received a “stunted microbiota” and mice that received a “healthy microbiota” induces a protective effect against stunting: the co-housed mice that received the “stunted microbiota” grow as well as their counterparts that received the “healthy microbiota”. Mice are coprophagic: they eat their cagemates’ faeces. Blanton and colleagues thus concluded that microbes protective against stunting transited from the gut of the mice that had received the “healthy microbiota”, into the gut of the co-house mice that had received the “stunted microbiota”. They then identified microbes initially present in the “healthy microbiota” that successfully colonize the gut of co-housed mice that received the “stunted microbiota”. They defined a consortium of 5 bacterial species that recapitulate the effect of a “healthy microbiota”: mice that received a “stunted microbiota” and the consortium grew better than mice that only received the “stunted microbiota” (Blanton et al., 2016a). At the same time, strains of another bacterial species, *Lactiplantibacillus plantarum*, was shown to promote the growth of undernourished infant mice. The growth-promoting effect of *L. plantarum* is strain-specific (some strains show a stronger growth-promoting phenotype than others) and mono-association with *L. plantarum* enhances the circulating titers of growth hormone (GH), insulin-like growth factor binding protein-3 (IGFBP-3) and the insulin-like growth factor-1 (IGF-1) (Schwarzer et al., 2016).

These findings are of preclinical importance, because stunted children fed a therapeutic renutrition foods fail to recover a height-for-age ratio similar to healthy children (Subramanian et al., 2014). Microbiota-directed complementary foods (*i.e.*, food designed to favour a microbiota composition close to the microbiota of healthy children) can improve the growth of undernourished piglets. Stunted children fed the microbiota-directed foods did not show an improvement of their height-for-age ratio over the course of a trial, but their plasma was enriched in proteins positively correlated with growth such as the insulin-like growth factor binding protein-3 (IGFBP-3), the

growth hormone receptor (GHR) and leptin. Moreover, the gut microbiota of the treated children was more similar to a “healthy microbiota” (Gehrig et al., 2019).

The beneficial effect of the gut microbiota on juvenile growth is thus promising, both in term of human health and for the food industry. However, the biology and mechanisms at play remain elusive.

4) Models of host-microbiota research

Mice are a powerful model to study host-microbiota interactions. They are genetically closer to humans than most other model animals: 99% of the mouse genes have a homolog in the human genome (Mouse Genome Sequencing Consortium et al., 2002). They provide relevant models for microbiota-related diseases such as obesity (Friedman, 2018), inflammatory bowel disease (IBD) (Mizoguchi, 2012), gut infection by pathogens (Ducarmon et al., 2019) and, as mentioned before, stunting (Blanton et al., 2016b). However, the physiology of the human gut and the mouse gut are quite different: especially, mice harbor a large caecum that shelters fermenting bacteria (Hugenholtz and de Vos, 2018). Moreover, the nutrition of mice is very different from human's: it relies greatly on fibers that are fermented by gut microbes and re-ingested upon coprophagy (Sakaguchi, 2003). Gut microbiota composition depends largely on phylogeny and nutrition (Nishida and Ochman, 2018); therefore, it is not surprising that the gut microbiota of mice is different from the one of humans: the murine microbiota and the human microbiota share some similarities at the genus level (thirteen of the twenty most abundant core genera in mice are also present in the twenty most abundant core genera in humans) but only 4% of the genes identified in the mouse's metagenome are found in the human metagenome. However, the murine microbiota and the human microbiota are more similar at the functional level: 95.2% of the KEGG orthologous groups are shared between the two species (Xiao et al., 2015). Most importantly, although GF mouse facilities have been running since the late 50' (Pleasant, 1959), they require complex isolators and are both costly and time-consuming.

Fortunately, simpler animal models for host-microbiota interactions have been developed for fundamental discovery. These models provide many practical advantages and allow to study the diversity of biological systems (Douglas, 2019; Leulier et al., 2017).

The zebra fish *Danio rerio* provides an interesting model of Vertebrate: its small size and high fecundity allows rearing in large quantities, and larvae can easily be maintained in gnotobiotic conditions. However, long-term maintenance of gnotobiotic adults is much more delicate (Melancon et al., 2017). The microbiota of zebra fish has been shown to modulate its host's nutrition (Semova et al., 2012), immune system (Rolig et al., 2015), behaviour (Borrelli et al., 2016) and to provide colonization resistance against pathogens (Stressmann et al., 2021).

In Invertebrates, the nematode worm *Caenorhabditis elegans* allows large-scale functional studies of host-microbes interactions. Though *C. elegans* is bacterivorous,

certain bacterial species can colonize its gut and form a *bona fide* microbiota (Dirksen et al., 2016). The short lifespan of *C. elegans* makes it a particularly convenient model of aging (Shen et al., 2018). *C. elegans*' microbiota can extend its host's longevity through production of nitric oxide (Gusarov et al., 2013) and can regulate the effects of the drug metformin on *C. elegans*' longevity through the production of agmatine (Pryor et al., 2019).

The Hawaiian bob-tailed squid *Euprymna scolopes* provides a unique example of host-symbiont interactions: its symbiotic bacterium *Vibrio fischeri* can colonize a specialized organ, the light organ, where it emits bioluminescence that allows its host to camouflage from predators below (Jones and Nishiguchi, 2004). The disadvantage of the squid-*Vibrio* model is that molecular tools to manipulate the squid's genome are lacking; however, it allowed to unravel unknown mechanisms of host-microbe interactions. For instance, production of the peptidoglycan fragment tracheal cytotoxin by *V. fischeri* causes apoptosis and regression of a part of the light organ, which is beneficial to the organ's function (Koropatnick et al., 2004). Moreover, *V. fischeri* produces the small non-coding RNA SsrA, which regulates the host's immune response and allows successful colonization of the light organ by the bacterium (Moriano-Gutierrez et al., 2020).

In my thesis, I used the fruit fly *Drosophila melanogaster* as a model to study the influence of symbiotic microbes on their host's growth, in several nutritional conditions. *Drosophila* has been used for decades to understand the mechanisms that govern the interactions between an animal host and microbes, pathogenic or commensal, as well as growth and nutrition. In the next two parts, I will present the state-of-the art on these topics, and how my thesis aims at addressing some of our current knowledge gaps.

II Drosophila as a model to study host-microbes interactions

1) Drosophila and pathogenic microbes

Historically, *Drosophila* has first been extensively used as a model for interaction with pathogenic microbes. *Drosophila* can be infected by viruses (Mussabekova et al., 2017), fungi (Lu and St Leger, 2016), protozoans (Chandler and James, 2013) and bacteria. Here I will focus on interactions with bacteria. *Drosophila* can be infected by extracellular natural pathogens such as *Pseudomonas entomophila* (Vodovar et al., 2005), opportunistic pathogens such as *Erwinia carotovora*, which is primarily a plant pathogen (Basset et al., 2000), and artificially infected by human pathogens in the lab (Neyen et al., 2014). *Drosophila* are a model of infection for *Vibrio cholerae* (Davoodi and Foley, 2019), *Pseudomonas aeruginosa* (Siva-Jothy et al., 2018), *Listeria monocytogenes* (Mansfield et al., 2003) and *Staphylococcus aureus* (Needham et al., 2004). Like all invertebrates, *Drosophila* does not have an adaptive immune system. Instead, *Drosophila* fights infection through its innate immune system (Imler, 2014), which relies mainly on the production of antimicrobial peptides (AMPs), reactive oxygen species (ROS) and activity of circulating cells including professional

phagocytes (Lemaitre and Hoffmann, 2007). Four signaling cascades allow *Drosophila* to sense, signal and respond to pathogenic bacteria.

The Toll pathway is homolog to the Toll-Like Receptor pathway in Mammals. It is expressed in macrophages and in the fat body (FB) (Buchon et al., 2014), a homolog to white adipose tissues and liver in Mammals (Søndergaard, 1993). Toll senses Lysin-type peptidoglycans, present in the cell wall of certain Gram-positive bacteria, through a complex formed by the peptidoglycan recognition protein SA (PGRP-SA) and the Gram-negative bacteria-binding protein 1 (GNBP1) (Gobert et al., 2003). The ligand-receptors complex triggers the cleavage of the cytokine Spätzle, which activates Toll and induce a cascade of effectors that lead to the transfer of the nuclear factor- κ B (NF- κ B) Dorsal-related immunity factor (Dif) into the nucleus (Meng et al., 1999). Dif then promote the transcription of Anti-Microbial Peptides (AMPs) that allow the fly to fight the pathogens (Lemaitre and Hoffmann, 2007). Of note, Toll is also involved in response to fungal pathogens (Lemaitre et al., 1996).

In parallel, the immune deficiency (IMD) pathway is the analog of the tumor necrosis factor (TNF) pathway in Mammals. It is expressed in the gut (Buchon et al., 2014), the FB (Lemaitre and Hoffmann, 2007), the macrophages (Bosch et al., 2019) and the Malphigian tubules, *i.e.* the excretory system of *Drosophila* (Cohen et al., 2020). The IMD pathway relies on sensing of Diaminopimelic acid (DAP)-type peptidoglycans, which are present in the cell wall of Gram-negative bacteria and certain Gram-positive bacteria such as *Bacilli*, by PGRP-LC and PGRP-LE (Aggrawal and Silverman, 2007; Leulier et al., 2003). PGRP-LC and PGRP-LE activate IMD. IMD then activates the TGF- β activated kinase 1 (Tak-1), which promotes the transfer of the nuclear factor- κ B (NF- κ B) Relish into the nucleus and transcription of a set of AMPs different from the AMPs induced by the Toll pathway (Kleino and Silverman, 2014).

Moreover, Tak-1 activates the c-Jun N-terminal kinase (JNK) pathway (Kleino and Silverman, 2014), which allows the shedding of infected enterocytes (Zhai et al., 2018) and stimulates AMP production by the FB (Delaney et al., 2006). It has been suggested that Tak-1 can also be activated independently of IMD through an unknown mechanism (Delaney et al., 2006), but this is subject to controversy (Tafesh-Edwards and Eleftherianos, 2020).

Finally, pathogenic bacteria produce uracil in the fly's gut as a byproduct of quorum-sensing (Kim et al., 2020). Uracil activates Hedgehog (Hh) in enterocytes (Lee et al., 2015), which leads to Ca^{2+} mobilization from endosomes and stimulates the production of ROS by the enzyme dual oxidase (Duox) (Lee et al., 2013).

Figure 1 summarizes the immune cascades engaged during the response of *Drosophila* to pathogenic bacteria.

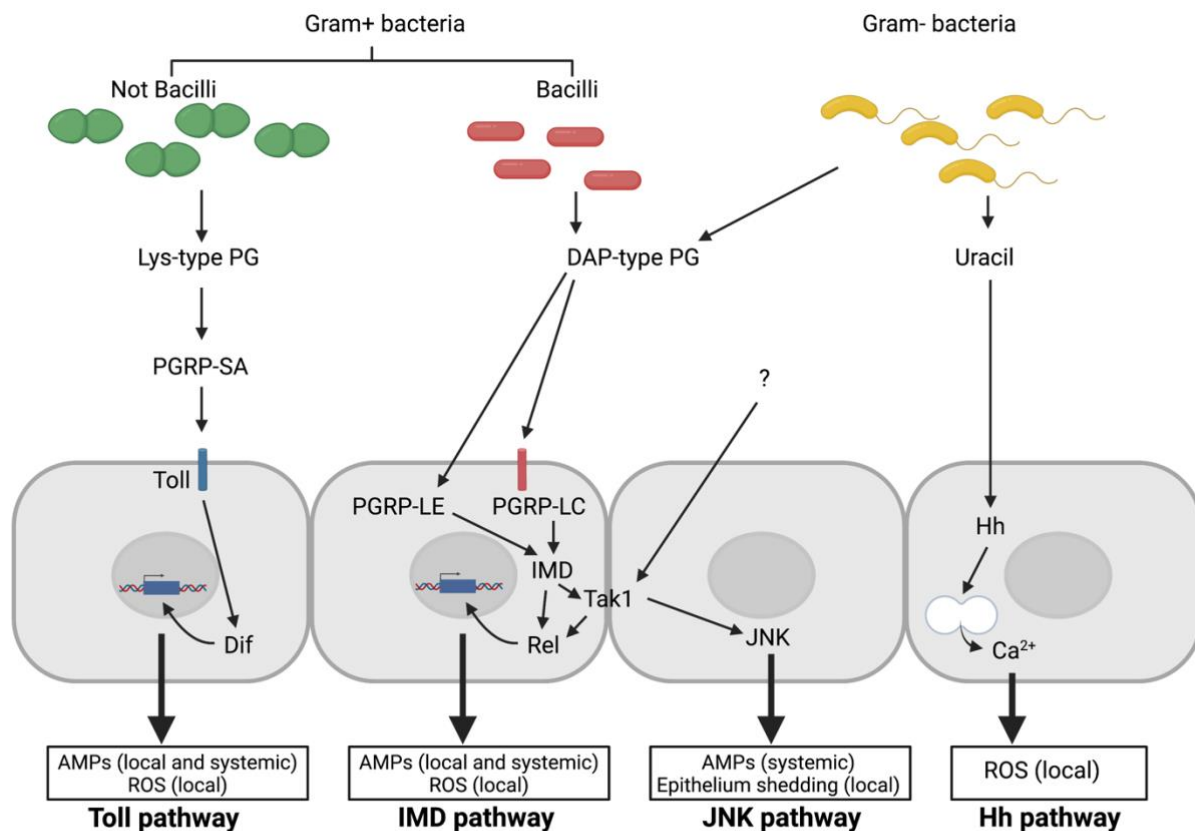


Fig 1. Immune response of *Drosophila* to pathogenic bacteria. Lys-type: Lysine-type. DAP: Diaminopimelic acid. PG: Peptidoglycan. PGRP: Peptidoglycan recognition protein. Dif: Dorsal-related immunity factor. IMD: Immune deficiency. Rel: Relish. Tak1: TGF- β activated kinase 1. JNK: c-Jun N-terminal kinase. Hh: Hedgehog. AMP: AntiMicrobial Peptides. ROS: Reactive Oxygen Species.

2) *Drosophila* and symbiotic microbes

Despite its robust immune system, *Drosophila* co-exists with many microbial species. *Drosophila*'s symbionts are either intracellular (endosymbionts such as *Wolbachia* (Clark et al., 2005) or *Spiroplasma* (Ventura et al., 2012)) or extracellular microbes mainly found in the gut lumen (Douglas, 2018a). Isolating microbes from the gut of a fly does not mean that these microbes reside in the fly's gut; they can be transient symbionts, acquired from the food and transiting through the gut. Yet, member strains of a few species isolated from wild flies were shown to persist in the gut of adults (Obadia et al., 2017). Moreover, two strains of *Acetobacter thailandicus* and *Acetobacter cibinongensis* show stable colonization of the adult crop (Pais et al., 2018). However, most *Drosophila* symbionts isolated from wild flies (Pais et al., 2018), and all symbionts isolated from lab-reared flies to date are transient: they grow on the food and transit through the gut in adults (Blum et al., 2013) and larvae (Storelli et al., 2018). For this reason, I will not use the term "gut microbiota" to describe *Drosophila*-associated bacteria, but rather "symbiotic bacteria" or simply "microbiota". As I will show in the next paragraphs, the fact that most symbiotic bacteria do not stably colonize the gut of their host does not mean that they do not interact with it. Transient

symbionts influence the biology of their host and are influenced by their host (Ma and Leulier, 2018).

The composition of *Drosophila*'s gut microbiota varies between lab-reared flies and wild flies. The presence of antimicrobial conservatives in the laboratory fly food, as well as its simple composition, imposes a strong selection pressure on symbiotic microbes (Téfit et al., 2018); therefore, the microbiota of lab-reared flies is generally less diverse than the one of wild flies (Staubach et al., 2013). However, even wild flies usually have a low microbial diversity, consisting in maximum 80 species belonging mostly to the families *Lactobacillaceae*, *Acetobacteraceae*, *Enterococcaceae*, *Corynebacteriaceae* and *Enterobacteriaceae* (Adair et al., 2018; Téfit et al., 2018). In addition to bacteria, wild flies are commonly associated with yeasts (Lachance et al., 1995). In the lab, flies are usually associated with 4-5 dominant species of bacteria belonging to the same families (Ren et al., 2007; Storelli et al., 2011). The microbiota composition is affected by the fly food: diets made of complex carbohydrates such as corn flour, with abundant conservatives such as the antifungal nipagin, tend to favor *Lactobacillaceae*, whereas diets made of simple sugars such as molasse, with less conservatives, tend to favor *Acetobacteraceae* (Obadia et al., 2018; Sharon et al., 2010). This explains some differences in the dominant strains/species found among different labs working on *Drosophila* microbiota. *Drosophila* can also shape its microbiota: association of 103 *Drosophila* lines with the same consortium of 5 bacterial species yielded an important between-lines variation in microbiota composition (Chaston et al., 2016). The presence of *Drosophila* enable *Lactobacilli* to overcome competition with *Acetobacteraceae* (Wong et al., 2015) and to persist longer on the fly food by consuming metabolites that are excreted by *Drosophila* larvae, such as N-acetylglucosamine (Storelli et al., 2018). The influence that *Drosophila* exerts on its microbiota relies partly on its immune system. Indeed, AMPs and ROS can kill both symbiotic and pathogenic bacteria indiscriminately. Moreover, the main cues that activate the immune system of *Drosophila*, *i.e.* the peptidoglycans, can be produced by symbionts as well as pathogens (uracil, on the contrary, seems to be produced by pathogens only as a byproduct of quorum-sensing (Kim et al., 2020)). Symbiotic bacteria are able to live in close association with *Drosophila* because they elicit an "immune tolerance": they do not trigger a strong immune response like pathogens do. Immune tolerance may rely on several mechanisms. First of all, on the abundance of peptidoglycans: pathogens, which highly proliferate during infection, may release more peptidoglycan fragments than symbionts. The localization of the peptidoglycan (in the gut lumen for symbionts, in the hemolymph for invading pathogens) may also be of importance. Finally, immune tolerance to symbionts is ensured by the action of immune modulators such as the Relish-inhibitor Caudal or PGRP-SD. Knocking-down Caudal in the posterior midgut increases the activity of the IMD pathway and alters the composition of the microbiota (Ryu et al., 2008). PGRP-SD is induced by the symbiont *L. plantarum* in a PGRP-LE dependent manner. It then allows regulation of the microbiota by modulating the expression of negative regulators of the IMD pathway (Iatsenko et al., 2018): *PGRP-LB* (Charroux et al., 2018), *PGRP-SCs* (Paredes et al., 2011) and *pirk* (Kleino et al., 2008).

Drosophila thus influences the composition and the abundance of its microbiota. In return, *Drosophila*'s microbiota has a profound influence on its host's biology. In the next paragraphs, I will discuss the influence of symbiotic microbes on *Drosophila*'s behaviour, metabolism, lifespan, fecundity and growth.

3) Microbiota and behaviour

First of all, symbionts affect *Drosophila*'s feeding behaviour. *Drosophila* are attracted to food that was previously in contact with CR larvae, but not by food that was in contact with GF larvae. This attractive effect of the microbiota can be recapitulated by some species (*L. plantarum* and *Levilactobacillus brevis*) (Venu et al., 2014). Moreover, *Drosophila* seem to be attracted by the microbes that they already carry: when larvae or adults are mono-associated with either *L. plantarum* or *Acetobacter pomorum*, they show attraction to food patches that were seeded with *L. plantarum* or *A. pomorum*, respectively; for adults at least, this attraction relies partly on olfactory sensing of microbial products (Wong et al., 2017). The emission of these olfactory cues depends on interactions between microbes: flies are more attracted by the odorants produced by a co-culture of the yeast *Saccharomyces cerevisiae* and the bacteria *Acetobacter malorum* and *L. plantarum* than by mono-cultures of these species. This attraction relies on metabolic cross-feeding between the three species, which allows the bacteria to produce attractive acetaldehyde derivatives and esters from the products of *S. cerevisiae*'s catabolism of ethanol (Fischer et al., 2017). However, not all microbial strains elicit olfactory attraction: *Drosophila* lacking odorant receptors lose attraction to the yeast *Saccharomyces cerevisiae*, but they are still attracted by *L. plantarum* (Qiao et al., 2019). Bacteria can thus also alter feeding behaviour through non-olfactory cues. Moreover, *Drosophila*'s microbiota affects the food choice of its host: compared to GF flies, flies associated with *A. pomorum* show a preference towards diets with a low protein:carbohydrate ratio (Wong et al., 2017). When they are deprived of essential amino acids (AA), GF flies show preference for proteins over sucrose and increase their food intake of proteins. Flies that are associated with symbiotic bacteria (Leitão-Gonçalves et al., 2017), especially with *A. pomorum* and *L. plantarum* (Henriques et al., 2020), lose this preference for proteins. A recent study by the lab of Won-Jae Lee proposes the following mechanism to explain the influence of symbionts on food choice: essential AA deprivation inhibits the target-of-rapamycin (TOR) pathway and activates the general control nonderepressible 2 (GCN2) pathway in enterocytes, which stimulate production of the neuropeptide CNMamide by enterocytes. CNMamide then activates the CNMamide Receptor in neurons, inducing preference for proteins. Symbiotic bacteria synthesize AA and provide them to the fly, which represses this gut brain-axis and protein preference (Kim et al., 2021).

Drosophila's microbiota can also influence its host's social behaviour. Flies bearing a knock-out (KO) mutation for the histone demethylase KDM5 (*kdm5^{-/-}*) display both reduced social behaviour and changes in the composition of their microbiota: they have higher titers of Proteobacteria and lower titers of *L. plantarum* compared to WT flies. Moreover, the reduced social behaviour is rescued in GF *kdm5^{-/-}* flies, and in *kdm5^{-/-}*

flies mono-associated with *L. plantarum*, which shows a causal relationship between the microbiota composition and social behaviour (Chen et al., 2019).

Furthermore, GF flies exhibit hyperactive locomotor behaviour: they walk faster than CR flies and make shorter pauses. Hyperactivity is rescued by association with certain species of symbiotic bacteria such as *L. brevis*. *L. brevis*' effect relies on the enzyme xylose isomerase, which activity in the bacterium alters the carbohydrate metabolism of *Drosophila*. Changes in carbohydrate availability then modify the locomotor behaviour through the activity of octopaminergic and tyraminergetic neurons (Schretter et al., 2018). However, these results are questioned by another study that did not show a robust hyperactivity of GF flies compared to CR flies (Selkrig et al., 2018). Similarly, Jia and colleagues did not observe differences in locomotor behaviour between GF flies and CR flies. However, they report that GF males are less aggressive than CR flies or flies associated with *L. plantarum* because symbiotic bacteria stimulate octopaminergic neurons that promote aggressive behaviours (Jia et al., 2021).

Finally, microbes influence *Drosophila*'s reproductive behaviour. Female flies prefer to lay eggs on food that contains symbiotic microbes. This behaviour is independent of olfactory receptors and may rather rely on gustatory receptors or other sensors (Liu et al., 2017; Qiao et al., 2019). The microbiota may also influence mating preferences of *Drosophila*, although this topic is subject to controversy. A study by Sharon and colleagues showed that *Drosophila* display mating preference toward flies that were raised on the same diet, versus flies that were raised on a different diet and thus have a different microbiota. Treating the flies with antibiotics abolishes the mating preference, and it can be restored by association with *L. plantarum*, demonstrating a causal relationship between symbionts and mating preference (Sharon et al., 2010). However, Leftwich and colleagues failed to reproduce these results: they did not observe the emergence of mating preference after raising *Drosophila* on the same two diets like Sharon and colleagues did. Moreover, treating the flies with *L. plantarum* did not induce mating preference either (Leftwich et al., 2017). Discrepancies between studies may be explained by differences in the initial microbiota of the flies, before they were raised on the two different diets (Obadia et al., 2018). More generally, diverging results in behavioural studies on *Drosophila* and its microbiota may be due to differences between rearing conditions: because different labs use different conditions to rear their *Drosophila* lines, especially different composition of fly foods, these lines can harbor different bacterial communities. Moreover, some effects of symbiotic bacteria are strain-specific: two strains of the same species may not have the same effect (Storelli et al., 2011). Therefore, it is considered good practice to work with defined consortia of bacterial strains, rather than use a "conventional" microbiota which composition can greatly vary between labs.

4) Microbiota and energy metabolism

Studies have compared the metabolomes of GF *Drosophila* and microbe-associated *Drosophila*. GF adults contain more triglycerides (TAG) and glucose than flies associated with microbes (Dobson et al., 2015). Only *Acetobacteraceae* and certain

species of *Lactobacillaceae* such as *L. plantarum* reduce the levels of TAG, whereas all bacteria tested can reduce the levels of glucose (Newell and Douglas, 2014). A metagenomic analysis showed a negative correlation between TAG levels in flies and the abundance of phosphotransferase system (PTS) in associated bacteria. PTS allow bacteria to uptake sugar; therefore, these data suggest that symbiotic bacteria can reduce the TAG levels of *Drosophila* by depleting the sugars in the diet (Kang and Douglas, 2020). Moreover, TAG levels are negatively correlated with acetic acid levels in flies. Acetic acid is mostly produced by *Acetobacteraceae*, which can reduce TAG levels in flies, and supplementation of acetic acid to GF flies reduce their TAG levels (McMullen et al., 2020), suggesting that acetic acid produced by symbionts such as *Acetobacteraceae* decrease TAG levels in *Drosophila*. The Watnick group has proposed a mechanism to explain this phenomenon. GF larvae have abundant lipid droplets in enterocytes, suggesting impaired lipid mobilization. Acetic acid produced by symbiotic bacteria is uptaken by enteroendocrine (EE) cells (cells in the *Drosophila* gut that produce hormones in response to several cues) through the transporter Targ. In EE cells, acetic acid abundance yields more AcetylCoA, which is used as a substrate by the Tip60-histone acetyltransferase (HAT) complex to regulate histone acetylation. Histone acetylation increases the expression of the immune gene *PGRP-LC* by EE cells (Jugder et al., 2021), which leads to the secretion of the hormone Tachykinin (Tk). Tk then promotes utilization of lipid resources in nearby enterocytes (Kamareddine et al., 2018).

Finally, gut microbes can also influence energy metabolism through interaction with mitochondria. Indeed, GF flies show reduced mitochondrial activity and ATP levels compared to bacteria-associated flies. This correlates with lower amounts of flavine adenine dinucleotide (FAD⁺), the active form of riboflavin, which is a required coenzyme for many enzymatic mitochondrial reactions. Because symbiotic bacteria provide riboflavin to *Drosophila* (Consuegra et al., 2020a; Wong et al., 2014), this suggests that FAD⁺-requiring mitochondrial activity, such as ATP generation from glucose and TAG, are promoted by symbiotic bacteria (Gnainsky et al., 2021).

5) Microbiota and lifespan

The influence of symbiotic bacteria on *Drosophila*'s lifespan has long been subject to controversy. Some studies reported that GF flies have a shorter lifespan than CR flies (Brummel et al., 2004; Keebaugh et al., 2018), while others showed that GF flies have an extended lifespan (Fast et al., 2018; Iatsenko et al., 2018; Lee et al., 2019). Whether symbiotic microbes can extend or shorten *Drosophila*'s lifespan depends on several parameters. First of all, it depends on the microbiota composition: depletion by low-dose oxidants of *Acetobacter acetii*, but not of *L. plantarum*, extends *Drosophila*'s lifespan (Obata et al., 2018). Association with *L. plantarum*, *Acetobacter tropicalis*, *Acetobacter orientalis* or a combination of these bacteria shorten lifespan, whereas mono-association with *L. brevis* or *Acetobacter pasteurianus* does not (Gould et al., 2018). Secondly, it depends on the diet: the symbiotic yeast *Issatchenkia orientalis* improves the lifespan of its host on a poor diet (0,1% yeast extract) (Keebaugh et al.,

2018) by improving amino acid harvest (Yamada et al., 2015). On the contrary, it shortens lifespan on a rich diet (5% yeast extract) (Keebaugh et al., 2019). Several mechanisms may explain the shortening of lifespan. First of all, some bacteria induce proliferation of intestinal stem cells (ISC). Lactic acid produced by *L. plantarum* is uptaken by enterocytes. It is then oxidized to pyruvate, which is accompanied by the reduction of NAD⁺ into NADH. NADH is the substrate of the enzyme Nox, which generates reactive oxygen species (ROS). ROS then stimulates ISC proliferation (Iatsenko et al., 2018). In young flies, induction of ISC proliferation by symbiotic bacteria through lactic acid may promote intestinal homeostasis (Jones et al., 2013); however, in aging flies the bacterial load increases due to immune senescence (the decline in immunity due to aging) (Min and Tatar, 2018). This causes overproliferation of ISCs in aging flies, dysplasia of the gut and eventually shortens lifespan (Iatsenko et al., 2018). On the contrary, another study reported that *L. plantarum* reduces the proliferation of ISCs in the aging gut (Fast et al., 2018). This contradictory result may be explained by strain specificity or by differences in the rearing diet (Douglas, 2018b). Moreover, a study in *C. elegans* has shown that upon supplementation of the drug metformin, the worm's commensal *Escherichia coli* produces agmatine, a metabolic derivative of arginine that increases fatty acid oxidation in the worm and extends its lifespan. The effect of agmatine on lifespan is conserved in *Drosophila*; however, it remains to be tested whether agmatine is actually produced by *Drosophila*'s symbiotic bacteria (Pryor et al., 2019).

6) Microbiota and fecundity

Like often in the field of *Drosophila*'s microbiota, the effect of *Drosophila*'s microbiota on its host fecundity depends strongly on the diet. GF flies reared on a nutrient-rich diet (~50 g.L⁻¹ of inactivated yeast) show the same fecundity as flies associated with symbiotic microbes (Ridley et al., 2012, 2013), whereas GF flies reared on a nutrient-poor diet (15 g.L⁻¹ of dry yeast or less) show reduced fecundity that can be rescued by symbiotic bacteria (Delbare et al., 2020; Elgart et al., 2016; Gnainsky et al., 2021; Gould et al., 2018). Enhancement of fecundity is also microbe-specific: *Lactobacillaceae* such as *L. plantarum* do not improve fecundity even on a nutrient-poor diet (Gould et al., 2018; Téfrit and Leulier, 2017), whereas *Acetobacteraceae* such as *A. pasteurianus*, *A. tropicalis* and *A. orientalis* strongly do. Association of *A. pasteurianus* with *L. plantarum* can further increase fecundity (Gould et al., 2018). The mechanisms seem to rely at least partly on the activity of the ovaries: on a nutrient-poor diet, GF female flies have less oocytes in their ovaries than CR flies. Moreover, the embryos of GF flies display a shorter embryonic development. These differences can be rescued by association with an isolated *Acetobacter*. The effect of *Acetobacter* relies on the enzyme Aldehyde dehydrogenase (Aldh) in the fly: *Acetobacter* increases *Aldh* expression, and *Aldh* is necessary and sufficient to increase the number of oocytes in the ovaries (Elgart et al., 2016). Interestingly, inhibiting mitochondria activity with drugs represses *Aldh* expression in the ovaries of *Acetobacter*-associated flies. As seen above, *Acetobacter* increase the mitochondrial activity of *Drosophila* by

providing FAD⁺. It is thus possible that *Acetobacter* increases *Aldh* expression and improves fecundity through the providing of FAD⁺ to the mitochondria of the ovaries (Gnainsky et al., 2021).

The effects of symbiotic bacteria on male fertility have been less studied. Males associated with *L. plantarum* are more fertile than male associated with *A. pomorum*, but the mechanisms are unknown (Morimoto et al., 2017). Moreover, CR females mated to GF males produce less eggs than CR females mated to CR males. This difference may be due to post-mating changes in the transcriptome of females, which are influenced by the male's microbiota status (Delbare et al., 2020).

7) Microbiota and post-embryonic growth

On a nutrient-rich diet, the growth of GF *Drosophila* larvae is similar to the growth of their CR counterparts (Storelli et al., 2011). However, on a nutrient-poor diet, GF larvae suffer from considerable growth delays compared to CR larvae. On a diet that contains only 10% of dry yeast, GF larvae take ~13,5 days to reach adulthood, whereas CR larvae need only ~10,5 days. This difference is due to a lengthening of the larval stages: the duration of the metamorphosis does not depend on the microbiota (Storelli et al., 2011). The less dry yeast is present in the diet, the more the effect of the microbiota is important: a 0.25% yeast diet yields a doubling of the duration of the larval phase between GF and CR conditions (Shin et al., 2011). *Drosophila*'s microbiota can thus rescue the deleterious effects of a poor nutrition on its host's growth. The effect of the whole microbiota can be mimicked by specific bacterial strains upon mono-association: *L. plantarum* Lp^{WJL} (Storelli et al., 2011) and *A. pomorum* Ap^{WJL} (Shin et al., 2011), for instance. Other strains of the same species (e.g. *L. plantarum*^{NIZO2877}) are less growth-promoting (Schwarzer et al., 2016). So far, most studies on growth promotion have focused on one microbial species, mostly from the genera *Lactobacilli* or *Acetobacter*. However, interactions between different microbes can strongly influence larval growth. Gould and colleagues tested the 32 possible combinations of GF, mono-, bi-, tri-, tetra- and penta-associations of 5 species of symbiotic bacteria and found that the most growth-promoting condition is a consortium of *L. brevis*, *A. pasteurianus* and *A. orientalis* (Gould et al., 2018). Moreover, bi-association of larvae with *A. pomorum* and *L. plantarum* greatly accelerate larval growth on a low-AA diet compared to mono-association with either bacterium. This synergy relies on lactic acid produced by *L. plantarum* through fermentation of dietary sugars, which triggers a metabolic switch in *A. pomorum* that is beneficial to larval growth (Consuegra et al., 2020b).

Since the first two articles describing the ability of *Drosophila*'s microbiota to promote its host's growth in undernutrition (Shin et al., 2011; Storelli et al., 2011), many studies have sought to understand the mechanisms at play. A first mechanism is the improvement of larval nutrition, either directly or indirectly. Direct improvement consists in the microbes providing nutrients. This aspect is discussed below in Chapter I: *Drosophila*-associated bacteria differentially shape the nutritional

requirements of their host during juvenile growth. Indirect improvement consists in enhancing the uptake of nutrients from the diet. *L. plantarum* stimulates the expression of proteases in larval enterocytes, which help the larvae digest dietary polypeptides. Proteases stimulation is partly mediated by sensing of *L. plantarum*'s peptidoglycans by the PGRP-LE/IMD/Relish cascade (Erkosar et al., 2015). In addition, a genetic screen on a library of loss-of-function mutants of *L. plantarum* showed that D-Alanylation of teichoic acids in the cell wall of *L. plantarum* further stimulates protease expression through an IMD-independent mechanism (Matos et al., 2017). Moreover, the symbiotic fungus *Issatchenkia orientalis* increases the flux of nutrients from the diet to its host by uptaking and concentrating dietary nutrients, which may improve development on a nutrient-low diet (Yamada et al., 2015). Improved nutrition stimulates growth through the activation of systemic signaling such as the AA-sensing target-of-rapamycin (TOR) in the fat body (Storelli et al., 2011) and insulin signaling (Shin et al., 2011). Regulation of growth by nutrient-dependent signaling is described in part III of the Introduction.

In addition to increasing the general availability of nutrients and stimulating systemic growth-regulating pathways, *Drosophila*'s microbiota has a local influence on its host's gut, which can lead to improved systemic growth. Symbiotic microbes can influence *Drosophila*'s development through the stimulation of ROS production in the gut. ROS are part of the local immune response: they are produced by enterocytes in response to infection (Lemaitre and Hoffmann, 2007), but also in response to symbiotic microbes: as previously described, lactate provided by *L. plantarum* stimulates ISC proliferation in adults through ROS production by enterocytes (Iatsenko et al., 2018). A similar mechanism may be at play in larvae. The larval gut contains stem cells called Adult Midgut Precursor (AMPs) that differentiate into epithelial cells and the adult ISCs during metamorphosis, forming a transitory "pupal gut" that ensures the integrity of the intestinal barrier during metamorphosis. Around adult emergence, adult ISCs become active and proliferate and differentiate to establish the adult midgut (Jiang and Edgar, 2009). *L. plantarum* stimulates the production of ROS in enterocytes, which increase the number of the AMPs through the secretion of the cytokine Unpaired 2 (Upd2). The authors did not test the influence of microbiota-induced AMP proliferation on larval growth, but they noticed that adults knocked-down for Upd2 in enterocytes are smaller than WT adults (Reedy et al., 2019). Moreover, GF larvae show an important variability in size due to cryptic genetic variation in developmental genes. *L. plantarum* can buffer this variability: when comparing groups of larvae with the same average size, larvae associated with *L. plantarum* display less variability in size than GF larvae. This "buffering effect" of symbiotic bacteria is lost upon supplementation with the antioxidant N-acetylcysteine, which suggests that it is ROS-dependent (Ma et al., 2019). Changes in the hosts' metabolism that are triggered by symbiotic microbes (see above) can impact larval growth. Several studies point to acetate as a crucial mediator of growth-promotion by symbiotic bacteria. A Metagenome-Wide Association Study on 41 strains of *Drosophila*'s symbionts identified bacterial genes and functions associated with higher growth-promoting effect. Especially, the enzymes required for

the biosynthesis of the respiratory cofactor pyrroloquinoline quinone positively correlate with growth-promoting ability (Chaston et al., 2014). Genes encoding these enzymes (PqqB, PqqC, and PQQ-Adh) were previously identified through a genetic screen on *A. pomorum*. *A. pomorum* deficient for these enzymes produce less acetate, which impairs their ability to promote larval growth (Shin et al., 2011). As described above, microbial acetate induces mobilization of lipid stores in enterocytes through IMD signaling in the EE cells. Supplementation of acetate and ectopic expression of the IMD pathway in EE cells both lead to lipid mobilization and improve the growth of GF larvae (Kamareddine et al., 2018). Through a study of experimental evolution, Martino and colleagues showed that a single mutation in the gene *ackA* could improve the growth-promoting ability of the strain *L. plantarum*^{NIZO2877}. *ackA* encodes an acetate kinase, and the evolved strain with the *ackA* mutation produces more N-acetyl-AA than the original strain. N-acetyl-Glutamine, especially, is capable of promoting the growth of GF larvae (Martino et al., 2018). Moreover, it decreases the expression of the IMD-regulator PGRP-SC1 in the gut (Gallo et al., 2021), suggesting a potential common mechanism with the acetate-IMD axis previously described (Jugder et al., 2021; Kamareddine et al., 2018). Figure 2 summarizes the mechanisms that may allow *Drosophila*'s microbiota to promote its host's growth. It is adapted from (Grenier and Leulier, 2020).

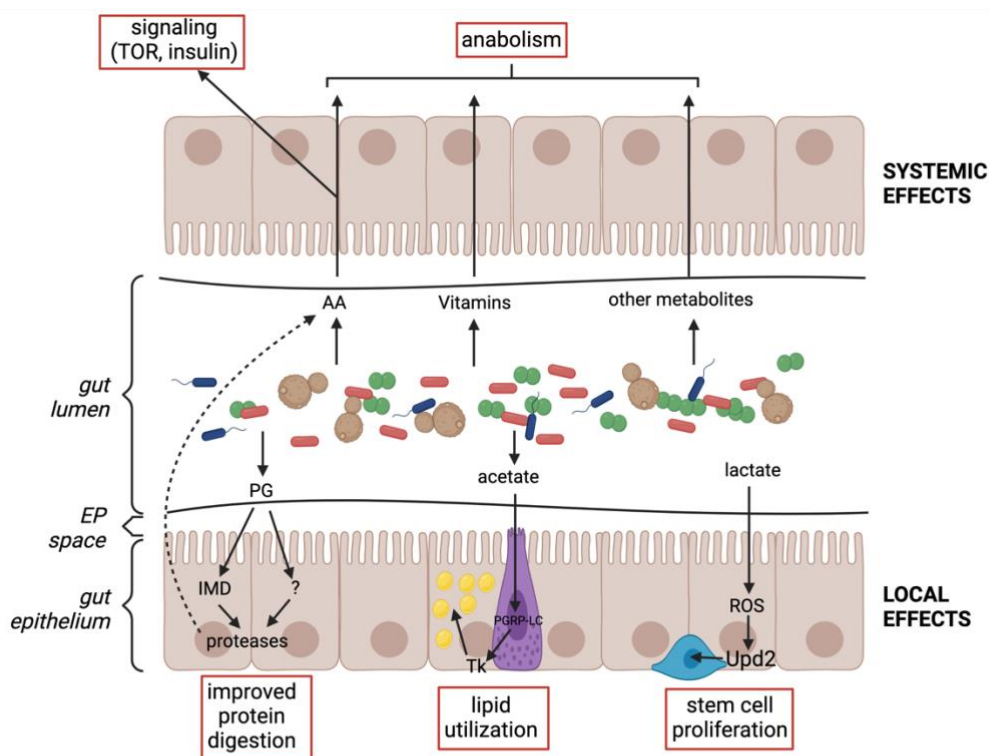


Fig 2. Mechanisms of growth promotion by *Drosophila*'s microbiome. AA: Amino acids. EP space: ectoperitrophic space between the peritrophic membrane (in black) and the epithelium. Epithelium: midgut epithelium composed of enterocytes (in brown), enteroendocrine cells (in purple) and stem cells (in blue). IMD: Immune Deficient Pathway. PG: peptidoglycans. PGRP-LC: Peptidoglycan Recognition Protein LC. ROS: Reactive Oxygen Species. Tk: Tachykinin. TOR: Target of Rapamycin kinase. Upd2: Unpaired2.

It is interesting to note that some of the pathways involved in growth promotion and lifespan shortening by symbiotic microbes are similar: increase of nutrient abundance can stimulate insulin pathways that accelerate growth (Storelli et al., 2011) and shorten lifespan (Clancy et al., 2001). Moreover, symbiotic microbes promote intestinal stem cells proliferation through ROS signaling in aging adults (Iatsenko et al., 2018) and in larvae (Reedy et al., 2019). Symbiotic microbes thus seem to favor a “live fast, die young” lifestyle for their host (Obata et al., 2018). In nature, this lifestyle probably benefits *Drosophila*'s fitness: the selective pressure on fast development is high, because it allows earlier reproduction, whereas the selective pressure on extended lifespan is low, because flies may die prematurely from predation or disease and fecundity decreases with age.

Drosophila is thus a powerful model to study interactions between host and microbes, especially in the context of growth. In the next part, I will discuss how *Drosophila* is also a powerful model to study the regulation of growth and nutrition.

III *Drosophila* as a model to study growth and nutrition

1) *Drosophila* and growth

Drosophila is a holometabolous insect. Its post-embryonic life is composed of three major stages: the larval stage, the metamorphosis or pupal stage, and adulthood. The systemic growth phase of *Drosophila* is concentrated into the larval stage: between hatching from the egg and entry into metamorphosis, *Drosophila* larvae go through three larval instars (L1, L2 and L3) and their body mass increases 200-fold (Tennessen and Thummel, 2011). Because *Drosophila* pupae are immobile and do not feed, the larvae need to accumulate all the resources that are necessary to go through metamorphosis and develop the adult organs ahead of pupariation. On a rich medium, the larval stage typically lasts 5 days, but this is highly dependent on environmental parameters in which diets play a major role (Layalle et al., 2008). After the L2-L3 molt, larvae can reach the “critical weight”: they achieve sufficient body mass to finish the larval stage and carry out metamorphosis. They are then committed to entering metamorphosis within a definite period of time, regardless of the amount of nutrients they ingest during the end of L3 stage. However, accumulation of nutrients after passing the critical weight determines the adult size: larvae starved after they reach their critical weight will yield smaller adults. On the contrary, the amount of nutrients accumulated before reaching the critical weight determines the length of the growth period: if larvae are starved before the critical weight checkpoint, their growth is stalled but they can then reach the same adult size as non-starved larvae if they encounter a richer food source (Tennessen and Thummel, 2011). *Drosophila* larvae thus have complex nutrient and physiological status sensing mechanisms, which allow them to synchronize their growth with the ingested nutrients. These mechanisms involve

nutrient sensors and hormonal relay that coordinate in a tissue and/or systemic manner the growth of the animal.

The main nutrient sensor regulating systemic growth in *Drosophila* is the target-of-rapamycin (TOR) kinase. TOR can form two complexes with its cofactors, mTORC1 and mTORC2. mTORC1 is activated by AA abundance (Laplante and Sabatini, 2009) through the action of AA transporters or intracellular AA-sensors (Goberdhan et al., 2016). In *Drosophila*, TOR is activated by the cationic AA transporter Slimfast (Colombani et al., 2003). Moreover, TOR is repressed by low energy status: high Adenosine Mono Phosphate levels activate the AMP-kinase (AMPK) (Braco et al., 2012), which in turn activates the TOR-inhibitor tuberous sclerosis complex 2 (TSC2) (Kim and Lee, 2015). Of note, TOR is a regulation hub that can also integrate other cues such as hypoxia (Texada et al., 2019). TOR activation has a cell-autonomous effect on tissue growth: it leads to the phosphorylation of the eIF4E-binding protein (4E-BP) and S6 kinase (S6K), which represses their capacity to inhibit translation and thus induces cell growth (Miron et al., 2003).

Moreover, *Drosophila* larva's fat body (FB) specializes in coupling local nutrient-sensing with systemic growth regulation. Activation of TOR in the larval FB regulates the release of four peptides: Growth Blocking Peptides (GBP) 1 and 2 (Koyama and Mirth, 2016), Stunted (Delanoue et al., 2016) and Eiger (Agrawal et al., 2016). These peptides can directly or indirectly modulate the production of *Drosophila* Insulin-Like Peptides (DILPs), especially DILP2, DILP3 and DILP5, in the Insulin-Producing Cells (IPCs) of the larval brain (Colombani et al., 2003). The FB can regulate DILP production in the IPCs in response to other nutritional cues, through the secretion of Unpaired2 (Upd2) in response to fat and sugar (Rajan and Perrimon, 2012), and CCHamide-2 (CCHA2) (Sano et al., 2015) and Dawdle (Daw) (Chng et al., 2014; Ghosh and O'Connor, 2014) in response to glucose levels. Moreover, DILP3 secretion by IPC is stimulated by the adipokinetic hormone (AKH) produced in the corpora cardiaca in response to trehalose, the main form of circulating carbohydrate in *Drosophila* (Kim and Neufeld, 2015). Finally, DILP production is cell-autonomously regulated by sensing of Leucine (Leu) by the transporter Minidisc in the IPCs (Manière et al., 2016).

DILPs are released in the hemolymph and activate the Insulin-Receptor (InR) in target cells. InR then triggers the phosphorylation cascade of Chico (Clancy et al., 2001), the phosphoinositide-3-kinase (PI3K) and the Akt kinase (Garofalo, 2002). Akt phosphorylates the forkhead transcription factor FOXO, which causes its sequestration into the cytoplasm and prevents it from activating its transcriptional targets such as the translation inhibitor 4E-BP (Jünger et al., 2003), resulting in cell growth. DILPs released by IPCs thus promote tissue growth in the whole larva (Ikeya et al., 2002). Moreover, after the larva has reached the critical weight, the FB directly regulates insulin signaling and promotes growth through the secretion of DILP6 (Okamoto et al., 2009).

On top of their direct effect on growth, DILPs indirectly control maturation by impacting ecdysone production. Ecdysone is a steroid hormone synthesized mostly by the prothoracic gland (PG) from sterols (Gilbert et al., 2002). It is converted into its active form, 20-hydroxyecdysone (20E) in peripheral organs (Petryk et al., 2003). During the growth phase, peaks of ecdysone induce the two molts that separate the three larval stages (Richards, 1981). Three small ecdysone pulses occur during the L3 stage: one controls the achievement of the critical weight, one triggers the production of a glue that will allow the pupa to stick to a surface, and the last one induces wandering behaviour: larvae stop feeding and “wander” until they find a place to undergo metamorphosis. A final large pulse of ecdysone triggers entry into metamorphosis (Kannangara et al., 2021; Warren et al., 2006). Ecdysone production by the PG integrates non-nutritional cues through the prothoracicotropic hormone (PTTH) pathway (McBrayer et al., 2007) and nutritional cues through the insulin pathway. Indeed, FOXO inhibits the transcription of the genes of the Halloween pathway, which are required for ecdysone synthesis (Koyama et al., 2014). InR activation by DILPs thus lead to derepression of ecdysone synthesis. Moreover, DILPs signaling in the PG activates the transcription of *warts (wts)*, which regulates ecdysone production by repressing the microRNA *bantam* (Moeller et al., 2017). Beside DILPs signaling, ecdysone synthesis is regulated by the nutritional status through three additional pathways: firstly, lipid and protein starvation trigger production of a lipoprotein-associated form of the protein Hedgehog (Hh) in the midgut. Hh reduces the expression of the Halloween genes and thus represses ecdysone synthesis (of note, Hh can also modulate growth in the FB through an unknown mechanism)(Rodenfels et al., 2014). Secondly, serotonergic neurons, which development is affected by nutrient availability (Sood et al., 2021), innervate the PG and modulate ecdysone production (Shimada-Niwa and Niwa, 2014). Finally, AA availability directly stimulate ecdysone production through the TOR pathway in the PG (Layalle et al., 2008). After the critical weight is reached, ecdysone causes a negative feedback loop on DILP induction by the FB and represses growth (Colombani et al., 2005).

Therefore, DILPs and ecdysone are the main factors that allow regulation of growth and maturation by nutrition. Inter-organ communication between the FB, the IPCs and the PG permits a fine-tuning of the development in response to nutrient availability: in nutrient abundance, DILPs boost tissue growth and fasten the peaks of ecdysone until the critical weight is reached. Once the critical weight is reached, ecdysone negatively feedbacks on DILP release and inhibits growth, committing the larva to metamorphosis. Fig. 3 summarizes the mechanisms of systemic growth regulation by nutrition in the *Drosophila* larva.

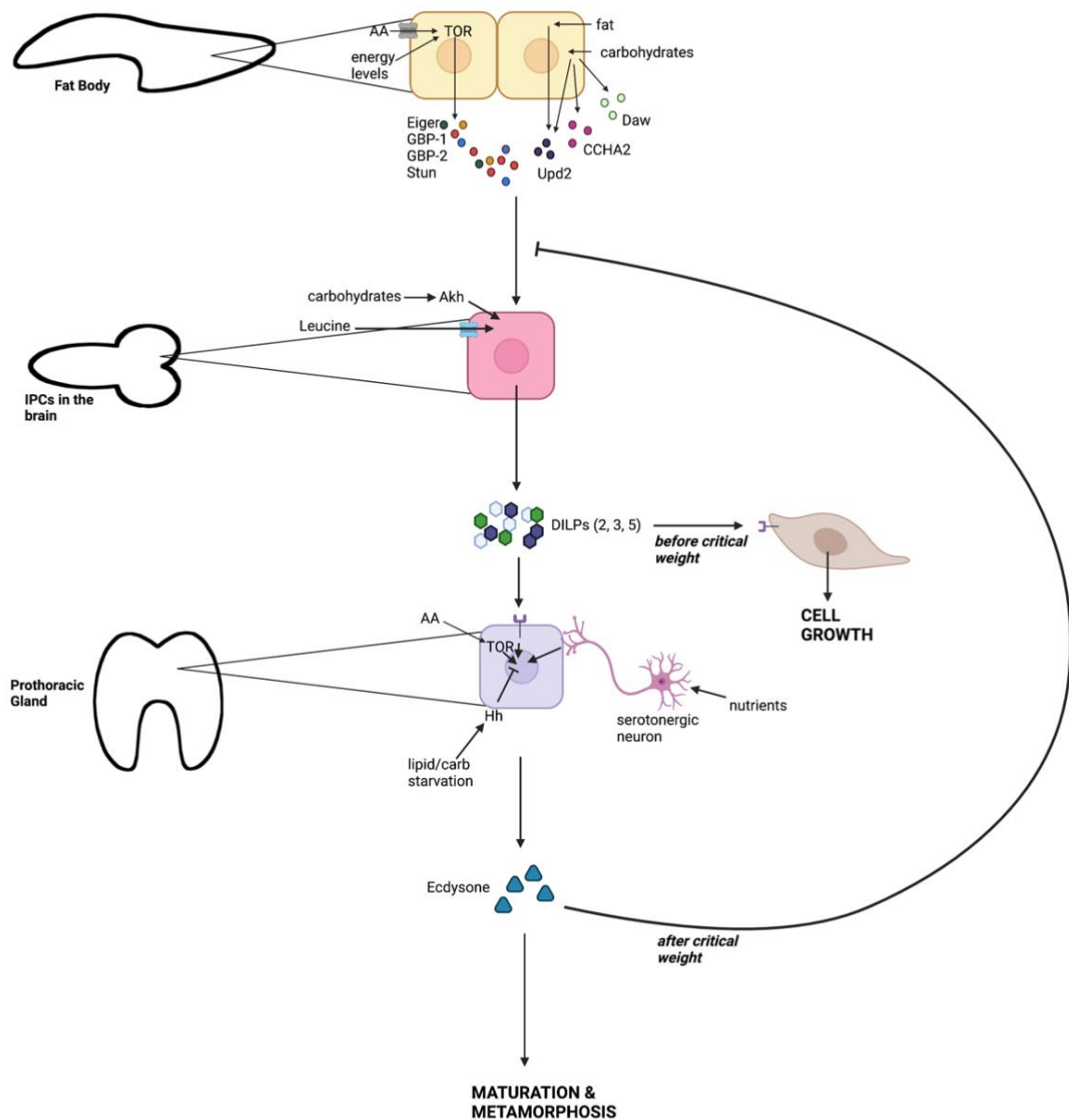


Fig 3. Growth regulation by nutrition on the *Drosophila* larva. AA: Amino acids. TOR: target of rapamycin. GBP: Growth Blocking Peptide. Stun: Stunted. Daw: Dawdle. CCHA2: CCHamide-2. Upd2: Unpaired2. Akh: Adipokinetic hormone. DILP: *Drosophila* Insulin-Like Peptides. IPC: Insulin-Producing Cells. Hh: Hedgehog.

In addition to a direct regulation of development through the TOR-insulin-ecdysone pathway, nutrient availability can regulate growth indirectly. Indeed, nutrient sensors allow to adapt the feeding behaviour to the food quality. Larvae can reject an unbalanced food and select a food which composition is closer to their nutritional needs. The ability of larvae to select optimal food can greatly impact growth. Nutrients can be sensed by Gustatory Receptors (GR), which are expressed in neurons of the head, the pharynx and the gut (Freeman and Dahanukar, 2015). Larvae can sense fructose through the receptor GR43a, expressed in the pharynx and the brain (Mishra et al., 2013). The Pickpockets receptors (encoded by *ppk11* and *ppk19*) (Liu et al.,

2003) and Serrano (Alves et al., 2014) allow detection of salt. Ribonucleosides and RNA are sensed through the family of receptors GR28 (Mishra et al., 2018). Finally, the ionotropic receptor *Hodor* allows sensing of zinc and activates TOR in enterocytes. Larvae knocked-out for *hodor* display reduced food intake and reduced DILP2 secretion, and suffer from developmental delays (Redhai et al., 2020).

An ionotropic receptor, *Ir76b*, is responsible of AA sensing in adults (Ganguly et al., 2017). In larvae, AA sensing relies mostly on the general control nonderepressible 2 kinase (GCN2). GCN2 was first discovered in yeast (Dever et al., 1992), but it is highly conserved among Eukaryotes. It contains a domain homolog to a histidyl-tRNA synthetase, an enzyme that binds the AA Histidine with its cognate tRNAs (Wek et al., 1989). This domain can bind uncharged His-tRNA, as well as uncharged tRNAs for other AA, which activates the kinase domain of the protein (Dong et al., 2000). Because uncharged tRNAs are more abundant when AA are scarce, GCN2 is a sensor of AA scarcity (Donnelly et al., 2013). When GCN2 binds an uncharged tRNA, it phosphorylates itself (Romano et al., 1998) and the eukaryotic elongation factor 2 α (eIF2 α) (Zhu et al., 1996). Phosphorylation of eIF2 α leads to the integrated stress response (ISR): translation of most mRNAs is repressed, except for a subset of them that allow adaptation to AA scarcity (Harding et al., 2003).

Of note, the ISR can be activated by other kinases: PERK, which senses endoplasmic reticulum stress, PKR and HRI in Mammals, which sense double-stranded RNA from viruses and heme scarcity, respectively (reviewed in (Donnelly et al., 2013)). Moreover, GCN2 can be activated by cues other than AA scarcity, though the mechanisms are unclear: glucose limitation (Yang et al., 2000), purine limitation (Rolfes and Hinnebusch, 1993), UV exposure (Grallert and Boye, 2007), viral (Krishnamoorthy et al., 2008) and bacterial infection (Tattoli et al., 2012), ribosomal RNA (Zhu and Wek, 1998) and stalled ribosomes (Harding et al., 2019; Inglis et al., 2019). The latter may also be a cue for AA starvation. Fig. 4 summarizes the mechanism of activation of the GCN2 pathway.

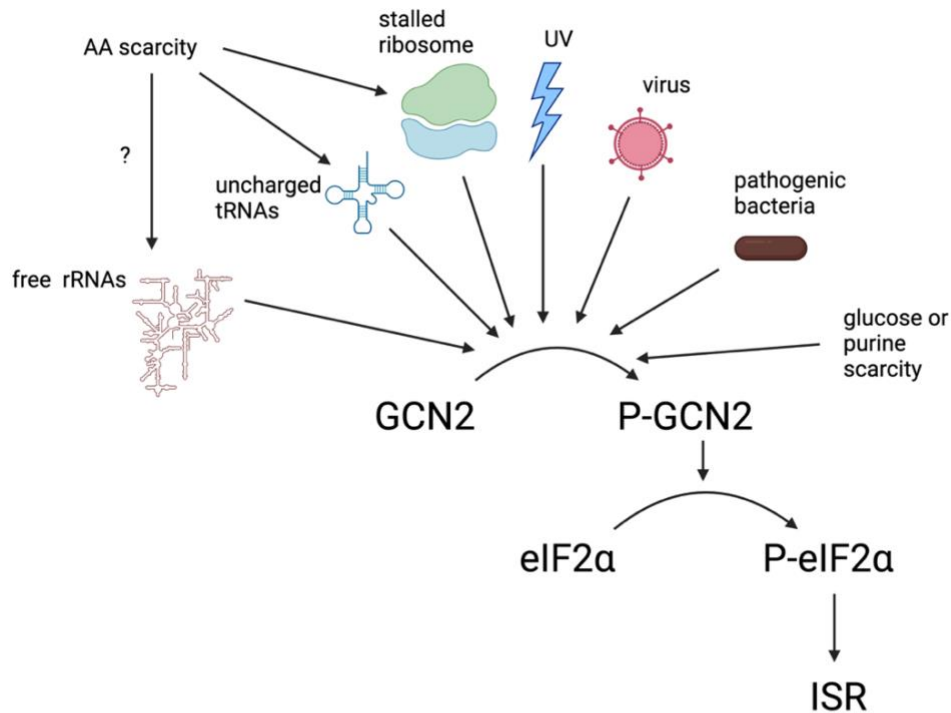


Fig 4. Mechanisms of GCN2 activation. AA: Amino acids. rRNAs: ribosomal RNA. tRNAs: transfer RNAs. UV: Ultraviolet light. GCN2: general control nonderepressible 2 kinase. P-GCN2: phosphorylated GCN2. eIF2 α : eukaryotic elongation factor 2 α . P-eIF2 α : phosphorylated eIF2 α . ISR: Integrated Stress Response.

In *Drosophila*, GCN2 has been mostly studied in regard to behaviour and immunity. Feeding *Drosophila* larvae a diet unbalanced in AA causes AA scarcity in the dopaminergic neurons, which activates GCN2 and leads to rejection of the diet. Ectopic activation of an activated form of GCN2 in dopaminergic neurons thus cause larvae to feed less and delays development (Bjorndal et al., 2014). GCN2 can also sense AA unbalance in the enterocytes, which alters the feeding behaviour of adults through the production of CNMAmide and signaling to neurons as described above (Kim et al., 2021). Moreover, bacterial infection activates GCN2, which promotes AMP production (Vasudevan et al., 2017) and inhibit epithelium renewal (Chakrabarti et al., 2012). In mice (Zhang et al., 2002) and in yeast (Zaborske et al., 2010), GCN2 is necessary for physiological adaptation to AA unbalance. However, this is not known in *Drosophila*. Moreover, it is not known whether GCN2 can be influenced by the microbiota. This will be discussed in the Chapter II: A symbiotic bacterium supports the growth of its host on an unbalanced diet through GCN2 activation in the intestine. *Drosophila* is thus a powerful model to understand the mechanisms controlling growth, and how they are regulated by nutrients. Moreover, the *Drosophila* model also allows control of the nutritional environment.

2) Drosophila and nutrition

In the wild, *Drosophila melanogaster* feeds and lays eggs on decaying fruits (Soto-Yéber et al., 2018). In the lab, optimized diets for *Drosophila* development are usually composed of agar, inactivated yeast, a sugar source and corn flour (Lesperance and Broderick, 2020). These diets are called oligidic diets, *i.e.* diets composed of complex nutrient sources (Piper, 2017). Many studies using oligidic diets have focused on the amount of yeast, which is the main source of proteins, lipids and vitamins. Decreasing the amount of yeast causes dietary restriction (DR), which differentially affects life history traits of *Drosophila*. DR has a non-linear effect on lifespan: as the quantity of nutrients decreases, lifespan increases until an optimum is reached; past this optimum, further decrease in nutrient abundance reduces lifespan (Partridge et al., 2005). DR also reduces the fecundity of female flies (Mirth et al., 2019) and lengthen the larval development (Robertson, 1963). Beyond the amount of yeast, the ratio of protein to carbohydrate (P:C) is a key parameter of *Drosophila* nutrition: lifespan is optimal at very low (1:16) P:C ratio, whereas the optimal fecundity is achieved at 1:4 P:C ratio (Simpson and Raubenheimer, 2009). Larval development is the shortest at intermediate (1:2) P:C ratio (Rodrigues et al., 2015).

Changing the quantity of yeast or carbohydrates in diets is the simplest way of manipulating *Drosophila*'s nutrition. However, there is an important limitation: decreasing the amount of yeast causes an indiscriminate decrease in all the components of yeast: AAs, lipids, vitamins and many other unidentified compounds that may be important for various aspects of *Drosophila*'s physiology. Holidic Diets (HDs) offer an opportunity to circumvent this limitation: they are synthetic media entirely composed of chemically pure nutrients. They thus allow to manipulate each nutrient individually. Moreover, they enable better comparisons of studies between laboratories because they are standardized (Lüersen et al., 2019). The first HD supporting the growth of *Drosophila* was developed in the late 1940s (Schultz et al., 1946), and further optimized in the 1950s (Hinton et al., 1951; Sang, 1956). A typical HD for *Drosophila* contains the 20 proteinogenic AAs, sucrose, B-vitamins, nucleotides, metals, minerals, choline, cholesterol, conservatives and agar (Piper et al., 2014). HDs sustains the full life cycle of *Drosophila* through several generations (Lee and Micchelli, 2013; Rapport et al., 1983), though development is longer than on yeast-based diet (Hinton et al., 1951). HDs have been used to test the importance of various nutrients on several life-history traits of *Drosophila* (Piper, 2017).

The use of HDs pinpointed the importance of single nutrients on lifespan. Removing the 10 essential AA (EAAs), B-vitamins, metals or cholesterol shortens flies' lifespan (Piper et al., 2014). Moreover, the HD composition in AA, rather than the total amount in AA, has an important impact on longevity. Decreasing the concentration of a single AA, Methionine, extends lifespan similarly to decreasing the P:C ratio on an oligidic diet (Troen et al., 2007). Lifespan increases when flies are fed a diet which AA composition is based on the AA composition of the fly's exome (Piper et al., 2017). Finally, addition of cholesterol partly rescues the detrimental effect of high P:C ratio on

longevity, presumably because females fed a high P:C diet lay more eggs, which consumes their stores of cholesterol and shortens their lifespan (Zanco et al., 2021). Sang and King tested the importance of each HD component for fecundity through single-omission experiments: they removed each component one by one and measured the consequence on the number of viable eggs per female. They observed that each EAAs, B-Vitamins (except for biotin) and some microelements are required for optimal fecundity (Sang and King, 1961). Like lifespan, fecundity is strongly impacted by AA composition: matching AA composition of the diet with AA composition of the fly's exome yields an optimum in fecundity (Piper et al., 2017).

Finally, HDs were extensively used to investigate the nutritional needs of growing *Drosophila* larvae. Through single-omission experiments, Hinton and colleagues (Hinton et al., 1951) and Sang (Sang, 1956) identified the nutrients that are essential to *Drosophila* larva's growth: the 10 essential AAs, several B-vitamins (biotin, thiamin, riboflavin, nicotinic acid, pantothenic acid, folic acid, pyridoxine), cholesterol, choline and several minerals and metals (K, P, Mg and Na). Larvae cannot synthesize these nutrients or, in the case of certain semi-essential AA such as Arginine (Arg), larvae can synthesize them at slow rate which does not support growth. Moreover, certain nutrients are not essential to larval growth but their absence lead to slower development: this is the case of certain non-essential AA (Cysteine, Glutamic Acid, Glycine) and nucleotides.

Importantly, nutritional requirements of *Drosophila* larvae were determined in a GF environment; therefore, it is not known to what extent symbiotic bacteria can fulfill these requirements. This point will be discussed in the Chapter I: *Drosophila*-associated bacteria differentially shape the nutritional requirements of their host during juvenile growth.

Besides nutrient omission, HD were used to study the importance of AA composition on development. Changing the concentration of each AA, while holding the total AA concentration the same, creates an unbalance in the limiting AAs. Piper and colleagues compared a HD which AA composition is based on the fly's exome (called FLY AA) to the historic HD which AA composition is based on the work from Hunt (called MM AA). They observed that at the same total AA amount, larval development is shorter on the FLY AA diet than on the MM AA diet. AA composition is thus crucial for larval development, with an AA-unbalanced diet causing a growth delay (Piper et al., 2017). This work was performed on conventionally-reared larvae, and it is not known whether or how their microbiota was affected by the HD. The influence of symbiotic bacteria on growth on an AA-unbalanced diet is thus unknown. It is discussed in the Chapter II: A symbiotic bacterium supports the growth of its host on an unbalanced diet through GCN2 activation in the intestine.

Objectives

The purpose of my thesis was to further unravel the mechanisms underlying the promotion of *Drosophila* larva's growth by symbiotic microbes. The model of study that I chose had to match several criteria:

Firstly, the phenotype of growth promotion depends widely on *Drosophila*'s nutrition. I thus used a holidic diet that allowed me to control finely *Drosophila*'s nutrition.

Secondly, I wanted to be able to perform genetic experiments in both the host and the microbes. *Drosophila* provides an immense genetic toolkit. As for the microbes, I focused on two bacterial species: *A. pomorum* and *L. plantarum* that both exhibit potent growth-promotion phenotypes (Shin et al., 2011; Storelli et al., 2011). Although the strain of *L. plantarum* that I used (Lp^{NC8}) was not isolated from a *Drosophila* but from grass silage (Axelsson et al., 2012), it exhibits the same growth-promoting phenotype as *Drosophila* isolates of the same species. Importantly, it has a high transformation efficiency and does not carry any plasmid, which makes it an ideal model for functional genetics (Matos et al., 2017).

Therefore, the model of study that I chose allowed me to manipulate the host's nutrition, the host's genetics and the microbes' genetics. I used it to focus on two questions:

First of all, I used a holidic diet (HD) to determine whether *Drosophila*'s symbionts could fulfill the nutritional requirements of growing larvae. Previous studies have investigated the nutritional requirements of GF *Drosophila* larvae, using a HD in a series of single-nutrient omissions to identify the nutrients that are essential to the growth of GF larvae. Here, we used genome-based metabolic network reconstruction and monitoring of microbial and larval growth on HD to identify which of these essential nutrients could be synthesized and provided to the host by the symbiotic bacteria *A. pomorum* and/or *L. plantarum*. We published this work in a research article that I am co-signing as first author. It is presented in Chapter I: *Drosophila*-associated bacteria differentially shape the nutritional requirements of their host during juvenile growth.

In a second part, I wondered whether my model of study could help identify mechanisms of growth promotion other than nutrient supply by the symbiotic bacteria. I thus generated a HD with AA unbalance due to limitation in Valine, because I knew from the first part that *L. plantarum* cannot synthesize and therefore provide Valine to the larva. Surprisingly, I found that *L. plantarum* is able to rescue the developmental delays due to limitation in Valine. This observation was an entry point to the second question of my thesis: how can a symbiotic bacterium rescue the growth delay of its host due to scarcity in an essential nutrient, without synthesizing the limiting nutrient? Through genetic experiments in both *Drosophila* and *L. plantarum*, we showed that rescue of limiting Valine by *L. plantarum* goes through stimulation of GCN2 in the larva's enterocytes by the bacterium, potentially via sensing of its r/tRNAs. Here in Chapter II, I report a draft manuscript that we are preparing for submission: A symbiotic

bacterium supports the growth of its host on an unbalanced diet through GCN2 activation in the intestine.

The main work of my thesis, which will be presented in the next parts, thus focus on the effect of mono-associations (with *L. plantarum* or *A. pomorum*) on the growth of the host. However, in nature animals are poly-associated with multiple microbes. The interactions of these microbes together may thus have important effects on the growth of the host as well. I participated to a study on the bi-association of *A. pomorum* and *L. plantarum*, and the effect of this bi-association on larval growth. This work is presented in Annex 1. Moreover, as discussed above, mutualism is bidirectional: the host benefits from the microbes, and the microbes benefit from the host. I participated to a study about how *L. plantarum* can itself benefit from the *Drosophila* larva. This work is presented in Annex 2. Finally, I wrote the review How commensal bacteria shape the physiology of *Drosophila melanogaster*. This work is presented in Annex 3.

References

- Adair, K.L., Wilson, M., Bost, A., and Douglas, A.E. (2018). Microbial community assembly in wild populations of the fruit fly *Drosophila melanogaster*. *The ISME Journal* 12, 959.
- Aggrawal, K., and Silverman, N. (2007). Peptidoglycan recognition in *Drosophila*. *Biochem Soc Trans* 35, 1496–1500.
- Agrawal, N., Delanoue, R., Mauri, A., Basco, D., Pasco, M., Thorens, B., and Léopold, P. (2016). The *Drosophila* TNF Eiger Is an Adipokine that Acts on Insulin-Producing Cells to Mediate Nutrient Response. *Cell Metabolism* 23, 675–684.
- Alves, G., Sallé, J., Chaudy, S., Dupas, S., and Manière, G. (2014). High-NaCl Perception in *Drosophila melanogaster*. *J. Neurosci.* 34, 10884–10891.
- Anukam, K., and Reid, G. (2007). Probiotics: 100 years (1907-2007) after Elie Metchnikoff's Observations. Undefined.
- Atarashi, K., Tanoue, T., Ando, M., Kamada, N., Nagano, Y., Narushima, S., Suda, W., Imaoka, A., Setoyama, H., Nagamori, T., et al. (2015). Th17 Cell Induction by Adhesion of Microbes to Intestinal Epithelial Cells. *Cell* 163, 367–380.
- Axelsson, L., Rud, I., Naterstad, K., Blom, H., Renckens, B., Boekhorst, J., Kleerebezem, M., van Hijum, S., and Siezen, R.J. (2012). Genome sequence of the naturally plasmid-free *Lactobacillus plantarum* strain NC8 (CCUG 61730). *J Bacteriol* 194, 2391–2392.
- Bar-On, Y.M., Phillips, R., and Milo, R. (2018). The biomass distribution on Earth. *PNAS* 115, 6506–6511.

Basset, A., Khush, R.S., Braun, A., Gardan, L., Boccard, F., Hoffmann, J.A., and Lemaitre, B. (2000). The phytopathogenic bacteria *Erwinia carotovora* infects *Drosophila* and activates an immune response. *Proc Natl Acad Sci U S A* *97*, 3376–3381.

Bercik, P., Denou, E., Collins, J., Jackson, W., Lu, J., Jury, J., Deng, Y., Blennerhassett, P., Macri, J., McCoy, K.D., et al. (2011). The Intestinal Microbiota Affect Central Levels of Brain-Derived Neurotrophic Factor and Behavior in Mice. *Gastroenterology* *141*, 599-609.e3.

Bermudez-Martin, P., Becker, J.A.J., Caramello, N., Fernandez, S.P., Costa-Campos, R., Canaguier, J., Barbosa, S., Martinez-Gili, L., Myridakis, A., Dumas, M.-E., et al. (2021). The microbial metabolite p-Cresol induces autistic-like behaviors in mice by remodeling the gut microbiota. *Microbiome* *9*, 157.

Bjordal, M., Arquier, N., Kniazeff, J., Pin, J.P., and Léopold, P. (2014). Sensing of Amino Acids in a Dopaminergic Circuitry Promotes Rejection of an Incomplete Diet in *Drosophila*. *Cell* *156*, 510–521.

Blanton, L.V., Charbonneau, M.R., Salih, T., Barratt, M.J., Venkatesh, S., Ilkaveya, O., Subramanian, S., Manary, M.J., Trehan, I., Jorgensen, J.M., et al. (2016a). Gut bacteria that prevent growth impairments transmitted by microbiota from malnourished children. *Science* *351*, aad3311.

Blanton, L.V., Barratt, M.J., Charbonneau, M.R., Ahmed, T., and Gordon, J.I. (2016b). Childhood undernutrition, the gut microbiota, and microbiota-directed therapeutics. *Science* *352*, 1533–1533.

Blum, J.E., Fischer, C.N., Miles, J., and Handelsman, J. (2013). Frequent replenishment sustains the beneficial microbiome of *Drosophila melanogaster*. *MBio* *4*, e00860-00813.

Borrelli, L., Aceto, S., Agnisola, C., De Paolo, S., Dipineto, L., Stilling, R.M., Dinan, T.G., Cryan, J.F., Menna, L.F., and Fioretti, A. (2016). Probiotic modulation of the microbiota-gut-brain axis and behaviour in zebrafish. *Sci Rep* *6*.

Bosch, P.S., Makhijani, K., Herboso, L., Gold, K.S., Baginsky, R., Woodcock, K.J., Alexander, B., Kukar, K., Corcoran, S., Jacobs, T., et al. (2019). Adult *Drosophila* Lack Hematopoiesis but Rely on a Blood Cell Reservoir at the Respiratory Epithelia to Relay Infection Signals to Surrounding Tissues. *Developmental Cell* *51*, 787-803.e5.

Bouskra, D., Brézillon, C., Bérard, M., Werts, C., Varona, R., Boneca, I.G., and Eberl, G. (2008). Lymphoid tissue genesis induced by commensals through NOD1 regulates intestinal homeostasis. *Nature* *456*, 507–510.

Braco, J.T., Gillespie, E.L., Alberto, G.E., Brenman, J.E., and Johnson, E.C. (2012). Energy-

Dependent Modulation of Glucagon-Like Signaling in *Drosophila* via the AMP-Activated Protein Kinase. *Genetics* 192, 457–466.

Brummel, T., Ching, A., Seroude, L., Simon, A.F., and Benzer, S. (2004). *Drosophila* lifespan enhancement by exogenous bacteria. *PNAS* 101, 12974–12979.

Buchon, N., Silverman, N., and Cherry, S. (2014). Immunity in *Drosophila melanogaster* — from microbial recognition to whole-organism physiology. *Nat Rev Immunol* 14, 796–810.

Caballero, S., Kim, S., Carter, R.A., Leiner, I.M., Sušac, B., Miller, L., Kim, G.J., Ling, L., and Pamer, E.G. (2017). Cooperating commensals restore colonization resistance to vancomycin-resistant *Enterococcus faecium*. *Cell Host Microbe* 21, 592-602.e4.

Cash, H.L., Whitham, C.V., Behrendt, C.L., and Hooper, L.V. (2006). Symbiotic Bacteria Direct Expression of an Intestinal Bactericidal Lectin. *Science* 313, 1126–1130.

Chakrabarti, S., Liehl, P., Buchon, N., and Lemaitre, B. (2012). Infection-Induced Host Translational Blockage Inhibits Immune Responses and Epithelial Renewal in the *Drosophila* Gut. *Cell Host & Microbe* 12, 60–70.

Chandler, J.A., and James, P.M. (2013). Discovery of Trypanosomatid Parasites in Globally Distributed *Drosophila* Species. *PLOS ONE* 8, e61937.

Charroux, B., Capo, F., Kurz, C.L., Peslier, S., Chaduli, D., Viallat-Lieutaud, A., and Royet, J. (2018). Cytosolic and Secreted Peptidoglycan-Degrading Enzymes in *Drosophila* Respectively Control Local and Systemic Immune Responses to Microbiota. *Cell Host Microbe* 23, 215-228.e4.

Chaston, J.M., Newell, P.D., and Douglas, A.E. (2014). Metagenome-wide association of microbial determinants of host phenotype in *Drosophila melanogaster*. *MBio* 5, e01631-01614.

Chaston, J.M., Dobson, A.J., Newell, P.D., and Douglas, A.E. (2016). Host Genetic Control of the Microbiota Mediates the *Drosophila* Nutritional Phenotype. *Appl Environ Microbiol* 82, 671–679.

Chen, K., Luan, X., Liu, Q., Wang, J., Chang, X., Snijders, A.M., Mao, J.-H., Secombe, J., Dan, Z., Chen, J.-H., et al. (2019). *Drosophila* Histone Demethylase KDM5 Regulates Social Behavior through Immune Control and Gut Microbiota Maintenance. *Cell Host & Microbe* 25, 537-552.e8.

Chevalier, G., Siopi, E., Guenin-Macé, L., Pascal, M., Laval, T., Rifflet, A., Boneca, I.G., Demangel, C., Colsch, B., Pruvost, A., et al. (2020). Effect of gut microbiota on depressive-like behaviors in mice is mediated by the endocannabinoid system. *Nat Commun* 11.

- Chng, W.-B.A., Sleiman, M.S.B., Schüpfer, F., and Lemaitre, B. (2014). Transforming growth factor β /activin signaling functions as a sugar-sensing feedback loop to regulate digestive enzyme expression. *Cell Rep* 9, 336–348.
- Clancy, D.J., Gems, D., Harshman, L.G., Oldham, S., Stocker, H., Hafen, E., Leivers, S.J., and Partridge, L. (2001). Extension of Life-Span by Loss of CHICO, a Drosophila Insulin Receptor Substrate Protein. *Science* 292, 104–106.
- Clark, M.E., Anderson, C.L., Cande, J., and Karr, T.L. (2005). Widespread prevalence of wolbachia in laboratory stocks and the implications for Drosophila research. *Genetics* 170, 1667–1675.
- Cohen, E., Sawyer, J.K., Peterson, N.G., Dow, J.A.T., and Fox, D.T. (2020). Physiology, Development, and Disease Modeling in the Drosophila Excretory System. *Genetics* 214, 235–264.
- Colombani, J., Raisin, S., Pantalacci, S., Radimerski, T., Montagne, J., and Léopold, P. (2003). A Nutrient Sensor Mechanism Controls Drosophila Growth. *Cell* 114, 739–749.
- Colombani, J., Bianchini, L., Layalle, S., Pondeville, E., Dauphin-Villemant, C., Antoniewski, C., Carré, C., Noselli, S., and Léopold, P. (2005). Antagonistic Actions of Ecdysone and Insulins Determine Final Size in Drosophila. *Science* 310, 667–670.
- Consuegra, J., Grenier, T., Baa-Puyoulet, P., Rahioui, I., Akherraz, H., Gervais, H., Parisot, N., Silva, P. da, Charles, H., Calevro, F., et al. (2020a). Drosophila-associated bacteria differentially shape the nutritional requirements of their host during juvenile growth. *PLOS Biology* 18, e3000681.
- Consuegra, J., Grenier, T., Akherraz, H., Rahioui, I., Gervais, H., da Silva, P., and Leulier, F. (2020b). Metabolic Cooperation among Commensal Bacteria Supports Drosophila Juvenile Growth under Nutritional Stress. *IScience* 23, 101232.
- Cremon, C., Barbaro, M.R., Ventura, M., and Barbara, G. (2018). Pre- and probiotic overview. *Current Opinion in Pharmacology* 43, 87–92.
- Davoodi, S., and Foley, E. (2019). Host-Microbe-Pathogen Interactions: A Review of *Vibrio cholerae* Pathogenesis in Drosophila. *Front Immunol* 10, 3128.
- Delaney, J.R., Stöven, S., Uvell, H., Anderson, K.V., Engström, Y., and Mlodzik, M. (2006). Cooperative control of Drosophila immune responses by the JNK and NF- κ B signaling pathways. *The EMBO Journal* 25, 3068–3077.
- Delanoue, R., Meschi, E., Agrawal, N., Mauri, A., Tsatskis, Y., McNeill, H., and Léopold, P. (2016). Drosophila insulin release is triggered by adipose Stunted ligand to brain Methuselah

receptor. *Science* 353, 1553–1556.

Delbare, S.Y.N., Ahmed-Braimah, Y.H., Wolfner, M.F., and Clark, A.G. (2020). Interactions between the microbiome and mating influence the female's transcriptional profile in *Drosophila melanogaster*. *Sci Rep* 10, 18168.

De Vadder, F., Kovatcheva-Datchary, P., Zitoun, C., Duchamp, A., Bäckhed, F., and Mithieux, G. (2016). Microbiota-Produced Succinate Improves Glucose Homeostasis via Intestinal Gluconeogenesis. *Cell Metabolism* 24, 151–157.

Dever, T.E., Feng, L., Wek, R.C., Cigan, A.M., Donahue, T.F., and Hinnebusch, A.G. (1992). Phosphorylation of initiation factor 2 α by protein kinase GCN2 mediates gene-specific translational control of GCN4 in yeast. *Cell* 68, 585–596.

Dick, G.J. (2019). The microbiomes of deep-sea hydrothermal vents: distributed globally, shaped locally. *Nat Rev Microbiol* 17, 271–283.

Dimidi, E., Christodoulides, S., Scott, S.M., and Whelan, K. (2017). Mechanisms of Action of Probiotics and the Gastrointestinal Microbiota on Gut Motility and Constipation. *Adv Nutr* 8, 484–494.

Dimijian, G.G. (2000). Evolving together: the biology of symbiosis, part 1. *Proc (Bayl Univ Med Cent)* 13, 217–226.

Dirksen, P., Marsh, S.A., Braker, I., Heitland, N., Wagner, S., Nakad, R., Mader, S., Petersen, C., Kowallik, V., Rosenstiel, P., et al. (2016). The native microbiome of the nematode *Caenorhabditis elegans*: gateway to a new host-microbiome model. *BMC Biol* 14.

Dobber, R., Hertogh-Huijbregts, A., Rozing, J., Bottomly, K., and Nagelkerken, L. (1992). The involvement of the intestinal microflora in the expansion of CD4⁺ T cells with a naive phenotype in the periphery. *Dev Immunol* 2, 141–150.

Dobson, A.J., Chaston, J.M., Newell, P.D., Donahue, L., Hermann, S.L., Sannino, D.R., Westmiller, S., Wong, A.C.-N., Clark, A.G., Lazzaro, B.P., et al. (2015). Host genetic determinants of microbiota-dependent nutrition revealed by genome-wide analysis of *Drosophila melanogaster*. *Nat Commun* 6, 6312.

Dong, J., Qiu, H., Garcia-Barrio, M., Anderson, J., and Hinnebusch, A.G. (2000). Uncharged tRNA Activates GCN2 by Displacing the Protein Kinase Moiety from a Bipartite tRNA-Binding Domain. *Molecular Cell* 6, 269–279.

Donnelly, N., Gorman, A.M., Gupta, S., and Samali, A. (2013). The eIF2 α kinases: their structures and functions. *Cell Mol Life Sci* 70, 3493–3511.

- Douglas, A.E. (2018a). The *Drosophila* model for microbiome research. *Lab Anim (NY)* 47, 157–164.
- Douglas, A.E. (2018b). Contradictory Results in Microbiome Science Exemplified by Recent *Drosophila* Research. *MBio* 9.
- Douglas, A.E. (2019). Simple animal models for microbiome research. *Nat Rev Microbiol* 17, 764–775.
- Duar, R.M., Lin, X.B., Zheng, J., Martino, M.E., Grenier, T., Pérez-Muñoz, M.E., Leulier, F., Gänzle, M., and Walter, J. (2017). Lifestyles in transition: evolution and natural history of the genus *Lactobacillus*. *FEMS Microbiol. Rev.* 41, S27–S48.
- Ducarmon, Q.R., Zwartink, R.D., Hornung, B.V.H., van Schaik, W., Young, V.B., and Kuijper, E.J. (2019). Gut Microbiota and Colonization Resistance against Bacterial Enteric Infection. *Microbiol Mol Biol Rev* 83.
- Elgart, M., Stern, S., Salton, O., Gnainsky, Y., Heifetz, Y., and Soen, Y. (2016). Impact of gut microbiota on the fly's germ line. *Nat Commun* 7, 11280.
- Erkosar, B., Storelli, G., Mitchell, M., Bozonnet, L., Bozonnet, N., and Leulier, F. (2015). Pathogen virulence impedes mutualist-mediated enhancement of host juvenile growth via inhibition of protein digestion. *Cell Host Microbe* 18, 445–455.
- Everard, A., Belzer, C., Geurts, L., Ouwerkerk, J.P., Druart, C., Bindels, L.B., Guiot, Y., Derrien, M., Muccioli, G.G., Delzenne, N.M., et al. (2013). Cross-talk between *Akkermansia muciniphila* and intestinal epithelium controls diet-induced obesity. *Proc Natl Acad Sci U S A* 110, 9066–9071.
- Falony, G., Joossens, M., Vieira-Silva, S., Wang, J., Darzi, Y., Faust, K., Kurilshikov, A., Bonder, M.J., Valles-Colomer, M., Vandeputte, D., et al. (2016). Population-level analysis of gut microbiome variation. *Science* 352, 560–564.
- Fassarella, M., Blaak, E.E., Penders, J., Nauta, A., Smidt, H., and Zoetendal, E.G. (2021). Gut microbiome stability and resilience: elucidating the response to perturbations in order to modulate gut health. *Gut* 70, 595–605.
- Fast, D., Duggal, A., and Foley, E. (2018). Monoassociation with *Lactobacillus plantarum* Disrupts Intestinal Homeostasis in Adult *Drosophila melanogaster*. *MBio* 9.
- Fischer, C.N., Trautman, E.P., Crawford, J.M., Stabb, E.V., Handelsman, J., and Broderick, N.A. (2017). Metabolite exchange between microbiome members produces compounds that influence *Drosophila* behavior. *ELife* 6, e18855.

Freeman, E.G., and Dahanukar, A. (2015). Molecular neurobiology of *Drosophila* taste. *Curr Opin Neurobiol* 34, 140–148.

Friedman, J.E. (2018). Developmental Programming of Obesity and Diabetes in Mouse, Monkey, and Man in 2018: Where Are We Headed? *Diabetes* 67, 2137–2151.

Funkhouser, L.J., and Bordenstein, S.R. (2013). Mom Knows Best: The Universality of Maternal Microbial Transmission. *PLOS Biology* 11, e1001631.

Gallo, M., Vento, J.M., Joncour, P., Quagliariello, A., Maritan, E., Beisel, C.L., and Martino, M.E. (2021). Beneficial *Lactiplantibacillus plantarum* promote *Drosophila* growth by down-regulating the expression of PGRP-SC1. *BioRxiv* 2021.07.16.452638.

Ganguly, A., Pang, L., Duong, V.-K., Lee, A., Schoniger, H., Varady, E., and Dahanukar, A. (2017). A molecular and cellular context-dependent role for *Ir76b* in detection of amino acid taste. *Cell Rep* 18, 737–750.

Gao, K., Mu, C., Farzi, A., and Zhu, W. (2020). Tryptophan Metabolism: A Link Between the Gut Microbiota and Brain. *Adv Nutr* 11, 709–723.

Garofalo, R.S. (2002). Genetic analysis of insulin signaling in *Drosophila*. *Trends Endocrinol Metab* 13, 156–162.

Gehrig, J.L., Venkatesh, S., Chang, H.-W., Hibberd, M.C., Kung, V.L., Cheng, J., Chen, R.Y., Subramanian, S., Cowardin, C.A., Meier, M.F., et al. (2019). Effects of microbiota-directed foods in gnotobiotic animals and undernourished children. *Science* 365.

Ghosh, A.C., and O'Connor, M.B. (2014). Systemic Activin signaling independently regulates sugar homeostasis, cellular metabolism, and pH balance in *Drosophila melanogaster*. *Proc Natl Acad Sci U S A* 111, 5729–5734.

Gilbert, J.A., Blaser, M.J., Caporaso, J.G., Jansson, J.K., Lynch, S.V., and Knight, R. (2018). Current understanding of the human microbiome. *Nat. Med.* 24, 392–400.

Gilbert, L.I., Rybczynski, R., and Warren, J.T. (2002). Control and biochemical nature of the ecdysteroidogenic pathway. *Annu Rev Entomol* 47, 883–916.

Gnainsky, Y., Zfanya, N., Elgart, M., Omri, E., Brandis, A., Mehlman, T., Itkin, M., Malitsky, S., Adamski, J., and Soen, Y. (2021). Systemic Regulation of Host Energy and Oogenesis by Microbiome-Derived Mitochondrial Coenzymes. *Cell Reports* 34, 108583.

Goberdhan, D.C.I., Wilson, C., and Harris, A.L. (2016). Amino Acid Sensing by mTORC1: Intracellular Transporters Mark the Spot. *Cell Metab* 23, 580–589.

Gobert, V., Gottar, M., Matskevich, A.A., Rutschmann, S., Royet, J., Belvin, M., Hoffmann, J.A., and Ferrandon, D. (2003). Dual activation of the *Drosophila* toll pathway by two pattern recognition receptors. *Science* *302*, 2126–2130.

Gould, A.L., Zhang, V., Lamberti, L., Jones, E.W., Obadia, B., Korasidis, N., Gavryushkin, A., Carlson, J.M., Beerenwinkel, N., and Ludington, W.B. (2018). Microbiome interactions shape host fitness. *Proc. Natl. Acad. Sci. U.S.A.* *115*, E11951–E11960.

Grallert, B., and Boye, E. (2007). The Gcn2 Kinase as a Cell Cycle Regulator. *Cell Cycle* *6*, 2768–2772.

Grenier, T., and Leulier, F. (2020). How commensal microbes shape the physiology of *Drosophila melanogaster*. *Curr Opin Insect Sci* *41*, 92–99.

Gusarov, I., Gautier, L., Smolentseva, O., Shamovsky, I., Eremina, S., Mironov, A., and Nudler, E. (2013). Bacterial nitric oxide extends the lifespan of *C. elegans*. *Cell* *152*, 818–830.

Harding, H.P., Zhang, Y., Zeng, H., Novoa, I., Lu, P.D., Calton, M., Sadri, N., Yun, C., Popko, B., Paules, R., et al. (2003). An Integrated Stress Response Regulates Amino Acid Metabolism and Resistance to Oxidative Stress. *Molecular Cell* *11*, 619–633.

Harding, H.P., Ordonez, A., Allen, F., Parts, L., Inglis, A.J., Williams, R.L., and Ron, D. (2019). The ribosomal P-stalk couples amino acid starvation to GCN2 activation in mammalian cells. *Elife* *8*.

Henriques, S.F., Dhakan, D.B., Serra, L., Francisco, A.P., Carvalho-Santos, Z., Baltazar, C., Elias, A.P., Anjos, M., Zhang, T., Maddocks, O.D.K., et al. (2020). Metabolic cross-feeding in imbalanced diets allows gut microbes to improve reproduction and alter host behaviour. *Nat Commun* *11*, 4236.

Hinton, T., Noyes, D.T., and Ellis, J. (1951). Amino acids and growth factors in a chemically defined medium for *Drosophila*. *Physiological Zoology* *24*, 335–353.

Hooper, L.V., Stappenbeck, T.S., Hong, C.V., and Gordon, J.I. (2003). Angiogenins: a new class of microbicidal proteins involved in innate immunity. *Nat Immunol* *4*, 269–273.

Hughenholz, F., and de Vos, W.M. (2018). Mouse models for human intestinal microbiota research: a critical evaluation. *Cell Mol Life Sci* *75*, 149–160.

Iatsenko, I., Boquete, J.-P., and Lemaitre, B. (2018). Microbiota-derived lactate activates production of Reactive Oxygen Species by the intestinal NADPH oxidase Nox and shortens *Drosophila* Lifespan. *Immunity* *49*, 929-942.e5.

- Ikeya, T., Galic, M., Belawat, P., Nairz, K., and Hafen, E. (2002). Nutrient-dependent expression of insulin-like peptides from neuroendocrine cells in the CNS contributes to growth regulation in *Drosophila*. *Curr Biol* *12*, 1293–1300.
- Imler, J.-L. (2014). Overview of *Drosophila* immunity: a historical perspective. *Dev Comp Immunol* *42*, 3–15.
- Inglis, A.J., Masson, G.R., Shao, S., Perisic, O., McLaughlin, S.H., Hegde, R.S., and Williams, R.L. (2019). Activation of GCN2 by the ribosomal P-stalk. *Proc Natl Acad Sci U S A* *116*, 4946–4954.
- Ishikawa, H., Tanaka, K., Maeda, Y., Aiba, Y., Hata, A., Tsuji, N.M., Koga, Y., and Matsumoto, T. (2008). Effect of intestinal microbiota on the induction of regulatory CD25+ CD4+ T cells. *Clin Exp Immunol* *153*, 127–135.
- Jia, Y., Jin, S., Hu, K., Geng, L., Han, C., Kang, R., Pang, Y., Ling, E., Tan, E.K., Pan, Y., et al. (2021). Gut microbiome modulates *Drosophila* aggression through octopamine signaling. *Nat Commun* *12*, 2698.
- Jiang, H., and Edgar, B.A. (2009). EGFR signaling regulates the proliferation of *Drosophila* adult midgut progenitors. *Development* *136*, 483–493.
- Joly, A., Leulier, F., and De Vadder, F. (2020). Microbial Modulation of the Development and Physiology of the Enteric Nervous System. *Trends Microbiol.*
- Jones, B.W., and Nishiguchi, M.K. (2004). Counterillumination in the Hawaiian bobtail squid, *Euprymna scolopes* Berry (Mollusca: Cephalopoda). *Marine Biology* *144*, 1151–1155.
- Jones, R.M., Luo, L., Ardita, C.S., Richardson, A.N., Kwon, Y.M., Mercante, J.W., Alam, A., Gates, C.L., Wu, H., Swanson, P.A., et al. (2013). Symbiotic lactobacilli stimulate gut epithelial proliferation via Nox-mediated generation of reactive oxygen species. *EMBO J.* *32*, 3017–3028.
- Jugder, B.-E., Kamareddine, L., and Watnick, P.I. (2021). Microbiota-derived acetate activates intestinal innate immunity via the Tip60 histone acetyltransferase complex. *Immunity* S1074-7613(21)00223-5.
- Jünger, M.A., Rintelen, F., Stocker, H., Wasserman, J.D., Végh, M., Radimerski, T., Greenberg, M.E., and Hafen, E. (2003). The *Drosophila* forkhead transcription factor FOXO mediates the reduction in cell number associated with reduced insulin signaling. *J. Biol.* *2*, 20.
- Kamareddine, L., Robins, W.P., Berkey, C.D., Mekalanos, J.J., and Watnick, P.I. (2018). The *Drosophila* Immune Deficiency Pathway Modulates Enteroendocrine Function and Host Metabolism. *Cell Metabolism*.

- Kang, D., and Douglas, A.E. (2020). Functional traits of the gut microbiome correlated with host lipid content in a natural population of *Drosophila melanogaster*. *Biol Lett* *16*, 20190803.
- Kannangara, J.R., Mirth, C.K., and Warr, C.G. (2021). Regulation of ecdysone production in *Drosophila* by neuropeptides and peptide hormones. *Open Biol* *11*, 200373.
- Keebaugh, E.S., Yamada, R., Obadia, B., Ludington, W.B., and Ja, W.W. (2018). Microbial quantity impacts *Drosophila* nutrition, development, and lifespan. *IScience* *4*, 247–259.
- Keebaugh, E.S., Yamada, R., and Ja, W.W. (2019). The Nutritional Environment Influences the Impact of Microbes on *Drosophila melanogaster* Life Span. *MBio* *10*.
- Kim, J., and Neufeld, T.P. (2015). Dietary sugar promotes systemic TOR activation in *Drosophila* through AKH-dependent selective secretion of Dilp3. *Nat Commun* *6*, 6846.
- Kim, M., and Lee, J.H. (2015). Identification of an AMPK phosphorylation site in *Drosophila* TSC2 (gigas) that regulate cell growth. *Int J Mol Sci* *16*, 7015–7026.
- Kim, B., Kanai, M.I., Oh, Y., Kyung, M., Kim, E.-K., Jang, I.-H., Lee, J.-H., Kim, S.-G., Suh, G.S.B., and Lee, W.-J. (2021). Response of the microbiome–gut–brain axis in *Drosophila* to amino acid deficit. *Nature* 1–5.
- Kim, E.-K., Lee, K.-A., Hyeon, D.Y., Kyung, M., Jun, K.-Y., Seo, S.H., Hwang, D., Kwon, Y., and Lee, W.-J. (2020). Bacterial Nucleoside Catabolism Controls Quorum Sensing and Commensal-to-Pathogen Transition in the *Drosophila* Gut. *Cell Host Microbe* *27*, 345–357.e6.
- Kim, S.G., Becattini, S., Moody, T.U., Shliaha, P.V., Littmann, E.R., Seok, R., Gjonbalaj, M., Eaton, V., Fontana, E., Amoretti, L., et al. (2019). Microbiota-derived lantibiotic restores resistance against vancomycin-resistant *Enterococcus*. *Nature* *572*, 665–669.
- Kleino, A., and Silverman, N. (2014). The *Drosophila* IMD pathway in the activation of the humoral immune response. *Dev Comp Immunol* *42*, 10.1016/j.dci.2013.05.014.
- Kleino, A., Myllymäki, H., Kallio, J., Vanha-aho, L.-M., Oksanen, K., Ulvila, J., Hultmark, D., Valanne, S., and Rämet, M. (2008). Pirk Is a Negative Regulator of the *Drosophila* Imd Pathway. *The Journal of Immunology* *180*, 5413–5422.
- Koropatnick, T.A., Engle, J.T., Apicella, M.A., Stabb, E.V., Goldman, W.E., and McFall-Ngai, M.J. (2004). Microbial factor-mediated development in a host-bacterial mutualism. *Science* *306*, 1186–1188.
- Koyama, T., and Mirth, C.K. (2016). Growth-Blocking Peptides As Nutrition-Sensitive Signals for Insulin Secretion and Body Size Regulation. *PLoS Biol* *14*.

- Koyama, T., Rodrigues, M.A., Athanasiadis, A., Shingleton, A.W., and Mirth, C.K. (2014). Nutritional control of body size through FoxO-Ultraspiracle mediated ecdysone biosynthesis. *ELife* 3, e03091.
- Krishnamoorthy, J., Mounir, Z., Raven, J., and Koromilas, A. (2008). The eIF2 α kinases inhibit vesicular stomatitis virus replication independently of eIF2 phosphorylation. *Cell Cycle* 7, 2346–2351.
- Lachance, M.-A., Gilbert, D.G., and Starmer, W.T. (1995). Yeast communities associated with *Drosophila* species and related flies in an eastern oak-pine forest: A comparison with western communities. *Journal of Industrial Microbiology* 14, 484–494.
- Laplante, M., and Sabatini, D.M. (2009). mTOR signaling at a glance. *J Cell Sci* 122, 3589–3594.
- Layalle, S., Arquier, N., and Léopold, P. (2008). The TOR Pathway Couples Nutrition and Developmental Timing in *Drosophila*. *Developmental Cell* 15, 568–577.
- Lee, W.-C., and Micchelli, C.A. (2013). Development and characterization of a chemically defined food for *Drosophila*. *PLOS ONE* 8, e67308.
- Lee, H.-Y., Lee, S.-H., Lee, J.-H., Lee, W.-J., and Min, K.-J. (2019). The role of commensal microbes in the lifespan of *Drosophila melanogaster*. *Aging (Albany NY)* 11, 4611–4640.
- Lee, K.-A., Kim, S.-H., Kim, E.-K., Ha, E.-M., You, H., Kim, B., Kim, M.-J., Kwon, Y., Ryu, J.-H., and Lee, W.-J. (2013). Bacterial-derived uracil as a modulator of mucosal immunity and gut-microbe homeostasis in *Drosophila*. *Cell* 153, 797–811.
- Lee, K.-A., Kim, B., Bhin, J., Kim, D.H., You, H., Kim, E.-K., Kim, S.-H., Ryu, J.-H., Hwang, D., and Lee, W.-J. (2015). Bacterial Uracil Modulates *Drosophila* DUOX-Dependent Gut Immunity via Hedgehog-Induced Signaling Endosomes. *Cell Host & Microbe* 17, 191–204.
- Leftwich, P.T., Clarke, N.V.E., Hutchings, M.I., and Chapman, T. (2017). Gut microbiomes and reproductive isolation in *Drosophila*. *PNAS* 114, 12767–12772.
- Leitão-Gonçalves, R., Carvalho-Santos, Z., Francisco, A.P., Fioreze, G.T., Anjos, M., Baltazar, C., Elias, A.P., Itskov, P.M., Piper, M.D.W., and Ribeiro, C. (2017). Commensal bacteria and essential amino acids control food choice behavior and reproduction. *PLOS Biology* 15, e2000862.
- Lemaitre, B., and Hoffmann, J. (2007). The Host Defense of *Drosophila melanogaster*. *Annu. Rev. Immunol.* 25, 697–743.

Lemaitre, B., Nicolas, E., Michaut, L., Reichhart, J.-M., and Hoffmann, J.A. (1996). The Dorsoventral Regulatory Gene Cassette *spätzle/Toll/cactus* Controls the Potent Antifungal Response in *Drosophila* Adults. *Cell* 86, 973–983.

Lesperance, D.N.A., and Broderick, N.A. (2020). Meta-analysis of Diets Used in *Drosophila* Microbiome Research and Introduction of the *Drosophila* Dietary Composition Calculator (DDCC). *G3 (Bethesda)* 10, 2207–2211.

Leulier, F., Parquet, C., Pili-Floury, S., Ryu, J.-H., Caroff, M., Lee, W.-J., Mengin-Lecreulx, D., and Lemaitre, B. (2003). The *Drosophila* immune system detects bacteria through specific peptidoglycan recognition. *Nat Immunol* 4, 478–484.

Leulier, F., MacNeil, L.T., Lee, W.-J., Rawls, J.F., Cani, P.D., Schwarzer, M., Zhao, L., and Simpson, S.J. (2017). Integrative Physiology: At the Crossroads of Nutrition, Microbiota, Animal Physiology, and Human Health. *Cell Metab* 25, 522–534.

Liu, L., Leonard, A.S., Motto, D.G., Feller, M.A., Price, M.P., Johnson, W.A., and Welsh, M.J. (2003). Contribution of *Drosophila* DEG/ENaC Genes to Salt Taste. *Neuron* 39, 133–146.

Liu, W., Zhang, K., Li, Y., Su, W., Hu, K., and Jin, S. (2017). Enterococci Mediate the Oviposition Preference of *Drosophila melanogaster* through Sucrose Catabolism. *Sci Rep* 7, 13420.

Lu, H.-L., and St Leger, R.J. (2016). Insect Immunity to Entomopathogenic Fungi. *Adv Genet* 94, 251–285.

Lüersen, K., Röder, T., and Rimbach, G. (2019). *Drosophila melanogaster* in nutrition research—the importance of standardizing experimental diets. *Genes Nutr* 14, 3.

Ma, D., and Leulier, F. (2018). The importance of being persistent: The first true resident gut symbiont in *Drosophila*. *PLOS Biology* 16, e2006945.

Ma, D., Bou-Sleiman, M., Joncour, P., Indelicato, C.-E., Frochoux, M., Braman, V., Litovchenko, M., Storelli, G., Deplancke, B., and Leulier, F. (2019). Commensal Gut Bacteria Buffer the Impact of Host Genetic Variants on *Drosophila* Developmental Traits under Nutritional Stress. *IScience* 19, 436–447.

Manière, G., Ziegler, A.B., Geillon, F., Featherstone, D.E., and Grosjean, Y. (2016). Direct Sensing of Nutrients via a LAT1-like Transporter in *Drosophila* Insulin-Producing Cells. *Cell Reports* 17, 137–148.

Mansfield, B.E., Dionne, M.S., Schneider, D.S., and Freitag, N.E. (2003). Exploration of

host-pathogen interactions using *Listeria monocytogenes* and *Drosophila melanogaster*. *Cell Microbiol* 5, 901–911.

Martino, M.E., Joncour, P., Leenay, R., Gervais, H., Shah, M., Hughes, S., Gillet, B., Beisel, C., and Leulier, F. (2018). Bacterial Adaptation to the Host's Diet Is a Key Evolutionary Force Shaping *Drosophila-Lactobacillus* Symbiosis. *Cell Host Microbe* 24, 109-119.e6.

Matos, R.C., Schwarzer, M., Gervais, H., Courtin, P., Joncour, P., Gillet, B., Ma, D., Bulteau, A.-L., Martino, M.E., Hughes, S., et al. (2017). D-Alanylation of teichoic acids contributes to *Lactobacillus plantarum*-mediated *Drosophila* growth during chronic undernutrition. *Nat Microbiol* 2, 1635–1647.

Mayer, E.A., Tillisch, K., and Gupta, A. (2015). Gut/brain axis and the microbiota. *J Clin Invest* 125, 926–938.

McBrayer, Z., Ono, H., Shimell, M., Parvy, J.-P., Beckstead, R.B., Warren, J.T., Thummel, C.S., Dauphin-Villemant, C., Gilbert, L.I., and O'Connor, M.B. (2007). Prothoracicotropic hormone regulates developmental timing and body size in *Drosophila*. *Dev Cell* 13, 857–871.

McMullen, J.G., Peters-Schulze, G., Cai, J., Patterson, A.D., and Douglas, A.E. (2020). How gut microbiome interactions affect nutritional traits of *Drosophila melanogaster*. *J Exp Biol* 223, jeb227843.

Melancon, E., De La Torre Canny, S.G., Sichel, S., Kelly, M., Wiles, T.J., Rawls, J.F., Eisen, J.S., and Guillemin, K. (2017). Best practices for germ-free derivation and gnotobiotic zebrafish husbandry. *Methods Cell Biol* 138, 61–100.

Meng, X., Khanuja, B.S., and Ip, Y.T. (1999). Toll receptor-mediated *Drosophila* immune response requires Dif, an NF- κ B factor. *Genes Dev.* 13, 792–797.

Milani, C., Duranti, S., Bottacini, F., Casey, E., Turrone, F., Mahony, J., Belzer, C., Delgado Palacio, S., Arboleya Montes, S., Mancabelli, L., et al. (2017). The First Microbial Colonizers of the Human Gut: Composition, Activities, and Health Implications of the Infant Gut Microbiota. *Microbiol Mol Biol Rev* 81.

Min, K.-J., and Tatar, M. (2018). Unraveling the Molecular Mechanism of Immunosenescence in *Drosophila*. *Int J Mol Sci* 19.

Miron, M., Lasko, P., and Sonenberg, N. (2003). Signaling from Akt to FRAP/TOR targets both 4E-BP and S6K in *Drosophila melanogaster*. *Mol Cell Biol* 23, 9117–9126.

Mirth, C.K., Nogueira Alves, A., and Piper, M.D. (2019). Turning food into eggs: insights from nutritional biology and developmental physiology of *Drosophila*. *Current Opinion in Insect Science* 31, 49–57.

Mishra, D., Miyamoto, T., Rezenom, Y.H., Broussard, A., Yavuz, A., Slone, J., Russell, D.H., and Amrein, H. (2013). The Molecular Basis of Sugar Sensing in *Drosophila* Larvae. *Current Biology* 23, 1466–1471.

Mishra, D., Thorne, N., Miyamoto, C., Jagge, C., and Amrein, H. (2018). The taste of ribonucleosides: novel macronutrients essential for larval growth are sensed by *Drosophila* gustatory receptor proteins. *PLOS Biology* 16, e2005570.

Mizoguchi, A. (2012). Animal Models of Inflammatory Bowel Disease. In *Progress in Molecular Biology and Translational Science*, P.M. Conn, ed. (Academic Press), pp. 263–320.

Moeller, M.E., Nagy, S., Gerlach, S.U., Soegaard, K.C., Danielsen, E.T., Texada, M.J., and Rewitz, K.F. (2017). Warts Signaling Controls Organ and Body Growth through Regulation of Ecdysone. *Current Biology* 27, 1652-1659.e4.

Moriano-Gutierrez, S., Bongrand, C., Essock-Burns, T., Wu, L., McFall-Ngai, M.J., and Ruby, E.G. (2020). The noncoding small RNA SsrA is released by *Vibrio fischeri* and modulates critical host responses. *PLOS Biology* 18, e3000934.

Morimoto, J., Simpson, S.J., and Ponton, F. (2017). Direct and trans-generational effects of male and female gut microbiota in *Drosophila melanogaster*. *Biol Lett* 13, 20160966.

Mouse Genome Sequencing Consortium, Waterston, R.H., Lindblad-Toh, K., Birney, E., Rogers, J., Abril, J.F., Agarwal, P., Agarwala, R., Ainscough, R., Alexandersson, M., et al. (2002). Initial sequencing and comparative analysis of the mouse genome. *Nature* 420, 520–562.

Munyaka, P.M., Khafipour, E., and Ghia, J.-E. (2014). External Influence of Early Childhood Establishment of Gut Microbiota and Subsequent Health Implications. *Front Pediatr* 2.

Mussabekova, A., Daeffler, L., and Imler, J.-L. (2017). Innate and intrinsic antiviral immunity in *Drosophila*. *Cell Mol Life Sci* 74, 2039–2054.

Needham, A.J., Kibart, M., Crossley, H., Ingham, P.W., and Foster, S.J. (2004). *Drosophila melanogaster* as a model host for *Staphylococcus aureus* infection. *Microbiology (Reading)* 150, 2347–2355.

Newell, P.D., and Douglas, A.E. (2014). Interspecies interactions determine the impact of the gut microbiota on nutrient allocation in *Drosophila melanogaster*. *Appl. Environ. Microbiol.* 80, 788–796.

Newton, I.L.G., and Rice, D.W. (2020). The Jekyll and Hyde Symbiont: Could *Wolbachia* Be a Nutritional Mutualist? *J Bacteriol* 202.

- Neyen, C., Bretscher, A.J., Binggeli, O., and Lemaitre, B. (2014). Methods to study *Drosophila* immunity. *Methods* 68, 116–128.
- Nishida, A.H., and Ochman, H. (2018). Rates of Gut Microbiome Divergence in Mammals. *Mol Ecol* 27, 1884–1897.
- van Nood, E., Vriese, A., Nieuwdorp, M., Fuentes, S., Zoetendal, E.G., de Vos, W.M., Visser, C.E., Kuijper, E.J., Bartelsman, J.F.W.M., Tijssen, J.G.P., et al. (2013). Duodenal Infusion of Donor Feces for Recurrent *Clostridium difficile*.
- Obadia, B., Güvener, Z.T., Zhang, V., Ceja-Navarro, J.A., Brodie, E.L., Ja, W.W., and Ludington, W.B. (2017). Probabilistic Invasion Underlies Natural Gut Microbiome Stability. *Curr. Biol.* 27, 1999-2006.e8.
- Obadia, B., Keebaugh, E.S., Yamada, R., Ludington, W.B., and Ja, W.W. (2018). Diet influences host–microbiota associations in *Drosophila*. *PNAS* 115, E4547–E4548.
- Obata, F., Fons, C.O., and Gould, A.P. (2018). Early-life exposure to low-dose oxidants can increase longevity via microbiome remodelling in *Drosophila*. *Nat Commun* 9, 975.
- Okamoto, N., Yamanaka, N., Yagi, Y., Nishida, Y., Kataoka, H., O’Connor, M.B., and Mizoguchi, A. (2009). A fat body-derived IGF-like peptide regulates postfeeding growth in *Drosophila*. *Dev Cell* 17, 885–891.
- Pais, I.S., Valente, R.S., Sporniak, M., and Teixeira, L. (2018). *Drosophila melanogaster* establishes a species-specific mutualistic interaction with stable gut-colonizing bacteria. *PLoS Biol* 16.
- Paredes, J.C., Welchman, D.P., Poidevin, M., and Lemaitre, B. (2011). Negative regulation by amidase PGRPs shapes the *Drosophila* antibacterial response and protects the fly from innocuous infection. *Immunity* 35, 770–779.
- Partridge, L., Piper, M.D.W., and Mair, W. (2005). Dietary restriction in *Drosophila*. *Mechanisms of Ageing and Development* 126, 938–950.
- Peterson, J.W. (1996). Bacterial Pathogenesis. In *Medical Microbiology*, S. Baron, ed. (Galveston (TX): University of Texas Medical Branch at Galveston), p.
- Petryk, A., Warren, J.T., Marqués, G., Jarcho, M.P., Gilbert, L.I., Kahler, J., Parvy, J.-P., Li, Y., Dauphin-Villemant, C., and O’Connor, M.B. (2003). Shade is the *Drosophila* P450 enzyme that mediates the hydroxylation of ecdysone to the steroid insect molting hormone 20-hydroxyecdysone. *Proc Natl Acad Sci U S A* 100, 13773–13778.

- Piper, M.D. (2017). Using artificial diets to understand the nutritional physiology of *Drosophila melanogaster*. *Curr Opin Insect Sci* 23, 104–111.
- Piper, M.D., Blanc, E., Leitão-Gonçalves, R., Yang, M., He, X., Linford, N.J., Hoddinott, M.P., Hopfen, C., Soultoukis, G.A., Niemeyer, C., et al. (2014). A holidic medium for *Drosophila melanogaster*. *Nat Methods* 11.
- Piper, M.D.W., Soultoukis, G.A., Blanc, E., Mesaros, A., Herbert, S.L., Juricic, P., He, X., Atanassov, I., Salmonowicz, H., Yang, M., et al. (2017). Matching dietary amino acid balance to the *in silico*-translated exome optimizes growth and reproduction without cost to lifespan. *Cell Metabolism* 25, 610–621.
- Pleasants, J.R. (1959). Rearing Germfree Cesarean-Born Rats, Mice, and Rabbits Through Weaning*. *Annals of the New York Academy of Sciences* 78, 116–126.
- Plovier, H., Everard, A., Druart, C., Depommier, C., Van Hul, M., Geurts, L., Chilloux, J., Ottman, N., Duparc, T., Lichtenstein, L., et al. (2017). A purified membrane protein from *Akkermansia muciniphila* or the pasteurized bacterium improves metabolism in obese and diabetic mice. *Nat Med* 23, 107–113.
- Podschun, R., and Ullmann, U. (1998). *Klebsiella* spp. as Nosocomial Pathogens: Epidemiology, Taxonomy, Typing Methods, and Pathogenicity Factors. *Clin Microbiol Rev* 11, 589–603.
- Pryor, R., Norvaisas, P., Marinos, G., Best, L., Thingholm, L.B., Quintaneiro, L.M., De Haes, W., Esser, D., Waschina, S., Lujan, C., et al. (2019). Host-Microbe-Drug-Nutrient Screen Identifies Bacterial Effectors of Metformin Therapy. *Cell* 178, 1299-1312.e29.
- Qiao, H., Keesey, I.W., Hansson, B.S., and Knaden, M. (2019). Gut microbiota affects development and olfactory behavior in *Drosophila melanogaster*. *J. Exp. Biol.* 222.
- Rajan, A., and Perrimon, N. (2012). *Drosophila* cytokine unpaired 2 regulates physiological homeostasis by remotely controlling insulin secretion. *Cell* 151, 123–137.
- Rapport, E.W., Stanley-Samuels, D., and Dadd, R.H. (1983). Ten generations of *Drosophila melanogaster* reared axenically on a fatty acid-free holidic diet. *Archives of Insect Biochemistry and Physiology* 1, 243–250.
- Redhai, S., Pilgrim, C., Gaspar, P., Giesen, L. van, Lopes, T., Riabinina, O., Grenier, T., Milona, A., Chanana, B., Swadling, J.B., et al. (2020). An intestinal zinc sensor regulates food intake and developmental growth. *Nature* 580, 263–268.
- Reedy, A.R., Luo, L., Neish, A.S., and Jones, R.M. (2019). Commensal microbiota-induced redox signaling activates proliferative signals in the intestinal stem cell microenvironment.

Development 146.

Ren, C., Webster, P., Finkel, S.E., and Tower, J. (2007). Increased internal and external bacterial load during *Drosophila* aging without life-span trade-off. *Cell Metab.* 6, 144–152.

Reyniers, J.A. (1946). Rearing germfree albino rats. *Lobund Reports* 1, 1.

Richards, G. (1981). The radioimmune assay of ecdysteroid titres in *Drosophila melanogaster*. *Mol Cell Endocrinol* 21, 181–197.

Ridaura, V.K., Faith, J.J., Rey, F.E., Cheng, J., Duncan, A.E., Kau, A.L., Griffin, N.W., Lombard, V., Henrissat, B., Bain, J.R., et al. (2013). Gut microbiota from twins discordant for obesity modulate metabolism in mice. *Science* 341, 1241214.

Ridley, E.V., Wong, A.C.-N., Westmiller, S., and Douglas, A.E. (2012). Impact of the Resident Microbiota on the Nutritional Phenotype of *Drosophila melanogaster*. *PLOS ONE* 7, e36765.

Ridley, E.V., Wong, A.C.N., and Douglas, A.E. (2013). Microbe-Dependent and Nonspecific Effects of Procedures To Eliminate the Resident Microbiota from *Drosophila melanogaster*. *Applied and Environmental Microbiology* 79, 3209–3214.

Robertson, F.W. (1963). The ecological genetics of growth in *Drosophila* 6. The genetic correlation between the duration of the larval period and body size in relation to larval diet. *Genetics Research* 4, 74–92.

Rodenfels, J., Lavrynenko, O., Ayciriex, S., Sampaio, J.L., Carvalho, M., Shevchenko, A., and Eaton, S. (2014). Production of systemically circulating Hedgehog by the intestine couples nutrition to growth and development. *Genes Dev* 28, 2636–2651.

Rodrigues, M.A., Martins, N.E., Balancé, L.F., Broom, L.N., Dias, A.J.S., Fernandes, A.S.D., Rodrigues, F., Sucena, É., and Mirth, C.K. (2015). *Drosophila melanogaster* larvae make nutritional choices that minimize developmental time. *Journal of Insect Physiology* 81, 69–80.

Rolfes, R.J., and Hinnebusch, A.G. (1993). Translation of the yeast transcriptional activator GCN4 is stimulated by purine limitation: implications for activation of the protein kinase GCN2. *Mol Cell Biol* 13, 5099–5111.

Rolig, A.S., Parthasarathy, R., Burns, A.R., Bohannon, B.J., and Guillemin, K. (2015). Individual members of the microbiota disproportionately modulate host innate immune responses. *Cell Host Microbe* 18, 613–620.

Romano, P.R., Garcia-Barrio, M.T., Zhang, X., Wang, Q., Taylor, D.R., Zhang, F., Herring, C., Mathews, M.B., Qin, J., and Hinnebusch, A.G. (1998). Autophosphorylation in the activation loop is required for full kinase activity in vivo of human and yeast eukaryotic

- initiation factor 2alpha kinases PKR and GCN2. *Mol Cell Biol* 18, 2282–2297.
- Rothschild, L.J., and Mancinelli, R.L. (2001). Life in extreme environments. *Nature* 409, 1092–1101.
- Ryu, J.-H., Kim, S.-H., Lee, H.-Y., Bai, J.Y., Nam, Y.-D., Bae, J.-W., Lee, D.G., Shin, S.C., Ha, E.-M., and Lee, W.-J. (2008). Innate immune homeostasis by the homeobox gene *Caudal* and commensal-gut mutualism in *Drosophila*. *Science* 319, 777–782.
- Sakaguchi, E. (2003). Digestive strategies of small hindgut fermenters. *Animal Science Journal* 74, 327–337.
- Sang, J.H. (1956). The quantitative nutritional requirements of *Drosophila melanogaster*. *Journal of Experimental Biology* 33, 45–72.
- Sang, J.H., and King, R.C. (1961). Nutritional requirements of axenically cultured *Drosophila melanogaster* adults. *Journal of Experimental Biology* 38, 793–809.
- Sano, H., Nakamura, A., Texada, M.J., Truman, J.W., Ishimoto, H., Kamikouchi, A., Nibu, Y., Kume, K., Ida, T., and Kojima, M. (2015). The Nutrient-Responsive Hormone CCHamide-2 Controls Growth by Regulating Insulin-like Peptides in the Brain of *Drosophila melanogaster*. *PLoS Genet* 11, e1005209.
- Schnorr, S.L., Candela, M., Rampelli, S., Centanni, M., Consolandi, C., Basaglia, G., Turroni, S., Biagi, E., Peano, C., Severgnini, M., et al. (2014). Gut microbiome of the Hadza hunter-gatherers. *Nat Commun* 5, 3654.
- Schretter, C.E., Vielmetter, J., Bartos, I., Marka, Z., Marka, S., Argade, S., and Mazmanian, S.K. (2018). A gut microbial factor modulates locomotor behaviour in *Drosophila*. *Nature* 563, 402.
- Schultz, J., St Lawrence, P., and Newmeyer, D. (1946). A chemically defined medium for the growth of *Drosophila melanogaster*. *Anat. Rec.* 96, 540.
- Schwarzer, M., Makki, K., Storelli, G., Machuca-Gayet, I., Srutkova, D., Hermanova, P., Martino, M.E., Balmand, S., Hudcovic, T., Heddi, A., et al. (2016). *Lactobacillus plantarum* strain maintains growth of infant mice during chronic undernutrition. *Science* 351, 854–857.
- Sczesnak, A., Segata, N., Qin, X., Gevers, D., Petrosino, J.F., Huttenhower, C., Littman, D.R., and Ivanov, I.I. (2011). The Genome of Th17 Cell-Inducing Segmented Filamentous Bacteria Reveals Extensive Auxotrophy and Adaptations to the Intestinal Environment. *Cell Host & Microbe* 10, 260–272.
- Sears, C.L. (2005). A dynamic partnership: Celebrating our gut flora. *Anaerobe* 11, 247–251.

Selkrig, J., Mohammad, F., Ng, S.H., Chua, J.Y., Tumkaya, T., Ho, J., Chiang, Y.N., Rieger, D., Pettersson, S., Helfrich-Förster, C., et al. (2018). The *Drosophila* microbiome has a limited influence on sleep, activity, and courtship behaviors. *Sci Rep* 8.

Semova, I., Carten, J.D., Stombaugh, J., Mackey, L.C., Knight, R., Farber, S.A., and Rawls, J.F. (2012). Microbiota regulate intestinal absorption and metabolism of fatty acids in the zebrafish. *Cell Host & Microbe* 12, 277–288.

Sender, R., Fuchs, S., and Milo, R. (2016). Revised Estimates for the Number of Human and Bacteria Cells in the Body. *PLoS Biol* 14.

Sharon, G., Segal, D., Ringo, J.M., Hefetz, A., Zilber-Rosenberg, I., and Rosenberg, E. (2010). Commensal bacteria play a role in mating preference of *Drosophila melanogaster*. *PNAS* 107, 20051–20056.

Shen, P., Yue, Y., and Park, Y. (2018). A living model for obesity and aging research: *Caenorhabditis elegans*. *Crit Rev Food Sci Nutr* 58, 741–754.

Shimada-Niwa, Y., and Niwa, R. (2014). Serotonergic neurons respond to nutrients and regulate the timing of steroid hormone biosynthesis in *Drosophila*. *Nat Commun* 5, 5778.

Shin, S.C., Kim, S.-H., You, H., Kim, B., Kim, A.C., Lee, K.-A., Yoon, J.-H., Ryu, J.-H., and Lee, W.-J. (2011). *Drosophila* microbiome modulates host developmental and metabolic homeostasis via insulin signaling. *Science* 334, 670–674.

Simpson, S.J., and Raubenheimer, D. (2009). Macronutrient balance and lifespan. *Aging (Albany NY)* 1, 875–880.

Siva-Jothy, J.A., Prakash, A., Vasanthakrishnan, R.B., Monteith, K.M., and Vale, P.F. (2018). Oral Bacterial Infection and Shedding in *Drosophila melanogaster*. *J Vis Exp* 57676.

Søndergaard, L. (1993). Homology between the mammalian liver and the *Drosophila* fat body. *Trends Genet* 9, 193.

Sood, C., Doyle, S.E., and Siegrist, S.E. (2021). Steroid hormones, dietary nutrients, and temporal progression of neurogenesis. *Current Opinion in Insect Science* 43, 70–77.

Soto-Yéber, L., Soto-Ortiz, J., Godoy, P., and Godoy-Herrera, R. (2018). The behavior of adult *Drosophila* in the wild. *PLoS One* 13, e0209917.

Staubach, F., Baines, J.F., Künzel, S., Bik, E.M., and Petrov, D.A. (2013). Host Species and Environmental Effects on Bacterial Communities Associated with *Drosophila* in the Laboratory and in the Natural Environment. *PLOS ONE* 8, e70749.

- Stewart, C.P., Iannotti, L., Dewey, K.G., Michaelsen, K.F., and Onyango, A.W. (2013). Contextualising complementary feeding in a broader framework for stunting prevention. *Maternal & Child Nutrition* 9, 27–45.
- Storelli, G. (2015). Caractérisation de l'interaction mutualiste liant *Drosophila melanogaster* à son symbionte *Lactobacillus plantarum*. These de doctorat. Lyon, École normale supérieure.
- Storelli, G., Defaye, A., Erkosar, B., Hols, P., Royet, J., and Leulier, F. (2011). *Lactobacillus plantarum* promotes *Drosophila* systemic growth by modulating hormonal signals through TOR-dependent nutrient sensing. *Cell Metab.* 14, 403–414.
- Storelli, G., Strigini, M., Grenier, T., Bozonnet, L., Schwarzer, M., Daniel, C., Matos, R., and Leulier, F. (2018). *Drosophila* Perpetuates Nutritional Mutualism by Promoting the Fitness of Its Intestinal Symbiont *Lactobacillus plantarum*. *Cell Metab.* 27, 362-377.e8.
- Stressmann, F.A., Bernal-Bayard, J., Perez-Pascual, D., Audrain, B., Rendueles, O., Briolat, V., Bruchmann, S., Volant, S., Ghozlane, A., Häussler, S., et al. (2021). Mining zebrafish microbiota reveals key community-level resistance against fish pathogen infection. *ISME J* 15, 702–719.
- Subramanian, S., Huq, S., Yatsunenkov, T., Haque, R., Mahfuz, M., Alam, M.A., Benezra, A., DeStefano, J., Meier, M.F., Muegge, B.D., et al. (2014). Persistent gut microbiota immaturity in malnourished Bangladeshi children. *Nature* 510, 417–421.
- Tafesh-Edwards, G., and Eleftherianos, I. (2020). JNK signaling in *Drosophila* immunity and homeostasis. *Immunology Letters* 226, 7–11.
- Tattoli, I., Sorbara, M.T., Vuckovic, D., Ling, A., Soares, F., Carneiro, L.A.M., Yang, C., Emili, A., Philpott, D.J., and Girardin, S.E. (2012). Amino Acid Starvation Induced by Invasive Bacterial Pathogens Triggers an Innate Host Defense Program. *Cell Host & Microbe* 11, 563–575.
- Téfit, M.A., and Leulier, F. (2017). *Lactobacillus plantarum* favors the early emergence of fit and fertile adult *Drosophila* upon chronic undernutrition. *J Exp Biol* 220, 900–907.
- Téfit, M.A., Gillet, B., Joncour, P., Hughes, S., and Leulier, F. (2018). Stable association of a *Drosophila*-derived microbiota with its animal partner and the nutritional environment throughout a fly population's life cycle. *Journal of Insect Physiology* 106, 2–12.
- Tennessen, J.M., and Thummel, C.S. (2011). Coordinating Growth and Review Maturation — Insights from *Drosophila*. *Curr Biol* 21, R750–R757.
- Texada, M.J., Jørgensen, A.F., Christensen, C.F., Koyama, T., Malita, A., Smith, D.K., Marple, D.F.M., Danielsen, E.T., Petersen, S.K., Hansen, J.L., et al. (2019). A fat-tissue

sensor couples growth to oxygen availability by remotely controlling insulin secretion. *Nat Commun* 10, 1955.

Troen, A.M., French, E.E., Roberts, J.F., Selhub, J., Ordovas, J.M., Parnell, L.D., and Lai, C.-Q. (2007). Lifespan modification by glucose and methionine in *Drosophila melanogaster* fed a chemically defined diet. *Age (Dordr)* 29, 29–39.

Turnbaugh, P.J., Hamady, M., Yatsunencko, T., Cantarel, B.L., Duncan, A., Ley, R.E., Sogin, M.L., Jones, W.J., Roe, B.A., Affourtit, J.P., et al. (2009). A core gut microbiome in obese and lean twins. *Nature* 457, 480–484.

Uma, G., Babu, M.M., Prakash, V.S.G., Nisha, S.J., and Citarasu, T. (2020). Nature and bioprospecting of haloalkaliphilics: a review. *World J Microbiol Biotechnol* 36, 66.

Vasudevan, D., Clark, N.K., Sam, J., Cotham, V.C., Ueberheide, B., Marr, M.T., and Ryoo, H.D. (2017). The GCN2-ATF4 signaling pathway induces 4E-BP to bias translation and boost antimicrobial peptide synthesis in response to bacterial infection. *Cell Reports* 21, 2039–2047.

Ventura, I.M., Martins, A.B., Lyra, M.L., Andrade, C.A.C., Carvalho, K.A., and Klaczko, L.B. (2012). Spiroplasma in *Drosophila melanogaster* populations: prevalence, male-killing, molecular identification, and no association with Wolbachia. *Microb Ecol* 64, 794–801.

Venu, I., Durisko, Z., Xu, J., and Dukas, R. (2014). Social attraction mediated by fruit flies' microbiome. *Journal of Experimental Biology* 217, 1346–1352.

Vodovar, N., Vinals, M., Liehl, P., Basset, A., Degrouard, J., Spellman, P., Boccard, F., and Lemaitre, B. (2005). *Drosophila* host defense after oral infection by an entomopathogenic *Pseudomonas* species. *Proc Natl Acad Sci U S A* 102, 11414–11419.

Warren, J.T., Yerushalmi, Y., Shimell, M.J., O'Connor, M.B., Restifo, L.L., and Gilbert, L.I. (2006). Discrete pulses of molting hormone, 20-hydroxyecdysone, during late larval development of *Drosophila melanogaster*: Correlations with changes in gene activity. *Developmental Dynamics* 235, 315–326.

Wek, R.C., Jackson, B.M., and Hinnebusch, A.G. (1989). Juxtaposition of domains homologous to protein kinases and histidyl-tRNA synthetases in GCN2 protein suggests a mechanism for coupling GCN4 expression to amino acid availability. *Proc Natl Acad Sci U S A* 86, 4579–4583.

Wong, A.C.-N., Dobson, A.J., and Douglas, A.E. (2014). Gut microbiota dictates the metabolic response of *Drosophila* to diet. *J. Exp. Biol.* 217, 1894–1901.

Wong, A.C.-N., Luo, Y., Jing, X., Franzenburg, S., Bost, A., and Douglas, A.E. (2015). The Host as the Driver of the Microbiota in the Gut and External Environment of *Drosophila melanogaster*. *Appl Environ Microbiol* 81, 6232–6240.

- Wong, A.C.-N., Wang, Q.-P., Morimoto, J., Senior, A.M., Lihoreau, M., Neely, G.G., Simpson, S.J., and Ponton, F. (2017). Gut microbiota modifies olfactory-guided microbial preferences and foraging decisions in *Drosophila*. *Current Biology* 27, 2397-2404.e4.
- Wu, W.-L., Adame, M.D., Liou, C.-W., Barlow, J.T., Lai, T.-T., Sharon, G., Schretter, C.E., Needham, B.D., Wang, M.I., Tang, W., et al. (2021). Microbiota regulate social behaviour via stress response neurons in the brain. *Nature* 1–6.
- Xiao, L., Feng, Q., Liang, S., Sonne, S.B., Xia, Z., Qiu, X., Li, X., Long, H., Zhang, J., Zhang, D., et al. (2015). A catalog of the mouse gut metagenome. *Nat Biotechnol* 33, 1103–1108.
- Yamada, R., Deshpande, S.A., Bruce, K.D., Mak, E.M., and Ja, W.W. (2015). Microbes promote amino acid harvest to rescue undernutrition in *Drosophila*. *Cell Rep*.
- Yang, R., Wek, S.A., and Wek, R.C. (2000). Glucose limitation induces GCN4 translation by activation of Gcn2 protein kinase. *Mol Cell Biol* 20, 2706–2717.
- Yatsunenکو, T., Rey, F.E., Manary, M.J., Trehan, I., Dominguez-Bello, M.G., Contreras, M., Magris, M., Hidalgo, G., Baldassano, R.N., Anokhin, A.P., et al. (2012). Human gut microbiome viewed across age and geography. *Nature* 486, 222–227.
- Zaborske, J.M., Wu, X., Wek, R.C., and Pan, T. (2010). Selective control of amino acid metabolism by the GCN2 eIF2 kinase pathway in *Saccharomyces cerevisiae*. *BMC Biochem* 11, 29.
- Zanco, B., Mirth, C.K., Sgrò, C.M., and Piper, M.D. (2021). A dietary sterol trade-off determines lifespan responses to dietary restriction in *Drosophila melanogaster* females. *Elife* 10.
- Zhai, Z., Boquete, J.-P., and Lemaitre, B. (2018). Cell-Specific Imd-NF- κ B Responses Enable Simultaneous Antibacterial Immunity and Intestinal Epithelial Cell Shedding upon Bacterial Infection. *Immunity* 48, 897-910.e7.
- Zhang, P., McGrath, B.C., Reinert, J., Olsen, D.S., Lei, L., Gill, S., Wek, S.A., Vattem, K.M., Wek, R.C., Kimball, S.R., et al. (2002). The GCN2 eIF2 α Kinase Is Required for Adaptation to Amino Acid Deprivation in Mice. *Mol Cell Biol* 22, 6681–6688.
- Zhu, S., and Wek, R.C. (1998). Ribosome-binding Domain of Eukaryotic Initiation Factor-2 Kinase GCN2 Facilitates Translation Control *. *Journal of Biological Chemistry* 273, 1808–1814.
- Zhu, S., Sobolev, A.Y., and Wek, R.C. (1996). Histidyl-tRNA synthetase-related sequences in

GCN2 protein kinase regulate in vitro phosphorylation of eIF-2. *J Biol Chem* 271, 24989–24994.

Zientz, E., Dandekar, T., and Gross, R. (2004). Metabolic interdependence of obligate intracellular bacteria and their insect hosts. *Microbiol Mol Biol Rev* 68, 745–770.

Chapter I:

Drosophila-associated bacteria differentially shape the nutritional requirements of their host during juvenile growth


Article published in PLOS Biology 2020 18(3), e3000681.

RESEARCH ARTICLE

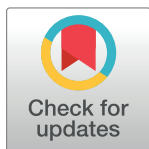
Drosophila-associated bacteria differentially shape the nutritional requirements of their host during juvenile growth

Jessika Consuegra¹, Théodore Grenier¹, Patrice Baa-Puyoulet², Isabelle Rahioui², Houssam Akherraz¹, Hugo Gervais¹, Nicolas Parisot², Pedro da Silva², Hubert Charles², Federica Calevro², François Leulier^{1*}

1 Institut de Génétique Fonctionnelle de Lyon, Université de Lyon, École Normale Supérieure de Lyon, Centre National de la Recherche Scientifique, Université Claude Bernard Lyon 1, UMR5242, Lyon, France, **2** Laboratoire Biologie Fonctionnelle, Insectes et Interactions, Université de Lyon, Institut National des Sciences Appliquées, Institut National de Recherche pour l'Agriculture, l'Alimentation et l'Environnement, UMR0203, Villeurbanne, France

 These authors contributed equally to this work.

* francois.leulier@ens-lyon.fr



OPEN ACCESS

Citation: Consuegra J, Grenier T, Baa-Puyoulet P, Rahioui I, Akherraz H, Gervais H, et al. (2020) *Drosophila*-associated bacteria differentially shape the nutritional requirements of their host during juvenile growth. PLoS Biol 18(3): e3000681. <https://doi.org/10.1371/journal.pbio.3000681>

Received: August 7, 2019

Accepted: March 4, 2020

Published: March 20, 2020

Peer Review History: PLOS recognizes the benefits of transparency in the peer review process; therefore, we enable the publication of all of the content of peer review and author responses alongside final, published articles. The editorial history of this article is available here: <https://doi.org/10.1371/journal.pbio.3000681>

Copyright: © 2020 Consuegra et al. This is an open access article distributed under the terms of the [Creative Commons Attribution License](https://creativecommons.org/licenses/by/4.0/), which permits unrestricted use, distribution, and reproduction in any medium, provided the original author and source are credited.

Data Availability Statement: All relevant data are within the paper and in [S1 Data](#) file. Metabolic network reconstructions and the resulting BioCyc metabolism databases are available at <http://artsymbiocyc.cycadsys.org>.

Abstract

The interplay between nutrition and the microbial communities colonizing the gastrointestinal tract (i.e., gut microbiota) determines juvenile growth trajectory. Nutritional deficiencies trigger developmental delays, and an immature gut microbiota is a hallmark of pathologies related to childhood undernutrition. However, how host-associated bacteria modulate the impact of nutrition on juvenile growth remains elusive. Here, using gnotobiotic *Drosophila melanogaster* larvae independently associated with *Acetobacter pomorum*^{WJL} (Ap^{WJL}) and *Lactobacillus plantarum*^{NC8} (Lp^{NC8}), 2 model *Drosophila*-associated bacteria, we performed a large-scale, systematic nutritional screen based on larval growth in 40 different and precisely controlled nutritional environments. We combined these results with genome-based metabolic network reconstruction to define the biosynthetic capacities of *Drosophila* germ-free (GF) larvae and its 2 bacterial partners. We first established that Ap^{WJL} and Lp^{NC8} differentially fulfill the nutritional requirements of the ex-GF larvae and parsed such difference down to individual amino acids, vitamins, other micronutrients, and trace metals. We found that *Drosophila*-associated bacteria not only fortify the host's diet with essential nutrients but, in specific instances, functionally compensate for host auxotrophies by either providing a metabolic intermediate or nutrient derivative to the host or by uptaking, concentrating, and delivering contaminant traces of micronutrients. Our systematic work reveals that beyond the molecular dialogue engaged between the host and its bacterial partners, *Drosophila* and its associated bacteria establish an integrated nutritional network relying on nutrient provision and utilization.

Introduction

Nutrition is the major environmental factor that determines to what extent an organism can realize its genetically-encoded growth potential [1]. The attributes of nutrition are defined by the quantity [2], quality [3], and bioavailability [4] of different nutrients in the diet. Nutrients

Funding: Research in FL's lab is supported by the "Fondation pour la Recherche Médicale" (Equipe FRM DEQ20180339196) and the Scientific Breakthrough Project from Université de Lyon "Microbehave." Research in PdS and FC's labs are supported by INRA and INSA Lyon. JC is funded by a postdoctoral fellowship from the "Fondation pour la Recherche Médicale" (FRM, SPF20170938612). TG is funded by a PhD fellowship from ENS de Lyon. The funders had no role in study design, data collection and analysis, decision to publish, or preparation of the manuscript.

Competing interests: The authors have declared that no competing interests exist.

Abbreviations: [ThiS]-COSH, [ThiS]-thiocarboxylate; a.u., arbitrary unit; Ap^{WJL}, *Acetobacter pomorum*^{WJL}; BCAA, branched-chain amino acid; CFU, colony-forming unit; CR, conventionally raised; CycADS, Cyc Annotation Database System; D₅₀, day when 50% of larvae population has entered metamorphosis; DGRP, *Drosophila* Genetic Reference Panel; DT, developmental timing; EAA^{Fly}, fly essential amino acid; EC, Enzyme Commission; FAD, Flavin Adenine Dinucleotide; FLYAA, fly exome-matched amino acid ratio; FMN, Flavin mononucleotide; FMOC, 9-fluorenylmethyl chloroformate; GF, germ-free; HD, Holidic Diet; HK, heat-killed; HPLC-MS, High-Performance Liquid Chromatography coupled with Mass Spectrometry; IIS, insulin/insulin-like growth factor signaling; LOD, limit of detection; Lp^{NC8}, *Lactobacillus plantarum*^{NC8}; MRS, De Man, Rogosa, and Sharpe; *MtnB/C*, genes encoding metallothionein B/C; NAL, nucleic acid and lipid; NCBI, National Center for Biotechnology Information; NEAA^{Fly}, fly nonessential amino acid; NMR, Nuclear Magnetic Resonance; OD_{max}, maximal optical density; OPA, ortho-phthalaldehyde; PC, phosphatidylcholine; PE, phosphatidylethanolamine; peg, protein encoding gene; PG, phosphatidylglycerol; PQQ-ADH, pyrroloquinoline-quinone-dependent alcohol dehydrogenase; Tn, transposon; TSP, Trimethylsilyl Propionic Acid; w¹¹¹⁸, *white*¹¹¹⁸; WT, wild type; yw, *yellow-white*.

are classified as nonessential or essential [3] based on the organism's biosynthetic capacities. Diets deficient in essential nutrients cause important growth and maturation delays or even growth arrest or "stunting", characterized by low height-for-age score [5]. In addition, some nutrients are conditionally essential. These nutrients can be synthesized by the organism but insufficiently under certain metabolically demanding conditions such as juvenile growth. Therefore, these conditionally essential nutrients also need to be retrieved from the diet like the essential ones. Deficient consumption of conditionally essential nutrients can also be detrimental for growth [3].

The intricate relationship between nutrition and growth is modulated by gut microbes. In a classical twin study in humans, Smith and colleagues unequivocally demonstrated that the gut microbiota composition of the juvenile subject suffering from stunting is significantly different from that of the healthy twin. When the fecal microbiota from the discordant twins were transplanted into genetically identical germ-free (GF) mice fed a poor diet, the recipients of the microbiota from the stunted twin performed poorly in terms of growth gain and weight recovery compared to the recipients of the microbiota of the healthy twin [6]. Furthermore, genomic analyses of gut microbiota from children experiencing strong acute malnutrition showed significant under-representation in pathways of amino acid biosynthesis and uptake, carbohydrate utilization, and B-vitamin metabolism [7]. Diets supplemented with nutrients favoring the growth of bacteria enriched in these under-represented pathways increase plasma biomarkers and levels of mediators of growth, bone formation, neurodevelopment, and immune function in children with moderate acute malnutrition [7]. These studies clearly show that microbes strongly impact how organisms respond to changes in their nutritional environment.

Diverse animal models are employed to decipher the physiological, ecological, genetic, and molecular mechanisms underpinning host/microbiota/diet interactions. Among them, *Drosophila melanogaster* is frequently chosen to study the impact of the nutritional environment on growth and development thanks to its short growth period as well as easy and cost-effective rearing conditions. During the juvenile phase of the *Drosophila* life cycle, larvae feed constantly and increase their body mass approximately 200 times until entry into metamorphosis [8]. However, the pace and duration of larval growth can be altered by the nutritional context and the host-associated microbes [9–11]. Like other animals, *Drosophila* live in constant association with microbes, including bacteria and yeast [12]. The impact of the host-associated microbes can be systematically assessed by generating gnotobiotic flies associated with a defined set of bacterial strains [13–15]. Lab-reared flies typically carry bacterial strains from only 4 to 8 species. The microbiota from wild flies are more complex. Nevertheless, they are usually dominated by members of the genera *Acetobacter* and *Lactobacillus* [16–22]. Most bacterial strains from these dominant genera are easy to culture in the lab, and some have even been genetically engineered for functional studies of host-microbe interactions [23–25]. These model bacteria are facultative symbionts that are constantly horizontally acquired [26–28]. Even though recent experimental evidence shows that wild bacterial isolates can persistently colonize the adult crop [22,29], bacteria associated to the larval gut are in fact transient; they constantly shuttle between the larval gut and the food substrate to establish a mutualistic cycle with the host [30,31].

We and others have previously shown that GF larvae raised in poor nutritional conditions show important developmental delays, and association with single model bacterial strains can accelerate *Drosophila* development under these nutritional challenges [20,25]. Specifically, *Acetobacter pomorum*^{WJL} (Ap^{WJL}) modulates developmental rate and final body size through the insulin/insulin-like growth factor signaling (IIS) pathway, and its intact acetate production machinery is critical [25]. *Lactobacillus plantarum*^{WJL} or *L. plantarum*^{NC8} (Lp^{NC8}) promotes

host juvenile growth and maturation partly through enhanced expression of intestinal peptidases upon sensing bacterial cell wall components by *Drosophila* enterocytes [20,23,32]. Interestingly, the growth-promoting effect of these bacteria is striking under nutritional scarcity, suggesting that besides the molecular dialogue engaged between the bacteria and their host to enhance protein digestion and compensate for reduced dietary macronutrient intake, bacteria-mediated growth promotion on globally scarce diets may also include specific compensation of essential nutrients, as recently reported for thiamin [33]. However, how the presence of such bacteria systematically alters the host's nutritional environment and satisfies the host's nutritional requirements remains unexplored. To do so, we assessed the bacterial contribution to *Drosophila* larval growth in 40 different and strictly controlled nutritional contexts based on chemically defined Holidic Diets (HDs).

HDs comprise a mixture of pure chemical ingredients that satisfy the different physiological requirements of the *Drosophila* host [34,35]. By altering the concentration of each or a combination of ingredients, one can exactly tailor the experiments by generating specific nutrient deficiencies or excess [36]. The first development of HDs supporting the growth of *Drosophila* can be traced back to the 1940s [37], and they were used to assess the direct impact of the nutritional environment on axenic larvae in the 1950s [38,39]. HDs were then used to investigate the links between nutrition and life span [40–43], fecundity [40–42,44], food choice behavior [45,46], nutrient sensing [47], and growth and maturation [33,40–42,48–50]. In this study, we adopted the recently developed fly exome-matched amino acid ratio (FLYAA) HD in which the amino acid concentrations are calculated so that they match the amino acid ratios found in the translated exome of the fly [40]. The FLYAA HD is optimal for both fecundity and life span of adults, and it can efficiently support larval growth, albeit not to the optimal growth and maturation rate obtained with rich oligidic diets [34]. Using this chemically defined HD, we aimed to deconstruct in a systematic manner the microbial contribution to the host's nutritional requirements down to individual nutrients.

To do so, we first needed to establish the biosynthetic capacities of GF larvae and 2 model *Drosophila*-associated bacteria: Ap^{WJL} and Lp^{NC8} on HD. We further complemented the in vivo study with automated metabolic network reconstruction based on the genome sequences of *D. melanogaster*, Ap^{WJL}, and Lp^{NC8}. In recent years, metabolic approaches based on genome-driven network reconstructions have been applied to predict the potential metabolic dependencies and metabolic exchanges between hosts and associated microbes [51–56]. The mutualistic association between the pea aphid *Acyrtosiphon pisum* and its obligate intracellular symbiont *Buchnera aphidicola* was the first symbiotic association for which genomic information were available on both partners and is a case study for a comprehensive survey of integrated host-symbiont metabolic interactions. In this model, decades of nutritional experiments using HDs and aposymbiotic aphids were reinterpreted in the light of newly available genomic data, thus changing the traditional paradigm that proposed a clear separation between the pathways of the host and its symbionts and revealing a particularly integrated metabolic network that is the result of the long coevolution of the insect with its obligate endosymbionts [57,58]. This example shows how important it is to integrate theoretical and experimental approaches to model metabolic pathways of symbiotic partners and properly dissect the functioning of their associations.

Here, we report that association of GF larvae with Ap^{WJL} or Lp^{NC8} modifies the nutritional requirements of ex-GF larvae in a specific manner for each bacterium. We show that Ap^{WJL} and Lp^{NC8} not only modify the nutritional environment of their host by fortifying diets with essential nutrients, they functionally compensate host auxotrophies despite not synthesizing the missing nutrient, probably by either providing a nutrient derivative to the host or by uptaking, concentrating, and delivering contaminant traces of the missing micronutrient.

Results and discussion

Metabolic network reconstruction of the host (*D. melanogaster*) and its associated bacteria, Ap^{WJL} and Lp^{NC8}, was automatically generated using the Cyc Annotation Database System (CycADS) pipeline [59]. The resulting BioCyc metabolism databases are available at <http://artsymbiocyc.cycadsys.org> for annotation and analysis purposes. We generated the enriched functional annotations of all the predicted proteins from the complete genomes of *D. melanogaster* (*Drosophila*, RefSeq GCF_000001215.4 release 6), *A. pomorum* strain DM001 (Ap^{WJL}, accession National Center for Biotechnology Information [NCBI] Bioproject PRJNA60787), and *L. plantarum* subsp. *plantarum* NC8 (Lp^{NC8}, NCBI Bioproject PRJNA67175). From the genomic analyses, we inferred all pathways allowing production of the organic compounds that are present in the exome-based FLYAA HD developed by Piper and colleagues [40]: fly essential and nonessential amino acids (EAAs^{Fly} ($n = 10$) and NEAAs^{Fly} ($n = 10$)), B-vitamins ($n = 7$), cholesterol ($n = 1$), and nucleic acids and lipid precursors (NALs, $n = 4$).

D. melanogaster biosynthetic capabilities inferred from genome-based metabolic network reconstruction

Although a BioCyc metabolic reconstruction of *D. melanogaster* is already publicly available (<https://biocyc.org/FLY>), we constructed an improved BioCyc database using a recent genome version and annotation [59]. This metabolic reconstruction identified 22,189 protein-encoding genes, including 5,061 enzymes and 156 transporters associated with 1,610 compounds assembled in a network of 331 pathways (versus the 227 pathways found in BioCyc). Like other metazoans, *Drosophila* possesses the gene repertoire to produce all the NEAAs^{Fly} but is unable to produce the EAAs^{Fly} (Fig 1A and S1 Table). *Drosophila* can also produce myoinositol, inosine, and uridine but is unable to synthesize vitamins from simple precursors (Fig 1B and S2 Table).

Ap^{WJL} biosynthetic capabilities inferred from genome-based metabolic network reconstruction

According to our metabolic reconstruction, the Ap^{WJL} genome comprises 4,268 protein-encoding genes including 1,326 enzymes and 46 transporters associated with 1,306 compounds assembled in a network of 313 pathways. Ap^{WJL} is a complete autotroph for all amino acids and possesses the genetic potential to produce the DNA bases inosine and uridine and 5 of the 7 vitamins present in the HD: biotin, folate, pantothenate, riboflavin, and thiamine (Fig 1A and 1B and S1 and S2 Tables). The first 2 steps of the nicotinate pathway (Enzyme Commission [EC] number 1.4.3.16 and 2.5.1.72) seem lacking in Ap^{WJL}. However, 3 candidate proteins (protein encoding genes [pegs].1228, 1229, and 1231) encode the succinate dehydrogenase enzymatic activity (EC 1.3.5.1). This enzyme can alternatively use oxygen or fumarate as an O-donor, depending on aerobic or anaerobic living conditions. Hence, this enzyme can switch between its aerobic condition activity (EC 1.3.5.1) towards its anaerobic condition activity (EC 1.4.3.16) using fumarate as a substrate and producing imminioaspartate. Hence, assuming that one of these genes can produce the activity at a sufficient rate in aerobic conditions in Ap^{WJL}, then the bacteria would be able to produce NAD⁺ and NADP⁺ from Asp (Fig 1B and S2 Table). The biosynthesis of pyridoxine is almost complete in Ap^{WJL}. Although we were not able to detect specific activities for the first 2 steps of the pathway, we propose (see below) that the bacteria have the capability to produce vitamin intermediates using enzymes with very close activities (S2 Table). Note that pyridoxine is reported as nonessential for acetic acid bacteria [60]. In summary, Ap^{WJL} genome analysis predicts that it is able to synthesize all

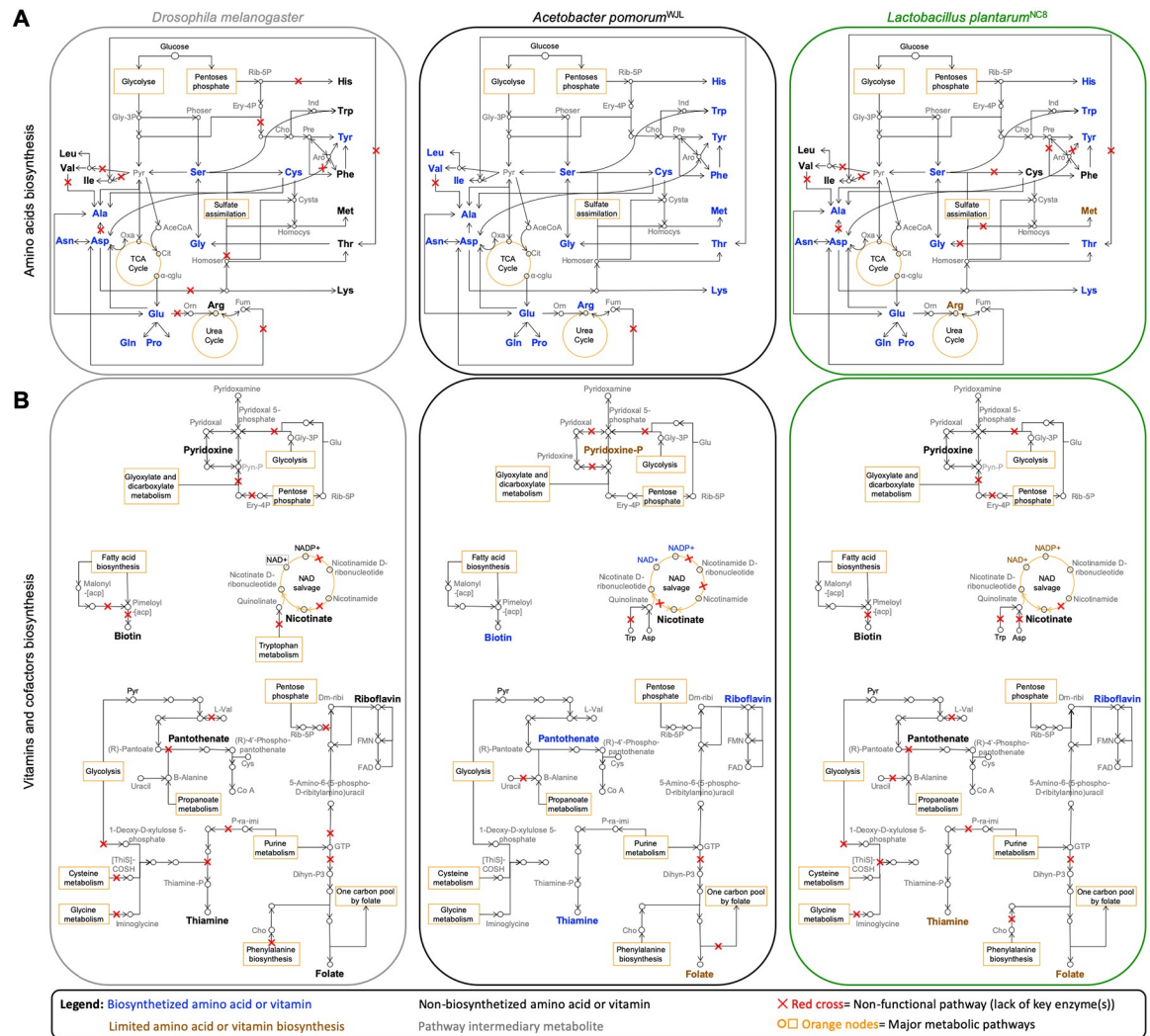


Fig 1. Expert automated genome annotation and metabolic network reconstruction of *Drosophila*, *Ap*^{WJL}, and *Lp*^{NC8}. (A) Amino acid biosynthetic pathways. (B) Vitamins and cofactors biosynthetic pathways. Left panels, *D. melanogaster*. Central panels, *Ap*^{WJL}. Right panels, *Lp*^{NC8}. Color code: blue, biosynthesized amino acids or vitamins; brown, limited amino acid or vitamin biosynthesis (biosynthesis of the metabolite may be possible, but it is limited and/or requires secondary metabolic pathways); black, nonbiosynthesized amino acids or vitamins; gray, pathway intermediary metabolites. Red cross: nonfunctional pathway (lack of key enzyme[s]). Orange nodes, major metabolic pathways. α -cglu, α -keto-glutarate; AceCoA, Acetyl-CoA; Ant, Antranilate; *Ap*^{WJL}, *A. pomorum*^{WJL}; Aro, Arogenate; Cho, chorismate; Cit, Citrate; Cysta, Cystathionine; Dihy-P3, 7,8-Dihydroneopterin-3'-P3; Dm-ribi, 6,7-Dimethyl-8-ribityllumazine; Ery-4P, Erythrose-4P; FAD, Flavin Adenine Dinucleotide; FMN, Flavin mononucleotide; Fum, Fumarate; Glc, Glucose; Gly-3P, Glycerate-3P; Homocys, Homocysteine; Homoser, Homoserine; Ind, Indole; *Lp*^{NC8}, *L. plantarum*^{NC8}; Orn, Ornithine; Oxa, Oxaloacetate; P-ra-imi, 1-(5'-Phospho-riboseyl)-5-aminoimidazole; Phoser, Phosphoserine; Pre, Prephenate; Pyn-P, Pyridoxine phosphate; Pyr, Pyruvate; Rib-5P, Ribose-5P; TCA, Tricarboxylic acid Cycle; [ThiS]-COSH, [ThiS]-thiocarboxylate.

<https://doi.org/10.1371/journal.pbio.3000681.g001>

amino acids, DNA bases, and the 7 B-vitamins (biotin, folate, pantothenate, riboflavin, thiamine, and intermediates of nicotinate and pyridoxine) present in HDs. However, we found no genomic support for the synthesis of choline and myoinositol in the *Ap*^{WJL} genome.

Lp^{NC8} biosynthetic capabilities inferred from genome-based metabolic network reconstruction

Metabolic reconstruction from the *Lp*^{NC8} genome generated a database that includes 2,868 protein-encoding genes, consisting of 973 enzymes and 74 transporters associated with 1,154

compounds, all assembled in a network of 246 metabolic pathways. From a genomic perspective (Fig 1A and S1 and S2 Tables), *Lp*^{NC8} is able to produce most amino acids from glucose or inner precursors with the exception of Phe, sulfur-containing amino acids (Cys, Met), and branched-chain amino acids (BCAAs; Ile, Leu, Val). Arg is known to be limiting [61] or essential to certain *L. plantarum* strains [62,63], yet the *Lp*^{NC8} genome encodes a complete Arg biosynthesis pathway. A manual curation of the pathway showed that the *Lp*^{NC8}'s *argCJBDF* operon should be functional because it does not contain stop codons, frameshifts, or deletions. *Lp*^{NC8} may produce Ala and Asp only using secondary metabolic routes (S1 Table). Therefore, *Lp*^{NC8} is expected to acquire these amino acids from the diet or to have an altered growth when they are absent from the diet. Similarly, biosynthesis of Thr is directly linked to Asp and Cys and is probably very limited in *Lp*^{NC8}.

Regarding vitamins and bases biosynthesis, *Lp*^{NC8} is able to produce folate, riboflavin, and thiamine (through the pyrimidine salvage pathway [2.1.7.49]), as well as all DNA bases including uridine and inosine (Fig 1B and S2 Table). *Lp*^{NC8} is not able to synthesize biotin, pyridoxine, pantothenate, choline, and myo-inositol. Based on our genomic analysis, *Lp*^{NC8} is not able to achieve the entire nicotinate biosynthetic pathway from Asp nor from Trp, as described in eukaryotes and in some bacteria [64]; even if the first step of the pathway could possibly be accomplished by the succinate dehydrogenase, as described above for *Ap*^{WJL}, the other 2 enzymes of the initial part of the pathway are missing (Fig 1B and S2 Table).

Collectively, our metabolic networks reconstruction shows that *Drosophila* and its associated bacteria have differential biosynthetic capacities. Indeed, some of the complete biosynthetic pathways are only present in one organism, while others are present in 2 or all 3 partners (Fig 2). In addition, we did not detect incomplete biosynthetic pathways potentially complemented between the host and its associated bacteria (Figs 1 and 2), as previously observed for obligate mutualistic partners [57,58].

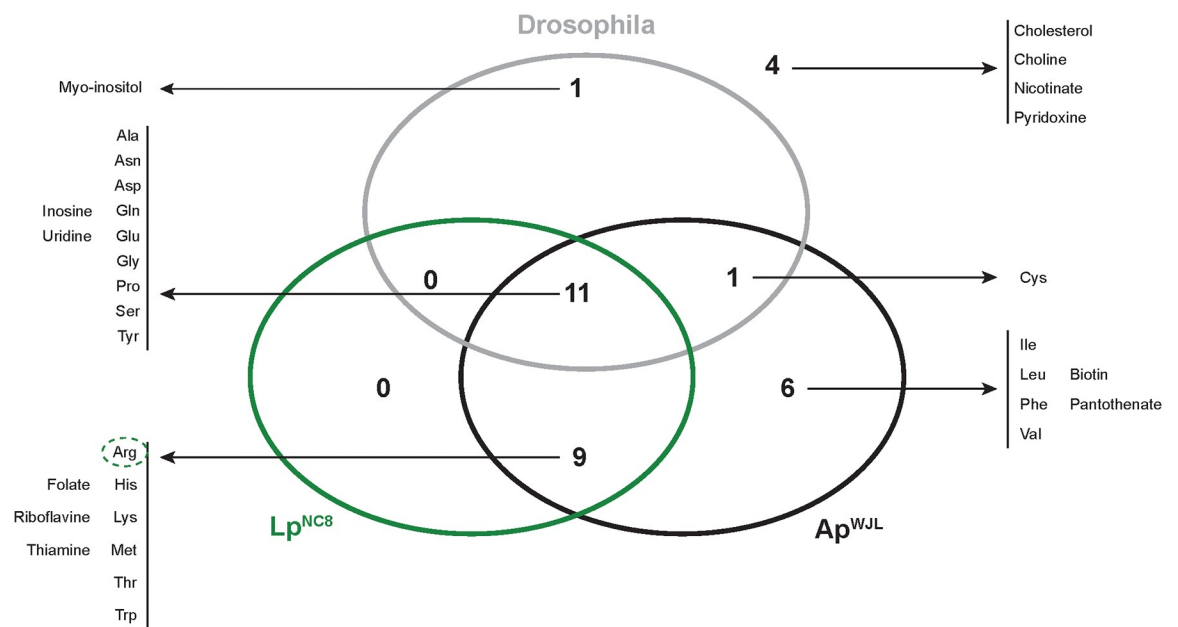


Fig 2. *Drosophila*, *Ap*^{WJL}, and *Lp*^{NC8} have differential biosynthetic capacities of nutrients contained in the HD. Venn diagram represents the number of nutrients present in the FLYAA HD that can be synthesized by each organism. The list of corresponding metabolites is provided. Dotted circles: biosynthesis of this metabolite by *Lp*^{NC8} (green) may be possible but might be limiting. *Ap*^{WJL}, *A. pomorum*^{WJL}; FLYAA, fly exome-matched amino acid ratio; HD, Holidic Diet; *Lp*^{NC8}, *L. plantarum*^{NC8}.

<https://doi.org/10.1371/journal.pbio.3000681.g002>

Experimental validation of *Drosophila*-associated bacteria auxotrophies using HDs

In order to experimentally test the metabolic potential of *Drosophila* and its associated bacteria predicted by our automated genome annotations and subsequent metabolic pathway reconstructions (see above), we adopted the exome-based FLYAA HD [40]. We systematically removed a single component at a time to generate 39 different fly nutritional substrates (henceforth named HDΔX, X being the nutrient omitted), plus one complete HD medium. This medium can also be prepared in a liquid version by omitting agar and cholesterol from the recipe. Liquid HDs can then be used to assess bacterial growth in 96-well plates, increasing the experimental throughput.

We first assessed *Ap*^{WJL} and *Lp*^{NC8} growth in each of the 40 different liquid HDs for 72 h, using maximal optical density (OD_{Max}) as a readout (Fig 3A and S3 Table). In the complete HD, both *Ap*^{WJL} and *Lp*^{NC8} grow well (Fig 3A, first line). On the deficient media, *Ap*^{WJL} can grow in HDΔSucrose, presumably using acetate from the acetate buffer as a carbon source. Also, its growth is not altered in the absence of any of EAAs^{Fly}, vitamins, or NALs. However, while *Ap*^{WJL} growth is not impacted by the lack of most NEAAs^{Fly}, it grows poorly in

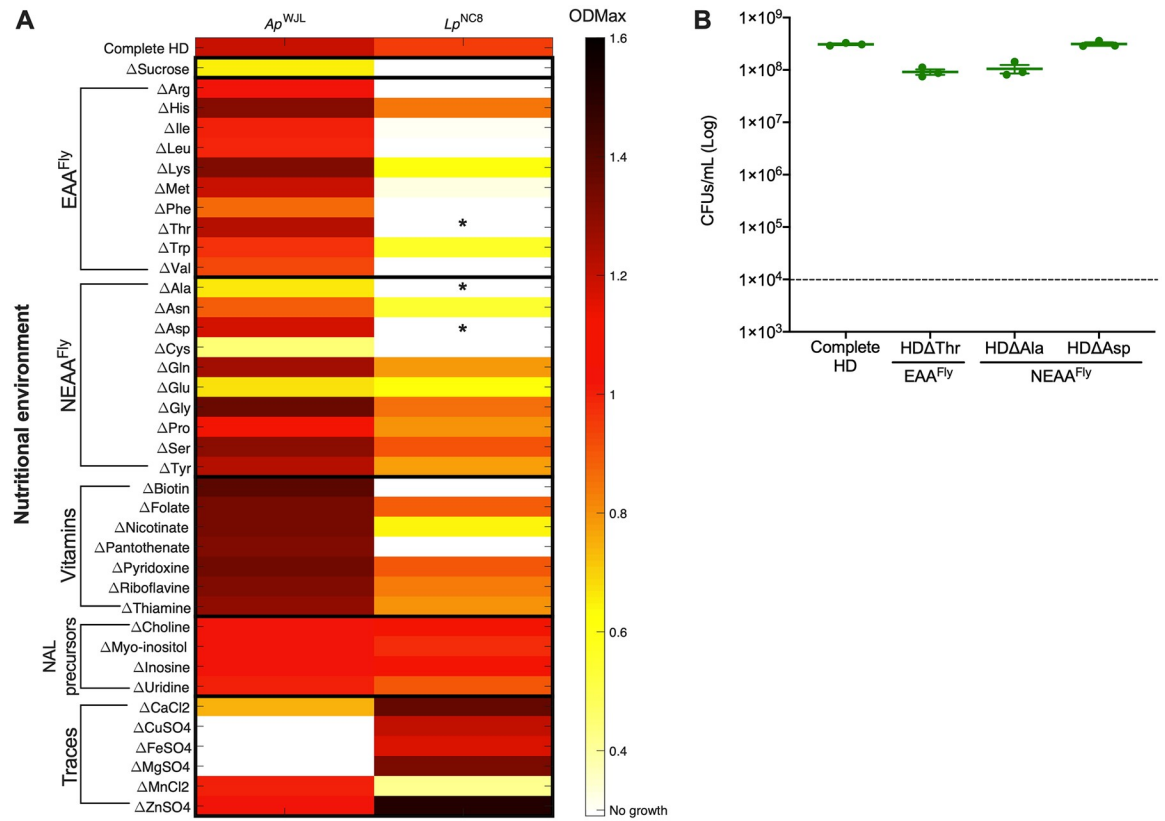


Fig 3. *Ap*^{WJL} and *Lp*^{NC8} auxotrophies detected in liquid fly HD. (A) Heat map representing the mean OD_{Max} reached by *Ap*^{WJL} or *Lp*^{NC8} after 72 h of culture. Each line shows growth in a different version of the liquid HD: complete HD (first line) or HD lacking nutrient X (ΔX, lines below). Cultures were made in 96-well plates under agitation. Asterisks (*) pinpoint contradictions with our metabolic pathway automated annotations, which are explained in panel B. (B) Growth of *Lp*^{NC8} in 4 versions of liquid HD: complete HD, HDΔThr, HDΔAla, and HDΔAsp in static conditions. Plot shows means with standard error based on 3 replicates by assay. Each dot represents an independent replicate. The dashed line represents the level of inoculation at *t* = 0 h (10⁴ CFUs per mL). *Ap*^{WJL}, *A. pomorum*^{WJL}; CFU, colony-forming unit; EAA^{Fly}, fly essential amino acid; HD, Holidic Diet; *Lp*^{NC8}, *L. plantarum*^{NC8}; NALs, nucleic acids and lipids; NEAA^{Fly}, fly nonessential amino acid; OD_{Max}, maximal optical density.

<https://doi.org/10.1371/journal.pbio.3000681.g003>

HD Δ Ala, HD Δ Cys, and HD Δ Glu. In addition, Ap^{WJL} fails to grow in HD Δ Cu, HD Δ Fe, and HD Δ Mg (Fig 3A, first column and S3 Table). The broad growth capacity of Ap^{WJL} in HDs correlates well with the wide range of environmental niches the genus *Acetobacter* can colonize. *Acetobacter* species are found in sugar-rich niches such as flowers and fruits but also in poorer niches such as soil and water, where they need to synthesize all the nutrients required for their own growth [65]. These findings corroborate our genome-based predictions (Fig 1). Furthermore, the genome-based metabolic pathway reconstruction predicted that Ap^{WJL} would not be able to synthesize choline and myoinositol; however, we observed that Ap^{WJL} grows in their absence. Choline is an important precursor of phosphatidylcholine (PC), which is a major component of *Acetobacter* membranes and plays an important role in conferring acetic acid tolerance. Despite its importance, PC is not essential for *Acetobacter* growth. Indeed, mutants precluding PC synthesis show a shift towards increased membrane content of phosphatidylethanolamine (PE) and phosphatidylglycerol (PG) and do not show any growth defects in standard medium [66]. Similarly, Ap^{WJL} likely does not need myoinositol for its growth because inositol compounds are absent from the membrane of most bacteria [67]. Regarding nicotinate and pyridoxine, the biosynthesis pathways of these 2 vitamins are only partial and do not support the production of the final molecules (Fig 1B and S2 Table); however, intermediates such as pyridoxine phosphate, pyridoxal-5-phosphate, and pyridoxamine or nicotinate-D-ribonucleotide, NAD⁺, and NADP⁺ may be synthesized and would support bacterial growth in nicotinate- or pyridoxine-depleted diets. Interestingly, Ap^{WJL} growth was only precluded in the absence of some metal ions: Cu, Fe, and Mg. Metal ions are important cofactors required for enzymatic activities [68]. Specifically, in acetic acid bacteria, Cu is an important cofactor of the energy-producing cytochromes of the respiratory chain [69], making it essential for Ap^{WJL} growth.

We detected far more nutritional auxotrophies for Lp^{NC8} on HDs (Fig 3A, second column and S3 Table). Lp^{NC8} fails to grow in HD Δ Sucrose because sucrose is the only suitable carbon source for this strain in the liquid HD. Also, Lp^{NC8} growth is precluded in the absence of 9 amino acids, including 6 EAAs^{Fly} (Arg, Ile, Leu, Phe, Thr, Val) and 3 NEAAs^{Fly} (Ala, Asp, Cys). It also grows poorly in media lacking the EAAs^{Fly} Lys, Met, and Trp and the NEAAs^{Fly} Asn and Glu. Moreover, Lp^{NC8} does not grow in HD Δ Biotin and HD Δ Pantothenate. However, it slightly grows in absence of nicotinate, despite the prediction from our genome-based metabolic pathway reconstruction that nicotinate could not be produced (Fig 1B and S2 Table). Finally, Lp^{NC8} growth is not affected by the lack of any NALs and even increased in the absence of certain metal ions such as Ca, Cu, Mg, and Zn. In contrast, Lp^{NC8} growth is significantly reduced in HD Δ Mn. These relatively elevated nutritional requirements of Lp^{NC8} were expected because *L. plantarum* is a species adapted to nutrient-rich environments [70]. Hence, many *L. plantarum* strains have lost the capacity to synthesize various nutrients that can easily be found in their natural habitats [70,71]. The inability of *L. plantarum* to synthesize important nutrients such as BCAAs (Ile, Leu, and Val) or the B-vitamin pantothenate was previously identified by both genome analyses [62] and growth studies in chemically defined minimal media [61,72,73]. Moreover, it is known that *L. plantarum* needs Mn to resist oxidative stress [74], which explains its poor growth in HD Δ Mn.

Our experimental data only partially correlate with the results of the genome-based predictions. Predicted auxotrophies for Ile, Leu, Val, Phe, Cys, pantothenate, and biotin were confirmed in vivo. The identified Arg auxotrophy was not surprising because, as mentioned above, Arg is often described as essential to *L. plantarum* in high-metabolic-demanding conditions even though all the genes necessary for Arg biosynthesis are present. However, auxotrophies of Lp^{NC8} to Thr, Ala, and Asp were not expected (Fig 3A, denoted by “*”), even though these amino acids were predicted to be limiting (see above). As mentioned previously, bacterial

growth in liquid HDs was assessed in 96-well plates using a microplate reader (see [Materials and methods](#)). Every cycle includes an agitation step to homogenize the solution to improve OD reading accuracy. This agitation step may oxygenate the media and thus negatively affects Lp^{NC8} growth in suboptimal nutritional conditions because *L. plantarum* strains are aerotolerant, but optimal growth is achieved under microaerophilic or anaerobic conditions [75]. To challenge these unexpected auxotrophies, we assessed Lp^{NC8} growth in liquid HD Δ Thr, HD Δ Ala, and HD Δ Asp in 15-mL closed falcon tubes without agitation. After 72 h of incubation, we determined colony-forming unit (CFU) counts in each media (Fig 3B). As predicted by our genomic analyses, Lp^{NC8} was now able to grow in each of the 3 deficient media in static conditions to the same extent as in the complete HD (Fig 3B). Therefore, Lp^{NC8} auxotrophies observed for Thr, Ala, and Asp in 96-well plates are likely due to excessive oxygenation. This could also explain the poor growth of Lp^{NC8} in the absence of the EAAs^{Fly} Lys, Met, and Trp and the NEAAs^{Fly} Asn and Glu.

Surprisingly, the ability of Lp^{NC8} to grow in HD Δ Choline, HD Δ Myoinositol, HD Δ Nicotinate, and HD Δ Pyridoxine does not correlate with our metabolic predictions. As for Ap^{WJL} (see above), Lp^{NC8} growth probably does not require choline or myoinositol. A previous study quantified choline and inositol compounds in *L. plantarum* cell extracts and found them to be extremely low and therefore most likely due to contaminations from the medium rather than components of *L. plantarum* biomass [76]. Pyridoxine is a precursor of pyridoxal-5-phosphate, a cofactor necessary for amino acid converting reactions. Teusink and colleagues [62] showed that *L. plantarum*^{WCSF1} requires exogenous sources of pyridoxine only in a minimal medium lacking amino acids. Because HD Δ Pyridoxine contains all amino acids, it is likely that pyridoxine is not essential for Lp^{NC8} growth in these conditions. Finally, the capacity of Lp^{NC8} to grow in HD Δ Nicotinate could be related to the presence of alternative pathways to nicotinate intermediate biosynthesis (Fig 1B and S2 Table). Indeed, this possibility has been previously reported in the genus *Lactobacillus* [71], which would explain the capacity to grow in absence of exogenous nicotinate.

Altogether, the complete HD is a suitable nutritional environment that allows the 2 model *Drosophila*-associated bacteria, Ap^{WJL} and Lp^{NC8} , to grow. Growth capacities in deficient media vary from one bacterium to another and are dictated by their individual genetic repertoires.

GF larvae exhibit 22 auxotrophies while developing on FLYAA HDs

We next sought to establish the nutritional requirements of GF larvae by assessing larval developmental timing (DT) in the complete HD and in each of the 39 deficient HDs (larvae were reared from eggs until pupae on the HDs; see [Materials and methods](#)). DT is expressed as D_{50} , which represents the day when 50% of the larvae population has entered metamorphosis in a specific nutritional condition. In agreement with previous studies [38,39], GF larvae fail to develop in all HD Δ EAAs^{Fly}, all HD Δ Vitamins, HD Δ Choline, HD Δ Cholesterol, HD Δ Zn, and HD Δ Mg (Fig 4A, first column). Over 60 years ago, Sang and colleagues reported that Zn was dispensable for GF larval development [38]. We suspect that the casein in the medium used in Sang and colleagues inadvertently provided trace amount of Zn, which could account for the discrepancy between our observation and that of Sang and colleagues. Also in accordance with previous studies [38,39,50], GF larvae were able to reach pupariation in HD Δ NEAAs^{Fly} (Δ Ala, Δ Cys, Δ Gln, Δ Glu, Δ Gly, Δ Pro), HD Δ Uridine, HD Δ Myoinositol, and HD Δ Mn at the same rate as on a complete HD (Fig 4A first column, S4 Table). The absence of sucrose, Tyr, inosine, Ca, Cu, and Fe did not prevent pupae emergence but increased the duration of larval development very significantly (Fig 4A first column, S4 Table). Surprisingly, GF larvae were able to

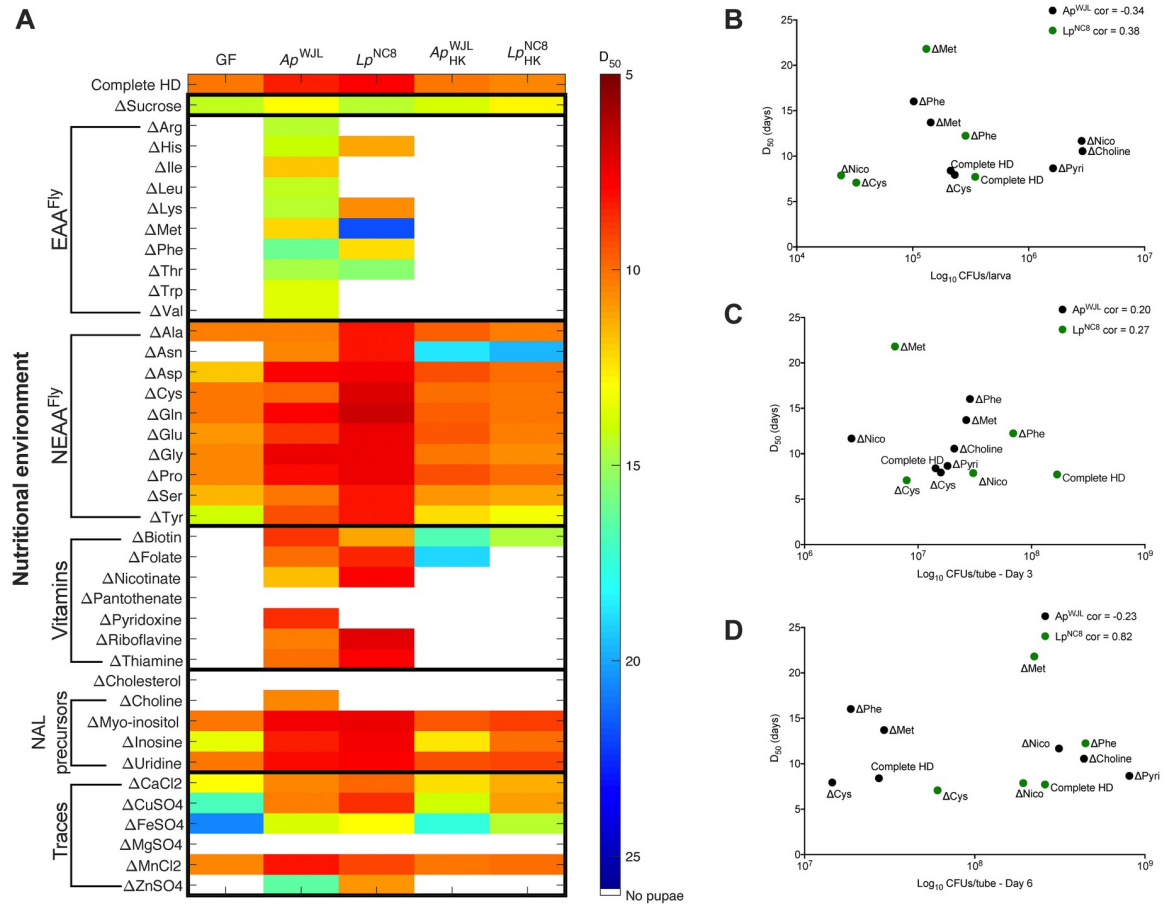


Fig 4. Ap^{WJL} and Lp^{NCS} can differentially fulfill their host's nutritional requirements in HDs. (A) Heat map representing the mean D_{50} of GF larvae (first column) and larvae associated with Ap^{WJL} , Lp^{NCS} , Ap^{WJL}_{HK} , and Lp^{NCS}_{HK} (columns 2, 3, 4, 5 respectively). Each line shows D_{50} in a different version of HD: complete HD (first line) or HDs lacking nutrient X (ΔX , lines below). White means larvae did not reach pupariation in these conditions. Means, standard errors of the mean and statistical tests (Dunn test of multiple comparisons) are detailed in [S4 Table](#). (B–D) Absence of correlation between time of development and quantity of bacteria. Y axis shows D_{50} , and X axis shows quantity of bacteria (Log_{10} CFUs) in the larval gut (B), in the diet in presence of larvae 3 days after inoculation (C), and in the diet in presence of larvae 6 days after inoculation (D). Each dot shows a different condition. Complete HD: on complete HD. ΔX : on HDs lacking nutrient X. Black dots: in monoassociation with Ap^{WJL} , green dots: in monoassociation with Lp^{NCS} . For each bacterium, we tested Pearson's product–moment correlation between D_{50} and quantity of bacteria. Ap^{WJL} , *A. pomorum*^{WJL}; CFU, colony-forming unit; cor, Pearson correlation coefficient for each bacterium; D_{50} , day when 50% of larvae population has entered metamorphosis; EAA^{Fly}, fly essential amino acid; GF, germ-free; HD, Holidic Diet; HK, heat-killed; Lp^{NCS} , *L. plantarum*^{NCS}; NALS, nucleic acids and lipids; NEAA^{Fly}, fly nonessential amino acid.

<https://doi.org/10.1371/journal.pbio.3000681.g004>

reach pupariation, albeit late, in HD Δ Sucrose. Indeed, all the HDs developed to date include carbohydrates (either sucrose or fructose) as a carbon source [34]. Larval development in the absence of carbohydrates suggests that GF larvae may use other components of the HD such as amino acids as carbon source. In summary, GF yellow-white (*yw*) larvae show 22 auxotrophies while developing on sterile HDs.

Our observations correlate well with our genome-based predictions of the metabolic capabilities of the 3 partners (Fig 1) with one exception: GF larvae did not reach pupariation in HD Δ Asn. This result was surprising because Asn is described as an NEAA in *Drosophila* and other animals [77]. To test whether Asn auxotrophy was specific to the *yw* fly line used in our lab, we assessed larval DT in 2 other *D. melanogaster* reference lines, the *Drosophila* Genetic Reference Panel (DGRP) line DGRP_25210 [78] and *white*¹¹¹⁸ (*w*¹¹¹⁸). Unlike *yw*, both *w*¹¹¹⁸

and DGRP_25210 larvae were able to develop in GF conditions in HD Δ Asn, albeit with a severe developmental delay (Fig 5A). Therefore, the complete Asn auxotrophy seen with our *yw* strain is an exception rather than a rule, an observation that correlates with our metabolic pathway reconstruction that was based on the genome sequence of the *D. melanogaster* reference genome strain (Bloomington stock #2057). We next sequenced the coding region of the enzyme AsnS, which converts Asp to Asn in *yw* flies, and did not detect any nonsynonymous mutation (S1 Fig). Further studies may thus be required to determine the origin of the Asn auxotrophy in our *yw* line on HD. However, these results indicate that Asn is not an EAA per se but remains a limiting NEAA, an observation that also applies to Tyr.

Bacterial cell wall sensing contributes to Lp^{NC8}-mediated larval growth promotion in complete chemically defined diets

We then investigated whether and how the association with bacteria affects the nutritional requirements of GF larvae during juvenile growth and maturation. To this end, we monoassociated GF embryos with Ap^{WJL} or Lp^{NC8} and measured D₅₀ and egg-to-pupa survival in complete and deficient HDs (Fig 4A, second and third columns, respectively, and S4 and S5 Tables). On a complete HD, monoassociation with either Ap^{WJL} or Lp^{NC8} accelerated larval DT with a mean D₅₀ of 8.4 and 7.7 days, respectively, whereas GF mean D₅₀ is 10.1 days (Fig 4A, first line). These growth-promoting effects upon monoassociation with either Ap^{WJL} or Lp^{NC8} have been previously reported on complex diets, and insights on the underlying molecular mechanisms were provided [20,25]. Shin and colleagues showed that when the associated larvae grow on a low-casamino-acid semiligidic diet, the pyrroloquinoline-quinone-dependent alcohol dehydrogenase (PQQ-ADH) activity of Ap^{WJL} modulates the developmental rate and body size through IIS. PQQ-ADH transposon (Tn) disruption in the Ap^{WJL}::Tnpqq mutant severely reduces acetic acid production, which has been proposed to alter the

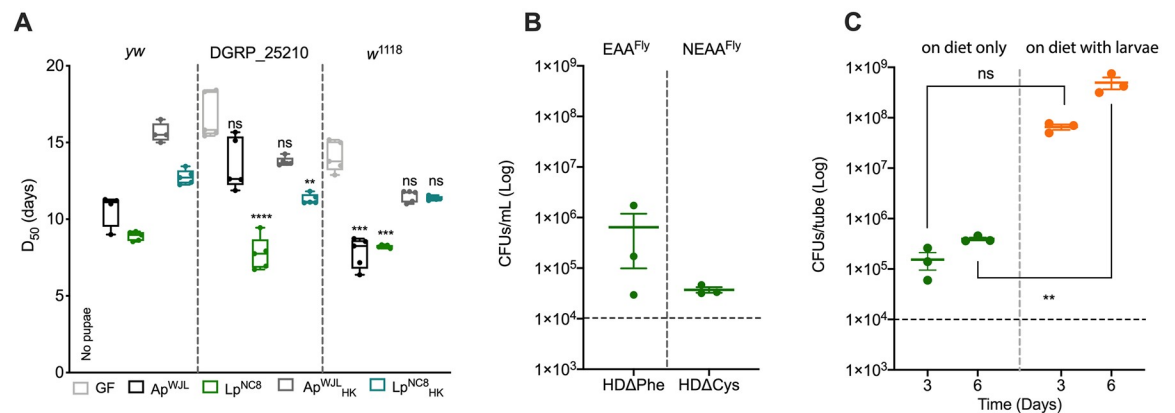


Fig 5. Evaluation of HD Δ Asn, HD Δ Phe, and HD Δ Cys contexts. (A) D₅₀ of *yw*, DGRP_25210, and *w*¹¹¹⁸ larvae on HD Δ Asn. Boxplots show minimum, maximum, and median. Each dot shows an independent replicate. GF *yw* larvae did not reach pupariation. For the other 2 lines, we performed a Kruskal–Wallis test followed by post hoc Dunn tests to compare each gnotobiotic condition to GF. ***p*-value < 0.005, ****p*-value < 0.0005, *****p*-value < 0.0001. (B) Growth of Lp^{NC8} in liquid HD Δ Phe and liquid HD Δ Cys, in static conditions, 3 days after inoculation. Plot shows mean with standard error. Each dot shows an independent replicate. The dashed line represents the level of inoculation at *t* = 0 h (10⁴ CFUs per mL). (C) Growth of Lp^{NC8} on solid HD Δ Cys, in absence and in presence of larvae, 3 days and 6 days after inoculation. Plot shows mean with standard error. Each dot represents an independent replicate. The dashed line represents the level of inoculation at *t* = 0 h (10⁴ CFUs per tube). We performed two-way ANOVA followed by post hoc Sidak test. ***p*-value < 0.005. Ap^{WJL}, *A. pomorum*^{WJL}; CFU, colony-forming unit; DGRP, XXX; D₅₀, day when 50% of larvae population has entered metamorphosis; EAA^{Fly}, fly essential amino acid; GF, germ-free; HD, Holidic Diet; HK, heat-killed; Lp^{NC8}, *L. plantarum*^{NC8}; NEAA^{Fly}, fly nonessential amino acid; ns, nonsignificant; *yw*, XXX.

<https://doi.org/10.1371/journal.pbio.3000681.g005>

regulation of developmental and metabolic homeostasis upon monoassociation [25]. Lp^{NC8} promotes host juvenile growth and maturation on a low-yeast-based oligidic diet, partly through enhanced expression of intestinal peptidases upon sensing of bacterial cell walls components by *Drosophila* enterocytes [20,23]. Deletion of the *dlt* operon, which encodes the molecular machinery involved in the D-alanylation of teichoic acids, leads to bacterial cell wall alteration with a complete loss of D-alanylation of teichoic acids, and consequently, cell walls purified from the $Lp^{NC8}\Delta dlt_{op}$ mutant trigger a reduced expression of peptidases in enterocytes [23]. Therefore, we first probed the importance of these molecular mechanisms on bacteria-mediated larval growth promotion on a complete HD. To this end, we tested in our HD setting the associations with the loss of function mutants $Ap^{WJL}::Tnpqq$ [25] and $Lp^{NC8}\Delta dlt_{op}$ [23]. In a complete HD, only the $Lp^{NC8}\Delta dlt_{op}$ mutant failed to support larval growth, reminiscent of the previous observation on the low-yeast oligidic diets (S2 Fig). Surprisingly, in complete HD, the $Ap^{WJL}::Tnpqq$ mutant actually triggered an enhanced growth promotion as compared to its wild-type (WT) reference strain. Shin and colleagues reported that $Ap^{WJL}::Tnpqq$ -associated larvae experienced growth delay, which can be rescued by acetic acid provision [25]. Therefore, the acetic-acid-based buffer in the HD may explain why $Ap^{WJL}::Tnpqq$ no longer behaves as a loss-of-function mutant in this setting; however, how it actually surpasses the WT strain on a complete HD remains elusive. Collectively, these results establish that sensing bacterial cell walls containing D-alanylated teichoic acids is also an important feature of the intrinsic growth-promoting ability of Lp^{NC8} in a complete chemically defined HD. Thus, the previously reported molecular sensing mechanism that mediates the growth-promoting effect of Lp^{NC8} during chronic undernutrition is also at play in synthetic diets.

Association with Ap^{WJL} fulfills 19 of the 22 nutrient requirements of GF larvae

Association with Ap^{WJL} sustained larval development (albeit to different degrees) in the absence of 19 out of 22 GF larvae essential nutrients (Fig 4A, second column). Ap^{WJL} -associated larvae reached pupariation in the absence of each EAA^{Fly} (though their development was slower than on complete HD), Asn, vitamins, choline, and Zn. Association with Ap^{WJL} also rescued the developmental delay observed in GF larvae in HD Δ Tyr, HD Δ inosine, HD Δ Cu, and HD Δ Fe. The only nutritional requirements of GF larvae that were not fulfilled by Ap^{WJL} were cholesterol, pantothenate, and Mg.

Association with Lp^{NC8} fulfills 12 of the 22 nutrient requirements of GF larvae

Compared to Ap^{WJL} , monoassociation with Lp^{NC8} compensated for a reduced number of the GF larvae nutritional deficiencies (12 out of 22; Fig 4A, third column). Lp^{NC8} -associated larvae reached pupariation in the absence of some EAAs^{Fly} (HD Δ His, HD Δ Lys, HD Δ Met, HD Δ Phe, HD Δ Thr), Asn, certain vitamins (HD Δ Biotin, HD Δ Folate, HD Δ Nicotinate, HD Δ Riboflavin, HD Δ Thiamine), and Zn. Moreover, Lp^{NC8} rescued the developmental delay observed in GF larvae on HD Δ Tyr, HD Δ inosine, HD Δ Cu, and HD Δ Fe.

Bacteria need to be metabolically active in order to fulfill larval nutritional requirements

Bacteria were grown in rich medium before association with larvae (see [Materials and methods](#)). Therefore, they might have accumulated nutrients that could be used later by the larvae to fulfill their nutritional requirements. To test for the nutritional input brought by the initial

bacterial inoculum, we associated GF larvae with 10× heat-killed (HK) bacteria (mimicking the maximal bacterial biomass found in the diet during the experiment, S3B Fig) and measured D_{50} in complete and deficient HDs (Fig 4A, fourth and fifth columns). In most cases, the D_{50} of larvae in HK and GF conditions was similar. Therefore, bacteria need to be metabolically active to fulfill the larval nutritional requirements on HDs. However, we found some exceptions. In HD Δ Asn, HD Δ Biotin, HD Δ Folate, HD Δ Cu, and HD Δ Fe, the addition of HK bacteria allowed the larvae to develop, though not as fast as in association with living bacteria. These results suggest that larvae only require a very small amount of these nutrients, which can be sufficiently derived from the inert bacterial inoculum.

On a low-protein oligidic diet, larval growth promotion by bacteria correlates positively with the quantity of microbes [79]. We wondered whether the differences that we observed in growth-promotion efficiency were due to differences in bacterial loads. Thus, we tested the correlation between bacterial loads and benefit to host growth in 3 contexts: (1) conditions in which both bacteria are beneficial to their host, complete HD; (2) conditions in which each bacterium differently impacts the host, HD Δ Met, HD Δ Phe, and HD Δ Nicotinate; and (3) conditions in which only one bacterium compensates for the lack of a nutrient, HD Δ Cys, HD Δ Pyr, and HD Δ Choline. We found no correlation between bacterial load in the larval gut (Fig 4B and S3A Fig) or in the diet (Fig 4B and 4C and S3B Fig) and the ability of the bacteria to impact host DT on the tested diets. These results reinforce the notion that, in our experimental settings, *Drosophila*-associated bacteria are biologically active partners, and their load, either in the diet or in the gut, does not dictate their functional impact on their host's nutrition or development.

The ability of bacteria to compensate nutritional deficiencies does not always correlate with the ability of bacteria to synthesize the nutrient

Next, based on the genome-based predictions and the experimentally revealed auxotrophies of GF larvae on FLYAA HD, we correlated the ability of each bacterium to synthesize a nutrient to its ability to fulfill the larval requirements in this nutrient. We identified 4 distinct situations related to the 19 compensations of the 22 auxotrophies shown by GF larvae.

Situation 1: the bacteria synthesize the missing nutrient in the diet and compensate for the related larval auxotrophy (15/19 auxotrophy compensations). In most of the tested conditions, when the bacteria can synthesize a nutrient, they can also fulfill the related nutritional requirements of the GF larvae. For Ap^{WJL}, this includes all EAAs^{Fly}, Asn, and most vitamins (except pantothenate). For Lp^{NC8}, the correlation between the nutritional complementation of ex-GF larva and the ability of Lp^{NC8} to synthesize the missing nutrient is more limited and only applies to the requirements of His, Lys, Met, Thr, Asn, and most vitamins. Nonetheless, these results suggest that bacteria can actively supply the nutrients lacking in the HD to the larvae. This phenomenon is reminiscent of previous observations using conventional and gnotobiotic hosts, in which microbial provision of riboflavin or thiamine by host-associated bacteria have been proposed [33,80]. Exceptions to this case seem to be Ap^{WJL} on HD Δ Pantothenate and Lp^{NC8} on HD Δ Trp. Specifically, Ap^{WJL} can produce pantothenate and grows in HD Δ Pantothenate, and similarly, Lp^{NC8} can produce Trp and grows in HD Δ Trp. However, neither supported larval development on the respective depleted HD. It is therefore probable that Ap^{WJL} and Lp^{NC8} produce enough pantothenate and Trp, respectively, to sustain their own growth in the depleted HD, but not sufficiently or in a manner inaccessible to the larvae, and thus fail to fulfill larval requirements for these nutrients.

Situation 2: the bacteria do not synthesize a nutrient, and they cannot fulfill larval nutrient requirements. Expectedly, we observed that when bacteria do not synthesize a nutrient, they

do not fulfill ex-GF larvae requirements for this nutrient. For instance, Lp^{NC8} cannot produce the BCAAs (Ile, Leu, and Val) nor grow in their absence, and thus, it cannot fulfill larval requirements for these amino acids. In some depleted diets, bacteria were able to grow (Fig 3A) even though they cannot synthesize the missing nutrient (Fig 1, S1 and S2 Tables), and they failed to fulfill the larvae requirements of these specific nutrients. This is observed for Ap^{WJL} and Lp^{NC8} on HD Δ Cholesterol. The likely explanation is that cholesterol is an animal sterol but is dispensable for bacterial growth [67,81]. Similarly, on HD Δ Choline and HD Δ Pyridoxine, Lp^{NC8} grows (Fig 3A) but is unable to fulfill larval requirements (Fig 4A) because according to genome-based predictions, it cannot synthesize these compounds (Fig 1 and S2 Table).

Situation 3: the bacteria do not synthesize a nutrient, but they can fulfill larval nutrient requirements (3/19 auxotrophy compensations). In most cases, we observe growth rescue by bacteria provision of the missing nutrients, but there are interesting exceptions. According to genome-based predictions, Ap^{WJL} is unable to synthesize de novo choline, pyridoxine, and nicotinate (Fig 1B and S2 Table). Surprisingly, it compensates larval auxotrophies on HD Δ Choline, HD Δ Pyridoxine, and HD Δ Nicotinate. Similarly, genome analysis predict that Lp^{NC8} cannot synthesize nicotinate (Fig 1B and S2 Table), but it compensates larval auxotrophy on HD Δ Nicotinate.

To confirm that the bacteria are incapable to synthesize these compounds, we assessed the presence of these compounds in bacterial supernatants using Nuclear Magnetic Resonance (NMR) spectroscopy and High-Performance Liquid Chromatography coupled with Mass Spectrometry (HPLC-MS). We were able to quantify choline in a complete HD using NMR spectroscopy (at 0.531 ± 0.003 mM for a theoretical concentration of 0.477 mM). However, we failed to detect it in the supernatant of Ap^{WJL} culture in HD Δ Choline (see Materials and methods section). Similarly, we did not detect any production of nicotinate by either Ap^{WJL} and Lp^{NC8} or production of pyridoxine by Ap^{WJL} in HD Δ Nicotinate or HD Δ Pyridoxine, although the analytical method used (HPLC-MS; see Materials and methods) was very sensitive, with a limit of detection of 15.625 nM and 0.977 nM for nicotinate and pyridoxine, respectively.

In the case of choline, Ap^{WJL} may synthesize other compounds that *Drosophila* can use to functionally replace choline. As stated before, *Acetobacter* mutants precluding PC synthesis shift their membrane composition towards increased content of PE and PG [66]. PE and PG have been reported to be part of the phospholipidic repertoire of *Drosophila* membranes [82], in which PE represents approximately 50% of their lipid composition [83]. We posit that ex-GF larvae growing on HD Δ Choline capitalize on ethanolamine or glycerol phosphoderivatives produced by Ap^{WJL} to compensate for the lack of choline in their diet.

In the case of pyridoxine, despite its inability to synthesize pyridoxine, Ap^{WJL} may fulfill larval requirements through the production of intermediates such as pyridoxine phosphate, pyridoxal-5-phosphate, or pyridoxamine, which are predicted to be synthesized based on genome analysis (Fig 1B and S2 Table).

Regarding nicotinate, both Ap^{WJL} and Lp^{NC8} grow on HD Δ Nicotinate and can also fulfill the larval requirements in this vitamin, even though they cannot synthesize it. However, genome-based metabolic predictions suggest that Ap^{WJL} may compensate for the lack of nicotinate by producing intermediates such as nicotinate-D-ribonucleotide, NAD⁺, and NADP⁺. In the case of Lp^{NC8} , we postulate the existence of alternative metabolic pathways leading to nicotinate intermediate biosynthesis.

Lp^{NC8} cannot grow in the absence of Phe (Fig 3A). The genomic analyses point to the possible loss of the gene coding for the enzyme prephenate dehydratase (4.2.1.51), the penultimate step on Phe biosynthesis, yet Lp^{NC8} can fulfill larval requirements for Phe (Fig 4A). We wondered whether the Phe auxotrophy we observed in 96-well plates (Fig 3A) was due to the oxygenation generated by the agitation through OD readings, as for Thr, Ala, and Asp (Fig 3B).

To test this, we set cultures of Lp^{NC8} in HD Δ Phe in static 15-mL closed falcon tubes and assessed bacterial growth after 3 days of culture. In contrast to agitation, Lp^{NC8} grows in HD Δ Phe up to 10^6 CFUs in static conditions (Fig 5B), whereas in the complete media (Fig 3B), Lp^{NC8} grows up to 5×10^8 CFUs. These results indicate that the rescue of larvae DT by Lp^{NC8} in HD Δ Phe is still mediated by bacterial nutrient supply. However, the poor growth of Lp^{NC8} in HD Δ Phe suggests the existence of an alternative pathway for Phe biosynthesis in absence of the prephenate dehydratase (Fig 1A). As suggested by Hadadi and colleagues [84], Phe might be produced from L-arogenate using a derivative catalysis through the 2.5.1.47 activity, which is encoded in Lp^{NC8} by the *cysD* gene (nc8_2167) (S2 Table).

A second such interesting case is larval development rescue by Lp^{NC8} on HD Δ Cys. Lp^{NC8} is an auxotroph for Cys (Fig 3A), even in static conditions (Fig 5B). Lp^{NC8} -associated larvae develop faster than GF larvae in HD Δ Cys, though GF larvae are not auxotrophic for Cys (Fig 4A). This beneficial effect of Lp^{NC8} on ex-GF larvae development on HD Δ Cys is similar to what is observed on a complete HD (Fig 4A, first row). Therefore, this result probably reflects the basal nutrient-independent growth-promoting effect of Lp^{NC8} , which relies on the sensing and signaling of the Lp^{NC8} cell wall by its host (S2 Fig) [23] and requires Lp^{NC8} to be metabolically active (Fig 4A, fifth column). Taken together, our results suggest that Lp^{NC8} is able to grow in HD Δ Cys only in the presence of *Drosophila* larvae. To test this hypothesis, we assessed Lp^{NC8} growth in solid HD Δ Cys in the absence and the presence of larvae (Fig 5C). Without larvae, Lp^{NC8} grew one log above the inoculum level (approximately 5×10^5 CFUs/tube) on solid HD Δ Cys (Fig 5C, “on diet only”). This minimal growth on solid HD Δ Cys could be due to the Cys reserves from Lp^{NC8} growth in rich media (De Man, Rogosa, and Sharpe [MRS] medium) prior to inoculation or from contaminants in the agar and cholesterol added to prepare the solid HD. Interestingly, in the presence of larvae in the HD Δ Cys, Lp^{NC8} CFU counts increased over time, reaching approximately 10^8 CFUs/tube at day 6 (Fig 5C, “on diet with larvae”). These results indicate that in HD Δ Cys, larvae support Lp^{NC8} growth, probably by supplying Cys or a precursor/derivative. In turn, Lp^{NC8} sensing and signaling in the host promote larval development and maturation. This observation extends the recent demonstration that *Drosophila* and *L. plantarum* engage in a mutualistic symbiosis, whereby the insect benefits the growth of the bacterium in their shared nutritional environment [30]. Here, we discover that Cys is an additional *Drosophila* symbiotic factor also previously referred to as “bacteria maintenance factor” [30].

Situation 4: Bacterial compensation of minerals and metal deficiencies by concentrating traces or by functional compensation (1/19 auxotrophy compensation). We observed that both Ap^{WJL} and Lp^{NC8} would compensate for Cu, Fe, and Zn deficiencies, but not Mg (Fig 4A, second and third columns). Requirements in Cu and Fe were also fulfilled by HK bacteria (Fig 4A, fourth and fifth columns), although larvae associated with HK bacteria in these conditions developed much slower than larvae associated with living bacteria. This suggests that the inert bacterial inoculum contains traces of Cu and Fe accumulated during the overnight growth in rich medium prior to inactivation and inoculation. These accumulated quantities allowed the larvae to develop when Cu and Fe were not supplied in the HD. Surprisingly, Zn requirements were fulfilled by living bacteria only (Fig 4A). We hypothesize that bacteria may concentrate contaminating traces of these elements in the HD and make them more available to larvae. Alternatively, this could be an interesting case of functional complementation that requires further investigation. Indeed, Zn is an important enzymatic cofactor in the biosynthesis of several metabolites by the larva [85]. In the absence of Zn, GF larvae would not produce these compounds; instead, they could be produced by the bacteria and supplied to the ex-GF larvae similarly to the nutritional complementation we observed above for choline (situation 3). Interestingly, a link between Zn response and the microbiota of *Drosophila* has been described

in previous studies. Expression of the Zn transporter *zip-3* is higher in GF *Drosophila* adults midguts than in their conventionally reared (CR) counterparts [27]. Moreover, the genes encoding metallothioneins B and C (*MtnB* and *MtnC*) are more expressed in flies harboring a microbiota than in GF flies [86]. Metallothioneins are intracellular proteins that can store Zn. Their expression, as well as expression of Zn transporters such as *zip-3*, is regulated by intracellular levels of Zn [87]. Altogether, these results suggest that host-associated bacteria may play an important role in the uptake of metals (especially Zn) by *Drosophila* larvae. This idea is reminiscent of recent reports in *Caenorhabditis elegans*, whereby a bacterium promotes worm development upon Fe scarcity by secreting a scavenging siderophore [88].

Drosophila-associated bacteria provide amino acids essential to larval development

Despite the interesting exceptions detailed above, our data establish that in many cases, *Drosophila*-associated bacteria complement the nutritional requirements of their host by synthesizing and supplying essential nutrients. Bacteria can actively excrete amino acids in their environment when they are produced in excess as intracellular byproducts of metabolic reactions [89]. Moreover, the bacterial cell wall is rich in D-amino acids, and it undergoes an important turnover [90,91]. In certain bacterial species, D-amino acids accumulate in the supernatant during growth and act as a signal to undergo stationary phase [92]. Thus, D-amino acids may also contribute to larval nutrition. Indeed, it has been previously shown that D-amino acids (D-Arg, D-His, D-Lys, D-Met, D-Phe, and D-Val) can support growth of GF larvae probably through the action of amino acid racemases [48]. We thus hypothesized that Ap^{WJL} and Lp^{NC8} could provide amino acids to their host by releasing them in the HD. To directly test this hypothesis, we cultured Ap^{WJL} and Lp^{NC8} in liquid HDs lacking each EAA^{Fly} and quantified the production of the corresponding missing EAA^{Fly}. We focused on EAAs^{Fly}, whose deficiency could be compensated by bacteria in our DT experiments (Fig 4A). In these assays, Ap^{WJL} was cultured under agitation and Lp^{NC8} cultures were grown in both agitated and static conditions (see Materials and methods). After 3 days, we quantified the amino acid concentration from bacterial supernatants using HPLC. We quantified amino acid production by Ap^{WJL} under agitation while growing in HDΔArg, HDΔHis, HDΔIle, HDΔLeu, HDΔLys, HDΔMet, HDΔPhe, HDΔThr, and HDΔVal and observed accumulation of all missing amino acids except for Lys and Met (Fig 6A). For Lp^{NC8}, we analyzed the supernatants of HDs that support Lp^{NC8} growth under agitation (Fig 3A): HDΔHis, HDΔLys, and HDΔMet. We also analyzed supernatants from static conditions, HDΔHis, HDΔLys, HDΔMet, HDΔPhe, and HDΔThr. Surprisingly, from all tested conditions, we only detected His accumulation in the supernatant of Lp^{NC8} grown on HDΔHis under agitation (Fig 6B). We did not detect Lys and Met in Ap^{WJL} culture supernatant or Lp^{NC8} culture under agitation supernatant nor His, Lys, Met, Phe, or Thr in Lp^{NC8} static culture supernatants. However, Ap^{WJL} or Lp^{NC8} can both fulfill larval requirements in an HD lacking these amino acids (Fig 4A). We only analyzed supernatants after 72 h of growth, it is therefore possible that we missed the peak of accumulation of the targeted amino acid, which may have taken place at another time point during the growth phase. Also, Ap^{WJL} and Lp^{NC8} may only secrete precursors or catabolites of those amino acids that we did not target in our analysis. Such amino acid derivatives may also be used by the larvae to compensate for the lack of the cognate amino acids in the diets (such as nicotinate or pyridoxine intermediates; see above). Alternatively, the culture conditions of bacteria on a liquid HD are likely to differ from the conditions encountered in the larval guts, and both Ap^{WJL} and Lp^{NC8} could be receiving cues from the larva itself to produce and/or secrete these nutrients. However, we detected Arg, His, Ile, Leu, Phe, Thr, and Val production by Ap^{WJL} and His

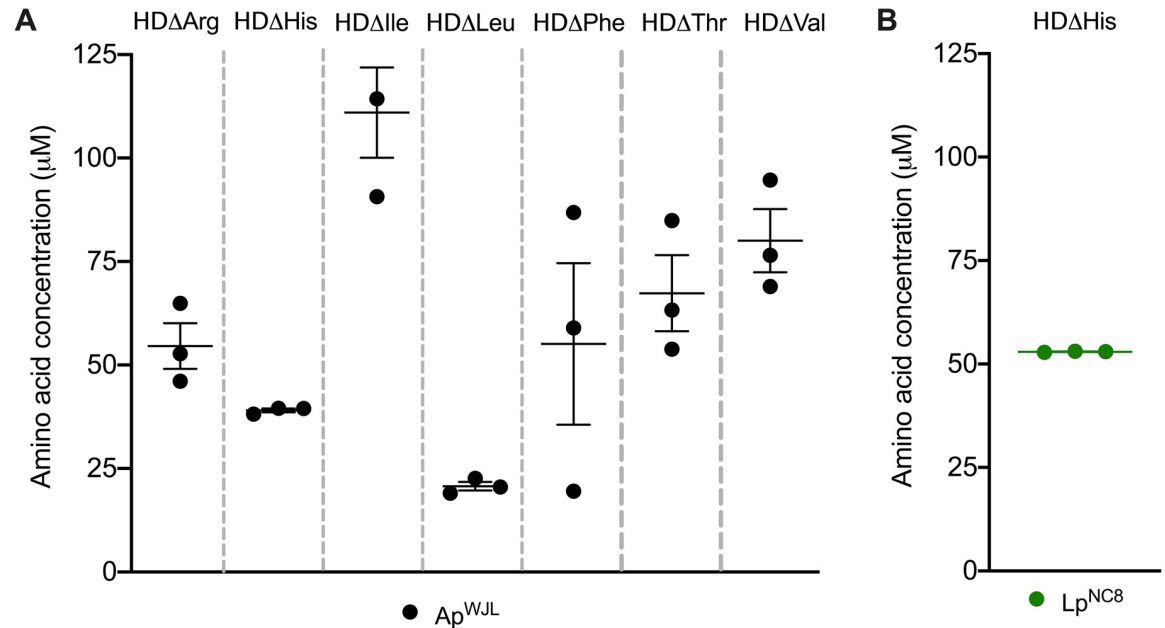


Fig 6. Ap^{WJL} and Lp^{NC8} can produce and release EAA^{Fly} during growth. (A) HPLC measured concentration of Arg, His, Ile, Leu, Phe, Thr, and Val in the supernatant of an Ap^{WJL} culture in HDΔArg, HDΔHis, HDΔIle, HDΔLeu, HDΔPhe, HDΔThr, and HDΔVal, respectively, 72 h after inoculation. Plot shows mean with standard error. Each dot shows an independent replicate. Each amino acid was not detected prior to microbial growth (S1 Data). (B) HPLC measured concentration of His in the supernatant of a Lp^{NC8} culture in HDΔHis, 72 h after inoculation. Plot shows mean with standard error. Each dot shows an independent replicate (53.08 μM, 52.82 μM, and 52.99 μM). Ap^{WJL}, *A. pomorum*^{WJL}; EAA^{Fly}, fly essential amino acid; HD, Holidic Diet; HPLC, High-Performance Liquid Chromatography; Lp^{NC8}, *L. plantarum*^{NC8}.

<https://doi.org/10.1371/journal.pbio.3000681.g006>

by Lp^{NC8}, a production that correlates with the respective abilities of Ap^{WJL} and Lp^{NC8} to compensate for the lack of these amino acids in the respective depleted HD. Of note, the concentration of newly synthesized amino acids accumulating in the supernatant is low compared to their concentration in a complete HD (20–150 μM in the former versus 1–5 mM in the latter). However, the bacterial supply of amino acids to the larvae is probably a continuous process, which may also be stimulated upon uptake and transit through the larval intestine. Thus, amino acids would directly be supplied to the larvae and will fulfill its nutritional requirements without the need to accumulate in the surrounding media.

Altogether, our results show that Ap^{WJL} and Lp^{NC8} are able to synthesize and excrete some EAA^{Fly} in their supernatants. These results confirm our hypothesis that *Drosophila*-associated bacteria Ap^{WJL} and Lp^{NC8} produce these EAA^{Fly} while growing on HDΔEAA^{Fly}. When associated with *Drosophila* larvae, Ap^{WJL} and Lp^{NC8} will therefore supply these amino acids to the larvae, allowing larval development on these deficient media as observed upon monoassociations (Fig 4A).

Conclusion

In this study, we have unraveled the interactions between the nutritional environment of *D. melanogaster* and 2 of its associated bacteria, as well as the functional importance of these interactions for *Drosophila* juvenile growth. We systematically characterized, both in genomes and in vivo, the biosynthetic capacities of growing GF larvae and 2 model bacterial strains behaving as natural partners of *Drosophila* (Ap^{WJL} and Lp^{NC8}). We show that both bacteria, each in its unique manner, alleviate the nutritional constraints in the environment to

accelerate host growth and maturation in diets depleted in essential nutrients (Fig 7). The capacity of the bacteria to fulfill 19 of the requirements in 22 essential nutrients for larvae correlated with their metabolic activity and, in most cases (15 out of 19), their ability to produce the missing nutrient. In contrast to obligate symbioses, our results highlight the clear separation between the metabolic pathways of the host and its associated bacteria and reveal a particularly integrated nutritional network between the insect and its facultative bacterial partners around the provision and utilization of nutrients.

Importantly, we further substantiate that the host requirement for essential nutrients can be fulfilled by bacterial provision of a metabolic intermediate of such nutrients (2 out of 19); for example, nicotinate intermediates by both Ap^{WJL} and Lp^{NC8} or pyridoxine intermediates by Ap^{WJL} . Interestingly, we also detected 2 situations in which nutrient compensation is not explained by a direct supply of the given nutrient or a metabolic intermediate: (i) the compensation of choline deficiency by Ap^{WJL} and (ii) the compensation of Zn deficiency by both Ap^{WJL} and Lp^{NC8} . We propose the existence of functional compensation mechanisms whereby Ap^{WJL} would complement choline deficiency by synthesizing and providing functional analogues of choline derivatives such as ethanolamine or glycerol derivatives. In addition, both *Drosophila*-associated bacteria would compensate Zn deficiency by uptaking, concentrating, and delivering contaminant traces of Zn to the host.

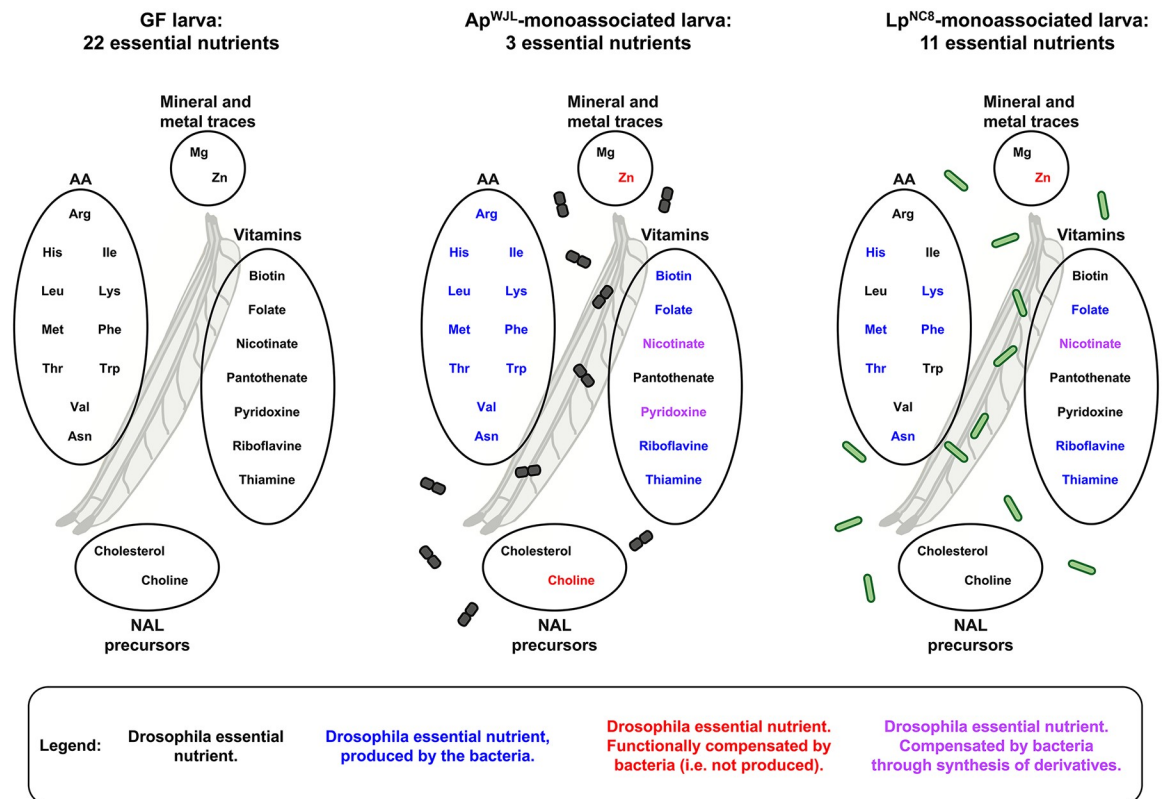


Fig 7. Ap^{WJL} and Lp^{NC8} differentially shape the nutritional requirements of their juvenile host. For each gnotobiotic condition, essential nutrients are represented in black and nonessential nutrients in color. Color code: blue, this nutrient can be synthesized by the bacteria; red, this nutrient cannot be synthesized by the bacteria, suggesting a mechanism of functional compensation. In purple: lack of this nutrient may be compensated by an intermediate metabolite or a derivative produced by the bacteria. AA, amino acid; Ap^{WJL} , *A. pomorum*^{WJL}; GF, germ-free; Lp^{NC8} , *L. plantarum*^{NC8}; NAL, nucleic acid and lipid.

<https://doi.org/10.1371/journal.pbio.3000681.g007>

Previous works have shown different mechanisms of growth promotion by microbes in a global low-nutrient context: *Drosophila* larvae can feed on inert microbes to extract nutrients [30,79,93], and living microbes can improve amino acid absorption by increasing the host's intestinal peptidase activity [23,32] and increasing nutrient-sensing-related hormonal signals [20,25]. Here, we show that in addition, the metabolic activities of live *Drosophila*-associated bacteria correct host auxotrophies. These results reveal a novel, to our knowledge, facet of the facultative nutritional mutualism engaged between *Drosophila* and its associated bacteria, which supports the host's nutritional versatility and may allow its juvenile forms to better cope with changes in nutrient availability during the critical phase of postnatal growth, hence ensuring optimal host fitness. Our work lays the basis for further mechanistic studies to investigate whether and how host-associated bacteria regulate the synthesis and release of essential nutrients for the host and whether the host influences this process. Dissecting how bacteria functionally compensate for nutrients that they cannot produce, catabolize excess nutrients, or detoxify toxic molecules also constitutes attractive perspectives for future investigations.

In some cases, the genome-based predictions of bacterial biosynthetic capabilities were incongruent with our *in vivo* assessment of bacterial auxotrophies (S6 Table). Such seeming discrepancies served as an entry point for us to discover novel, to our knowledge, phenomena and interactions that would have been missed had we only adopted a single approach. One such interesting example is the Asn auxotrophy unique to the *Drosophila yw* line in GF conditions. Another one is the larval provision of Cys (or its derivatives) to Lp^{NC8} to maintain a mutualistic nutritional exchange between host and associated bacteria. Previously, a combination of genomic and *in vivo* approaches has been successfully used for bacteria [62] but not applied to complex symbiotic systems such as facultative host-bacteria nutritional interactions. Indeed, reports characterized these interactions at the genome level [94], but they were not confirmed *in vivo*. Our work fills this gap and emphasizes the importance of using parallel systematic genome-based annotation, pathway reconstruction, and *in vivo* approaches for understanding the intricate relationships between the microbial and the nutritional environments and their impact on animal juvenile growth.

Materials and methods

Expert automated genome annotation and reconstruction of the biosynthetic potential of *D. melanogaster*, Ap^{WJL}, and Lp^{NC8}

We used the CycADS [59], an automated annotation management system, to integrate protein annotations from the complete genomes of *D. melanogaster* (RefSeq GCF_000001215.4 release 6), *A. pomorum* strain DM001 (accession: NCBI Bioproject PRJNA60787), and *L. plantarum* subsp. *plantarum* NC8 (NCBI Bioproject PRJNA67175). CycADS collects protein annotation results from different annotation methods, including KAAS [95], PRIAM [96], Blast2GO [97,98], and InterProScan [99], in order to obtain Enzyme Commission numbers and Gene Ontology annotations. All annotation information was then processed in the CycADS SQL database and automatically extracted to generate appropriate input files to build the 3 BioCyc databases using the Pathway Tools software v22.5 [100]. The BioCyc databases and their associated metabolic networks are available in the EcoCyc database [101]. From the genomic analyses, we inferred the biosynthetic capabilities of the 3 organisms and manually inspected all pathways allowing production of the organic compounds that are present in the exome-based FLYAA HD [40]. For each gap found in biosynthetic pathways or nonconventional enzymatic catalysis, TBLASTN [102] searches were performed in the 3 genomes to look for unpredicted protein activities. Alternative pathways were searched in the literature or using the BioCyc “Metabolic Route Search” tool [103].

Drosophila diets, stocks, and breeding

D. melanogaster stocks were reared as described previously [32]. Briefly, flies were kept at 25 °C with 12:12-h dark/light cycles on a yeast/cornmeal medium containing 50 g/L of inactivated yeast, 80 g/L of cornmeal, 7.4 g/L of agar, 4 mL/L of propionic acid, and 5.2 g/L of nipagin. GF stocks were established as described previously [86] and maintained in yeast/cornmeal medium supplemented with an antibiotic cocktail composed of kanamycin (50 µg/mL), ampicillin (50 µg/mL), tetracycline (10 µg/mL), and erythromycin (5 µg/mL). Axenicity was tested by plating fly media on nutrient agar plates. *D. melanogaster yw* flies were used as the reference strain in this work. Other *D. melanogaster* lines used include a WT strain from the DGRP collection, DGRP_25210 [78], and the *w*¹¹¹⁸ line [104].

Experiments were performed on HD without preservatives. Complete HD, with a total of 8 g/L of amino acids, was prepared as described by Piper and colleagues using the FLYAAs [40]. Briefly, sucrose, agar, and amino acids with low solubility (Ile, Leu, and Tyr), as well as stock solutions of metal ions and cholesterol, were combined in an autoclavable bottle with milli-Q water up to the desired volume, minus the volume of solutions to be added after autoclaving. After autoclaving at 120 °C for 15 min, the solution was allowed to cool down at room temperature to approximately 60 °C. Acetic acid buffer and stock solutions for the essential and non-essential amino acids, vitamins, nucleic acids, and lipids were added. Single-nutrient-deficient HD was prepared following the same recipe, excluding the nutrient of interest (named HDΔX, X being the nutrient omitted). Tubes used to pour the HD were sterilized under UV for 20 min. HD was stored at 4 °C until use for no longer than 1 week.

Bacterial strains and growth conditions

Ap^{WJL} [25], Lp^{NC8} [105], Ap^{WJL::Tnpqq} [25], and Lp^{NC8Δdlt_{op}} [23] were used in this study. Ap^{WJL} has been isolated from the midgut of a laboratory-raised adult *Drosophila* [19]. Lp^{NC8} has been isolated from grass silage [105], but we previously showed that it associates effectively with *Drosophila* and benefit its juvenile growth [23]. We use this strain as a model *Drosophila*-associated bacteria thanks to its genetic tractability (no plasmid and high transformation efficiency). *A. pomorum* strains were cultured in 10 mL of Mannitol Broth (Bacto peptone 3 g/L [Becton Dickinson, Sparks, MD USA], yeast extract 5 g/L [Becton Dickinson], D-mannitol 25 g/L [Carl Roth, Karlsruhe, Germany]) in a 50-mL flask at 30 °C under 180 rpm during 24 h. *L. plantarum* strains were cultured in 10 mL of MRS broth (Carl Roth) in 15-mL culture tubes at 37 °C, without agitation, overnight. Liquid or solid cultures of Ap^{WJL::Tnpqq} were supplemented with kanamycin (Sigma-Aldrich, Darmstadt, Germany) at a final concentration of 50 µg/mL. CFU counts were performed for all strains on MRS agar (Carl Roth) plated using the Easyspiral automatic plater (Interscience, Saint-Nom-la-Bretèche, France). The MRS agar plates were then incubated for 24–48 h at 30 °C for Ap^{WJL} or 37 °C for Lp^{NC8}. CFU counts were done using the automatic colony counter Scan1200 (Interscience) and its counting software.

Bacterial growth in liquid HD

To assess bacterial growth in the fly nutritional environment, we developed a liquid HD comprising all HD components except agar and cholesterol. Liquid HD was prepared as described for HD. Single-nutrient-deficient liquid HD was prepared following the same recipe, excluding the nutrient of interest. After growth in culture media, PBS-washed Ap^{WJL} or Lp^{NC8} was inoculated at a final concentration of approximately 10⁶ CFU/mL in 200 µL of either complete liquid HD or nutrient-deficient liquid HD. Cultures were incubated in 96-well microtiter plates (Nunc Edge 2.0; Thermo Fisher Scientific, Waltham, MA, USA) at 30 °C for 72 h.

Growth was monitored using an SPECTROstar^{Nano} (BMG Labtech GmbH, Ortenberg, Germany) by measuring the optical density at 600 nm (OD_{600}) every 30 min. Heatmap in Fig 3A represents the maximal OD detected during the 72 h of growth (average of 3 replicates). The whole experiment was repeated at least twice. Fig 3A was created using the `imagesc` function in MATLAB (version 2016b; The MathWorks, Natick, MA, USA). *Lp*^{NC8} growth in static conditions was performed in 10 mL of liquid HD in 15-mL falcon tubes inoculated at a final concentration of approximately 10^4 CFU/mL. Cultures were incubated at 30 °C for 72 h. After incubation, cultures were diluted in PBS and plated on MRS agar as described above.

Bacterial growth in solid HD

Bacterial CFUs in HD Δ Cys were assessed in presence or absence of *Drosophila* larvae. Microtubes containing 400 μ L of HD and 0.75- to 1-mm glass microbeads were inoculated with approximately 10^4 CFUs of *Lp*^{NC8}. Five first-instar larvae, collected from eggs laid on HD Δ Cys, were added. The tubes were incubated at 30 °C for 0, 3, or 6 days. After incubation, 600 μ L of PBS was added directly into the microtubes. Samples were homogenized with the Precellys 24 tissue homogenizer (Bertin Technologies, Montigny-le-Bretonneux, France). Lysate dilutions (in PBS) were plated on MRS, and CFU counts were assessed as described above.

DT determination

Axenic adults were placed in sterile breeding cages overnight to lay eggs on sterile HD. The HD used to collect embryos always matched the experimental condition. Fresh axenic embryos were collected the next morning and seeded by pools of 40 in tubes containing the HD to test. For the monoassociated conditions, a total of approximately 10^7 CFUs of *Ap*^{WJL} or approximately 10^8 CFUs of *Lp*^{NC8}, washed in PBS, were inoculated on the substrate and the eggs. Inoculation of *Ap*^{WJL} was limited to approximately 10^7 CFUs because higher inoculums decreased egg-to-pupa survival. For HK conditions, washed cells of *Ap*^{WJL} or *Lp*^{NC8} were incubated for 3 h at 65 °C. Once at room temperature, embryos were inoculated with approximately 10^8 HK CFUs and approximately 10^9 HK CFUs, respectively. In the GF conditions, bacterial suspensions were replaced with sterile PBS. Tubes were incubated at 25 °C with 12:12-h dark/light cycles. The emergence of pupae was scored every day until all pupae had emerged. The experiment was stopped when no pupae emerged after 30 days. Each gnotobiotic or nutritional condition was inoculated in 5 replicates. Means, standard error of the mean, and statistical tests (Dunn test of multiple comparisons) are detailed in S4 Table. Because larvae are cannibalistic and can find missing nutrients by eating their siblings [106,107], we therefore excluded replicates with low egg-to-pupa survival (<25%, i.e., $n < 10$). Moreover, we considered that larvae failed to develop in one condition if the mean egg-to-pupa survival of the 5 replicates was inferior to 25% (for details on egg-to-pupae survival, see S5 Table). D_{50} was determined using D50App (<http://paulinejoncour.shinyapps.io/D50App>) as described previously [23]. The whole experiment was repeated at least twice. D_{50} heatmap represents the average of the 5 replicates of each gnotobiotic and nutritional condition. Fig 4A was done using the `imagesc` function on MATLAB (version 2016b; The MathWorks).

Nicotinate and pyridoxine quantification by HPLC/MS

After growth in culture media, PBS-washed *Ap*^{WJL} or *Lp*^{NC8} was inoculated in triplicates at a final concentration of approximately 10^6 CFU/mL into 10 mL of liquid HD Δ Nicotinate Δ Pyridoxine Δ Choline and HD Δ Nicotinate, respectively. *Ap*^{WJL} was grown under agitated conditions (50-mL flasks incubated at 30 °C under 180 rpm). *Lp*^{NC8} was grown under static conditions (15-mL falcon tubes at 30 °C). Samples were taken at times 0 h and 72 h. Samples

were centrifuged (5,000 rpm, 5 min). Supernatants were collected and stored at -20°C until use. Supernatants were separated on a PFP column (150×2.1 mm i.d., particle size 5 μm ; Supelco, Bellefonte PA, USA). Solvent A was 0.1% formic acid in H_2O , and solvent B was 0.1% formic acid in acetonitrile at a flow rate of 250 $\mu\text{L}/\text{min}$. Solvent B was varied as follows: 0 min, 2%; 2 min, 2%; 10 min, 5%; 16 min, 35%; 20 min, 100%; and 24 min, 100%. The column was then equilibrated for 6 min at the initial conditions before the next sample was analyzed. The volume of injection was 5 μL . High-resolution experiments were performed with a Vanquish HPLC system coupled to an Orbitrap Qexactive+ mass spectrometer (Thermo Fisher Scientific) equipped with a heated electrospray ionization probe. MS analyses were performed in positive FTMS mode at a resolution of 70,000 (at 400 m/z) in full-scan mode, with the following source parameters: the capillary temperature was 320°C , the source heater temperature 300°C , the sheath gas flow rate 40 a.u. (arbitrary unit), the auxiliary gas flow rate 10 a.u., the S-Lens RF level 40%, and the source voltage 5 kV. Metabolites were determined by extracting the exact mass with a tolerance of 5 ppm. The limit of detection was determined following the ERACHEM guideline [108]. Nicotinate and pyridoxine standards were mixed at 5 μM and diluted 13 times up to 0.48×10^{-3} μM . Each solution was injected 3 times. The limit of detection was determined as $\text{LOD} = 3 \times s'/0$, where $s'/0$ is the standard deviation of the intercept.

Choline quantification by RMN

After growth in culture media, PBS-washed Ap^{WJL} was inoculated in triplicates at a final concentration of approximately 10^6 CFU/mL into 10 mL of liquid $\text{HD}\Delta\text{Nicotinate}\Delta\text{Pyridoxine}\Delta\text{Choline}$. Ap^{WJL} was then grown under agitated conditions (50-mL flasks incubated at 30°C under 180 rpm). Samples were taken at times 0 h and 72 h. Samples were centrifuged (5,000 rpm, 5 min). Supernatants were collected and stored at -20°C until use. Supernatants were analyzed by 1H 1D NMR on a Bruker Ascend 800 MHz spectrometer (Bruker, Billerica, MA, USA) equipped with a CPCI 5-mm cryoprobe. A volume of 540 μL of supernatant was mixed to 60 μL of Trimethylsilyl Propionic Acid (TSP) 10 mM solution in D_2O for spectra calibration. A 1D 1H NMR sequence with water presaturation and a pulse angle of 30° and a complete relaxation delay of 7 s was used. An acquisition of 64,000 points was acquired (2 s acquisition time) and processed with 256,000 points.

DNA extraction and *AsnS* locus analyses

Genomic DNA from 2 adult *yw* flies was extracted as previously described [109]. Briefly, flies were ground in microtubes containing 0.75- to 1-mm glass microbeads and 500 μL of lysis buffer (Tris-HCl 10 mM, EDTA 1 mM, NaCl 1 mM [pH 8.2]) using the Precellys 24 tissue homogenizer (Bertin Technologies). Then, we added Proteinase K (PureLink Genomic DNA extraction kit; Invitrogen, Carlsbad, CA, USA) at a final concentration of 200 $\mu\text{g}/\text{mL}$ and incubated the samples at 56°C under 700 rpm agitation for 1 h. Samples were centrifuged at $10,000 \times g$ for 2 min, and we collected the supernatant. *AsnS* coding sequence was amplified by PCR (Q5 Pol High Fidelity M0491S; New England BioLabs, Ipswich, MA, USA) using the primers *AsnS_F* (CGGGCCGCTTCGTTAAAAA) and *AsnS_R* (TGGAATTCCTCAGACTTGCCA) with a Veriti Thermal Cycler (Applied BioSystems, Foster City, CA, USA). PCR products were purified using the NucleoSpin Gel and PCR Cleanup kit (Macherey-Nagel, Düren, Germany) following manufacturer's instructions. Sequencing was done by Sanger sequencing (Genewiz, Leipzig, Germany) using the following primers: *AsnS_F*, *AsnS_R*, *AsnS1* (AGGATTATGGAAAGGATCTTCTGCA), *AsnS2* (CTCCGGTCGGATTTGCATCA), *AsnS3* (TAATGCCAAAGGGGTCTCGG), and *AsnS4* (GTGCGCCAGCTGCATTTATC). The whole coding sequence was then assembled and analyzed using Geneious (version 10.1.3;

Biomatters Ltd., Auckland, New Zealand) by mapping on the reference *D. melanogaster* genome (RefSeq GCF_000001215.4 release 6).

Amino acid quantification by HPLC

After growth in culture media, PBS-washed Ap^{WJL} or Lp^{NC8} was inoculated in triplicates at a final concentration of approximately 10⁶ CFU/mL into 10 mL of each liquid HDΔEAA^{Fly} shown to support their growth and in which they fulfill larval requirements (Figs 3A and 4A). For Ap^{WJL}, this includes liquid HDΔArg, HDΔHis, HDΔIle, HDΔLeu, HDΔLys, HDΔMet, HDΔPhe, HDΔThr, and HDΔVal in agitated conditions. For Lp^{NC8}, this includes liquid HDΔHis, HDΔLys, and HDΔMet in agitated conditions and liquid HDΔHis, HDΔLys, HDΔMet, HDΔPhe, and HDΔThr in static conditions. For agitated conditions, cultures were done in 50-mL flasks and incubated at 30 °C under 180 rpm. Static conditions were performed in 15-mL falcon tubes at 30 °C. Samples were taken at times 0 h and 72 h. Samples were centrifuged (5,000 rpm, 5 min). Supernatants were collected and stored at −20 °C until use.

Amino acid quantification was performed by HPLC from the supernatants obtained at 0 h and 72 h. Samples were crushed in 320 μL of ultrapure water with a known quantity of norvaline used as the internal standard. Each sample was submitted to a classical protein hydrolysis in sealed glass tubes with Teflon-lined screw caps (6N HCl, 115 °C, for 22 h). After air vacuum removal, tubes were purged with nitrogen. All samples were stored at −20 °C and then mixed with 50 μL of ultrapure water for amino acid analyses. Amino acid analysis was performed by HPLC (Agilent 1100; Agilent Technologies, Massy, France) with a guard cartridge and a reverse phase C18 column (Zorbax Eclipse-AAA 3.5 μm, 150 × 4.6 mm; Agilent Technologies). Prior to injection, samples were buffered with borate at pH 10.2, and primary or secondary amino acids were derivatized with ortho-phthalaldehyde (OPA) or 9-fluorenylmethyl chloroformate (FMOC), respectively. The derivatization process, at room temperature, was automated using the Agilent 1313A autosampler. Separation was carried out at 40 °C, with a flow rate of 2 mL/min, using 40 mM NaH₂PO₄ (eluent A [pH 7.8], adjusted with NaOH) as the polar phase and an acetonitrile/methanol/water mixture (45:45:10, v/v/v) as the nonpolar phase (eluent B). A gradient was applied during chromatography, starting with 20% of B and increasing to 80% at the end. Detection was performed by a fluorescence detector set at 340 and 450 nm of excitation and emission wavelengths, respectively (266/305 nm for proline). These conditions do not allow for the detection and quantification of cysteine and tryptophan, so only 18 amino acids were quantified. For this quantification, norvaline was used as the internal standard, and the response factor of each amino acid was determined using a 250 pmol/μL standard mix of amino acids. The software used was the ChemStation for LC 3D Systems (Agilent Technologies).

Supporting information

S1 Fig. The Asn auxotrophy of the *yw* line is not due to mutations in the *AsnS* gene. Pair-wise alignment of the *AsnS* coding region sequenced from *D. melanogaster yw* and the *AsnS* coding region from *D. melanogaster* reference genome, Bloomington #2057. *yw*, *yellow-white*. (TIF)

S2 Fig. Lp^{NC8}Δ*dlt*_{op}, but not Ap^{WJL}::*Tnpqq*, shows a loss of function of its intrinsic growth-promoting ability in HD. D₅₀ of GF larvae and larvae associated with Ap^{WJL}, Ap^{WJL}::*Tnpqq*, Lp^{NC8}, and Lp^{NC8}Δ*dlt*_{op}, reared on complete HD. We performed a Kruskal–Wallis test followed by post hoc Dunn tests to compare each gnotobiotic condition to GF. **p*-value < 0.05, ****p*-value < 0.0001. Ap^{WJL}, *A. pomorum*^{WJL}; *dlt*, XXX; D₅₀, day when 50% of larvae

population has entered metamorphosis; GF, germ-free; HD, Holidic Diet; Lp^{NC8}, *L. plantarum*^{NC8}; ns, nonsignificant; *pqq*, pyrroloquinoline-quinone-dependent; Tn, transposon. (TIF)

S3 Fig. Quantity of Ap^{WJL} and Lp^{NC8} on different HDs in presence of larvae. (A) Bacterial load per larva at day 6 postinoculation. Boxplots show minimum, maximum, and median. Each dot shows an independent replicate. (B) Load of Ap^{WJL} and Lp^{NC8} in solid HD in presence of larvae 3 days and 6 days after inoculation. Plot shows mean with standard error based on 3 replicates by assay. Each dot represents an independent replicate. The dashed line represents the level of inoculation at $t = 0$ h (10^4 CFUs per tube). Ap^{WJL}, *A. pomorum*^{WJL}; CFU, colony-forming unit; HD, Holidic Diet; Lp^{NC8}, *L. plantarum*^{NC8}. (TIF)

S1 Table. Inference from genomic analysis of the biosynthetic capabilities for amino acid production in *D. melanogaster*, Ap^{WJL}, and Lp^{NC8}. Ap^{WJL}, *A. pomorum*^{WJL}; f/i, targeted amino acid biosynthesis is feasible/impossible in a depleted medium; Lp^{NC8}, *L. plantarum*^{NC8}. (XLSX)

S2 Table. Inference from genomic analysis of the biosynthetic capabilities for vitamins production in *D. melanogaster*, Ap^{WJL}, and Lp^{NC8}. Ap^{WJL}, *A. pomorum*^{WJL}; f/i, targeted vitamin biosynthesis is feasible/impossible in a depleted medium; Lp^{NC8}, *L. plantarum*^{NC8}. (XLSX)

S3 Table. OD_{Max} of Ap^{WJL} and Lp^{NC8} grown in 39 HDs. Mean and SEM of OD_{Max} reached by Ap^{WJL} or Lp^{NC8} grown in complete liquid HD (first line) or liquid HD lacking nutrient X (ΔX , lines below) during 72 h of growth. Ap^{WJL}, *A. pomorum*^{WJL}; HD, Holidic Diet; Lp^{NC8}, *L. plantarum*^{NC8}; OD_{Max}, maximal optical density; SEM, Standard Error of the Mean. (XLSX)

S4 Table. D₅₀ of larvae in 40 HDs and 5 gnotobiotic conditions. Mean and SEM of D₅₀ of GF larvae or larvae associated with Ap^{WJL}, Lp^{NC8}, Ap^{WJL}_{HK}, and Lp^{NC8}_{HK}. n: number of independent replicates for each condition. For each gnotobiotic condition, we performed a Kruskal–Wallis test followed by post hoc Dunn test to compare each nutritional environment to complete HD. Ap^{WJL}, *A. pomorum*^{WJL}; D₅₀, day when 50% of larvae population has entered metamorphosis; GF, germ-free; HD, Holidic Diet; HK, heat-killed; Lp^{NC8}, *L. plantarum*^{NC8}; SEM, Standard Error of the Mean. (XLSX)

S5 Table. Egg-to-pupa survival in 40 HDs and 5 gnotobiotic conditions. Mean and SEM of egg-to-pupa survival of GF larvae or larvae associated with Ap^{WJL}, Lp^{NC8}, Ap^{WJL}_{HK}, and Lp^{NC8}_{HK}. n: number of independent replicates for each condition. For each gnotobiotic condition, we performed a Kruskal–Wallis test followed by post hoc Dunn test to compare each nutritional environment to complete HD. Ap^{WJL}, *A. pomorum*^{WJL}; GF, germ-free; HD, Holidic Diet; HK, heat-killed; Lp^{NC8}, *L. plantarum*^{NC8}; SEM, Standard Error of the Mean. (XLSX)

S6 Table. Comparison of genome-based metabolic predictions with in vivo auxotrophies and bacterial complementation of larval nutritional deficiencies. Can partner A synthesize nutrient X? Prediction from automated annotation and metabolic reconstruction (from Fig 1, S1 and S2 Tables). Can partner A grow in the absence of nutrient X? Auxotrophy observed in vivo (from Fig 3A and 3B). Can bacterial partner A promote larval growth on HD ΔX ? In vivo complementation of ex-GF larvae requirements (from Fig 4A), y: yes (green), n: no (red).

Hypothesis to explain contradiction: why the different approaches do not always lead to the same conclusion. GF, germ-free; HD, Holidic Diet; NA, Nonapplicable.

(XLSX)

S1 Data. All experimental data used to generate graphs of this manuscript.

(XLSX)

Acknowledgments

We would like to thank Dali Ma for critical reading and editing of the manuscript and valuable suggestions; members of the Ribeiro and Piper labs for advice on how to effectively implement HD preparations; Edern Cahoreau, Maud Heuillet, and Floriant Bellvert from the Metatoul platform of Genopole Toulouse for NMR and LC/MS analysis; the ArthroTools platform of the SFR Biosciences (UMS3444/US8) for fly equipment and facility; and the Bloomington Stock Center for fly lines.

Author Contributions

Conceptualization: Jessika Consuegra, Théodore Grenier, François Leulier.

Data curation: Jessika Consuegra, Théodore Grenier, Patrice Baa-Puyoulet, Nicolas Parisot, Hubert Charles, Federica Calevro.

Formal analysis: Jessika Consuegra, Théodore Grenier, Patrice Baa-Puyoulet, Nicolas Parisot, Hubert Charles, Federica Calevro.

Funding acquisition: Federica Calevro, François Leulier.

Investigation: Jessika Consuegra, Théodore Grenier, Patrice Baa-Puyoulet, Isabelle Rahioui, Houssam Akherraz, Hugo Gervais, Nicolas Parisot, Pedro da Silva, Hubert Charles.

Methodology: Jessika Consuegra, Théodore Grenier.

Project administration: François Leulier.

Resources: Patrice Baa-Puyoulet, Nicolas Parisot, Pedro da Silva, Hubert Charles, Federica Calevro.

Software: Patrice Baa-Puyoulet, Nicolas Parisot, Hubert Charles, Federica Calevro.

Supervision: Jessika Consuegra, François Leulier.

Validation: Jessika Consuegra, Théodore Grenier.

Visualization: Jessika Consuegra, Théodore Grenier, Patrice Baa-Puyoulet.

Writing – original draft: Jessika Consuegra, Théodore Grenier.

Writing – review & editing: Jessika Consuegra, Théodore Grenier, Patrice Baa-Puyoulet, Isabelle Rahioui, Houssam Akherraz, Hugo Gervais, Nicolas Parisot, Pedro da Silva, Hubert Charles, Federica Calevro, François Leulier.

References

1. Lifshitz F. Nutrition and growth. *J Clin Res Pediatr Endocrinol*. 2009; 1: 157–163. <https://doi.org/10.4274/jcrpe.v1i4.39> PMID: 21274290
2. Shanley DP, Kirkwood TBL. Calorie restriction and aging: a life-history analysis. *Evolution*. 2000; 54: 740–750. <https://doi.org/10.1111/j.0014-3820.2000.tb00076.x> PMID: 10937249

3. Chipponi JX, Bleier JC, Santi MT, Rudman D. Deficiencies of essential and conditionally essential nutrients. *Am J Clin Nutr.* 1982; 35: 1112–1116. <https://doi.org/10.1093/ajcn/35.5.1112> PMID: 6805293
4. Fairweather-Tait SJ, Southon S. Bioavailability of nutrients. In: Caballero B, editor. *Encyclopedia of Food Sciences and Nutrition (Second Edition)*. Oxford: Academic Press; 2003. pp. 478–484. <https://doi.org/10.1016/B0-12-227055-X/00096-1>
5. Stewart CP, Iannotti L, Dewey KG, Michaelsen KF, Onyango AW. Contextualising complementary feeding in a broader framework for stunting prevention. *Matern Child Nutr.* 2013; 9: 27–45. <https://doi.org/10.1111/mcn.12088> PMID: 24074316
6. Smith MI, Yatsunenkov T, Manary MJ, Trehan I, Mkakosya R, Cheng J, et al. Gut microbiomes of Malawian twin pairs discordant for kwashiorkor. *Science.* 2013; 339: 548–554. <https://doi.org/10.1126/science.1229000> PMID: 23363771
7. Gehrig JL, Venkatesh S, Chang H-W, Hibberd MC, Kung VL, Cheng J, et al. Effects of microbiota-directed foods in gnotobiotic animals and undernourished children. *Science.* 2019; 365(6449): eaau4732. <https://doi.org/10.1126/science.aau4732> PMID: 31296738
8. Tennessen JM, Thummel CS. Coordinating growth and repressing maturation—insights from *Drosophila*. *Curr Biol CB.* 2011; 21: R750–R757. <https://doi.org/10.1016/j.cub.2011.06.033> PMID: 21959165
9. Douglas AE. The *Drosophila* model for microbiome research. *Lab Anim.* 2018; 47: 157–164. <https://doi.org/10.1038/s41684-018-0065-0> PMID: 29795158
10. Erkosar B, Storelli G, Defaye A, Leulier F. Host-intestinal microbiota mutualism: “learning on the fly”. *Cell Host Microbe.* 2013; 13: 8–14. <https://doi.org/10.1016/j.chom.2012.12.004> PMID: 23332152
11. Lee K-A, Lee W-J. *Drosophila* as a model for intestinal dysbiosis and chronic inflammatory diseases. *Dev Comp Immunol.* 2014; 42: 102–110. <https://doi.org/10.1016/j.dci.2013.05.005> PMID: 23685204
12. Broderick NA, Lemaitre B. Gut-associated microbes of *Drosophila melanogaster*. *Gut Microbes.* 2012; 3: 307–321. <https://doi.org/10.4161/gmic.19896> PMID: 22572876
13. Bakula M. The persistence of a microbial flora during postembryogenesis of *Drosophila melanogaster*. *J Invertebr Pathol.* 1969; 14: 365–374. [https://doi.org/10.1016/0022-2011\(69\)90163-3](https://doi.org/10.1016/0022-2011(69)90163-3) PMID: 4904970
14. Koyle ML, Veloz M, Judd AM, Wong AC-N, Newell PD, Douglas AE, et al. Rearing the fruit fly *Drosophila melanogaster* under axenic and gnotobiotic conditions. *J Vis Exp JoVE.* 2016;(113):e54219. <https://doi.org/10.3791/54219> PMID: 27500374
15. Ma D, Storelli G, Mitchell M, Leulier F. Studying host-microbiota mutualism in *Drosophila*: harnessing the power of gnotobiotic flies. *Biomed J.* 2015; 38: 285–293. <https://doi.org/10.4103/2319-4170.158620> PMID: 26068125
16. Brummel T, Ching A, Seroude L, Simon AF, Benzer S. *Drosophila* lifespan enhancement by exogenous bacteria. *Proc Natl Acad Sci.* 2004; 101: 12974–12979. <https://doi.org/10.1073/pnas.0405207101> PMID: 15322271
17. Cox CR, Gilmore MS. Native microbial colonization of *Drosophila melanogaster* and its use as a model of *Enterococcus faecalis* pathogenesis. *Infect Immun.* 2007; 75: 1565–1576. <https://doi.org/10.1128/IAI.01496-06> PMID: 17220307
18. Ren C, Webster P, Finkel SE, Tower J. Increased internal and external bacterial load during *Drosophila* aging without life-span trade-off. *Cell Metab.* 2007; 6: 144–152. <https://doi.org/10.1016/j.cmet.2007.06.006> PMID: 17681150
19. Ryu J-H, Kim S-H, Lee H-Y, Bai JY, Nam Y-D, Bae J-W, et al. Innate immune homeostasis by the homeobox gene *Caudal* and commensal-gut mutualism in *Drosophila*. *Science.* 2008; 319: 777–782. <https://doi.org/10.1126/science.1149357> PMID: 18218863
20. Storelli G, Defaye A, Erkosar B, Hols P, Royet J, Leulier F. *Lactobacillus plantarum* promotes *Drosophila* systemic growth by modulating hormonal signals through TOR-dependent nutrient sensing. *Cell Metab.* 2011; 14: 403–414. <https://doi.org/10.1016/j.cmet.2011.07.012> PMID: 21907145
21. Adair KL, Wilson M, Bost A, Douglas AE. Microbial community assembly in wild populations of the fruit fly *Drosophila melanogaster*. *ISME J.* 2018; 12: 959. <https://doi.org/10.1038/s41396-017-0020-x> PMID: 29358735
22. Pais IS, Valente RS, Sporniak M, Teixeira L. *Drosophila melanogaster* establishes a species-specific mutualistic interaction with stable gut-colonizing bacteria. *PLoS Biol.* 2018; 16. <https://doi.org/10.1371/journal.pbio.2005710> PMID: 29975680
23. Matos RC, Schwarzer M, Gervais H, Courtin P, Joncour P, Gillet B, et al. D-Alanylation of teichoic acids contributes to *Lactobacillus plantarum*-mediated *Drosophila* growth during chronic undernutrition. *Nat Microbiol.* 2017; 2: 1635–1647. <https://doi.org/10.1038/s41564-017-0038-x> PMID: 28993620

24. Schretter CE, Vielmetter J, Bartos I, Marka Z, Marka S, Argade S, et al. A gut microbial factor modulates locomotor behaviour in *Drosophila*. *Nature*. 2018; 563: 402. <https://doi.org/10.1038/s41586-018-0634-9> PMID: 30356215
25. Shin SC, Kim S-H, You H, Kim B, Kim AC, Lee K-A, et al. *Drosophila* microbiome modulates host developmental and metabolic homeostasis via insulin signaling. *Science*. 2011; 334: 670–674. <https://doi.org/10.1126/science.1212782> PMID: 22053049
26. Blum JE, Fischer CN, Miles J, Handelsman J. Frequent replenishment sustains the beneficial microbiome of *Drosophila melanogaster*. *mBio*. 2013; 4: e00860–00813. <https://doi.org/10.1128/mBio.00860-13> PMID: 24194543
27. Broderick NA, Buchon N, Lemaitre B. Microbiota-induced changes in *Drosophila melanogaster* host gene expression and gut morphology. *mBio*. 2014; 5: e01117–14. <https://doi.org/10.1128/mBio.01117-14> PMID: 24865556
28. Winans NJ, Walter A, Chouaia B, Chaston JM, Douglas AE, Newell PD. A genomic investigation of ecological differentiation between free-living and *Drosophila*-associated bacteria. *Mol Ecol*. 2017; 26: 4536–4550. <https://doi.org/10.1111/mec.14232> PMID: 28667798
29. Obadia B, Güvener ZT, Zhang V, Ceja-Navarro JA, Brodie EL, Ja WW, et al. Probabilistic invasion underlies natural gut microbiome stability. *Curr Biol* CB. 2017; 27: 1999–2006.e8. <https://doi.org/10.1016/j.cub.2017.05.034> PMID: 28625783
30. Storelli G, Strigini M, Grenier T, Bozonnet L, Schwarzer M, Daniel C, et al. *Drosophila* perpetuates nutritional mutualism by promoting the fitness of its intestinal symbiont *Lactobacillus plantarum*. *Cell Metab*. 2018; 27: 362–377.e8. <https://doi.org/10.1016/j.cmet.2017.11.011> PMID: 29290388
31. Ma D, Leulier F. The importance of being persistent: The first true resident gut symbiont in *Drosophila*. *PLoS Biol*. 2018; 16: e2006945. <https://doi.org/10.1371/journal.pbio.2006945> PMID: 30071013
32. Erkosar B, Storelli G, Mitchell M, Bozonnet L, Bozonnet N, Leulier F. Pathogen virulence impedes mutualist-mediated enhancement of host juvenile growth via inhibition of protein digestion. *Cell Host Microbe*. 2015; 18: 445–455. <https://doi.org/10.1016/j.chom.2015.09.001> PMID: 26439865
33. Sannino DR, Dobson AJ, Edwards K, Angert ER, Buchon N. The *Drosophila melanogaster* gut microbiota provisions thiamine to its host. *mBio*. 2018; 9: e00155–18. <https://doi.org/10.1128/mBio.00155-18> PMID: 29511074
34. Piper MD. Using artificial diets to understand the nutritional physiology of *Drosophila melanogaster*. *Curr Opin Insect Sci*. 2017; 23: 104–111. <https://doi.org/10.1016/j.cois.2017.07.014> PMID: 29129274
35. Staats S, Lüersen K, Wagner AE, Rimbach G. *Drosophila melanogaster* as a versatile model organism in food and nutrition research. *J Agric Food Chem*. 2018; 66: 3737–3753. <https://doi.org/10.1021/acs.jafc.7b05900> PMID: 29619822
36. Lüersen K, Röder T, Rimbach G. *Drosophila melanogaster* in nutrition research—the importance of standardizing experimental diets. *Genes Nutr*. 2019; 14: 3. <https://doi.org/10.1186/s12263-019-0627-9> PMID: 30766617
37. Schultz J, St Lawrence P, Newmeyer D. A chemically defined medium for the growth of *Drosophila melanogaster*. *Anat Rec*. 1946; 96: 540.
38. Sang JH. The quantitative nutritional requirements of *Drosophila melanogaster*. *J Exp Biol*. 1956; 33: 45–72.
39. Hinton T, Noyes DT, Ellis J. Amino acids and growth factors in a chemically defined medium for *Drosophila*. *Physiol Zool*. 1951; 24: 335–353.
40. Piper MDW, Soultoukis GA, Blanc E, Mesaros A, Herbert SL, Juricic P, et al. Matching dietary amino acid balance to the *in silico*-translated exome optimizes growth and reproduction without cost to lifespan. *Cell Metab*. 2017; 25: 610–621. <https://doi.org/10.1016/j.cmet.2017.02.005> PMID: 28273481
41. Jang T, Lee KP. Comparing the impacts of macronutrients on life-history traits in larval and adult *Drosophila melanogaster*: the use of nutritional geometry and chemically defined diets. *J Exp Biol*. 2018; 221(Pt. 21): jeb.181115. <https://doi.org/10.1242/jeb.181115> PMID: 30171098
42. Piper MDW, Blanc E, Leitão-Gonçalves R, Yang M, He X, Linford NJ, et al. A holdic medium for *Drosophila melanogaster*. *Nat Methods*. 2014; 11: 100–105. <https://doi.org/10.1038/nmeth.2731> PMID: 24240321
43. Troen AM, French EE, Roberts JF, Selhub J, Ordovas JM, Parnell LD, et al. Lifespan modification by glucose and methionine in *Drosophila melanogaster* fed a chemically defined diet. *Age Dordr Neth*. 2007; 29: 29–39. <https://doi.org/10.1007/s11357-006-9018-4> PMID: 19424828
44. Sang JH, King RC. Nutritional requirements of axenically cultured *Drosophila melanogaster* adults. *J Exp Biol*. 1961; 38: 793–809.
45. Leitão-Gonçalves R, Carvalho-Santos Z, Francisco AP, Fioreze GT, Anjos M, Baltazar C, et al. Commensal bacteria and essential amino acids control food choice behavior and reproduction. *PLoS Biol*. 2017; 15: e2000862. <https://doi.org/10.1371/journal.pbio.2000862> PMID: 28441450

46. Wu Q, Yu G, Park SJ, Gao Y, Ja WW, Yang M. Excreta quantification (EX-Q) for longitudinal measurements of food intake in *Drosophila*. *iScience*. 2019; 23: 100776. <https://doi.org/10.1016/j.isci.2019.100776> PMID: 31901635
47. Mishra D, Thorne N, Miyamoto C, Jagge C, Amrein H. The taste of ribonucleosides: novel macronutrients essential for larval growth are sensed by *Drosophila* gustatory receptor proteins. *PLoS Biol*. 2018; 16: e2005570. <https://doi.org/10.1371/journal.pbio.2005570> PMID: 30086130
48. Geer BW. Utilization of D-amino acids for growth by *Drosophila melanogaster* larvae. *J Nutr*. 1966; 90: 31–39. <https://doi.org/10.1093/jn/90.1.31> PMID: 5918848
49. Lee W-C, Micchelli CA. Development and characterization of a chemically defined food for *Drosophila*. *PLoS ONE*. 2013; 8: e67308. <https://doi.org/10.1371/journal.pone.0067308> PMID: 23844001
50. Rapport EW, Stanley-Samuels D, Dadd RH. Ten generations of *Drosophila melanogaster* reared axenically on a fatty acid-free holidic diet. *Arch Insect Biochem Physiol*. 1983; 1: 243–250. <https://doi.org/10.1002/arch.940010307>
51. i5K Consortium. The i5K Initiative: advancing arthropod genomics for knowledge, human health, agriculture, and the environment. *J Hered*. 2013; 104: 595–600. <https://doi.org/10.1093/jhered/est050> PMID: 23940263
52. Baa-Puyoulet P, Parisot N, Febvay G, Huerta-Cepas J, Vellozo AF, Gabaldón T, et al. ArthropodaCyc: a CycADS powered collection of BioCyc databases to analyse and compare metabolism of arthropods. *Database J Biol Databases Curation*. 2016; 2016: baw081. <https://doi.org/10.1093/database/baw081> PMID: 27242037
53. Cottret L, Milreu PV, Acuña V, Marchetti-Spaccamela A, Stougie L, Charles H, et al. Graph-based analysis of the metabolic exchanges between two co-resident intracellular symbionts, *Baumannia cicadellinicola* and *Sulcia muelleri*, with their insect host, *Homalodisca coagulata*. *PLoS Comput Biol*. 2010; 6: e1000904. <https://doi.org/10.1371/journal.pcbi.1000904> PMID: 20838465
54. Magnúsdóttir S, Heinken A, Kutt L, Ravcheev DA, Bauer E, Noronha A, et al. Generation of genome-scale metabolic reconstructions for 773 members of the human gut microbiota. *Nat Biotechnol*. 2017; 35: 81–89. <https://doi.org/10.1038/nbt.3703> PMID: 27893703
55. Ankrah NYD, Chouaia B, Douglas AE. The cost of metabolic interactions in symbioses between Insects and Bacteria with reduced genomes. *mBio*. 2018; 9: e01433–18. <https://doi.org/10.1128/mBio.01433-18> PMID: 30254121
56. Opatovsky I, Santos-Garcia D, Ruan Z, Lahav T, Ofaim S, Mouton L, et al. Modeling trophic dependencies and exchanges among insects' bacterial symbionts in a host-simulated environment. *BMC Genomics*. 2018; 19: 402. <https://doi.org/10.1186/s12864-018-4786-7> PMID: 29801436
57. Wilson ACC, Ashton PD, Calevro F, Charles H, Colella S, Febvay G, et al. Genomic insight into the amino acid relations of the pea aphid, *Acyrtosiphon pisum*, with its symbiotic bacterium *Buchnera aphidicola*. *Insect Mol Biol*. 2010; 19 Suppl 2: 249–258. <https://doi.org/10.1111/j.1365-2583.2009.00942.x> PMID: 20482655
58. Russell CW, Bouvaine S, Newell PD, Douglas AE. Shared metabolic pathways in a coevolved insect-bacterial symbiosis. *Appl Environ Microbiol*. 2013; 79: 6117–6123. <https://doi.org/10.1128/AEM.01543-13> PMID: 23892755
59. Vellozo AF, Véron AS, Baa-Puyoulet P, Huerta-Cepas J, Cottret L, Febvay G, et al. CycADS: an annotation database system to ease the development and update of BioCyc databases. *Database J Biol Databases Curation*. 2011; 2011: bar008. <https://doi.org/10.1093/database/bar008> PMID: 21474551
60. Rao MRR, Stokes JL. Nutrition of the acetic acid bacteria. *J Bacteriol*. 1953; 65: 405–412. PMID: 13069394
61. Saguir FM, de Nadra MCM. Improvement of a chemically defined medium for the sustained growth of *Lactobacillus plantarum*: nutritional requirements. *Curr Microbiol*. 2007; 54: 414–418. <https://doi.org/10.1007/s00284-006-0456-0> PMID: 17503149
62. Teusink B, van Enckevort FHJ, Francke C, Wiersma A, Wegkamp A, Smid EJ, et al. *In silico* reconstruction of the metabolic pathways of *Lactobacillus plantarum*: comparing predictions of nutrient requirements with those from growth experiments. *Appl Environ Microbiol*. 2005; 71: 7253–7262. <https://doi.org/10.1128/AEM.71.11.7253-7262.2005> PMID: 16269766
63. Bringel F, Hubert J-C. Extent of genetic lesions of the arginine and pyrimidine biosynthetic pathways in *Lactobacillus plantarum*, *L. paraplantarum*, *L. pentosus*, and *L. casei*: prevalence of CO(2)-dependent auxotrophs and characterization of deficient arg genes in *L. plantarum*. *Appl Environ Microbiol*. 2003; 69: 2674–2683. <https://doi.org/10.1128/AEM.69.5.2674-2683.2003> PMID: 12732536
64. Kurnasov O, Goral V, Colabroy K, Gerdes S, Anantha S, Osterman A, et al. NAD biosynthesis: identification of the tryptophan to quinolinate pathway in bacteria. *Chem Biol*. 2003; 10: 1195–1204. <https://doi.org/10.1016/j.chembiol.2003.11.011> PMID: 14700627

65. Matsushita K, Toyama H, Tonouchi N, Okamoto-Kainuma A, editors. Acetic acid bacteria: ecology and physiology. Tokyo: Springer Japan; 2016.
66. Hanada T, Kashima Y, Kosugi A, Koizumi Y, Yanagida F, Udaka S. A gene encoding phosphatidylethanolamine N-methyltransferase from *Acetobacter aceti* and some properties of its disruptant. *Biosci Biotechnol Biochem*. 2001; 65: 2741–2748. <https://doi.org/10.1271/bbb.65.2741> PMID: 11826972
67. Sohlenkamp C, Geiger O. Bacterial membrane lipids: diversity in structures and pathways. *FEMS Microbiol Rev*. 2016; 40: 133–159. <https://doi.org/10.1093/femsre/fuv008> PMID: 25862689
68. Chandrangsu P, Rensing C, Helmann JD. Metal homeostasis and resistance in bacteria. *Nat Rev Microbiol*. 2017; 15: 338–350. <https://doi.org/10.1038/nrmicro.2017.15> PMID: 28344348
69. Rosenberg E, DeLong EF, Lory S, Stackebrandt E, Thompson F, editors. The Prokaryotes: *Alphaproteobacteria* and *Betaproteobacteria*. 4th ed. Berlin Heidelberg: Springer-Verlag; 2014.
70. Siezen RJ, Tzeneva VA, Castioni A, Wels M, Phan HTK, Rademaker JLW, et al. Phenotypic and genomic diversity of *Lactobacillus plantarum* strains isolated from various environmental niches. *Environ Microbiol*. 2010; 12: 758–773. <https://doi.org/10.1111/j.1462-2920.2009.02119.x> PMID: 20002138
71. Martino ME, Bayjanov JR, Caffrey BE, Wels M, Joncour P, Hughes S, et al. Nomadic lifestyle of *Lactobacillus plantarum* revealed by comparative genomics of 54 strains isolated from different habitats. *Environ Microbiol*. 2016; 18: 4974–4989. <https://doi.org/10.1111/1462-2920.13455> PMID: 27422487
72. Teusink B, Wiersma A, Molenaar D, Francke C, de Vos WM, Siezen RJ, et al. Analysis of growth of *Lactobacillus plantarum* WCFS1 on a complex medium using a genome-scale metabolic model. *J Biol Chem*. 2006; 281: 40041–40048. <https://doi.org/10.1074/jbc.M606263200> PMID: 17062565
73. Wegkamp A, Teusink B, De Vos Wm, Smid Ej. Development of a minimal growth medium for *Lactobacillus plantarum*. *Lett Appl Microbiol*. 2010; 50: 57–64. <https://doi.org/10.1111/j.1472-765X.2009.02752.x> PMID: 19874488
74. Groot MNN, Klaassens E, de Vos WM, Delcour J, Hols P, Kleerebezem M. Genome-based in silico detection of putative manganese transport systems in *Lactobacillus plantarum* and their genetic analysis. *Microbiology*. 2005; 151: 1229–1238. <https://doi.org/10.1099/mic.0.27375-0> PMID: 15817790
75. Vos P, Garrity G, Jones D, Krieg NR, Ludwig W, Rainey FA, et al., editors. *Bergey's manual of systematic bacteriology: volume 3: the Firmicutes*. 2nd ed. New York: Springer-Verlag; 2009.
76. Ikawa M. Nature of the lipids of some lactic acid bacteria. *J Bacteriol*. 1963; 85: 772–781. PMID: 14044942
77. Patterson MK, Orr GR. Asparagine biosynthesis by the Novikoff Hepatoma isolation, purification, property, and mechanism studies of the enzyme system. *J Biol Chem*. 1968; 243: 376–380. PMID: 4295091
78. Mackay TFC, Richards S, Stone EA, Barbadilla A, Ayroles JF, Zhu D, et al. The *Drosophila melanogaster* Genetic Reference Panel. *Nature*. 2012; 482: 173–178. <https://doi.org/10.1038/nature10811> PMID: 22318601
79. Keebaugh ES, Yamada R, Obadia B, Ludington WB, Ja WW. Microbial quantity impacts *Drosophila* nutrition, development, and lifespan. *iScience*. 2018; 4: 247–259. <https://doi.org/10.1016/j.isci.2018.06.004> PMID: 30240744
80. Wong AC-N, Dobson AJ, Douglas AE. Gut microbiota dictates the metabolic response of *Drosophila* to diet. *J Exp Biol*. 2014; 217: 1894–1901. <https://doi.org/10.1242/jeb.101725> PMID: 24577449
81. Huang Z, London E. Cholesterol lipids and cholesterol-containing lipid rafts in bacteria. *Chem Phys Lipids*. 2016; 199: 11–16. <https://doi.org/10.1016/j.chemphyslip.2016.03.002> PMID: 26964703
82. Hammad LA, Cooper BS, Fisher NP, Montooth KL, Karty JA. Profiling and quantification of *Drosophila melanogaster* lipids using liquid chromatography/mass spectrometry: Lipid composition of *Drosophila melanogaster*. *Rapid Commun Mass Spectrom*. 2011; 25: 2959–2968. <https://doi.org/10.1002/rcm.5187> PMID: 21913275
83. Jones HE, Harwood JL, Bowen ID, Griffiths G. Lipid composition of subcellular membranes from larvae and prepupae of *Drosophila melanogaster*. *Lipids*. 1992; 27: 984–987. <https://doi.org/10.1007/bf02535576> PMID: 1487960
84. Hadadi N, MohammadiPeyhani H, Miskovic L, Seijo M, Hatzimanikatis V. Enzyme annotation for orphan and novel reactions using knowledge of substrate reactive sites. *Proc Natl Acad Sci U S A*. 2019; 116: 7298–7307. <https://doi.org/10.1073/pnas.1818877116> PMID: 30910961
85. Navarro JA, Schneuwly S. Copper and zinc homeostasis: lessons from *Drosophila melanogaster*. *Front Genet*. 2017; 8: 223. <https://doi.org/10.3389/fgene.2017.00223> PMID: 29312444
86. Combe BE, Defaye A, Bozonnet N, Puthier D, Royet J, Leulier F. *Drosophila* microbiota modulates host metabolic gene expression via IMD/NF- κ B signaling. *PLoS ONE*. 2014; 9: e104120. <https://doi.org/10.1371/journal.pone.0094729> PMID: 24733183

87. Hennigar SR, Kelley AM, McClung JP. Metallothionein and zinc transporter expression in circulating human blood cells as biomarkers of zinc status: a systematic review. *Adv Nutr.* 2016; 7: 735–746. <https://doi.org/10.3945/an.116.012518> PMID: 27422508
88. Qi B, Han M. Microbial siderophore enterobactin promotes mitochondrial iron uptake and development of the host via interaction with ATP synthase. *Cell.* 2018; 175: 571–582.e11. <https://doi.org/10.1016/j.cell.2018.07.032> PMID: 30146159
89. Goffin P, van de Bunt B, Giovane M, Leveau JHJ, Höppener-Ogawa S, Teusink B, et al. Understanding the physiology of *Lactobacillus plantarum* at zero growth. *Mol Syst Biol.* 2010; 6: 413. <https://doi.org/10.1038/msb.2010.67> PMID: 20865006
90. Typas A, Banzhaf M, Gross CA, Vollmer W. From the regulation of peptidoglycan synthesis to bacterial growth and morphology. *Nat Rev Microbiol.* 2011; 10: 123–136. <https://doi.org/10.1038/nrmicro2677> PMID: 22203377
91. Boothby D, Daneo-Moore L, Higgins ML, Coyette J, Shockman GD. Turnover of bacterial cell wall peptidoglycans. *J Biol Chem.* 1973; 248: 2161–2169. PMID: 4632249
92. Lam H, Oh D-C, Cava F, Takacs CN, Clardy J, de Pedro MA, et al. D-amino acids govern stationary phase cell wall re-modeling in Bacteria. *Science.* 2009; 325: 1552–1555. <https://doi.org/10.1126/science.1178123> PMID: 19762646
93. Yamada R, Deshpande SA, Bruce KD, Mak EM, Ja WW. Microbes promote amino acid harvest to rescue undernutrition in *Drosophila*. *Cell Rep.* 2015; 10(6): 865–872. <https://doi.org/10.1016/j.celrep.2015.01.018> PMID: 25683709
94. Newell PD, Chaston JM, Wang Y, Winans NJ, Sannino DR, Wong ACN, et al. In vivo function and comparative genomic analyses of the *Drosophila* gut microbiota identify candidate symbiosis factors. *Front Microbiol.* 2014; 5: 576. <https://doi.org/10.3389/fmicb.2014.00576> PMID: 25408687
95. Moriya Y, Itoh M, Okuda S, Yoshizawa AC, Kanehisa M. KAAS: an automatic genome annotation and pathway reconstruction server. *Nucleic Acids Res.* 2007; 35: W182–185. <https://doi.org/10.1093/nar/gkm321> PMID: 17526522
96. Claudel-Renard C, Chevalet C, Faraut T, Kahn D. Enzyme-specific profiles for genome annotation: PRIAM. *Nucleic Acids Res.* 2003; 31: 6633–6639. <https://doi.org/10.1093/nar/gkg847> PMID: 14602924
97. Conesa A, Götz S, García-Gómez JM, Terol J, Talón M, Robles M. Blast2GO: a universal tool for annotation, visualization and analysis in functional genomics research. *Bioinforma Oxf Engl.* 2005; 21: 3674–3676. <https://doi.org/10.1093/bioinformatics/bti610> PMID: 16081474
98. Conesa A, Götz S. Blast2GO: A comprehensive suite for functional analysis in plant genomics. *Int J Plant Genomics.* 2008; 2008: 619832. <https://doi.org/10.1155/2008/619832> PMID: 18483572
99. Jones P, Binns D, Chang H-Y, Fraser M, Li W, McAnulla C, et al. InterProScan 5: genome-scale protein function classification. *Bioinforma Oxf Engl.* 2014; 30: 1236–1240. <https://doi.org/10.1093/bioinformatics/btu031> PMID: 24451626
100. Karp PD, Latendresse M, Paley SM, Krummenacker M, Ong QD, Billington R, et al. Pathway Tools version 19.0 update: software for pathway/genome informatics and systems biology. *Brief Bioinform.* 2016; 17: 877–890. <https://doi.org/10.1093/bib/bbv079> PMID: 26454094
101. Karp PD, Weaver D, Paley S, Fulcher C, Kubo A, Kothari A, et al. The EcoCyc Database. *EcoSal Plus.* 2014; 6: ecosalplus.ESP-0009-2013. <https://doi.org/10.1128/ecosalplus.ESP-0009-2013> PMID: 26442933
102. Altschul SF, Gish W, Miller W, Myers EW, Lipman DJ. Basic local alignment search tool. *J Mol Biol.* 1990; 215: 403–410. [https://doi.org/10.1016/S0022-2836\(05\)80360-2](https://doi.org/10.1016/S0022-2836(05)80360-2) PMID: 2231712
103. Latendresse M, Krummenacker M, Karp PD. Optimal metabolic route search based on atom mappings. *Bioinforma Oxf Engl.* 2014; 30: 2043–2050. <https://doi.org/10.1093/bioinformatics/btu150> PMID: 24642060
104. Teixeira L, Ferreira Á, Ashburner M. The Bacterial Symbiont *Wolbachia* Induces Resistance to RNA Viral Infections in *Drosophila melanogaster*. *PLoS Biol.* 2008; 6: e1000002. <https://doi.org/10.1371/journal.pbio.1000002> PMID: 19222304
105. Axelsson L, Rud I, Naterstad K, Blom H, Renckens B, Boekhorst J, et al. Genome sequence of the naturally plasmid-free *Lactobacillus plantarum* strain NC8 (CCUG 61730). *J Bacteriol.* 2012; 194: 2391–2392. <https://doi.org/10.1128/JB.00141-12> PMID: 22493200
106. Ahmad M, Chaudhary SU, Afzal AJ, Tariq M. Starvation-induced dietary behaviour in *Drosophila melanogaster* larvae and adults. *Sci Rep.* 2015; 5: 14285. <https://doi.org/10.1038/srep14285> PMID: 26399327
107. Vijendravarma RK, Narasimha S, Kawecki TJ. Predatory cannibalism in *Drosophila melanogaster* larvae. *Nat Commun.* 2013; 4: 1789. <https://doi.org/10.1038/ncomms2744> PMID: 23653201

108. Magnusson, B., Örnemark, U. The fitness for purpose of analytical methods: a laboratory guide to method validation and related topics. 2014 [cited 2020 Jan 14]. <https://www.eurachem.org/>.
109. Green MR, Sambrook J. Molecular cloning: a laboratory manual, fourth edition. 4th edition. Cold Spring Harbor, NY: Cold Spring Harbor Laboratory Press US; 2012.

Chapter II:

A symbiotic bacterium supports the growth of its host on an unbalanced diet through GCN2 activation in the intestine

Article in preparation.

A symbiotic bacterium supports the growth of its host on an unbalanced diet through GCN2 activation in the intestine

Grenier T.¹, Consuegra J.¹, Akherraz H.¹, Hugues S.¹, Gillet B.¹, Matos R.¹, Leulier F^{1*}.

¹. Institut de Génomique Fonctionnelle de Lyon (IGFL), Ecole Normale Supérieure de Lyon, CNRS UMR 5242, Université Claude Bernard Lyon 1, 69364 Lyon Cedex 07, France

*corresponding author : francois.leulier@ens-lyon.fr

Abstract

Animals have evolved and are living in constant association with microbes. One important feature of such symbiosis is the optimization of host growth in situation of malnutrition. However, how symbionts achieve this remains partly elusive. Our lab and others have showed that *Drosophila*'s symbiotic bacteria such as *Lactiplantibacillus plantarum* (Lp) buffer the developmental delay in *Drosophila* larvae facing a global amino acids (AA) scarcity. Here we wondered whether Lp could also buffer the developmental delay due to alterations in AA composition. To test this, we fed the larvae a diet composed of chemically pure nutrients, which allows us to manipulate AA composition. We generated AA unbalance by reducing the amount of Valine, an essential AA. We observed that AA unbalance by Valine reduction delays the growth of Germ-Free (GF) larvae, and this delay can be rescued by association with Lp. Lp cannot synthesize Valine, which indicates that buffering of AA unbalance by Lp does not rely on AA providing. In order to understand the mechanisms underlying Lp's effect, we tested the implication of growth-regulating AA-sensing pathways such as GCN2. GCN2 is a kinase that is activated by unloaded tRNAs, a proxy for AA scarcity, and allows adaptation to AA scarcity in all Eukaryotes. We showed that expression of GCN2 in the larval midgut is necessary for Lp to buffer AA unbalance. Moreover, we showed that Lp can activate GCN2 in a specific region of the larval midgut. Through a genetic screen in Lp using a library of insertion mutants, we found that 3 different operons encoding ribosomal and transfer RNAs are necessary for Lp to rescue AA unbalance and to activate GCN2 in the larval midgut. These results indicate that r/tRNAs produced by Lp are necessary to activate GCN2. Finally, we analysed the larval anterior midgut's transcriptome and identified transcriptional signatures of activation of GCN2 by Lp that may explain the rescue of growth delay by Lp on unbalanced diet. Our work provides a novel mechanistical understanding of the host-symbionts molecular dialogue shaping animal growth in response to altered nutritional environments.

Introduction

Nutrition is one of the major factors influencing the growth trajectory of animals (Lifshitz, 2009). Juvenile animals that feed on an inadequate source of nutrients (either in term of nutrient quantity or quality, *i.e.* malnutrition) face important growth alteration. The gut microbiota (*i.e.* the communities of microorganisms that are found in the intestinal tract of animals) plays a major role in the interplay between nutrition and growth (Schwarzer et al., 2018). Especially, certain strains of bacteria promote growth of young Mammals suffering from chronic undernutrition (*i.e.* fed a nutrient-poor diet for a long period of time) (Blanton et al., 2016; Schwarzer et al., 2016), which has inspired the development of microbiota-guided renutrition strategies for undernourished children (Gehrig et al., 2019). However, the mechanisms underlying the growth-supporting activities of bacterial strains during malnutrition remain largely elusive.

The fruit fly *Drosophila melanogaster* (hereinafter referred to as *Drosophila*) is a powerful model to study the influence of bacteria on animal growth. Indeed, *Drosophila* harbours simple bacterial communities, which individual component can be cultured and genetically engineered. Moreover, the *Drosophila* growth phase (larval stages) is short (4-5 days in optimal nutritional conditions, up to 15-20 days in severe malnutrition conditions) (Erkosar et al., 2013; Tennessen and Thummel, 2011). Reducing the quantity of nutrients greatly delays the development of Germ-Free (GF) *Drosophila* larvae (*i.e.* larvae lacking a microbiota) and such delay can be buffered by the association of GF animals with certain strains of symbiotic bacteria (Keebaugh et al., 2018; Shin et al., 2011; Storelli et al., 2011). In this context, sensing of symbiotic bacteria by gut cells leads to the production of digestive enzymes (Erkosar et al., 2015) and the mobilization of lipid stores (Kamareddine et al., 2018) which support juvenile growth.

Previous studies on the effect of *Drosophila*'s microbiota on growth rely on oligidic diets, *i.e.* diets made of nutritionally complex components such as dry yeast and cornflour. Such diets allow to grossly manipulate nutrient quantity (for instance, by decreasing the amount of dry yeast) but not nutrient composition; reducing the amount of dry yeast leads to an indiscriminate decrease of all amino acids, vitamins, lipids, cholesterol and many other unidentified compounds present in yeast cells. On the contrary, holidic diets (diets made of chemically pure nutrients) allow to finely control the nutritional composition of *Drosophila*'s diet (Piper, 2017). Especially, the holidic diet (HD) developed by Hinton and colleagues in the early 50' (Hinton et al., 1951), and later improved by others (Piper et al., 2014, 2017; Sang, 1956), contains all 20 proteinogenic amino acids (AA), allowing the precise control over the quantity of each AA in experimental diets.

AA are among the most important nutrients for juvenile growth (Wu, 2009): beside being the building blocks of proteins, they can fuel the energy metabolism through

gluconeogenesis (Grasmann et al., 2019), act as methyl donors (Niculescu and Zeisel, 2002) or as precursors for vitamins biosynthesis (Castro-Portuguez and Sutphin, 2020). Moreover, they are major regulators of cell and organismal physiology through two AA-sensing pathways engaging the target-of-rapamycin (TOR) and the general control nonderepressible 2 (GCN2) kinases (Gallinetti et al., 2013). Both kinases were first described in yeast (Dever et al., 1992; Heitman et al., 1991) and orthologous pathways were found in virtually all eukaryotes, including *Drosophila* (Olsen et al., 1998; Zhang et al., 2002). The TOR kinase forms two proteic complexes: mTORC1 and mTORC2, which can be activated by many cues (Laplante and Sabatini, 2009). Especially, mTORC1 responds to high intracellular AA levels through the action of AA transporters and AA-binding cytosolic proteins (Goberdhan et al., 2016). Once activated, TOR increases translation through phosphorylation of 4E-BP and S6K (Ma and Blenis, 2009). GCN2 is activated by binding to uncharged tRNAs, a signature of hampered protein synthesis due to a scarcity of intracellular AA (Masson, 2019). Activation of GCN2 causes a global translational repression through phosphorylation of the Eukaryotic Initiation Factor 2 (eIF2 α) (Teske et al., 2011). In addition to their cell-autonomous effects, TOR and GCN2 pathways have systemic effects. In *Drosophila*, activation of TOR by AA in the fat body stimulates juvenile growth (Colombani et al., 2003a) through the modulation of Insulin-Like Peptides secretion in the brain (Géminard et al., 2009; Marshall et al., 2012) and ecdysone production in the prothoracic gland (Layalle et al., 2008; Ohhara et al., 2017). Ubiquitous knock-down of GCN2 in *Drosophila* larvae causes developmental delay but the tissue specificity of the phenotype and the underlying mechanisms coupling GCN2 activity to systemic growth remain elusive (Malzer et al., 2013). Moreover, activation of GCN2 in dopaminergic neurons of the larval brain (Bjordal et al., 2014) or in the enterocytes of adult flies (Kim et al., 2021) trigger a marked behavioural response leading to the avoidance of diets with an unbalanced AA composition. AA unbalance causes marked developmental delays in *Drosophila* larvae (Piper et al., 2017). Indeed, Piper and colleagues recently designed a HD which AA composition mirrors the composition of *Drosophila*'s exome, which they called FLY AA (Piper et al., 2017). The FLY AA diet was compared to the historical MM1 AA diet (Hinton et al., 1951), which has the same overall quantity of AA and other nutrients, but a different AA composition. The FLY AA diet is superior to the MM1 AA diet to support *Drosophila*'s lifespan, fecundity and development, which indicates that AA composition in diets and not just quantity greatly influences these parameters.

Given the role of the microbiota in buffering growth defects during chronic undernutrition, we wondered if and how symbiotic bacteria would buffer growth delays due to malnutrition in the form of dietary AA unbalance. Moreover, we wondered whether the TOR and/or GCN2 AA-sensing pathways would regulate juvenile growth upon AA unbalance, and if yes, whether the symbiotic bacteria would engage these major regulators of cell and organismal physiology to support systemic growth. To this end, we used Holidic Diets to determine the contribution of *Lactiplantibacillus plantarum* (Lp), a major symbiotic bacterium of *Drosophila*, to larval development on

diets with unbalanced AA compositions. We found that GF larvae are severely impacted by dietary AA unbalance. Moreover, Lp-association improves the growth of larvae fed an AA-unbalanced diet, even when the unbalance is based on a decrease of Branch-Chain AA that Lp cannot synthesize. We found that this Lp-mediated support to growth during dietary AA unbalance requires the activation of the GCN2 pathway by Lp in enterocytes of the anterior larval midgut. We performed a genetic screen of Lp's genome to understand how Lp can activate GCN2, and our results suggest that it may rely on the sensing of bacterial ribosomal and/or transfer RNAs by host GCN2. Finally, we used *Drosophila* transcriptomics to illustrate the biological processes downstream GCN2 that may contribute to the support of larval growth by symbiotic bacteria on an AA-unbalanced diet.

Results

I Association with Lp rescues amino-acid unbalance

In order to test the effect of AA unbalance on *Drosophila* growth independently of any microbial influence, we compared the development of GF larvae reared on the FLY AA diet, which AA composition is based on *Drosophila*'s exome, to larvae reared on the historical MM1 AA diet (Piper et al., 2017). FLY AA and MM1 AA diet show the same total concentration of AA (10,7 g.L⁻¹) but differ in AA composition (Fig. 1A). GF larvae reared on the MM1 AA diet show an important growth delay compared to GF larvae reared on the FLY AA diet (Fig. 1B, grey curves). Consistently with previous observations made on conventionally-reared larvae (Piper et al., 2017), Lp-associated larvae are slightly delayed on the MM1 AA diet compared to the FLY AA diet; however, the difference is much less important than observed for GF larvae (Fig. 1B), indicating that association with Lp rescues to a large extent the developmental delay due to dietary AA unbalance.

We next wondered whether the developmental delay of GF larvae on unbalanced diet was due to the limiting quantity of specific essential AA (EAA). To test this hypothesis, we generated AA unbalance by selectively and uniquely decreasing the concentration of each EAA by 60% from the FLY AA diet. As expected, decreasing the concentration of any EAA causes growth delay in GF larvae. Decreasing the amount of certain EAA (Ile, Lys, Thr, Trp, Val) results in a particularly important growth delay. Decreasing the amount of the other EAA (Arg, His, Met, Leu, Phe) causes only a minor delay in GF larvae development compared to the balanced diet. In most cases, association with Lp significantly improves growth on unbalanced diets compared to the balanced diet, except for the diets scarce in Arg and Phe (Fig. 1C). It was previously shown that *Drosophila*'s symbiotic bacteria can synthesize AA and provide them to their host to compensate for AA scarcity (Consuegra et al., 2020a; Kim et al., 2021). However, Lp has limited AA biosynthetic capacities: its genome does not encode the enzymes necessary for the synthesis of Branched-Chain AA (BCAA: Leucine, Isoleucine and

Valine) (Martino et al., 2016; Saguir and de Nadra, 2007; Teusink et al., 2005), and thus it cannot provide them to its host (Consuegra et al., 2020a; Kim et al., 2021). Therefore, we were interested by the fact that Lp rescues the developmental delay caused by an AA unbalance due to a decrease in BCAA which it cannot synthesize *de novo*. We decided to focus on diets reduced in Valine (Val) to decipher the mechanisms underlying Lp's effect. We thereafter refer to the FLY AA diet as "balanced diet", and to the FLY AA -60% Val diet as "unbalanced diet" (Fig. 1D). Decreasing Val by 60% results in a strong delay in the growth of GF larvae, which is almost completely rescued by association with Lp (Fig. 1E). Of note, further decreasing Val concentration (-80%, -90%) is lethal to GF larvae, but not to Lp-associated larvae (Fig. S1A). Completely removing Val from the diet is lethal to both GF larvae and Lp-associated larvae (Consuegra et al., 2020a). On the contrary, increasing Val by 100% compared to its initial levels does not change the development of GF or Lp-associated larvae (Fig. S1B). Egg-to-pupa survival is not impacted by AA unbalance nor by association with Lp (Fig. S1C). Replacing the missing Val with an equal quantity of another EAA (Leu or His) does not improve the development of GF larvae (Fig. S1D). This shows that the delay observed on unbalanced diet is due to AA unbalance rather than total AA scarcity. Moreover, supplementing the GF larvae with Heat-Killed (HK) Lp does not to rescue the effects of an unbalanced diet on larval growth, which indicates that the Val brought by the inoculation of Lp at the beginning of the experiment is not sufficient to restore Val levels required for larval growth (Fig. S1E). Taken together, these results suggest that Lp can rescue the effects of dietary AA unbalance on larval growth through a mechanism independent of AA providing. Instead, we posit that Lp promotes adaptation of its host's physiology to dietary AA unbalance to support larval growth.

Figure 1

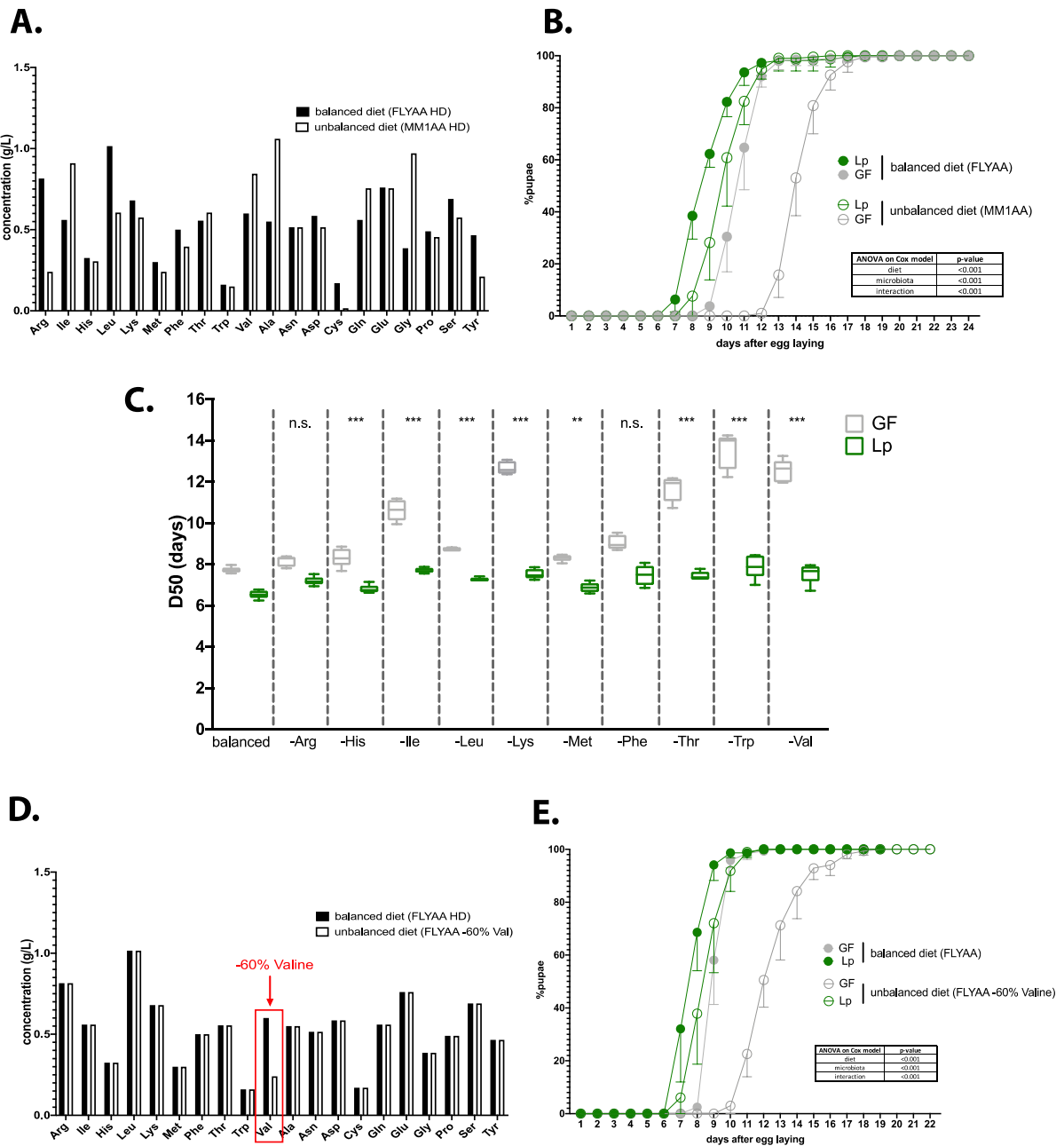


Fig. 1 Lp rescues the developmental delay due to AA unbalance.

(A) AA composition of the balanced diet (FLY AA, black bars) and the unbalanced diet (MM1 AA, white bars). The Y-axis represents the concentration of each AA in the diet ($\text{g}\cdot\text{L}^{-1}$). (B) Developmental timing of larvae raised on balanced diet (FLY AA, filled circles) or unbalanced diet (MM1 AA, empty circles) in GF condition (grey circles) or Lp-associated conditions (green circles). The graph represents the total fraction of emerged pupae over time as a percentage of the final number of pupae. We used a Cox proportional hazards model to test the effect of the diet, the association with Lp, and the interaction between these two parameters. (C) Developmental timing of GF larvae (grey) and Lp-associated larvae

(green) on diets with a -60% decrease of each EAA. Boxplots show maximum, minimum and median D50 (median time of pupariation) of each replicate. For each diet, we used a Cox proportional hazards model to test the effect of the diet, association with Lp, and the interaction between these two parameters. We show the p-values of the interactions between diet and association Lp after correction by the Holm method. n.s.: non-significant, **: p-value<0.01, ***: p-value<0.001. (D) AA composition of the balanced diet (FLY AA, black bars) and the unbalanced diet (FLY AA-60% Val, white bars). The Y-axis represents the concentration of each AA in the diet (g.L⁻¹). (E) Developmental timing of larvae raised on balanced diet (FLY AA, filled circles) or unbalanced diet (FLY AA-60% Val, empty circles) in GF condition (grey circles) or Lp-associated conditions (green circles). The graph represents the total fraction of emerged pupae over time as a percentage of the final number of pupae. We used a Cox proportional hazards model to test the effect of the diet, association with Lp, and the interaction between these two parameters.

II Rescue of AA unbalance by Lp requires GCN2 in the larval midgut

Eukaryotes adapt their cellular and systemic physiology to AA availability through TOR or GCN2 pathways. We therefore wondered whether the association with Lp during dietary AA unbalance functionally interacts with the activity of these pathways. In *Drosophila*, it was previously reported that AA (or lack of) engage the TOR and/or GCN2 pathways in fat body cells (Colombani et al., 2003b; Géminard et al., 2009; Koyama et al., 2020), in brain dopaminergic neurons (Bjordal et al., 2014; Manière et al., 2020) or enterocytes of the midgut (Kim et al., 2021). Given that GCN2 activity in dopaminergic neurons of the larval brain promotes avoidance to EAA-deficient diets (Bjordal et al., 2014), we first tested whether Lp association alter larval food intake in our experimental conditions where larvae have no food choice to operate. We observed that Lp does not change the food intake on balanced diet (Fig. S2A) or on unbalanced diet (Fig. S2B).

Next, using tissue specific *in vivo* RNAi (Dietzl et al., 2007), we altered the expression of the TOR (Fig. 2A,B) or GCN2 (Fig. 2C,D) kinases in either fat-body cells (Fig. 2A,C) or enterocytes (Fig. 2B,D) and followed the developmental timing of GF or Lp-associated animals on dietary AA unbalanced conditions. Knocking-down TOR expression in fat body cells (Fig. 2A) or enterocytes (Fig. 2B), or knocking-down GCN2 expression in fat body cells (Fig. 2C) has no impact on the development of Lp-associated larvae fed an unbalanced diet. On the contrary, GCN2 knock-down (Fig. S2C) in enterocytes causes a significant developmental delay in Lp-associated larvae compared to control animals (Fig. 2D), a phenotype that we did not observe while Lp-associated larvae develop on an AA balanced diet (Fig. S2D) and that we confirmed using two other GCN2 RNAi lines (Fig. 2E,F). Importantly, GCN2 knock-down in enterocytes does not alter Lp intestinal loads (Fig. S2E). TOR pathway is required both in the fat body and enterocytes to support growth of GF larvae only (Fig. 2A,B). Taken together these results indicate that the support provided by Lp to animals developing on AA unbalanced diets requires a functional GCN2 pathway in enterocytes. This phenotype is independent of the intrinsic role or the TOR kinase in supporting larval development in GF animals. Of note, these results are in sharp contrast with chronic undernutrition conditions, whereby TOR pathway activity in the fat body does contribute to Lp-mediated growth promotion (Storelli et al., 2011).

We next wondered whether GCN2 is necessary to rescue AA unbalance due to scarcity in the other EAA. We thus decreased the amount of each EAA identified in Fig. 1B as important for GF larvae (Ile, Lys, Thr and Trp) by 60% and measured the growth of larvae knocked-down for GCN2. We found that GCN2 is necessary for Lp to rescue the scarcity in Ile or Thr, but not in Trp or Lys (Fig.S2F-I). Lp can synthesize Lys and Trp, but not Ile (Consuegra et al., 2020a); therefore, it seems that GCN2 is necessary only when the limiting AA cannot be provided by Lp. Lp can produce Thr, but in limiting quantity (Consuegra et al., 2020a), which may explain why GCN2 is also necessary for Lp to rescue the delay due to Thr scarcity. Moreover, we observed that association with a strain of *Acetobacter pomorum* (Ap), another symbiotic bacterium often found in the *Drosophila* midgut, can also rescue AA unbalance due to Val scarcity. Conversely to Lp, Ap's support to larval development upon Val scarcity is independent of GCN2 expression in the gut and likely explained by the ability of Ap to produce Val and rescue the host's auxotrophy to Val (Fig. S2J, (Consuegra et al., 2020a)). Taken together, our results thus demonstrate the specific role of GCN2 pathway in enterocytes to mediate Lp's support to larval development despite dietary AA unbalance.

Figure 2

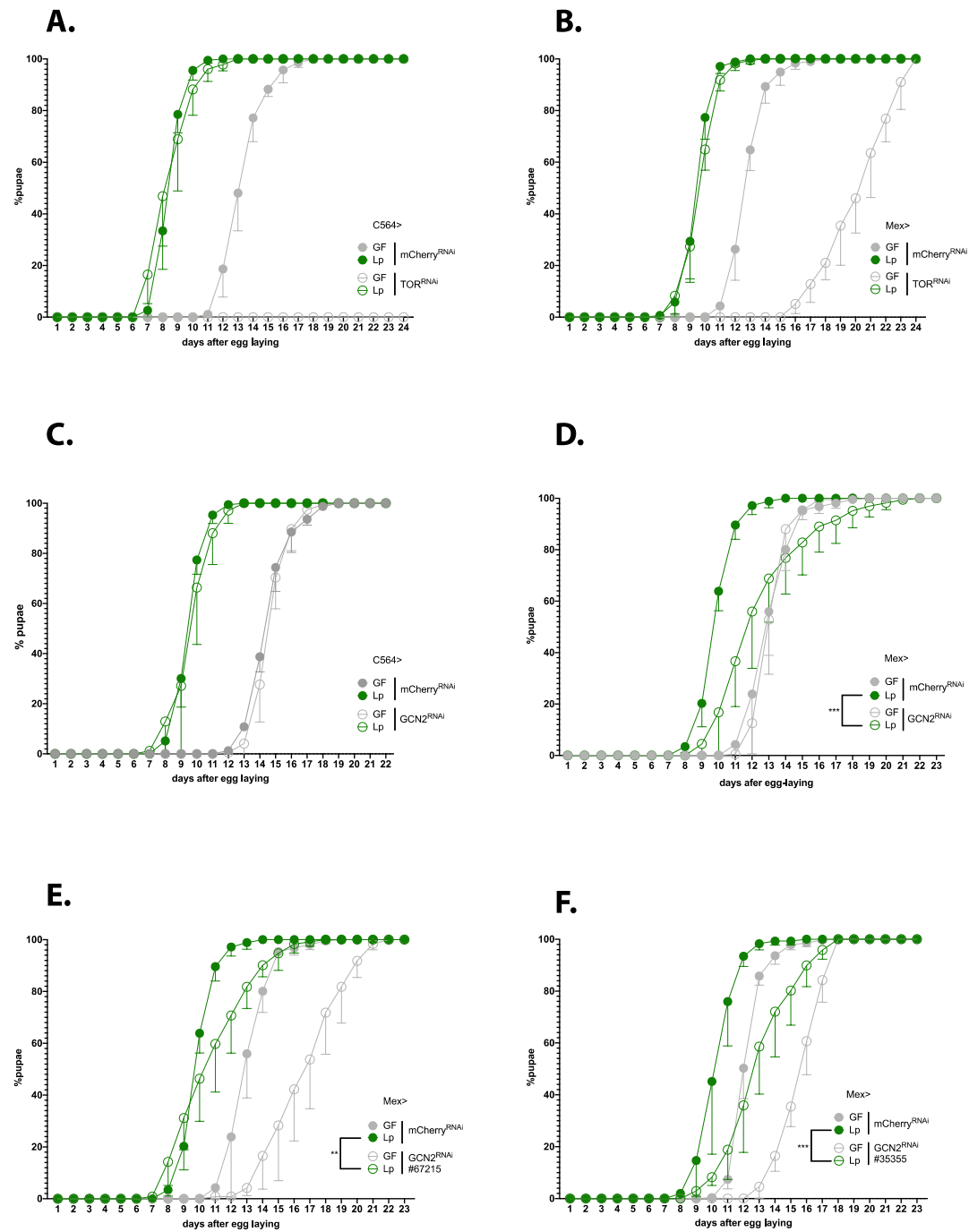


Fig. 2 Expression of GCN2 in the gut is necessary for Lp to rescue the delay due to AA unbalance.

All panels show developmental timing of larvae raised on unbalanced diet (FLY AA -60% Val) in GF condition (grey circles) or Lp-associated conditions (green circles), in a control background (Mex>mCherry^{RNAi}, filled circles) or in a knock-down background (empty circles). The graphs represent the total fraction of emerged pupae over time as a percentage of the final number of pupae. (A) TOR knock-down in the fat body. (B) TOR knock-down in the enterocytes. (C) GCN2 knock-down in the fat body. (D-F) GCN2 knock-down in the enterocytes using the lines #KK103976 (D), #BL67215 (E) and #BL35355 (F). We used a Cox proportional hazards model to compare the effect of Lp in the control background and in the GCN2 knock-down background. **: p-value<0.01. ***: p-value<0.001.

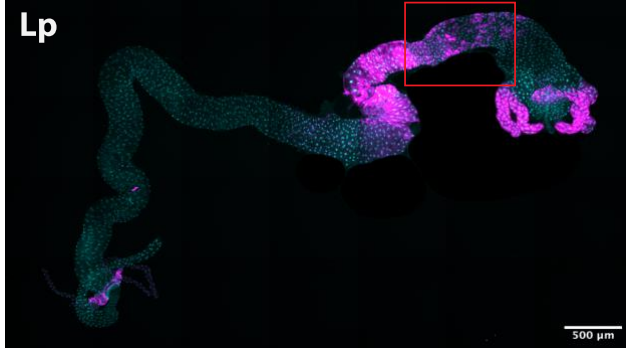
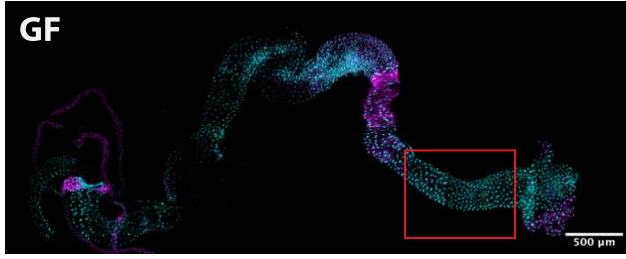
III Lp activates GCN2 in the anterior midgut

GCN2 activation allows adaptation to nutrient-scarce conditions (Gallinetti et al., 2013). Moreover, we showed that the expression of GCN2 in enterocytes is necessary for Lp to support development on AA unbalanced diets. Therefore, we hypothesized that Lp may activate GCN2 in the larva's enterocytes, promoting adaptation to an unbalanced diet. Activation of GCN2 causes phosphorylation of eIF2 α . This results in repression of translation, except for a subset of mRNAs which translation is increased (Donnelly et al., 2013). One of the mRNAs which translation is increased by eIF2 α phosphorylation is the transcription factor ATF4 (crc in *Drosophila*) (B'chir et al., 2013). In *Drosophila*, ATF4 can bind to recognition sites in the first intron of the gene *4E-BP* (*Thor* in *Drosophila*) and activate its transcription. Kang and colleagues generated the transgenic line *4E-BP^{intron}dsRed*, which carries a fluorophore under the transcriptional control of the first intron of *4E-BP*. This reporter thus allows to visualize the pattern of activity of ATF4 downstream of GCN2 (Kang et al., 2017; Vasudevan et al., 2017). Therefore, we used the *4E-BP^{intron}dsRed* reporter as a readout to probe GCN2 activity in the larval midgut. Fig. 3A shows the pattern of expression of the *4E-BP^{intron}dsRed* reporter in dissected guts of larvae fed an unbalanced diet, either GF (top panel) or Lp-associated (bottom panel). Similarly to what was previously reported (Kang et al., 2017), we observed *4E-BP^{intron}dsRed* reporter activation in the gastric caeca, the proventriculus and in the middle midgut, in a region known as the acidic zone (Overend et al., 2016). This pattern is conserved between GF larvae and Lp-associated larvae. Conversely, the *4E-BP^{intron}dsRed* reporter is activated in the anterior midgut specifically in Lp-associated larvae, while this signal is absent from GF guts (red square and quantification of signal in Fig. 3B,C). Importantly, we confirmed by RT-qPCR that endogenous GCN2-dependant *4E-BP* expression was induced in the anterior midgut upon Lp-association on unbalanced diet (Fig. S3). Interestingly, activation of *4E-BP^{intron}dsRed* reporter in this region depends on the association with Lp, but not on AA unbalance as we observed it in larvae raised on either unbalanced diet (Fig. 3B) or balanced diet (Fig. 3C). Lp can thus activate the *4E-BP^{intron}dsRed* reporter specifically in the anterior midgut, independently of dietary AA unbalance.

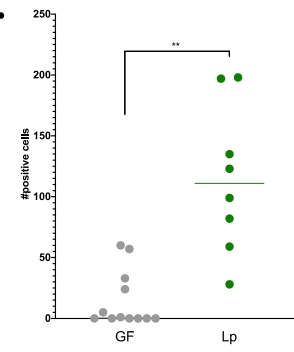
ATF4 is activated by eIF2 α , which can be phosphorylated by GCN2 but also by other kinases such as PERK (Teske et al., 2011). In order to test whether the *4E-BP^{intron}dsRed* reporter indeed mirrors GCN2 activity, we looked at its pattern of expression in a GCN2 knock-down background (Fig. 3D). Inhibition of GCN2 by RNAi completely abrogate the activation of the *4E-BP^{intron}dsRed* reporter by Lp in the anterior midgut of larvae reared on unbalanced diet (Fig. 3E) or balanced diet (Fig. 3F). Therefore, our results establish that Lp can activate GCN2 activity in the anterior midgut of larvae, independently of AA unbalance.

Figure 3

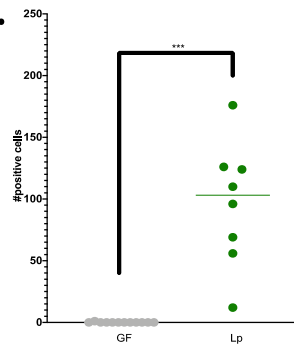
A.



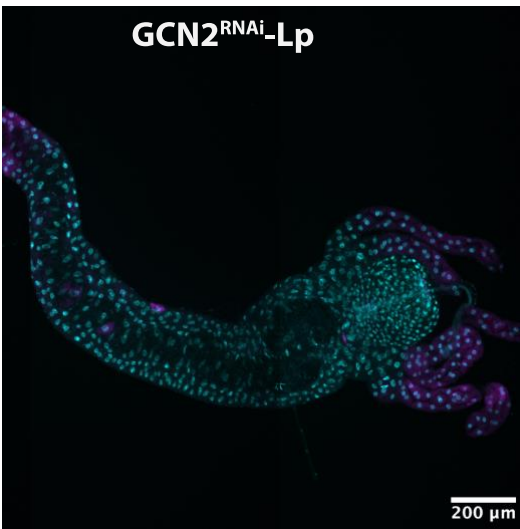
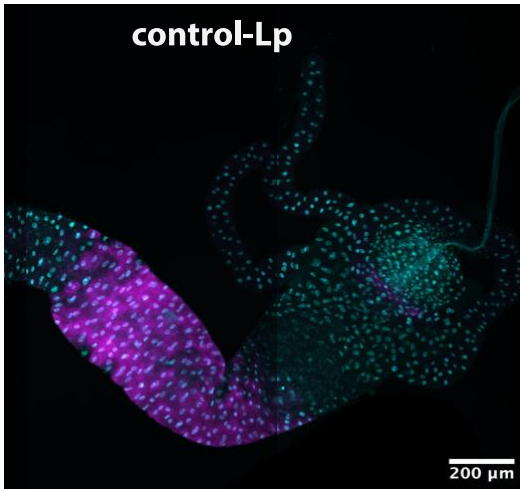
B.



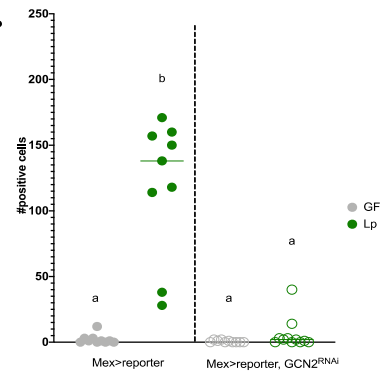
C.



D.



E.



F.

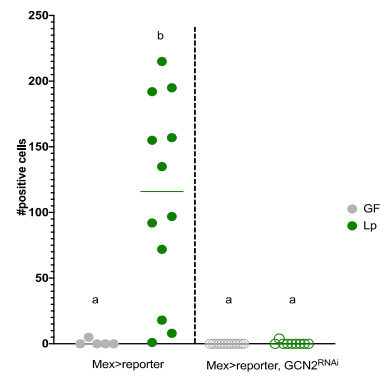


Fig. 3 Association with Lp activates GCN2 in the larval anterior midgut.

(A) Representative pictures of the full gut of a GF larva (top panel) and a Lp-associated larva (bottom panel) fed an unbalanced diet. Cyan: DAPI. Magenta: 4E-BP^{intron}dsRed reporter. The red square shows the region of the anterior midgut where Lp activates the 4E-BP^{intron}dsRed reporter. (B-C) Quantification of the 4E-BP^{intron}dsRed reporter's activity in the anterior midgut of GF larvae (grey circles) or Lp-associated larvae (green circles) fed an unbalanced (B) or balanced (C) diet. Each dot represents one sample. The bar shows the mean. We performed a Mann-Whitney test to compare the GF and Lp-associated conditions. **: p-value<0.01. ***: p-value<0.001. (D) Representative pictures of the anterior midgut of a control (Mex-Gal4 x 4E-BP^{intron}dsRed reporter) Lp-associated larva (top panel) and a GCN2 knock-down (Mex-Gal4 x 4E-BP^{intron}dsRed reporter; UAS-GCN2^{RNAi}) Lp-associated larva (bottom panel) fed an unbalanced diet. Cyan: DAPI. Magenta: 4E-BP^{intron}dsRed reporter. (E-F) Quantification of the 4E-BP^{intron}dsRed reporter's activity in the anterior midgut of GF larvae (grey circles) or Lp-associated larvae (green circles) fed an unbalanced (B) or balanced (C) diet. Filled circles: control condition (Mex-Gal4 x 4E-BP^{intron}dsRed reporter). Empty circles: GCN2 knock-down (Mex-Gal4 x 4E-BP^{intron}dsRed reporter; UAS-GCN2^{RNAi}). For each nutritional condition, we performed a Kruskal-Wallis test followed by post-hoc Dunn's tests to compare all conditions together. a: the conditions are not significantly different from each other (p-value>0.05). b: the condition is significantly different from other conditions (p-value<0.01).

IV Rescue of AA unbalance by Lp requires r/tRNAs operons in Lp

In order to identify the mechanism of GCN2 activation by Lp, we performed a genetic screen using a transposon insertion library of Lp (Fig. 4A). This library is composed of 2091 mutants, each carrying a transposon randomly inserted in the chromosome, including 1218 insertions inside ORFs (Matos et al., 2017). To render the screening process scalable, we analyzed each mutant of the library upon mono-association to GF larvae and looked for transposon insertions in Lp's genome altering the capacity of Lp to support larval development on a severely unbalanced diet (FLY AA -80%, Fig. S1A). For each mutant, we calculated the D50 (median time of development of associated larvae) and normalized it into a z-score. We applied a threshold of 2.5 and identified 32 mutants which z-scores are above the threshold: association with these mutants thus result in a delayed time of larval development on a severely unbalanced diet (Fig. 4B). To validate the 32 candidates selected from the initial screen, we individually re-tested them in multiple (5) replicates. We compared the development of larvae associated with the 32 candidates to larvae associated with an intergenic region insertion strain showing a WT-like phenotype (mutant B02.04, z-score=0.65). Thus, we discarded 23 false positives and retained only 9 candidates which result in a significant developmental delay on an unbalanced diet upon association (Fig. 4C). Lp grows on the food and transits through the larval gut (Storelli et al., 2018), and so the quantity of live bacteria present in the food can greatly impact the growth-promoting capacity of Lp (Consuegra et al., 2020b). As a consequence, a Lp strain that grows poorly on the food matrix would not support larval growth. Since we wanted to exclude such candidates, we tested the growth of the 9 candidates on unbalanced HD, in the presence of larvae (Fig. 4D). 3 candidates (B08.06, F09.11 and H04.06) show growth defects and thus were not retained for further analysis. On the contrary, the remaining 6 candidates show no growth defect. Moreover, they do not show any impairment at colonizing the larval gut (Fig. 4E). Next, we sequenced the genomes of the 6 selected candidates to determine which genes were affected by transposon insertion.

Interestingly, 4 out of the 6 candidates (mutants C09.09, D12.09, D12.16 and F07.08) showed independent transposon insertions in operons encoding transfer RNA (tRNAs) and ribosomal RNAs (rRNA) (Fig. 4F).

Figure 4

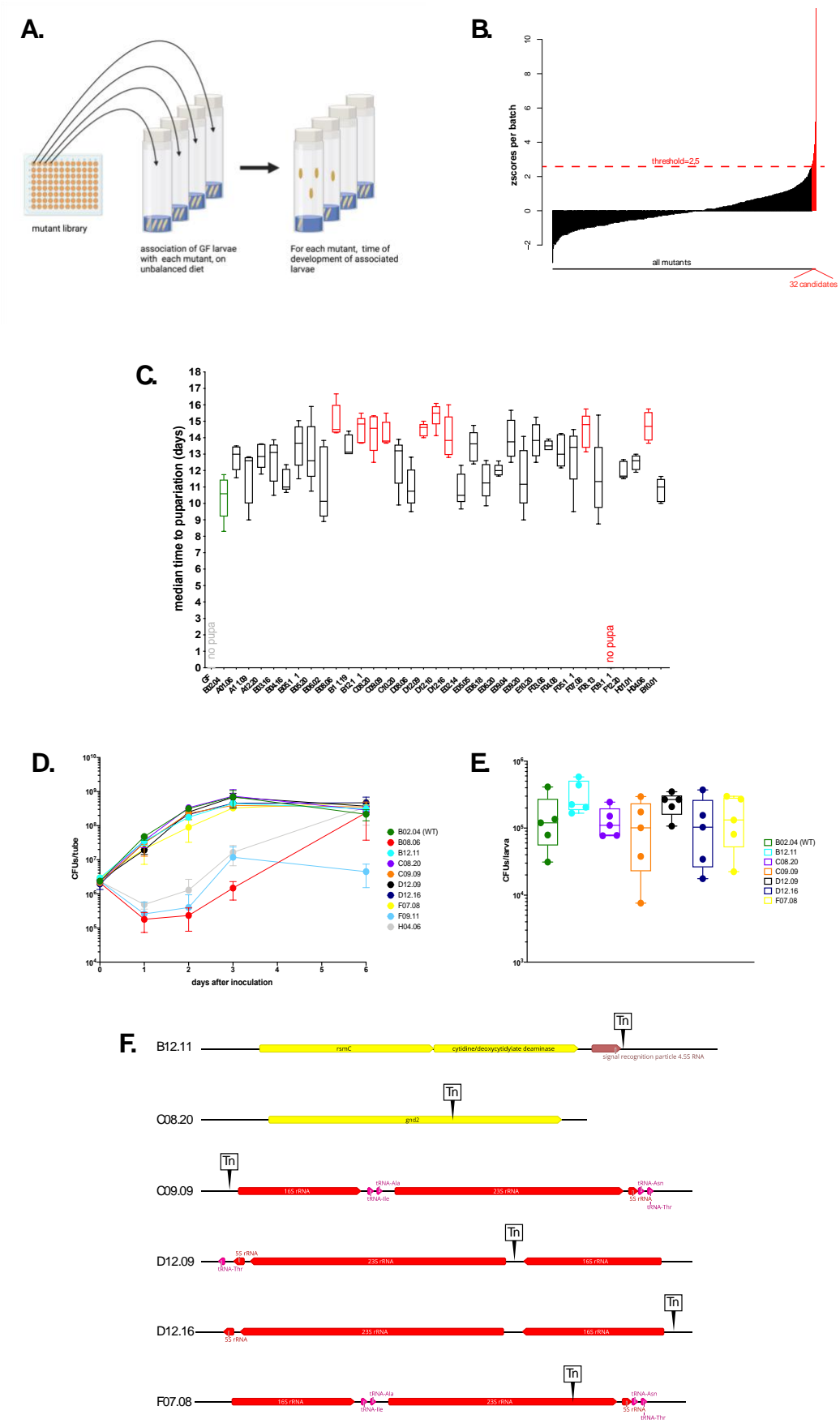


Fig. 4 The operons encoding ribosomal and transfer RNAs in Lp are necessary for Lp to rescue the delay due to AA unbalance.

(A) Representation of the genetic screen. (B) Result of the screen: for each mutant (X-axis), we calculated the median time of development of associated larvae and normalized it into a z-score (Y-axis). We selected the 32 candidates that yielded a z-score > 2.5 (C) Developmental timing of GF larvae (grey) and larvae associated with WT-like Tn mutant B02.04 (green) or the 32 candidate Tn mutants from the genetic screen, on a severely unbalanced diet (FLY AA -80% Val). GF larvae and larvae associated with mutant F09.11 did not reach pupariation. Boxplots show maximum, minimum and median of D50 (median time of pupariation) of each replicate. We performed a Kruskal-Wallis test followed by post-hoc Dunn's tests to compare all mutants to B02.04. In red: statistically significant difference with B02.04 (p-value < 0.05). (D) Growth of the 9 candidates on unbalanced diet (FLY AA -60% Val), in association with larvae. The graph shows the quantity of Colony-Forming Units (CFUs) of Lp over time. (E) Colonization of the larva gut by the 6 remaining candidates, on unbalanced diet (FLY AA -60% Val). The graph shows the quantity of Colony-Forming Units (CFUs) of Lp per larva. We performed a Kruskal-Wallis test followed by post-hoc Dunn's tests to compare each candidate to B02.04 and found no statistically significant difference. (F) Representation of the six transposon insertion. Tn: transposon. *rspC*: 16S rRNA methyltransferase. *gnd2*: phosphogluconate dehydrogenase. Of note, C09.09 and F07.08 show two independent insertions in the same r/tRNA operon.

V Lp may activate GCN2 through secretion of r/t RNAs

r/tRNA encoding operons are thus necessary for Lp to rescue AA unbalance. In eukaryotic cells, GCN2 is activated by unloaded tRNAs, which are a proxy for AA scarcity (Masson, 2019). Moreover, rRNAs can bind and activate GCN2 through a double-stranded RNA-binding domain (Zhu and Wek, 1998). Therefore, we wondered whether bacterial ribosomal and/or transfer RNAs produced by Lp could be activating GCN2 in the larval midgut. We first tested interaction between GCN2 knock-down and Lp r/tRNA mutation. To do so, we focused on the mutant F07.08, which carries transposon insertion in an operon encoding the three rRNAs and four tRNAs. As expected, control larvae reared on unbalanced diet in association with F07.08 show a developmental delay compared to larvae associated with WT-like B02.04 (Fig. 5A). On the contrary, larvae knocked-down for GCN2 in the enterocytes do not show a difference between association with F07.08 and association with B02.04 (Fig. 5B); in other words, the effect of the r/tRNA mutation is only observed when GCN2 is present.

We then used the 4E-BP^{intron}dsRed reporter to test the activation of GCN2 by F07.08-association (Fig. 5C). On AA unbalanced diet, F07.08-associated larvae show a reduced activation of GCN2 compared to B02.04-associated larvae, though the difference is not statistically significant (Fig. 5D). On an AA balanced diet, GCN2 activation in the midgut in F07.08-associated larvae is altered: it is comparable to GCN2 activation in GF larvae, and significantly different from GCN2 activation in control B02.04-associated larvae (Fig. 5E). The lesser difference observed on unbalanced diet might be due to longer association of the larvae with F08.08: indeed, in order to size-match the larvae, we collect them 24h before the emergence of the first pupae, which is D6 after egg-laying for B02.04 and D8 after egg-laying for F07.08. To ensure comparable association with the two mutants, we performed short-term association of GF larvae with B02.04 or F07.08: the larvae were reared GF, associated

with B02.04 or F07.08 at D8 after egg-laying, and collected for dissection at D10 after egg-laying. In short-term association on an unbalanced diet, activation of GCN2 was significantly reduced in F07.08-associated larvae compared to B02.04-associated larvae (Fig. 5F-G). Taken together these results establish a genetic interaction between the r/tRNA mutation in Lp, and GCN2 activity in the host, suggesting a functional interaction between the two processes.

It is unknown whether bacterial r/tRNAs can activate GCN2. We therefore tested this hypothesis by feeding purified bacterial tRNAs to GF larvae carrying the 4E-BP^{intron}dsRed reporter. At the highest dose tested (625 µg), bacterial tRNAs significantly increase the expression of the reporter in the anterior midgut (Fig. S4A). This increase is comparable to the effect of feeding eukaryotic tRNAs to these larvae, though slightly inferior. However, the effect is minimal as compared to the association of larvae with Lp (Fig. S4B). These results therefore suggest that Lp's tRNA may be direct activators of GCN2 in enterocytes. However, we cannot exclude that Lp's rRNAs or an indirect mechanism dependent on a functional Lp r/tRNA operon is at play.

Figure 5

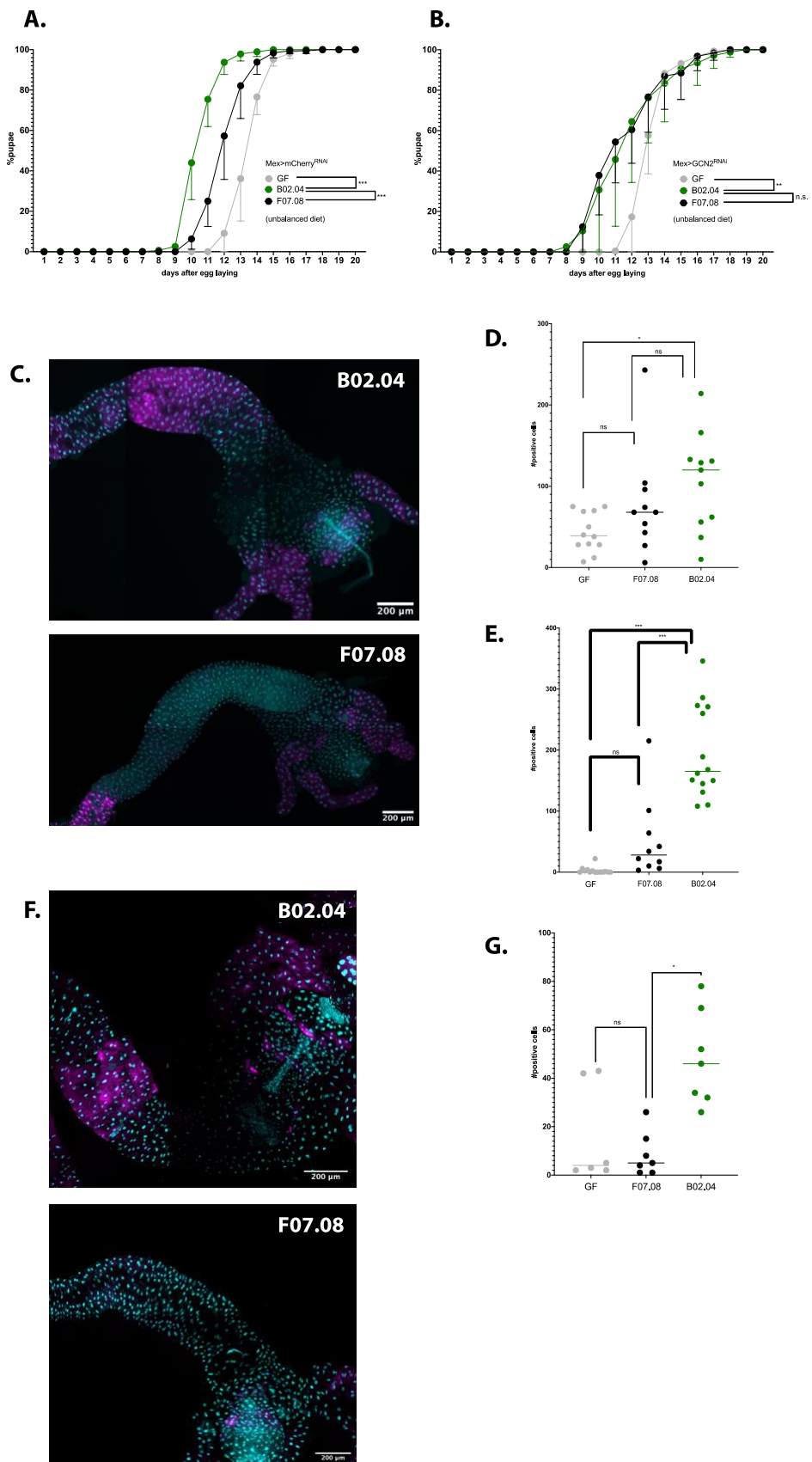


Fig. 5 r/tRNAs produced by Lp may activate GCN2 in the anterior midgut.

(A-B) Developmental timing of GF larvae (grey), larvae associated with Lp Tn::r/t RNA mutant F07.08 (black) and larvae associated with Lp Tn::WT mutant B02.04 (green) on unbalanced diet (FLY AA -60% Val). We used a Cox proportional hazards model to compare the effect of B02.04-association with F07.08-association and GF condition. n.s.: non-significant, **: p-value<0.01, ***: p-value<0.001. (A) Control larvae (Mex>mCherry^{RNAi}). (B) Larvae knocked-down for GCN2 in enterocytes (Mex>GCN2^{RNAi}). (C) Representative pictures of the anterior midgut of larvae associated with B02.04 (top panel) and F07.08 (bottom panel) fed a balanced diet. Cyan: DAPI. Magenta: 4E-BP^{intron}dsRed reporter. (D-F) Quantification of the 4E-BP^{intron}dsRed reporter's activity in the anterior midgut of GF larvae (grey), larvae associated with F07.08 (black) and larvae associated with B02.04 (green) on unbalanced diet (D) or balanced diet (E). The bar shows the mean. We performed a Kruskal-Wallis test followed by post-hoc Dunn's tests to compare the conditions together. n.s.: non-significant. *: p-value<0.05. ***: p-value<0.001. (F) Representative pictures of the anterior midgut of larvae associated with B02.04 (top panel) and F07.08 (bottom panel) fed a balanced diet upon short-term association. Cyan: DAPI. Magenta: 4E-BP^{intron}dsRed reporter. (G) Quantification of the 4E-BP^{intron}dsRed reporter's activity in the anterior midgut of GF larvae (grey), larvae associated with F07.08 (black) and larvae associated with B02.04 (green) on unbalanced diet upon short-term association. The bar shows the mean. We performed a Kruskal-Wallis test followed by post-hoc Dunn's tests to compare the conditions together. n.s.: non-significant. *: p-value<0.05.

VI Alterations in the gut transcriptome after GCN2 induction by Lp

We next wondered how GCN2 activation by Lp's r/tRNA operon may support larval growth on an AA unbalanced diet. When GCN2 is activated, it phosphorylates eIF2 α . Phosphorylation of eIF2 α inhibits translation, except for a subset of mRNAs including the transcription factor ATF4 which translation is increased (Donnelly et al., 2013). ATF4 then activates the transcription of genes involved in stress response. In *Drosophila*, one of these genes is the eIF4E-binding protein 4E-BP (Kang et al., 2017). 4E-BP activation promotes cap-independent translation, which boosts Anti-Microbial Peptides (AMPs) production in the fat body (Vasudevan et al., 2017) and can alter the composition of the microbiota (Vandehoef et al., 2020). Therefore, we tested whether ATF4 and 4E-BP acting downstream of GCN2 are also necessary for Lp to support larval development upon dietary AA unbalance. We observed that knocking-down ATF4 or 4E-BP in the enterocytes delays the development of GF larvae on an unbalanced diet. However, such knock-downs do not affect the development of Lp-associated larvae like GCN2 knock-down does. ATF4 and 4E-BP are thus not required for Lp to support larval development upon dietary AA unbalance (Fig. 6A).

Therefore, we analyzed the larval midgut GCN2-dependent, ATF4-independent, r/tRNA operon-dependent transcriptomic response to Lp association. To this end, we analyzed the transcriptome of the anterior midgut of larvae fed an unbalanced diet in 8 different conditions: Mex>control^{RNAi}, Mex>GCN2^{RNAi} and Mex>ATF4^{RNAi}, each in GF and Lp-associated background, and Mex>control^{RNAi} in association with B02.04 and F07.08.

We thus applied four successive filters to our sequencing data: we looked for genes 1) differentially regulated upon GCN2 knock-down (in association with Lp) 2) NOT

differentially regulated upon ATF4 knock-down (in association with Lp) 3) differentially regulated between F07.08 association and B02.04 association 4) differentially regulated between Lp association and GF. (Fig. 6B).

We applied the four filters to up-regulated genes (Fig. 6C) and to down-regulated genes (Fig. 6D). This approach resulted in a very reduced pool of candidate genes. 5 genes were found to be upregulated by Lp in a GCN2-dependent, ATF4-independent and r/tRNA operon-dependent manner: *CG16995*, *CG12780*, *ITP*, *PGRP-LB* and *Glu4EF*. Fig. S5A shows the normalized counts for these genes in all 8 conditions. 6 genes were found to be downregulated by Lp in a GCN2-dependent, ATF4-independent and r/tRNA operon-dependent manner: *MalA1*, *fiz*, *UQCR-14*, *CG7322*, *AANATL2* and *Akr1B*. Fig. S5B shows the normalized count for these genes in all 8 conditions.

We identified three main signatures from our transcriptomic data. First of all, we found that Lp up-regulates certain immune genes through the r/tRNA operon and GCN2: *PGRP-LB*, which is a negative regulator of the Immune deficiency (IMD) pathway that fosters immune tolerance to symbiotic bacteria (Charroux et al., 2018); and *CG12780*, a homolog of the *Gram-negative bacteria-binding protein 1 (GNBP1)* (Jiggins and Kim, 2006). GNBP1 is a co-factor of PGRP-SA, which senses Lys-type peptidoglycans and triggers the Toll pathway. *CG12780* was previously found to be activated in response to infection by Gram+ and Gram- bacteria (De Gregorio et al., 2001; Irving et al., 2001). Although *PGRP-LB* and *CG12780* went through the four filters that we applied, examination of the normalized counts show that their expression does not differ markedly between GF *Mex>ATF4^{RNAi}* larvae and Lp-associated *Mex>ATF4^{RNAi}*. Induction of these genes by Lp thus seems to be both GCN2- and ATF4-dependent, as previously described for other immune-related genes (Vasudevan et al., 2017). Therefore, their induction by Lp is unlikely to explain the rescue of larval development on unbalanced diet.

The second signature that we identified is linked to glucose metabolism and mitochondrial respiration. Lp down-regulates *Mal-A1*, *UQCR-14* and *CG7322* through the r/tRNA operon and GCN2, independently of ATF4. Mal-A1 is an alpha-glucosidase, which may catalyze the release of glucose from sucrose, the only carbohydrate present in the HD (Tanimura et al., 1979). UQCR-14 is a subunit of the respiratory chain in the mitochondria and CG7322 is a carbonyl reductase predicted to be involved in glucose metabolism (Gaudet et al., 2011). It thus seems that association with Lp causes a down-regulation of mitochondrial respiration and upstream glucose metabolism in the anterior midgut through GCN2 and the r/tRNA operon, independently of ATF4.

Finally, we found several signatures of ecdysone (Ecd) signaling. Firstly, association with Lp up-regulates the expression of *CG16995* and *ion transport peptide (ITP)*. *CG16995* is a protein of unknown function. It was previously shown to be upregulated in the gut of CR flies vs GF flies (Broderick et al., 2014), and it is up-regulated during metamorphosis in an Ecd-Receptor-dependent manner (Beckstead et al., 2005). It may thus be a target of Ecd signaling. ITP is an antidiuretic hormone peptide of the

crustacean hyperglycemic hormone (CHH) family that regulates water absorption in response to dehydration in adults (Gáliková et al., 2018). In Crabs, the endocrine cells of the gut synthesize CHH, which triggers molting (Chung et al., 1999), possibly through the biosynthesis and metabolism of ecdysteroids (Chung, 2010). ITP may thus also regulate Ecd signaling in flies, though this hypothesis has not been tested (Dircksen et al., 2008). Moreover, association with Lp down-regulates the expression of *Akr1B* and *fezzik* (*fiz*) through GCN2 and the r/t RNA operon, independently of ATF4. *Akr1B* encodes an aldose-reductase, orthologous to the aldo-keto reductase family 1 in humans (Rižner and Penning, 2014). Enzymes of this family play an important role in synthesis and degradation of steroid hormones in humans, but it is not known whether this role is conserved in flies. *fiz* encodes an Ecd oxidase, which catalyzes the transformation of Ecd into inactive 3-epiecdysteroids and can thus repress Ecd signaling (Takeuchi et al., 2005). Importantly, a hypomorphic allele of *fiz* or a knock-down of *Fiz* in the whole organism result in increased larval growth rate, larger larvae at all stages and larger adults (Glaser-Schmitt and Parsch, 2018).

Therefore, our transcriptomics data suggest that induction of GCN2 by Lp through the r/tRNA operon results in an ATF4-dependent immune response (induction of *PGRP-LC* and *CG12780*) and two ATF4-independent responses: repression of glucose metabolism and mitochondrial respiration (down-regulation of *Mal-A1*, *UQCR-14* and *CG7322*) and induction of Ecd signaling (up-regulation of *CG16995* and *ITP*, down-regulation of *fiz* and *Akr1B*). In insects, Ecd is mostly synthesized by the prothoracic gland during Ecd peaks, that trigger molting and entry into metamorphosis (Gilbert et al., 2002). In addition to its canonical role, Ecd was recently found to stimulate the proliferation and growth of intestinal stem cells in mated females. This is expected to increase the nutrient absorption by the gut, and to increase nutrient availability for other organs. In adult females, knocking-down the Ecd receptor in the gut decreases fecundity (Ahmed et al., 2020). We hypothesize that a similar mechanism may be at play in larvae: Ecd signaling triggered by Lp through GCN2 may promote gut growth, which may improve the absorption of nutrients, especially of the limiting AA and thus support systemic growth. Of note, unpublished data from our lab suggest that Ecd signaling increases gut growth upon Lp-association on an oligidic diet (Ramos et al., in prep). We also observed that mitochondrial respiration seems to be decreased by Lp through GCN2 and the r/t RNA operon, which may suggest that enterocytes of Lp-associated larvae rely on fermentation, rather than respiration, for energy metabolism. Fermentation is less effective than respiration for ATP production, but it allows the synthesis of intermediates such as NADPH and ribose-5-phosphate that are necessary for anabolism and cell growth (Weinberg and Chandel, 2009). This phenomenon, which was first described in cancer cells (Warburg, 1956), may participate to increase gut growth and indirectly systemic growth by supporting increase nutrient absorption in Lp-associated larvae. We used the microscopy images that we took for Fig. 3 and Fig. 5 to measure the width of the anterior midgut in different conditions, on unbalanced diet. The anterior midgut of Lp-associated larvae is wider than the anterior midgut of GF larvae (Fig. S6A). This effect depends on GCN2: Lp-associated larvae knocked-down for GCN2 show anterior midgut width similar to GF larvae (Fig. S6B). Finally, the

width of the anterior midgut of larvae associated with F07.08 in chronic (Fig. S6C) or short-term association (Fig. S6D) seems reduced compared to B02.04-associated larvae (although the difference is not statistically significant). It thus appears that Lp stimulates anterior midgut growth through GCN2 activation and Lp's r/tRNA operon.

Figure 6

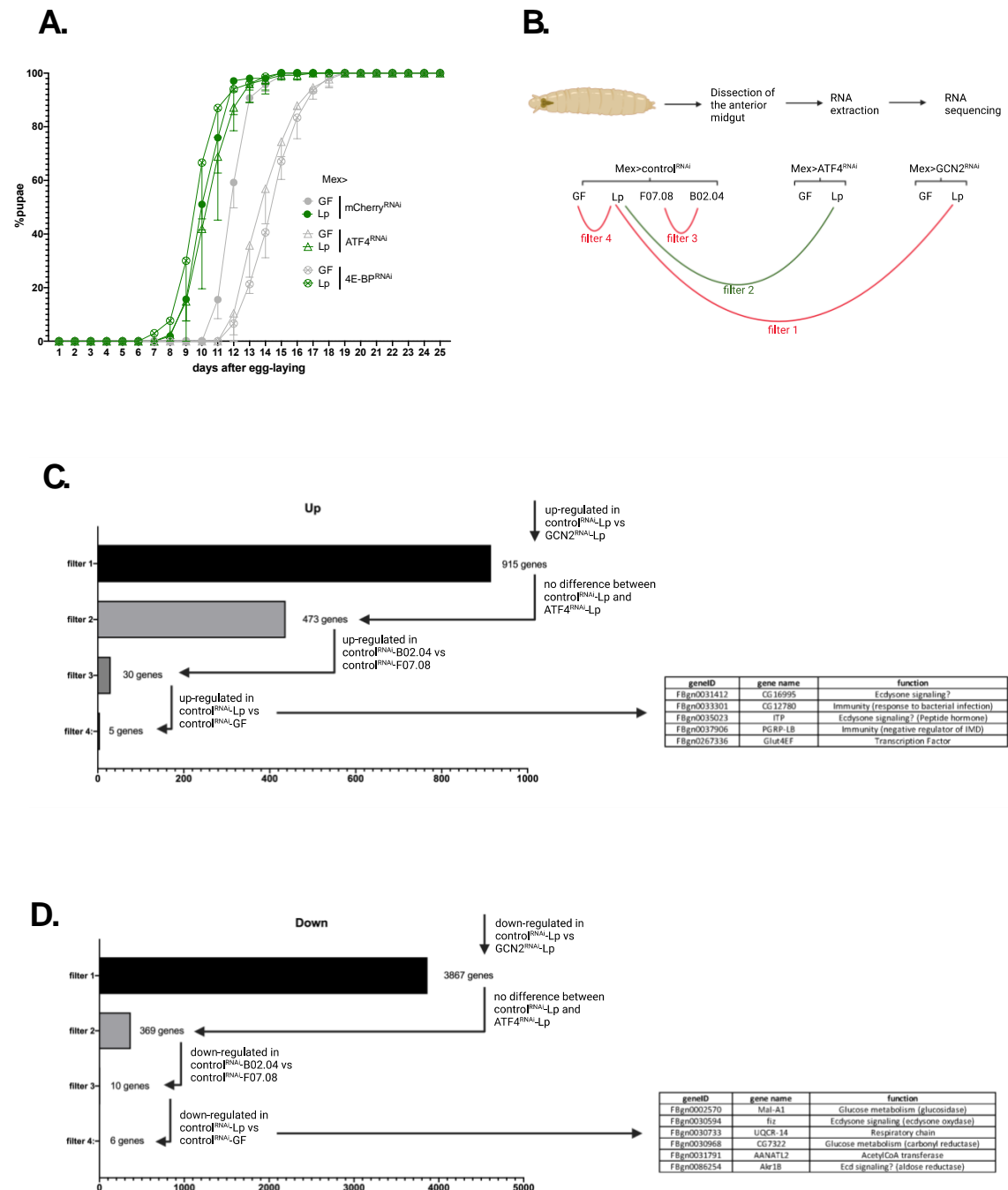


Fig. 6 Alterations in the gut transcriptome after GCN2 induction by Lp

(A) Developmental timing of larvae raised on unbalanced diet in GF condition (grey) or Lp-associated conditions (green), in a control background (Mex>mCherry^{RNAi}, filled circles), an ATF4 knock-down

background (Mex>ATF4^{RNAi}, empty triangles) or a 4E-BP knock-down background (Mex>4E-BP^{RNAi}, empty circles). The graph represents the total fraction of emerged pupae over time as a percentage of the final number of pupae. (B) Representation of the RNAseq strategy. We looked for genes that were differentially expressed (red lines) or not differentially expressed (green line) between conditions. (C) Filtering of up-regulated genes. The table shows the five genes that passed through the four filters. (D) Filtering of down-regulated genes. The table shows the six genes that passed through the four filters.

Discussion

It is well-known that symbiotic microbes can promote the postnatal growth of their host in a nutrient-poor diet by directly or indirectly modifying their diet. Pea aphids' symbiotic bacteria provide EAA precursors to their host (Akman Gündüz and Douglas, 2009; Russell et al., 2013). *Drosophila*'s symbiotic bacteria provide B-vitamins and certain EAAs to the developing larvae (Consuegra et al., 2020a; Sannino et al., 2018). The microbiota of termites (Brune and Dietrich, 2015), ruminants (Cammack et al., 2018) and rodents (Sakaguchi, 2003) degrades plant fibres into metabolites that can fuel their host's metabolism. Symbiotic microbes can also modify their host's diet indirectly: for instance, *Lp* stimulates the production of digestive enzymes including proteases by *Drosophila*'s enterocytes, which allows the larva to retrieve AA from dietary polypeptides (Erkosar et al., 2015; Matos et al., 2017).

Here, we show that the symbiotic bacterium *Lp* can rescue the developmental delay of its host due to AA unbalance without 1) providing the limiting AA (because *Lp* is not capable of synthesizing Val (Consuegra et al., 2020a; Kim et al., 2021; Teusink et al., 2005)) or 2) increasing degradation of dietary polypeptides (because the HD contains only free AA). We show that *Lp*'s effect depends on the action of *Drosophila*'s GCN2 in enterocytes. GCN2 is known to be active in *Drosophila*'s enterocytes: it is required for lifespan extension under dietary restriction (Kim et al., 2020) and influence food choice behavior under AA scarcity (Kim et al., 2021) and response to bacterial infection (Chakrabarti et al., 2012). We now report that GCN2 activation in the enterocytes is necessary for growth promotion by symbiotic bacteria on an AA-unbalanced diet. Of note, GCN2 is unnecessary when the symbiotic bacteria can provide the limiting AA.

We then used the reporter 4E-BP^{intron}dsRed to demonstrate that *Lp* activates GCN2 in a subset of enterocytes of the anterior midgut. This region of the midgut is located just before the acidic zone, which inactivates many *Lp* cells passing through it (Storelli et al., 2018). It is thus in this anterior region that most live *Lp* cells interact with enterocytes. The pattern of expression of 4E-BP^{intron}dsRed slightly differs from the pattern observed by Kang and colleagues (Kang et al., 2017): upon AA scarcity, they observed activation of the reporter in the gastric caeca, the acidic region and the proventriculus like we did, but not in the anterior midgut. Because those experiments were done in conventionally-reared larvae where the microbial status of the animals was not reported, this difference with our findings suggests that GCN2 activation by symbiotic bacteria may be species-dependent or strain-dependent; an alternative explanation is that frequently flipped conventional fly stocks or crosses may carry very

low microbial titers and therefore present GF-like phenotypes. Moreover, we found that inhibition of GCN2 completely abolishes the induction of the 4E-BP^{intron}dsRed by Lp in the anterior midgut. The activity of the 4E-BP^{intron}dsRed in the rest of the gut (gastric caeca, proventriculus, acidic region) appears decreased, but not completely abolished, by GCN2 knock-down in this context. *Drosophila* possesses only two eIF2 α kinases: GCN2 and PERK (Malzer et al., 2013). These results thus suggest PERK activity in the gastric caeca, the proventriculus and the acidic region. Surprisingly, we found that GCN2 activation in the anterior midgut is marginally impacted by dietary AA unbalance: GF larvae on an unbalanced diet show a slightly increased activation compared to GF larvae on a balanced diet, but the difference is not statistically significant. On the contrary, the presence of Lp dramatically increases the activation of GCN2 in this region. Previous studies have shown that GCN2 can be activated by factors others than AA scarcity: UV exposure (Grallert and Boye, 2007), viral (Krishnamoorthy et al., 2008) and bacterial infection (Chakrabarti et al., 2012; Tattoli et al., 2012; Vasudevan et al., 2017). Tattoli and colleagues proposed that GCN2 can be activated by AA depletion triggered by intracellular infection by *Shigella* (Tattoli et al., 2012); however, this mechanism seems unlikely in our situation because Lp is not intracellular, and because association with Lp fosters rescue of AA unbalance.

In order to understand how Lp activates GCN2, we performed a genetic screen using a library of insertion mutants of Lp. We identified six candidates that are impaired in their ability to support larval development upon dietary AA unbalance, without displaying any growth or colonization defects. Four out of these six candidates were independent insertions of transposons in operons encoding ribosomal and transfer RNAs. The genome of Lp contains five operons encoding the rRNA (5S, 16S, 23S) associated with tRNAs. Several copies of each tRNA are present on the chromosome; therefore, we assume that insertion of a transposon in a r/tRNA operon decreases the global synthesis of r/tRNAs, but it does not impact the viability and the growth of the mutant because of the other copies of the genes in the genome. Of note, one of the mutants (D12.16) shows disruption of an operon that encodes only rRNAs. However, synthesis of tRNAs is regulated by ribosomal activity (Gourse et al., 1985); therefore, tRNAs production may be indirectly altered in D12.16 as well. The other two candidates might also be linked to r/tRNA production: C08.20 has a transposon insertion of the gene *gnd2* that encodes a phosphogluconate dehydrogenase of the Pentose Phosphate Pathway (PPP). One product of the PPP is the 5-phosphoribosyl- α -1-pyrophosphate (PRPP), which is a precursor for the biosynthesis of nucleotides (Kilstrup et al., 2005). It is thus possible that disruption of *gnd2* might alter production of RNAs by the cells. Moreover, B12.11 displays an insertion in the end of an operon encoding *rsmC*, *lp_0696* and *lp_sRNA01*. *rsmC* encodes a 16S rRNA methyltransferase. Methylation of rRNA stabilizes ribosomes and improves translation in other bacteria (Wong et al., 2013). *lp_0696* encodes a cytidine/deoxycytidylate deaminase, which catalyzes conversion of cytidine into uridine. *lp_sRNA01* encodes the signal recognition particle (SRP), a small non-coding RNA which addresses membrane proteins to the membrane during their translation (Kuhn et al., 2017).

Disruption of this operon may thus directly alter RNA production and/or ribosomal function, which can negatively regulate r/tRNA synthesis (Gourse et al., 1985). Further work is needed to measure how the mutations that we identified impact the synthesis of each family of r/tRNA.

Lp mutants for operons encoding r/tRNAs fail to rescue AA unbalance in control larvae. Yet, association with a r/tRNA mutant does not affect the growth of larvae knocked-down for GCN2. Moreover, it yields a reduced activation of the 4E-BP^{intron}dsRed reporter of GCN2 activity. Uncharged eukaryotic tRNAs are the canonical activators of GCN2. tRNAs bind a domain of GCN2 that shares homology with the histidyl-tRNA synthetase (HisRS), an enzyme that catabolizes loading of His-tRNA on the AA Histidine (His) (Masson, 2019). However, this domain is not specific to His-tRNAs: it can bind other tRNAs as well, such as tRNAs for Phenylalanine, Valine, Tyrosine and Lysine (Dong et al., 2000; Wek et al., 1995). Moreover, the HisRS domain can bind viral dsRNA, leading to GCN2 activation in response to viral infection (Berlanga et al., 2006). Therefore, binding of prokaryotic tRNAs by *Drosophila*'s HisRS domain of GCN2 may be possible. Using the 4E-BP^{intron}dsRed reporter, we observed that feeding larvae bacterial tRNAs or eukaryotic tRNAs both activate GCN2. We thus propose that tRNAs produced by Lp activate GCN2 in their host's enterocytes. Of note, tRNA-derived small RNAs were previously described as signaling molecules in the symbiotic nodules of plants (Ren et al., 2019) and in humans macrophages after *Mycobacterium tuberculosis* infection through binding to Toll-Like Receptor 7 (Pawar et al., 2020). Unconventional mechanisms of activation of GCN2 might be at play as well: GCN2 can also be activated by rRNA (Zhu and Wek, 1998) and by stalled ribosomes (Inglis et al., 2019). Finally, alteration of GCN2 activation in r/tRNA mutants may also be an indirect effect of translation defects in these mutants and reduced expression of unidentified GCN2 elicitors.

We do not know yet if and how Lp's r/tRNAs are delivered to enterocytes. *M. tuberculosis*' tRNAs activating macrophages were found inside extracellular vesicles (Pawar et al., 2020). Similarly, the squid symbiont *Vibrio fischeri* delivers the small non-coding RNA SsrA to its host in outer membrane vesicles (Moriano-Gutierrez et al., 2020). *Lactocaseibacillus casei* produces extracellular vesicles that contain r/tRNA (Domínguez Rubio et al., 2017). Moreover, extracellular vesicles from *Limosilactobacillus reuteri* influences gut motility in mice (West et al., 2020) and extracellular vesicles from *L. plantarum*^{WCFS1} increase the expression of immunity genes in worms and cultured colonocytes (Li et al., 2017). Therefore, it is possible that Lp may deliver r/tRNAs to *Drosophila*'s enterocytes via extracellular vesicles. This could explain why providing tRNAs directly to the larva does not fully recapitulate the effect of Lp on GCN2 activation. This hypothesis remains to be tested.

We wondered how GCN2 activation by Lp may improve growth in situation of AA unbalance. The GCN2-eIF2 α -ATF4-4E-BP pathway is the best-studied in *Drosophila*. However, it does not seem to be involved here because Lp can rescue AA unbalance

in larvae knock-down for ATF4 or 4E-BP in enterocytes. Instead, rescue of AA unbalance may occur independently of eIF2 α , through other substrates of GCN2. eIF2 α is the only known substrate of GCN2; however, Dang Do and colleagues showed that in the mouse liver, GCN2 does not regulate the same set of genes as PERK, another eIF2 α -kinase. This suggests that additionally to their common substrate eIF2 α , GCN2 and PERK have distinct substrates (Dang Do et al., 2009). eIF2 α -independent action of GCN2 was described in response to UV exposure (Grallert and Boye, 2007) and viral infection (Krishnamoorthy et al., 2008). Alternatively, rescue of AA unbalance may rely on eIF2 α targets other than ATF4. ATF4-independent regulation of gene expression by eIF2 α was described in *Drosophila* (Malzer et al., 2018), mice (Guo and Cavener, 2007) and Mammalian cells (Harding et al., 2003; Wek and Cavener, 2007). To understand how GCN2 activation by Lp may improve growth in situation of AA unbalance, we analyzed the transcriptome of the anterior midgut of larvae. We found signatures of increased Ecd signaling upon association with Lp, which are reduced when GCN2 is knocked-down or when larvae are associated with Lp mutant for a r/tRNA operon. Moreover, we found that Lp down-regulates the expression of genes encoding enzymes of glucose metabolism and mitochondrial respiration, in a GCN2-dependent and r/tRNAs operon-dependent manner. Ecd signaling in the gut of adults stimulates gut growth (Ahmed et al., 2020) and a metabolic switch from respiration to fermentation allows the production of intermediates that favor anabolism and cell growth (Weinberg and Chandel, 2009). We observed that Lp increases the width of the anterior midgut in a GCN2-dependent manner. Therefore, we hypothesize that stimulation of the anterior midgut growth through GCN2 activation by Lp may result in an increase in nutrients uptake, and thus allows the Lp-associated larvae to improve recovery of the limiting AA from the unbalanced diet.

In conclusion, we showed that the symbiotic bacterium Lp can rescue the effects of AA unbalance on growth through GCN2 activation in enterocytes, possibly through secretion of r/tRNAs and modification of Ecd signaling and/or glucose metabolism in the gut. Sensing of bacteria through GCN2 was previously described in the context of infection (Chakrabarti et al., 2012; Tattoli et al., 2012; Vasudevan et al., 2017). These studies and ours emphasize the role of GCN2 in the sensing of bacteria, on top of its canonical role of sensing uncharged tRNAs of the self as a proxy of AA scarcity (Donnelly et al., 2013). It raises the question of the evolutionary origin of GCN2: could GCN2 have primarily evolved as a sensor for bacterial tRNAs, like Toll and Peptidoglycan-Recognition Proteins did for peptidoglycans, before developing a new function of sensing AA scarcity?

Our study emphasizes the importance of GCN2 in enterocytes for the regulation and support of juvenile growth. GCN2 is highly conserved across Eukaryotes (Donnelly et al., 2013), and it was previously shown to be important for mouse adaptation to an AA unbalanced diet (Anthony et al., 2004; Guo and Cavener, 2007; Laeger et al., 2016;

Zhang et al., 2002). Our study therefore paves the way to testing whether the mechanisms that we discovered are also at play in juvenile mice. Finally, tumors can rely on GCN2 to adapt to AA-limiting conditions (Saavedra-García et al., 2021; Ye et al., 2010). As increasing attention is being paid to the links between microbiota and cancer (Rajagopala et al., 2017), further research may also address the potential activation of GCN2 in tumors by commensal bacteria.

Material and Methods

Drosophila lines and breeding

Drosophila stocks were maintained at 25°C with 12:12-h dark/light cycles on a yeast/cornmeal medium composed of 50 g.L⁻¹ of inactivated yeast, 80 g.L⁻¹ of cornmeal, 4 mL.L⁻¹ of propionic acid, 5.2 g.L⁻¹ of nipagin and 7.4 g.L⁻¹ of agar. All experiments were conducted in gnotobiotic flies derived from GF stocks. GF stocks were established as previously described (Combe et al., 2014) and maintained on yeast/cornmeal medium supplemented with antibiotics (50 µg/mL of kanamycin, 50 µg/mL of ampicillin, 10 µg/mL of tetracyclin and 5 µg/mL of erythromycin). We verified axenicity by grinding GF flies using a Precellys 24 tissue homogenizer (Bertin Technologies, Montigny-le-Bretonneux, France) and plating the lysate on Man-Rogosa-Sharp (MRS) Agar (Carl Roth) and LB Agar (Carl Roth). We used *yw* flies (BDSC #1495) as a reference strain. The following lines were used: UAS-mCherry^{RNAi} (BDSC #35785), UAS-KK^{RNAi} (VDRC #60100), UAS-TOR^{RNAi} (BDSC #33951), UAS-GCN2^{RNAi}-1 (VRDC #103976, gift from P. Leopold's lab), UAS-GCN2^{RNAi}-2 (BDSC #35355), UAS-GCN2^{RNAi}-3 (BDSC 67215), UAS-ATF4^{RNAi} (VDRC #109014), UAS-4E-BP^{RNAi} (VDRC #36667), 4E-BP^{intron}dsRed (gift from H.D. Ryoo's lab), Mex1-Gal4 and C564-Gal4 from out stocks. We generated the line 4E-BP^{intron}dsRed, UAS-GCN2^{RNAi} by recombining the lines 4E-BP^{intron}dsRed and UAS-GCN2^{RNAi}-1.

Holidic diets

We performed all our experiments on holidic diets (HD) without antibiotics. The HDs were prepared following the protocol of Piper and colleagues (Piper, 2017) at a total AA concentration of 10.7 g.L⁻¹. We made two changes to Piper and colleagues' protocol: we used a lower concentration of sucrose (5 g.L⁻¹) because we noted that this concentration is the best for GF larvae: higher sucrose concentrations are toxic and slightly delay development of GF larvae (data not shown). Moreover, we omitted the conservatives (propionic acid or nipagin). We worked in sterile conditions: tubes and egg-laying cages were UV-treated or autoclaved, and solutions were either autoclaved (first part containing agar, Leu, Ile, Tyr, sucrose, cholesterol and traces, as well as the acetate buffer solution) or filter-sterilized (stock solutions of EAA, NEAA, Glu, Cys, Vitamins, Nucleic Acids and Lipids precursors, Folate). For all experiments

involving transposon mutants, we supplemented the HD with erythromycin ($5 \mu\text{g}\cdot\text{mL}^{-1}$). HD was stored at 4°C for maximum one week before use.

Bacteria and culture conditions

We used the strain Lp^{NC8} of *Lactiplantibacillus plantarum* and the strain Ap^{WJL} of *Acetobacter pomorum*. Conversely to other strains of *L. plantarum*, Lp^{NC8} was not isolated from a fly but from grass silage (Axelsson et al., 2012); we used it because it is as growth promoting as fly isolates and it can be efficiently targeted for genetic modifications (Matos et al., 2017). Ap^{WJL} was isolated from a fly's intestine (Ryu et al., 2008). The Lp mutant library was generated by transposon insertion by Matos and colleagues from Lp^{NC8} (Matos et al., 2017). Lp was grown overnight at 37°C without agitation in MRS (Carl Roth). All Lp mutants were grown for 24h in MRS supplemented with Erythromycin at $5 \mu\text{g}\cdot\text{mL}^{-1}$. Ap^{WJL} was grown for 24h in Mannitol Broth composed of $3 \text{g}\cdot\text{L}^{-1}$ of Bacto peptone (Becton Dickinson), $5 \text{g}\cdot\text{L}^{-1}$ of yeast extract (Becton Dickinson) and $25 \text{g}\cdot\text{L}^{-1}$ of D-mannitol (Carl Roth) in a flask at 30°C under 180 rpm agitation.

Developmental timing experiments

GF flies were placed in a sterile breeding cage overnight to lay eggs on a dish of HD similar to the HD used for the experiment. At d0, we collected the eggs and placed them in the tubes containing the HD. Unless stated otherwise, each experimental condition consisted in 5 tubes each containing 40 eggs. Eggs were then inoculated with $100 \mu\text{L}$ of sterile PBS 1X (GF condition) or with $100 \mu\text{L}$ of an overnight culture of bacteria resuspended in PBS 1X (yielding in $\sim 2 \times 10^8$ CFUs of Lp and $\sim 10^7$ CFUs of Ap per tube). For the Heat-Killed (HK) condition, the resuspension of Lp in PBS was incubated 3h at 65°C . After inoculation, the larvae were kept at 25°C with 12:12-h dark/light cycles. The number of newly emerged pupae was scored every day until all pupae have emerged. The data are represented either as pupariation curves or as the median time of pupariation (D50) calculated using the D50App (<http://paulinejoncour.shinyapps.io/D50App>). We then used the R package Survival (Therneau and Grambsch, 2000) to make a Cox proportional hazard model adapted to pupariation curves, replacing the event "death" with the event "pupariation" (Rodrigues et al., 2018). We then either performed analysis of variance (ANOVA) to identify the effects of the different parameters and their interaction, or multiple comparisons followed by correction with the Holm method to compare the effect of Lp in different conditions.

Genetic screen

The genetic screen was performed in the same conditions as other Developmental timing experiments, but we used 20 eggs per condition in small tubes and one replicate per condition. Each condition consisted in the inoculation of one transposon insertion mutant. The screen was divided into four batches. For each batch, we calculated the

D50 of each mutant, and the associated z-score. We then pooled the z-scores from the four batches and selected the ones above a threshold of 2.5. The 32 candidates were re-tested in a Developmental timing experiment of 5 replicates. For each candidate, we calculated the D50 and performed a Kruskal-Wallis test followed by post-hoc Dunn's tests to compare it to the WT-like transposon insertion mutant B02.04 (transposon inserted in an intergenic region downstream *dnaJ*).

Mapping of insertion by Whole Genome Sequencing (WGS)

The transposons inserted in the mutant's genomes are not bar-coded. To map them, we extracted the genomic DNA of each candidate using a kit UltraClean Microbial DNA isolation (MoBio). Samples were quality-checked using a Qubit 4.0 HS DNA. To sequence genomic bacterial DNA, libraries were built using the Nextera DNA Flex Library Prep (Illumina) starting from 500ng of DNA (except for 2 samples for which 350ng and 280ng were used) and following the provider's recommendations. The 17 dual-indexed libraries were pooled in an equimolar manner and sequenced on a paired-end mode (2x75bp) using a NextSeq500 Illumina sequencer and a mid-output run. More than 155M of reads were obtained for the run generating between 7M to 12M of reads by sample. Data were analyzed using Galaxy (Afgan et al., 2016). Briefly, for each mutant, we filtered all pairs of reads which had one of the two reads mapped on the transposon sequence. We gathered the paired reads and mapped them on the genome of *Lp*^{NC8} (Axelsson et al., 2012) to identify the region in contact of the transposon. The genome of *Lp*^{NC8} contains five operons encoding r/tRNAs that share high sequence similarities. Therefore, sequencing did not allow us to identify in which operon the insertion took place. We thus used operon-specific PCR to identify in which operon the transposon was inserted for each mutant. For each mutant, we used two primers specific of the transposon (OLB215: ATGGCCGCGGGATTACGACTCC and OLB221: AGCTATGCATCCAACGCGTTGGG) and one primer specific of each r/tRNA operon (op1: CAAACGGGTGCTGGATGAAA, op2: TTAGCCCAGGACTTGCAAGA, op3: AGGAAGTTACCCCGAACCTG, op4: GCTAGATTTCCGGCACACTG and op5: GAAGGCGGATGGGACTAAGT).

Microscopy

4E-BP^{intron}dsRed larvae were reared on HD as for Developmental timing experiments. We collected them at pre-wandering mid-L3, 1 day before the emergence of the first pupae (typically D5 after egg-laying (AEL) for *Lp*-associated larvae on balanced diet, D6 AEL for *Lp*-associated larvae on unbalanced diet or GF larvae on balanced diet, D7 AEL for GCN2 knocked-down *Lp*-associated larvae on unbalanced diet, D10 AEL for GF larvae on unbalanced diet, D6 AEL for B02.04-associated larvae on unbalanced diet and D8 AEL for F07.08-associated larvae on unbalanced diet). For short-term association, GF larvae were reared on unbalanced diet until D8 AEL, associated with B02.04 and F07.08 as previously described and collected at D10 AEL. Larvae were

dissected in PBS 1X. The guts were fixed in paraformaldehyde (PFA) 4% in PBS 1X 1h at room temperature, washed in PBS 1X, washed three times in PBS Triton 0.2%, washed in PBS1X and mounted in ROTI®Mount FluorCare DAPI (Carl Roth HP20.1). Pictures were acquired with a confocal microscope Zeiss LSM 780. We analyzed the images using a custom macro on ImageJ: the macro identifies the reporter-positive regions above a defined threshold, and count the number of DAPI-positive particles inside. Anterior midgut width was measured with ImageJ.

Bacterial growth on HD

Microtubes containing 400 μ L of unbalanced HD were inoculated with $\sim 10^6$ of each candidate mutant. 5 L1 GF larvae were added to each tube, and the tubes were incubated at 25°C. Each day, 3 samples per condition were collected for CFUs counting: we added 600 μ L of sterile PBS 1X and grinded them using a Precellys 24 tissue homogenizer (Bertin Technologies, Montigny-le-Bretonneux, France. Settings: 6000 rpm, 2x30s, 30s pause). The homogenates were diluted at the appropriate concentration and plated on MRS Agar using an Easyspiral automatic plater (Interscience, Saint-Nom-la-Breteche, France). Plates were incubated at 37°C for 48h, and the number of CFUs was assessed using an automatic colony counter Scan1200 (Interscience) and its counting software.

Colonization of the larval gut

Larvae were reared on unbalanced diet as for Developmental timing experiments. 6 days AEL, larvae were collected, surface-sterilized in ethanol 70% and grinded using a Precellys 24 tissue homogenizer (Bertin Technologies, Montigny-le-Bretonneux, France. Settings: 6000 rpm, 2x30s, 30s pause). The CFUs were then counted as described above.

tRNAs feeding

4E-BP^{intron}dsRed larvae were reared on balanced diet as for Developmental timing experiments. At d0, d2, d4 and d5 AEL, the tubes were supplemented with 50 μ L of a solution of tRNAs dissolved in Millipore water to reach a total concentration in the tube of 5, 25 and 125 μ g.mL⁻¹. GF controls were supplemented with the same volume of Millipore water. We purchased the purified tRNAs at Sigma-Aldrich (bacterial tRNAs from *Escherichia coli* 10109541001, eukaryotic tRNAs from yeast 10109517001). Larvae were dissected 6 days AEL and treated as described above.

Food intake experiments

Larvae were reared on unbalanced diet as for Developmental timing experiments. Larvae were collected 1 day before the emergence of the first pupae and placed on unbalanced diet containing Erioglaucline disodium salt (Sigma-Aldrich 861146) at

0.8%. Every hour, we collected 5 larvae in 5 replicates per condition, rinsed them in PBS and placed them in a microtube with beads and 500 μ L PBS. Larvae were grinded using a Precellys 24 tissue homogenizer (Bertin Technologies, Montigny-le-Bretonneux, France. Settings: 6000 rpm, 2x30s, 30s pause). Optical Density at 0.629 nm was measured using a spectrophotometer SPECTROstarNano (BMG Labtech GmbH, Ortenberg, Germany).

RNA extraction

Larvae were reared as for Developmental timing experiments and collected 1 day before the emergence of the first pupae. Larvae were dissected in PBS, and dissected anterior midguts were kept in RNAlater (Thermofisher AM7021) before they were transferred to a microtube and flash-frozen. We used 10 guts for each replicate, and made 5 replicates for each condition. Samples were grinded using a Precellys 24 tissue homogenizer (Bertin Technologies, Montigny-le-Bretonneux, France. Settings: 6500 rpm, 2x30s, 30s pause) and total RNA was extracted using a RNeasy kit (Macherey-Nagel 740955.50) following the instructions of the manufacturer.

RT-qPCR

We adjusted RNA concentrations and performed Reverse-Transcription (RT) on extracted RNAs using a SuperScript II RT kit (Thermofisher 18064022) and random primers (Invitrogen) following the instructions of the manufacturer. We then performed quantitative PCR using the primers:

GCN2-forward: TGGCGCCCCTAGATGGCTCAATCCCAAGAGCTACG,

GCN2-reverse: TAGCCTCCCTAGCGCGGAAGTAGAGCGTCTCCGTG,

4E-BP-forward: CAGATGCCCGAGGTGTACTC,

4E-BP-reverse: CATGAAAGCCCGCTCGTAGA,

rp49-forward: GACGCTTCAAGGGACAGTATCTG,

rp49-reverse: AAACGCGGTTCTGCATGA on a Biorad CFX96 apparatus (Biorad) using SYBR GreenER qPCR Supermix (Invitrogen).

RNA sequencing

Both UAS-GCN2^{RNAi} and UAS-ATF4^{RNAi} are KK lines from VDRC. In order to reduce transcriptional noise, we thus used the KK line VDRC-60100 crossed to Mex-Gal4 as the control condition for RNA sequencing. 40 samples of total RNA isolated as previously described (5 replicates per condition) were used to build libraries using the SENSE mRNA-Seq Library Prep Kit V2 from Lexogen and following the RTS protocol. The libraries were single-indexed and pooled together in an equimolar manner in order to sequence 20 libraries at a time on a high-output run in a single-end mode (1x86bp) using a NextSeq500 Illumina sequencer. The two runs performed generated more than 535M reads each, resulting in an average of around 26-27 million reads per sample.

Transcriptome analysis

Reads were analyzed using Galaxy (Afgan et al., 2016). Briefly, we verified the quality of the samples using MultiQC. We then used RNAstar to map the reads on *Drosophila*'s genome (BDGP6.32). We used Deseq2 to compare the conditions together and generate lists of genes with their differential expression, as well as rLog normalized tables. We applied filters to the lists of genes using RStudio. For filter 1 (genes differentially regulated between Lp-associated control and Lp-associated GCN2^{RNAi} Lp), filter 3 (genes differentially regulated between B02.04-associated control and F07.08-associated control) and filter 4 (genes differentially regulated between GF control and Lp-associated control), we applied a cutoff of fold-change >1.5 or <-1.5 for up-regulation and down-regulation, respectively, and a cutoff of p-value <0.05 (p-value adjusted for multiple testing with the Benjamini-Hochberg procedure which controls false discovery rate (FDR)). For filter 2, (genes not differentially regulated between Lp-associated control and Lp-associated ATF4^{RNAi} Lp), we applied a cutoff of -1.5 < fold-change < 1.5 and adjusted p-value > 0.05.

Figures

Figures were created using the Prism GraphPad software and Biorender (BioRender.com).

Supporting Information

Figure S1

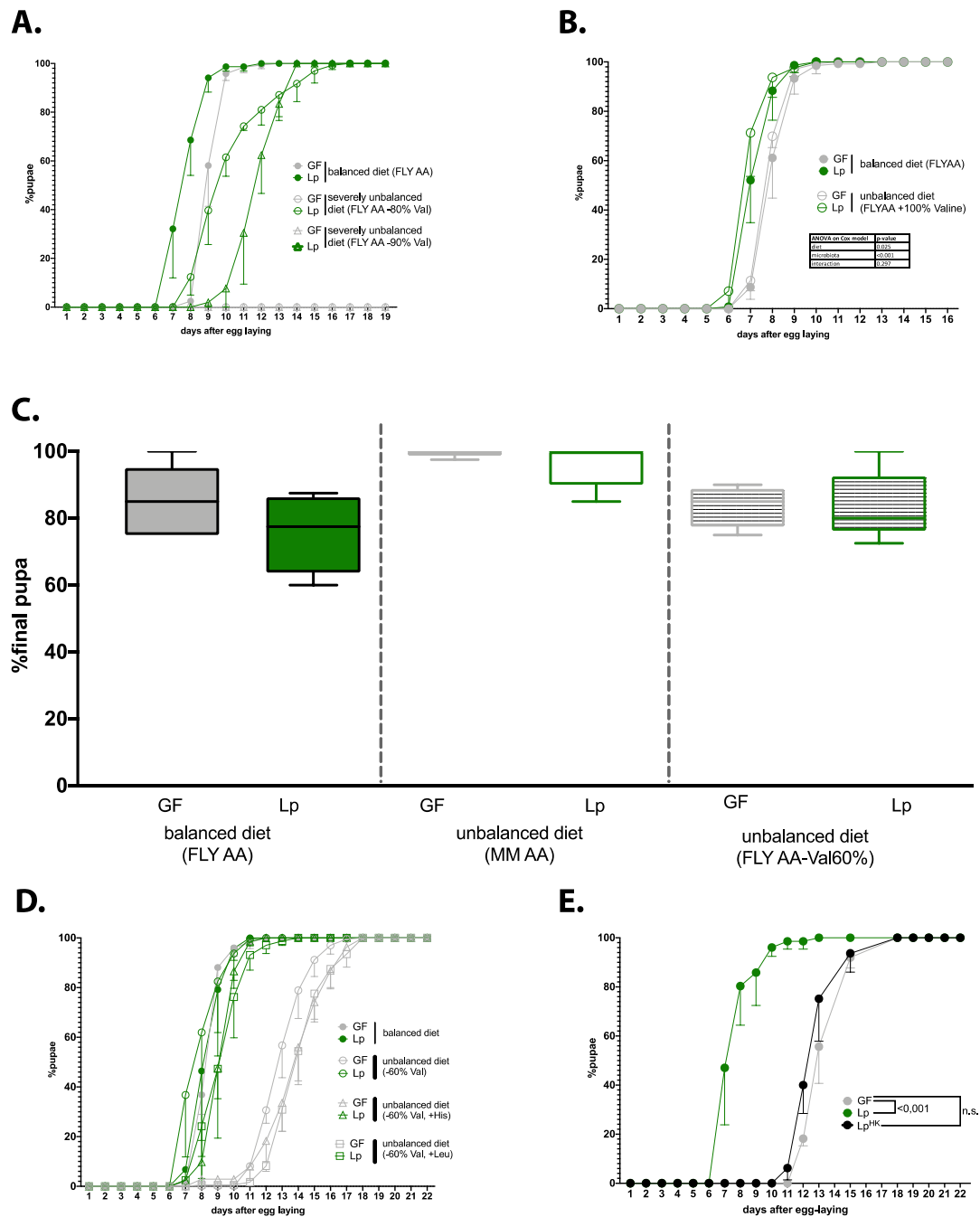


Fig. S1

(A) Developmental timing of larvae raised on balanced diet (FLY AA, filled circles) or on severely unbalanced diets (FLY AA -80% Val, empty circles, FLY AA -90% Val, empty triangles) in GF condition (grey) or Lp-associated conditions (green). The graph represents the total fraction of emerged pupae over time as a percentage of the final number of pupae. GF larvae on severely unbalanced diet did not reach pupariation. (B) Developmental timing of larvae raised on balanced diet (FLY AA, filled circles) or

on unbalanced diet due to excess Val (FLY AA +60% Val, empty circles). We used a Cox proportional hazards model to test the effect of the diet, the association with Lp, and the interaction between these two parameters. (C) Egg-to-pupa survival of GF larvae (in grey) and Lp-associated larvae (green) on balanced diet and unbalanced diets. Survival was calculated as the final number of pupae divided by the initial number of eggs (*i.e.* 40 per replicate). We performed a Kruskal-Wallis test followed by post-hoc Dunn's tests to compare each condition to the condition GF on balanced diet and found no statistically significant difference. (D) Developmental timing of larvae in GF condition (grey) or Lp-associated conditions (green). Larvae were raised on balanced diet (FLY AA, filled circles), on unbalanced diet (FLY AA Val-60%, empty circles), on unbalanced diet adjusted with His (FLY AA Val -60% + His, triangles) or on unbalanced diet adjusted with Leu (FLY AA Val -60% + Leu, squares). (E) Developmental timing of larvae raised on unbalanced diet (FLY AA Val -60%) in GF conditions (grey), in Lp-associated conditions (green) or after supplementation with the same quantity of Heat-Killed (HK) Lp (black). We used a Cox proportional hazards model to compare the effect of Lp and HK Lp to the GF condition.

Figure S2

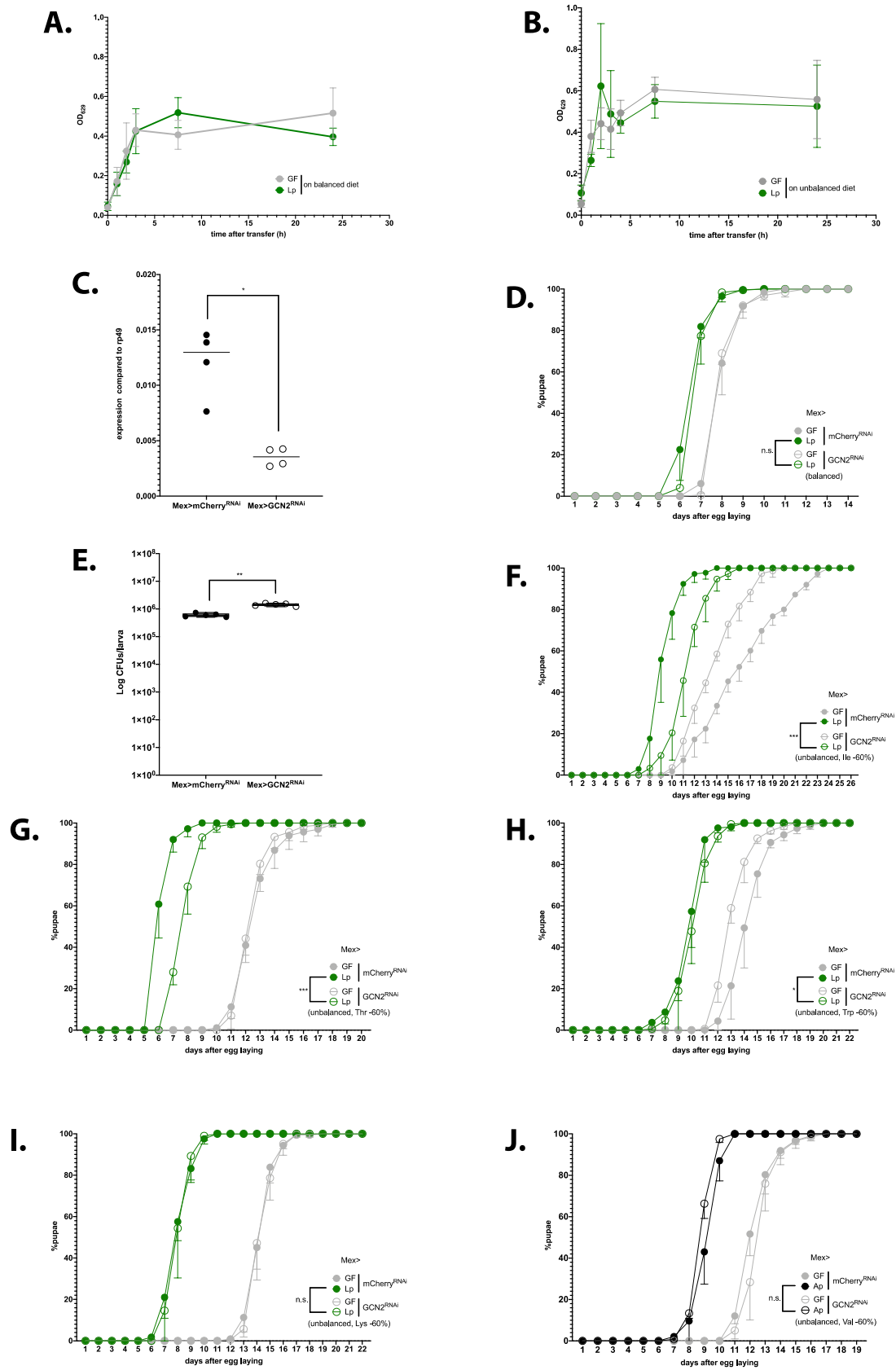
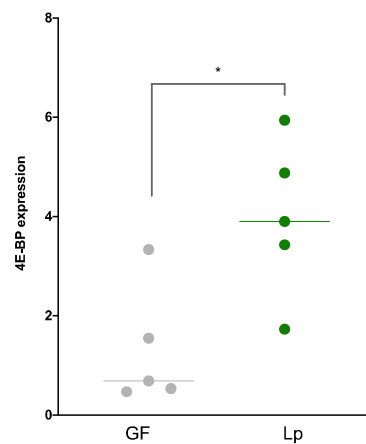


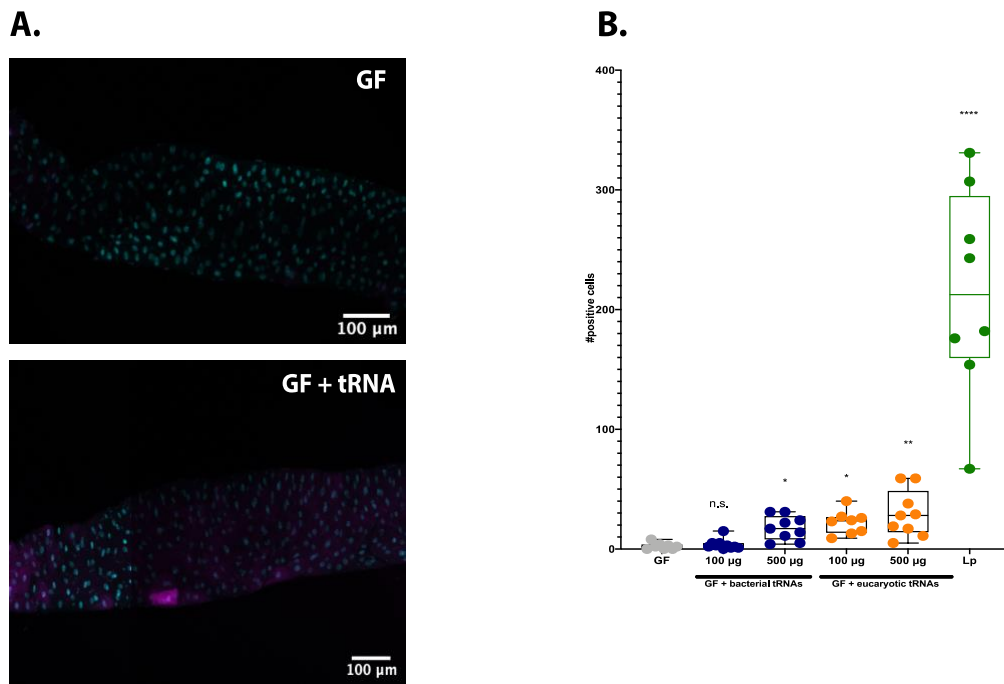
Fig. S2

(A-B) Food intake of larvae reared in GF conditions (grey) or Lp-associated conditions (green) on balanced diet (A) or unbalanced diet (B). Larvae were transferred on coloured food, and food intake was calculated as the Optical Density (OD) of the food ingested by the larvae over time. (C) Expression of *GCN2* in the anterior midgut of control larvae (*Mex>mCherry^{RNAi}*) or *GCN2* knock-down larvae (*Mex>GCN2^{RNAi}*). Expression is normalized with the expression of *rp49* using the formula $2^{Cq(rp49)-Cq(GCN2)}$. We performed a Mann-Whitney test to compare the two conditions, * p-value<0.05. (D) Developmental timing of larvae reared on balanced diet in GF conditions (grey) or Lp-associated conditions (green) in a control background (*Mex>mCherry^{RNAi}*, filled circles) or in a *GCN2* knock-down background (empty circles). We used a Cox proportional hazards model to compare the effect of Lp in the control background and in the *GCN2* knock-down background. n.s.: non-significant. (E) Colonization of the gut by Lp in control larvae (*Mex>mCherry^{RNAi}*, filled circles) or *GCN2* knock-down larvae (*Mex>GCN2^{RNAi}*, empty circles). We performed a Mann-Whitney test to compare the two conditions. **: p-value<0.01. (F-I) Developmental timing of larvae in GF conditions (grey) or Lp-associated conditions (green) in a control background (*Mex>mCherry^{RNAi}*, filled circles) or *GCN2* knock-down larvae (*Mex>GCN2^{RNAi}*, empty circles). Larvae were reared on unbalanced diet FLY AA Ile -60% (F), FLY AA Thr -60% (G), FLY AA Trp -60% (H) and FLY AA Lys -60% (I). for each nutritional condition, we used a Cox proportional hazards model to compare the effect of Lp in the control background and in the *GCN2* knock-down background. The p-values were adjusted by the Holm method. n.s.: non-significant. *: p-value<0.05. ***: p-value<0.001. (J) Developmental timing of larvae reared on unbalanced diet (FLY AA Val-60%) in GF conditions (grey) or Ap-associated conditions (black) in a control background (*Mex>mCherry^{RNAi}*, filled circles) or *GCN2* knock-down larvae (*Mex>GCN2^{RNAi}*, empty circles). We used a Cox proportional hazards model to compare the effect of Ap in the control background and in the *GCN2* knock-down background. n.s.: non-significant.

Figure S3**Fig. S3**

4E-BP expression in the anterior midgut of larvae reared on unbalanced diet in GF conditions (grey) or Lp-associated conditions (green). Expression is normalized with the expression of *rp49* using the formula $2^{Cq(rp49)-Cq(4E-BP)}$. We performed a Mann-Whitney test to compare the two conditions. *: p-value<0.05.

Figure S4

**Fig. S4**

(A) Representative images of 4E-BP^{intron}dsRed GF larvae (top panel) and 4E-BP^{intron}dsRed GF larvae fed 500 μg of bacterial tRNAs (bottom panel) on balanced diet (FLY AA). Cyan: DAPI. Magenta: 4E-BP^{intron}dsRed reporter. (B) Quantification of the 4E-BP^{intron}dsRed reporter's activity in the anterior midgut of GF larvae (grey), GF larvae fed with increasing concentrations of bacterial tRNAs (blue) or yeast tRNAs (orange) and Lp-associated larvae (green) on balanced diet (FLY AA). We performed a Kruskal-Wallis test followed by post-hoc Dunn's tests to compare each condition to GF. n.s.: non-significant. *: p-value<0.05. **: p-value<0.01. ***: p-value<0.001.

Figure S5

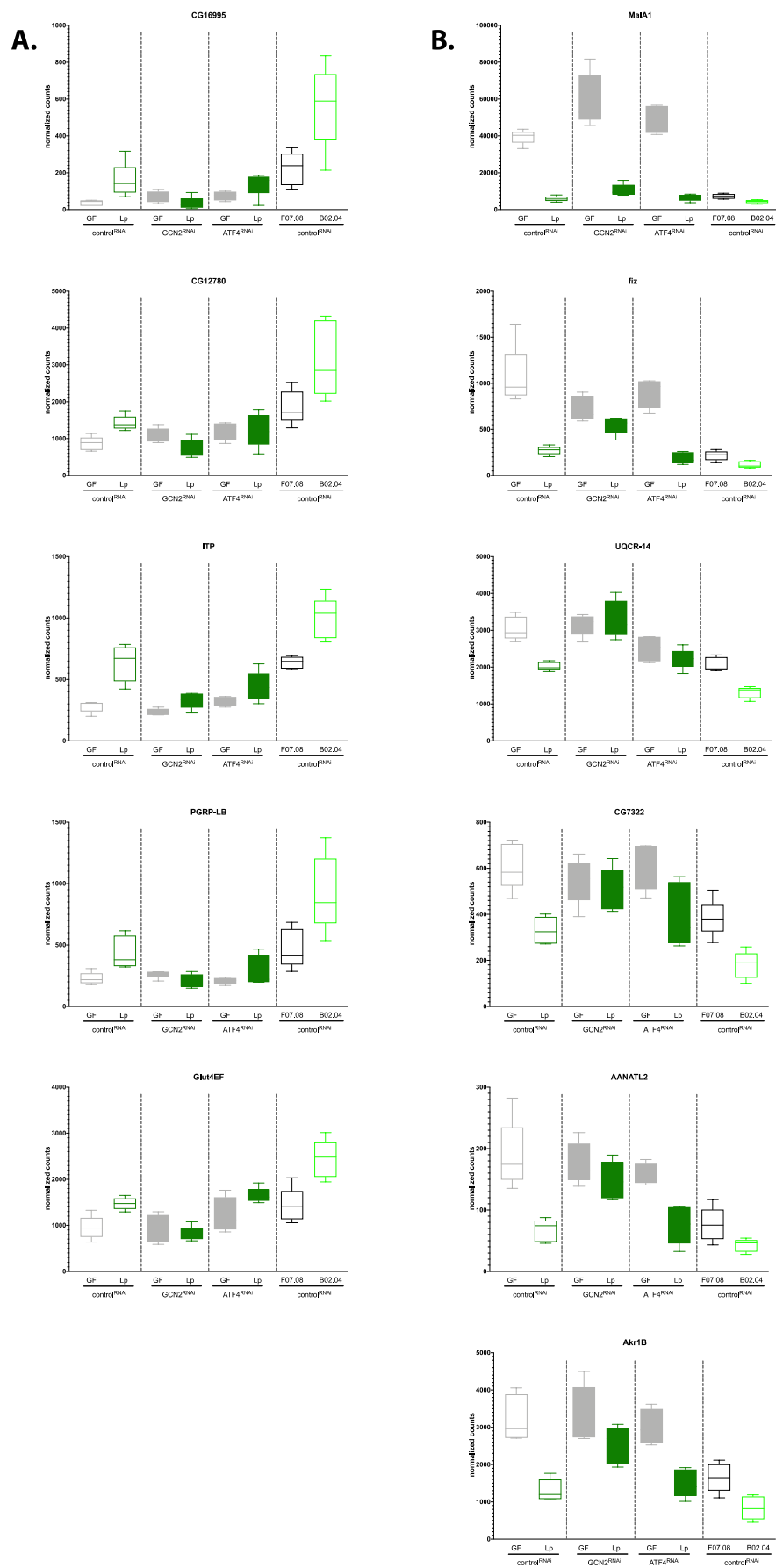
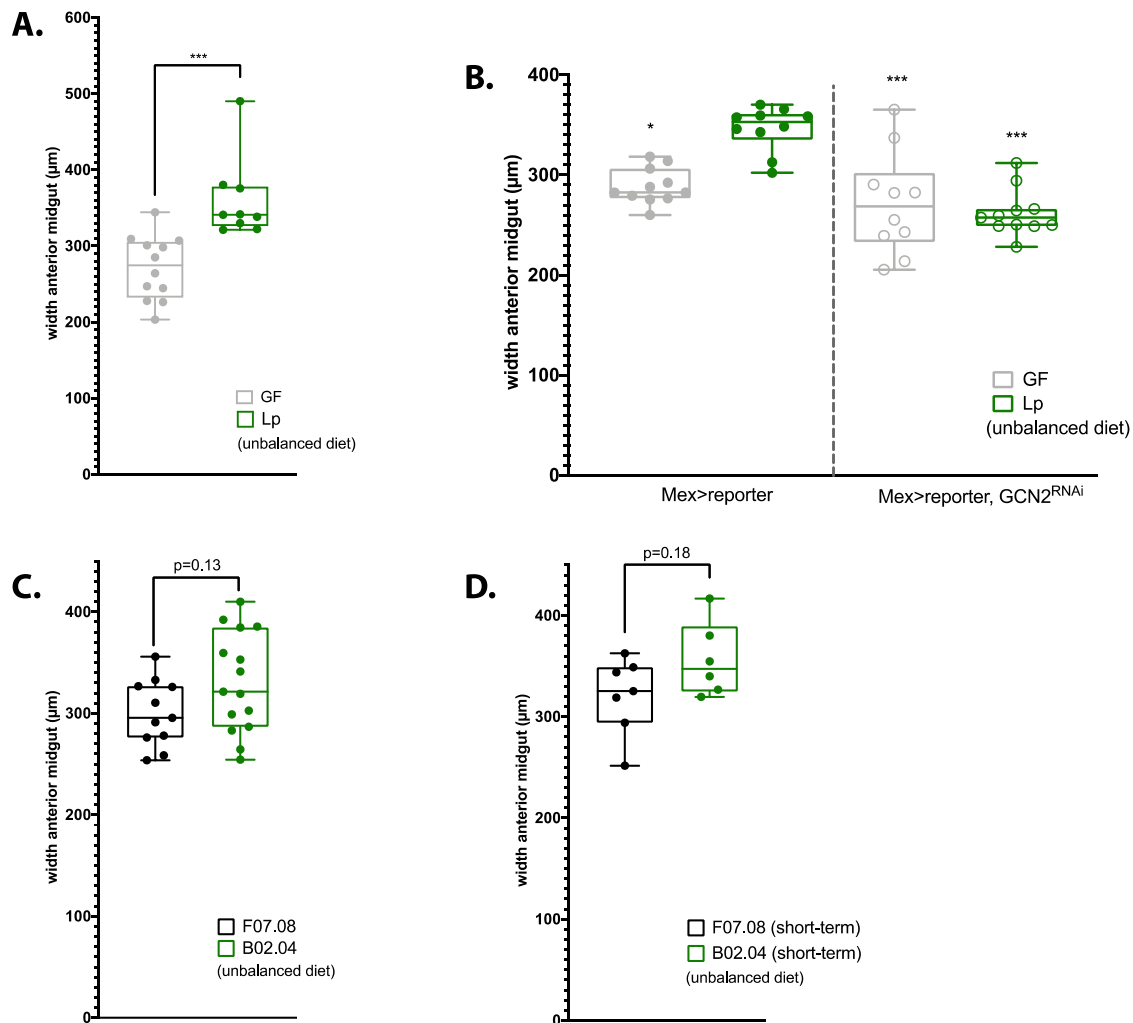


Fig. S5

Normalized counts of the genes identified in the transcriptome analysis. The boxplots show min, max and median expression of the genes (5 replicates per condition). (A) Genes identified as up-regulated in response to Lp in a GCN2-dependent, r/tRNA operon-dependent, ATF4-independent manner. (B) Genes identified as down-regulated in response to Lp in a GCN2-dependent, r/tRNA operon-dependent, ATF4-independent manner.

Fig. S6**Fig. S6**

Maximal width of the anterior midgut (µm) of larvae fed an unbalanced diet. (A) 4E-BP^{intron}dsRed GF (grey) and Lp-associated larvae (green). We performed a Mann-Whitney test to compare the two conditions. ***: p-value < 0.001. (B) Mex>4E-BP^{intron}dsRed (control condition, filled circles) and Mex>4E-BP^{intron}dsRed, GCN2^{RNAi} (GCN2 knock-down, empty circles), in GF conditions (grey) or Lp-associated conditions (green). We performed a Kruskal-Wallis test followed by post-hoc Dunn's tests to compare each condition to the Lp-associated control condition. *: p-value < 0.05, ***: p-value < 0.001. (C-D) 4E-BP^{intron}dsRed in chronic (B) or short-term (C) association with F07.08 (black) and B02.04 (green). We performed a Mann-Whitney test to compare the two conditions. The p-values are indicated on the graphs.

References

- Afgan, E., Baker, D., van den Beek, M., Blankenberg, D., Bouvier, D., Čech, M., Chilton, J., Clements, D., Coraor, N., Eberhard, C., et al. (2016). The Galaxy platform for accessible, reproducible and collaborative biomedical analyses: 2016 update. *Nucleic Acids Res* *44*, W3–W10.
- Ahmed, S.M.H., Maldera, J.A., Kronic, D., Paiva-Silva, G.O., Pénalva, C., Teleman, A.A., and Edgar, B.A. (2020). Fitness trade-offs incurred by ovary-to-gut steroid signalling in *Drosophila*. *Nature* *584*, 415–419.
- Akman Gündüz, E., and Douglas, A.E. (2009). Symbiotic bacteria enable insect to use a nutritionally inadequate diet. *Proc Biol Sci* *276*, 987–991.
- Anthony, T.G., McDaniel, B.J., Byerley, R.L., McGrath, B.C., Cavener, D.R., McNurlan, M.A., and Wek, R.C. (2004). Preservation of liver protein synthesis during dietary leucine deprivation occurs at the expense of skeletal muscle mass in mice deleted for eIF2 kinase GCN2. *J Biol Chem* *279*, 36553–36561.
- Axelsson, L., Rud, I., Naterstad, K., Blom, H., Renckens, B., Boekhorst, J., Kleerebezem, M., van Hijum, S., and Siezen, R.J. (2012). Genome sequence of the naturally plasmid-free *Lactobacillus plantarum* strain NC8 (CCUG 61730). *J Bacteriol* *194*, 2391–2392.
- B'chir, W., Maurin, A.-C., Carraro, V., Averous, J., Jousse, C., Muranishi, Y., Parry, L., Stepien, G., Fafournoux, P., and Bruhat, A. (2013). The eIF2 α /ATF4 pathway is essential for stress-induced autophagy gene expression. *Nucleic Acids Res* *41*, 7683–7699.
- Beckstead, R.B., Lam, G., and Thummel, C.S. (2005). The genomic response to 20-hydroxyecdysone at the onset of *Drosophila* metamorphosis. *Genome Biology* *6*, R99.
- Berlanga, J.J., Ventoso, I., Harding, H.P., Deng, J., Ron, D., Sonenberg, N., Carrasco, L., and de Haro, C. (2006). Antiviral effect of the mammalian translation initiation factor 2 α kinase GCN2 against RNA viruses. *EMBO J* *25*, 1730–1740.
- Bjordal, M., Arquier, N., Kniazeff, J., Pin, J.P., and Léopold, P. (2014). Sensing of Amino Acids in a Dopaminergic Circuitry Promotes Rejection of an Incomplete Diet in *Drosophila*. *Cell* *156*, 510–521.
- Blanton, L.V., Charbonneau, M.R., Salih, T., Barratt, M.J., Venkatesh, S., Ilkaveya, O., Subramanian, S., Manary, M.J., Trehan, I., Jorgensen, J.M., et al. (2016). Gut bacteria that prevent growth impairments transmitted by microbiota from malnourished children. *Science* *351*, aad3311.
- Broderick, N.A., Buchon, N., and Lemaitre, B. (2014). Microbiota-induced changes in *drosophila melanogaster* host gene expression and gut morphology. *MBio* *5*, e01117-01114.
- Brune, A., and Dietrich, C. (2015). The Gut Microbiota of Termites: Digesting the Diversity in the Light of Ecology and Evolution. *Annual Review of Microbiology* *69*, 145–166.
- Cammack, K.M., Austin, K.J., Lamberson, W.R., Conant, G.C., and Cunningham, H.C. (2018). Ruminant nutrition symbiosis: Tiny but mighty: the role of the rumen microbes in

livestock production. *J. Anim. Sci.* *96*, 752–770.

Castro-Portuguez, R., and Sutphin, G.L. (2020). Kynurenine pathway, NAD⁺ synthesis, and mitochondrial function: Targeting tryptophan metabolism to promote longevity and healthspan. *Exp Gerontol* *132*, 110841.

Chakrabarti, S., Liehl, P., Buchon, N., and Lemaitre, B. (2012). Infection-Induced Host Translational Blockage Inhibits Immune Responses and Epithelial Renewal in the *Drosophila* Gut. *Cell Host & Microbe* *12*, 60–70.

Charroux, B., Capo, F., Kurz, C.L., Peslier, S., Chaduli, D., Viallat-Lieutaud, A., and Royet, J. (2018). Cytosolic and Secreted Peptidoglycan-Degrading Enzymes in *Drosophila* Respectively Control Local and Systemic Immune Responses to Microbiota. *Cell Host Microbe* *23*, 215-228.e4.

Chung, J.S. (2010). Hemolymph ecdysteroids during the last three molt cycles of the blue crab, *Callinectes sapidus*: quantitative and qualitative analyses and regulation. *Archives of Insect Biochemistry and Physiology* *73*, 1–13.

Chung, J.S., Dirksen, H., and Webster, S.G. (1999). A remarkable, precisely timed release of hyperglycemic hormone from endocrine cells in the gut is associated with ecdysis in the crab *Carcinus maenas*. *PNAS* *96*, 13103–13107.

Colombani, J., Raisin, S., Pantalacci, S., Radimerski, T., Montagne, J., and Léopold, P. (2003a). A Nutrient Sensor Mechanism Controls *Drosophila* Growth. *Cell* *114*, 739–749.

Colombani, J., Raisin, S., Pantalacci, S., Radimerski, T., Montagne, J., and Léopold, P. (2003b). A Nutrient Sensor Mechanism Controls *Drosophila* Growth. *Cell* *114*, 739–749.

Combe, B.E., Defaye, A., Bozonnet, N., Puthier, D., Royet, J., and Leulier, F. (2014). *Drosophila* microbiota modulates host metabolic gene expression via IMD/NF- κ B signaling. *PLoS One* *9*.

Consuegra, J., Grenier, T., Baa-Puyoulet, P., Rahioui, I., Akherraz, H., Gervais, H., Parisot, N., Silva, P. da, Charles, H., Calevro, F., et al. (2020a). *Drosophila*-associated bacteria differentially shape the nutritional requirements of their host during juvenile growth. *PLOS Biology* *18*, e3000681.

Consuegra, J., Grenier, T., Akherraz, H., Rahioui, I., Gervais, H., da Silva, P., and Leulier, F. (2020b). Metabolic Cooperation among Commensal Bacteria Supports *Drosophila* Juvenile Growth under Nutritional Stress. *IScience* *23*, 101232.

Dang Do, A.N., Kimball, S.R., Cavener, D.R., and Jefferson, L.S. (2009). eIF2 α kinases GCN2 and PERK modulate transcription and translation of distinct sets of mRNAs in mouse liver. *Physiol Genomics* *38*, 328–341.

De Gregorio, E., Spellman, P.T., Rubin, G.M., and Lemaitre, B. (2001). Genome-wide analysis of the *Drosophila* immune response by using oligonucleotide microarrays. *Proc Natl Acad Sci U S A* *98*, 12590–12595.

- Dever, T.E., Feng, L., Wek, R.C., Cigan, A.M., Donahue, T.F., and Hinnebusch, A.G. (1992). Phosphorylation of initiation factor 2 α by protein kinase GCN2 mediates gene-specific translational control of GCN4 in yeast. *Cell* 68, 585–596.
- Dietzl, G., Chen, D., Schnorrer, F., Su, K.-C., Barinova, Y., Fellner, M., Gasser, B., Kinsey, K., Oettel, S., Scheiblaue, S., et al. (2007). A genome-wide transgenic RNAi library for conditional gene inactivation in *Drosophila*. *Nature* 448, 151–156.
- Dirksen, H., Tesfai, L.K., Albus, C., and Nässel, D.R. (2008). Ion transport peptide splice forms in central and peripheral neurons throughout postembryogenesis of *Drosophila melanogaster*. *Journal of Comparative Neurology* 509, 23–41.
- Domínguez Rubio, A.P., Martínez, J.H., Martínez Casillas, D.C., Coluccio Leskow, F., Piuri, M., and Pérez, O.E. (2017). *Lactobacillus casei* BL23 Produces Microvesicles Carrying Proteins That Have Been Associated with Its Probiotic Effect. *Front Microbiol* 8.
- Dong, J., Qiu, H., Garcia-Barrio, M., Anderson, J., and Hinnebusch, A.G. (2000). Uncharged tRNA Activates GCN2 by Displacing the Protein Kinase Moiety from a Bipartite tRNA-Binding Domain. *Molecular Cell* 6, 269–279.
- Donnelly, N., Gorman, A.M., Gupta, S., and Samali, A. (2013). The eIF2 α kinases: their structures and functions. *Cell Mol Life Sci* 70, 3493–3511.
- Erkosar, B., Storelli, G., Defaye, A., and Leulier, F. (2013). Host-intestinal microbiota mutualism: “learning on the fly.” *Cell Host & Microbe* 13, 8–14.
- Erkosar, B., Storelli, G., Mitchell, M., Bozonnet, L., Bozonnet, N., and Leulier, F. (2015). Pathogen virulence impedes mutualist-mediated enhancement of host juvenile growth via inhibition of protein digestion. *Cell Host Microbe* 18, 445–455.
- Gáliková, M., Dirksen, H., and Nässel, D.R. (2018). The thirsty fly: Ion transport peptide (ITP) is a novel endocrine regulator of water homeostasis in *Drosophila*. *PLOS Genetics* 14, e1007618.
- Gallinetti, J., Harputlugil, E., and Mitchell, J.R. (2013). Amino acid sensing in dietary-restriction-mediated longevity: roles of signal-transducing kinases GCN2 and TOR. *Biochem J* 449, 1–10.
- Gaudet, P., Livstone, M.S., Lewis, S.E., and Thomas, P.D. (2011). Phylogenetic-based propagation of functional annotations within the Gene Ontology consortium. *Briefings in Bioinformatics* 12, 449–462.
- Gehrig, J.L., Venkatesh, S., Chang, H.-W., Hibberd, M.C., Kung, V.L., Cheng, J., Chen, R.Y., Subramanian, S., Cowardin, C.A., Meier, M.F., et al. (2019). Effects of microbiota-directed foods in gnotobiotic animals and undernourished children. *Science* 365.
- Géminard, C., Rulifson, E.J., and Léopold, P. (2009). Remote Control of Insulin Secretion by Fat Cells in *Drosophila*. *Cell Metabolism* 10, 199–207.
- Gilbert, L.I., Rybczynski, R., and Warren, J.T. (2002). Control and biochemical nature of the

ecdysteroidogenic pathway. *Annu Rev Entomol* 47, 883–916.

Glaser-Schmitt, A., and Parsch, J. (2018). Functional characterization of adaptive variation within a cis-regulatory element influencing *Drosophila melanogaster* growth. *PLOS Biology* 16, e2004538.

Goberdhan, D.C.I., Wilson, C., and Harris, A.L. (2016). Amino Acid Sensing by mTORC1: Intracellular Transporters Mark the Spot. *Cell Metab* 23, 580–589.

Gourse, R.L., Takebe, Y., Sharrock, R.A., and Nomura, M. (1985). Feedback regulation of rRNA and tRNA synthesis and accumulation of free ribosomes after conditional expression of rRNA genes. *Proc Natl Acad Sci U S A* 82, 1069–1073.

Grallert, B., and Boye, E. (2007). The Gcn2 Kinase as a Cell Cycle Regulator. *Cell Cycle* 6, 2768–2772.

Grasmann, G., Smolle, E., Olschewski, H., and Leithner, K. (2019). Gluconeogenesis in cancer cells – repurposing of a starvation-induced metabolic pathway? *Biochim Biophys Acta Rev Cancer* 1872, 24–36.

Guo, F., and Cavener, D.R. (2007). The GCN2 eIF2 α Kinase Regulates Fatty-Acid Homeostasis in the Liver during Deprivation of an Essential Amino Acid. *Cell Metabolism* 5, 103–114.

Harding, H.P., Zhang, Y., Zeng, H., Novoa, I., Lu, P.D., Calton, M., Sadri, N., Yun, C., Popko, B., Paules, R., et al. (2003). An Integrated Stress Response Regulates Amino Acid Metabolism and Resistance to Oxidative Stress. *Molecular Cell* 11, 619–633.

Heitman, J., Movva, N.R., and Hall, M.N. (1991). Targets for cell cycle arrest by the immunosuppressant rapamycin in yeast. *Science* 253, 905–909.

Hinton, T., Noyes, D.T., and Ellis, J. (1951). Amino acids and growth factors in a chemically defined medium for *Drosophila*. *Physiological Zoology* 24, 335–353.

Inglis, A.J., Masson, G.R., Shao, S., Perisic, O., McLaughlin, S.H., Hegde, R.S., and Williams, R.L. (2019). Activation of GCN2 by the ribosomal P-stalk. *Proc Natl Acad Sci U S A* 116, 4946–4954.

Irving, P., Troxler, L., Heuer, T.S., Belvin, M., Kopczynski, C., Reichhart, J.-M., Hoffmann, J.A., and Hetru, C. (2001). A genome-wide analysis of immune responses in *Drosophila*. *Proc Natl Acad Sci U S A* 98, 15119–15124.

Jiggins, F.M., and Kim, K.-W. (2006). Contrasting Evolutionary Patterns in *Drosophila* Immune Receptors. *J Mol Evol* 63, 769–780.

Kamareddine, L., Robins, W.P., Berkey, C.D., Mekalanos, J.J., and Watnick, P.I. (2018). The *Drosophila* Immune Deficiency Pathway Modulates Enteroendocrine Function and Host Metabolism. *Cell Metabolism*.

Kang, M.-J., Vasudevan, D., Kang, K., Kim, K., Park, J.-E., Zhang, N., Zeng, X., Neubert,

- T.A., Marr, M.T., and Ryoo, H.D. (2017). 4E-BP is a target of the GCN2–ATF4 pathway during *Drosophila* development and aging. *J Cell Biol* 216, 115–129.
- Keebaugh, E.S., Yamada, R., Obadia, B., Ludington, W.B., and Ja, W.W. (2018). Microbial quantity impacts *Drosophila* nutrition, development, and lifespan. *IScience* 4, 247–259.
- Kilstrup, M., Hammer, K., Ruhdal Jensen, P., and Martinussen, J. (2005). Nucleotide metabolism and its control in lactic acid bacteria. *FEMS Microbiology Reviews* 29, 555–590.
- Kim, B., Kanai, M.I., Oh, Y., Kyung, M., Kim, E.-K., Jang, I.-H., Lee, J.-H., Kim, S.-G., Suh, G.S.B., and Lee, W.-J. (2021). Response of the microbiome–gut–brain axis in *Drosophila* to amino acid deficit. *Nature* 1–5.
- Kim, K., Park, J.-E., Yeom, J., Park, N., Trần, T.-X.T., and Kang, M.-J. (2020). Tissue-specific roles of GCN2 in aging and autosomal dominant retinitis pigmentosa. *Biochem Biophys Res Commun* 533, 1054–1060.
- Koyama, T., Texada, M.J., Halberg, K.A., and Rewitz, K. (2020). Metabolism and growth adaptation to environmental conditions in *Drosophila*. *Cell Mol Life Sci* 77, 4523–4551.
- Krishnamoorthy, J., Mounir, Z., Raven, J., and Koromilas, A. (2008). The eIF2 α kinases inhibit vesicular stomatitis virus replication independently of eIF2 phosphorylation. *Cell Cycle* 7, 2346–2351.
- Kuhn, A., Koch, H.-G., and Dalbey, R.E. (2017). Targeting and Insertion of Membrane Proteins. *EcoSal Plus* 7.
- Laeger, T., Albarado, D.C., Burke, S.J., Trosclair, L., Hedgepeth, J.W., Berthoud, H.-R., Gettys, T.W., Collier, J.J., Münzberg, H., and Morrison, C.D. (2016). Metabolic Responses to Dietary Protein Restriction Require an Increase in FGF21 that Is Delayed by the Absence of GCN2. *Cell Reports* 16, 707–716.
- Laplante, M., and Sabatini, D.M. (2009). mTOR signaling at a glance. *J Cell Sci* 122, 3589–3594.
- Layalle, S., Arquier, N., and Léopold, P. (2008). The TOR Pathway Couples Nutrition and Developmental Timing in *Drosophila*. *Developmental Cell* 15, 568–577.
- Li, M., Lee, K., Hsu, M., Nau, G., Mylonakis, E., and Ramratnam, B. (2017). Lactobacillus-derived extracellular vesicles enhance host immune responses against vancomycin-resistant enterococci. *BMC Microbiol* 17.
- Lifshitz, F. (2009). Nutrition and growth. *J Clin Res Pediatr Endocrinol* 1, 157–163.
- Ma, X.M., and Blenis, J. (2009). Molecular mechanisms of mTOR-mediated translational control. *Nat Rev Mol Cell Biol* 10, 307–318.
- Malzer, E., Szajewska-Skuta, M., Dalton, L.E., Thomas, S.E., Hu, N., Skaer, H., Lomas, D.A., Crowther, D.C., and Marciniak, S.J. (2013). Coordinate regulation of eIF2 α phosphorylation by PPP1R15 and GCN2 is required during *Drosophila* development. *J Cell*

Sci 126, 1406–1415.

Malzer, E., Dominicus, C.S., Chambers, J.E., Dickens, J.A., Mookerjee, S., and Marciniak, S.J. (2018). The integrated stress response regulates BMP signalling through effects on translation. *BMC Biol* 16.

Manière, G., Alves, G., Berthelot-Grosjean, M., and Grosjean, Y. (2020). Growth regulation by amino acid transporters in *Drosophila* larvae. *Cell. Mol. Life Sci.*

Marshall, L., Rideout, E.J., and Grewal, S.S. (2012). Nutrient/TOR-dependent regulation of RNA polymerase III controls tissue and organismal growth in *Drosophila*. *EMBO J* 31, 1916–1930.

Martino, M.E., Bayjanov, J.R., Caffrey, B.E., Wels, M., Joncour, P., Hughes, S., Gillet, B., Kleerebezem, M., van Hijum, S.A.F.T., and Leulier, F. (2016). Nomadic lifestyle of *Lactobacillus plantarum* revealed by comparative genomics of 54 strains isolated from different habitats. *Environ. Microbiol.* 18, 4974–4989.

Masson, G.R. (2019). Towards a model of GCN2 activation. *Biochem Soc Trans* 47, 1481–1488.

Matos, R.C., Schwarzer, M., Gervais, H., Courtin, P., Joncour, P., Gillet, B., Ma, D., Bulteau, A.-L., Martino, M.E., Hughes, S., et al. (2017). D-Alanylation of teichoic acids contributes to *Lactobacillus plantarum*-mediated *Drosophila* growth during chronic undernutrition. *Nat Microbiol* 2, 1635–1647.

Moriano-Gutierrez, S., Bongrand, C., Essock-Burns, T., Wu, L., McFall-Ngai, M.J., and Ruby, E.G. (2020). The noncoding small RNA SsrA is released by *Vibrio fischeri* and modulates critical host responses. *PLOS Biology* 18, e3000934.

Niculescu, M.D., and Zeisel, S.H. (2002). Diet, Methyl Donors and DNA Methylation: Interactions between Dietary Folate, Methionine and Choline. *J Nutr* 132, 2333S–2335S.
Ohhara, Y., Kobayashi, S., and Yamanaka, N. (2017). Nutrient-Dependent Endocycling in Steroidogenic Tissue Dictates Timing of Metamorphosis in *Drosophila melanogaster*. *PLoS Genet* 13, e1006583.

Olsen, D.S., Jordan, B., Chen, D., Wek, R.C., and Cavener, D.R. (1998). Isolation of the gene encoding the *Drosophila melanogaster* homolog of the *Saccharomyces cerevisiae* GCN2 eIF-2alpha kinase. *Genetics* 149, 1495–1509.

Overend, G., Luo, Y., Henderson, L., Douglas, A.E., Davies, S.A., and Dow, J.A.T. (2016). Molecular mechanism and functional significance of acid generation in the *Drosophila* midgut. *Sci Rep* 6, 27242.

Pawar, K., Shigematsu, M., Sharbati, S., and Kirino, Y. (2020). Infection-induced 5'-half molecules of tRNA^{His}GUG activate Toll-like receptor 7. *PLOS Biology* 18, e3000982.

Piper, M.D. (2017). Using artificial diets to understand the nutritional physiology of *Drosophila melanogaster*. *Curr Opin Insect Sci* 23, 104–111.

- Piper, M.D., Blanc, E., Leitão-Gonçalves, R., Yang, M., He, X., Linford, N.J., Hoddinott, M.P., Hopfen, C., Soultoukis, G.A., Niemeyer, C., et al. (2014). A holidic medium for *Drosophila melanogaster*. *Nat Methods* 11.
- Piper, M.D.W., Soultoukis, G.A., Blanc, E., Mesaros, A., Herbert, S.L., Juricic, P., He, X., Atanassov, I., Salmonowicz, H., Yang, M., et al. (2017). Matching dietary amino acid balance to the *in silico*-translated exome optimizes growth and reproduction without cost to lifespan. *Cell Metabolism* 25, 610–621.
- Rajagopala, S.V., Vashee, S., Oldfield, L.M., Suzuki, Y., Venter, J.C., Telenti, A., and Nelson, K.E. (2017). The Human Microbiome and Cancer. *Cancer Prev Res (Phila)* 10, 226–234.
- Ren, B., Wang, X., Duan, J., and Ma, J. (2019). Rhizobial tRNA-derived small RNAs are signal molecules regulating plant nodulation. *Science* 365, 919–922.
- Rižner, T.L., and Penning, T.M. (2014). Role of aldo–keto reductase family 1 (AKR1) enzymes in human steroid metabolism. *Steroids* 79, 49–63.
- Rodrigues, Y.K., Bergen, E. van, Alves, F., Duneau, D., and Beldade, P. (2018). Complex effects of day and night temperature fluctuations on thermally plastic traits in a seasonal plasticity model. *BioRxiv* 207258.
- Russell, C.W., Bouvaine, S., Newell, P.D., and Douglas, A.E. (2013). Shared metabolic pathways in a coevolved insect-bacterial symbiosis. *Appl. Environ. Microbiol.* 79, 6117–6123.
- Ryu, J.-H., Kim, S.-H., Lee, H.-Y., Bai, J.Y., Nam, Y.-D., Bae, J.-W., Lee, D.G., Shin, S.C., Ha, E.-M., and Lee, W.-J. (2008). Innate immune homeostasis by the homeobox gene *Caudal* and commensal-gut mutualism in *Drosophila*. *Science* 319, 777–782.
- Saavedra-García, P., Roman-Trufero, M., Al-Sadah, H.A., Blighe, K., López-Jiménez, E., Christoforou, M., Penfold, L., Capece, D., Xiong, X., Miao, Y., et al. (2021). Systems level profiling of chemotherapy-induced stress resolution in cancer cells reveals druggable trade-offs. *PNAS* 118.
- Saguir, F.M., and de Nadra, M.C.M. (2007). Improvement of a chemically defined medium for the sustained growth of *Lactobacillus plantarum*: nutritional requirements. *Curr. Microbiol.* 54, 414–418.
- Sakaguchi, E. (2003). Digestive strategies of small hindgut fermenters. *Animal Science Journal* 74, 327–337.
- Sang, J.H. (1956). The quantitative nutritional requirements of *Drosophila melanogaster*. *Journal of Experimental Biology* 33, 45–72.
- Sannino, D.R., Dobson, A.J., Edwards, K., Angert, E.R., and Buchon, N. (2018). The *Drosophila melanogaster* gut microbiota provisions thiamine to its host. *MBio* 9, e00155-18.
- Schwarzer, M., Makki, K., Storelli, G., Machuca-Gayet, I., Srutkova, D., Hermanova, P.,

- Martino, M.E., Balmand, S., Hudcovic, T., Heddi, A., et al. (2016). *Lactobacillus plantarum* strain maintains growth of infant mice during chronic undernutrition. *Science* 351, 854–857.
- Schwarzer, M., Strigini, M., and Leulier, F. (2018). Gut Microbiota and Host Juvenile Growth. *Calcified Tissue International* 102, 387–405.
- Shin, S.C., Kim, S.-H., You, H., Kim, B., Kim, A.C., Lee, K.-A., Yoon, J.-H., Ryu, J.-H., and Lee, W.-J. (2011). *Drosophila* microbiome modulates host developmental and metabolic homeostasis via insulin signaling. *Science* 334, 670–674.
- Storelli, G., Defaye, A., Erkosar, B., Hols, P., Royet, J., and Leulier, F. (2011). *Lactobacillus plantarum* promotes *Drosophila* systemic growth by modulating hormonal signals through TOR-dependent nutrient sensing. *Cell Metab.* 14, 403–414.
- Storelli, G., Strigini, M., Grenier, T., Bozonnet, L., Schwarzer, M., Daniel, C., Matos, R., and Leulier, F. (2018). *Drosophila* perpetuates nutritional mutualism by promoting the fitness of its intestinal symbiont *Lactobacillus plantarum*. *Cell Metab* 27, 362-377.e8.
- Takeuchi, H., Rigden, D.J., Ebrahimi, B., Turner, P.C., and Rees, H.H. (2005). Regulation of ecdysteroid signalling during *Drosophila* development: identification, characterization and modelling of ecdysone oxidase, an enzyme involved in control of ligand concentration. *Biochem J* 389, 637–645.
- Tanimura, T., Kitamlira, K., Fukuda, T., and Kikuchi, T. (1979). Purification and Partial Characterization of Three Forms of α -Glucosidase from the Fruit Fly *Drosophila melanogaster*. *The Journal of Biochemistry* 85, 123–130.
- Tattoli, I., Sorbara, M.T., Vuckovic, D., Ling, A., Soares, F., Carneiro, L.A.M., Yang, C., Emili, A., Philpott, D.J., and Girardin, S.E. (2012). Amino Acid Starvation Induced by Invasive Bacterial Pathogens Triggers an Innate Host Defense Program. *Cell Host & Microbe* 11, 563–575.
- Tennessen, J.M., and Thummel, C.S. (2011). Coordinating growth and review maturation — insights from *Drosophila*. *Curr Biol* 21, R750–R757.
- Teske, B.F., Baird, T.D., and Wek, R.C. (2011). Chapter Nineteen - Methods for Analyzing eIF2 Kinases and Translational Control in the Unfolded Protein Response. In *Methods in Enzymology*, P.M. Conn, ed. (Academic Press), pp. 333–356.
- Teusink, B., van Enkevort, F.H.J., Francke, C., Wiersma, A., Wegkamp, A., Smid, E.J., and Siezen, R.J. (2005). *In silico* reconstruction of the metabolic pathways of *Lactobacillus plantarum*: comparing predictions of nutrient requirements with those from growth experiments. *Appl Environ Microbiol* 71, 7253–7262.
- Therneau, T.M., and Grambsch, P.M. (2000). *Modeling Survival Data: Extending the Cox Model* (New York: Springer-Verlag).
- Vandehoef, C., Molaei, M., and Karpac, J. (2020). Dietary Adaptation of Microbiota in *Drosophila* Requires NF- κ B-Dependent Control of the Translational Regulator 4E-BP. *Cell Rep* 31, 107736.

Vasudevan, D., Clark, N.K., Sam, J., Cotham, V.C., Ueberheide, B., Marr, M.T., and Ryoo, H.D. (2017). The GCN2-ATF4 signaling pathway induces 4E-BP to bias translation and boost antimicrobial peptide synthesis in response to bacterial infection. *Cell Reports* 21, 2039–2047.

Warburg, O. (1956). On the Origin of Cancer Cells. *Science* 123, 309–314.

Weinberg, F., and Chandel, N.S. (2009). Mitochondrial Metabolism and Cancer. *Annals of the New York Academy of Sciences* 1177, 66–73.

Wek, R.C., and Cavener, D.R. (2007). Translational Control and the Unfolded Protein Response. *Antioxidants & Redox Signaling* 9, 2357–2372.

Wek, S.A., Zhu, S., and Wek, R.C. (1995). The histidyl-tRNA synthetase-related sequence in the eIF-2 alpha protein kinase GCN2 interacts with tRNA and is required for activation in response to starvation for different amino acids. *Mol Cell Biol* 15, 4497–4506.

West, C.L., Stanisiz, A.M., Mao, Y.-K., Champagne-Jorgensen, K., Bienenstock, J., and Kunze, W.A. (2020). Microvesicles from *Lactobacillus reuteri* (DSM-17938) completely reproduce modulation of gut motility by bacteria in mice. *PLOS ONE* 15, e0225481.

Wong, S.Y., Javid, B., Addepalli, B., Piszczek, G., Strader, M.B., Limbach, P.A., and Barry, C.E. (2013). Functional role of methylation of G518 of the 16S rRNA 530 loop by GidB in *Mycobacterium tuberculosis*. *Antimicrob. Agents Chemother.* 57, 6311–6318.

Wu, G. (2009). Amino acids: metabolism, functions, and nutrition. *Amino Acids* 37, 1–17.

Ye, J., Kumanova, M., Hart, L.S., Sloane, K., Zhang, H., De Panis, D.N., Bobrovnikova-Marjon, E., Diehl, J.A., Ron, D., and Koumenis, C. (2010). The GCN2-ATF4 pathway is critical for tumour cell survival and proliferation in response to nutrient deprivation. *The EMBO Journal* 29, 2082–2096.

Zhang, P., McGrath, B.C., Reinert, J., Olsen, D.S., Lei, L., Gill, S., Wek, S.A., Vattam, K.M., Wek, R.C., Kimball, S.R., et al. (2002). The GCN2 eIF2 α Kinase Is Required for Adaptation to Amino Acid Deprivation in Mice. *Mol Cell Biol* 22, 6681–6688.

Zhu, S., and Wek, R.C. (1998). Ribosome-binding Domain of Eukaryotic Initiation Factor-2 Kinase GCN2 Facilitates Translation Control *. *Journal of Biological Chemistry* 273, 1808–1814.

Conclusion and perspectives

Conclusions and perspectives

Symbiotic microbes can promote the growth of their host in situation of undernutrition in mice (Schwarzer et al., 2016), flies (Shin et al., 2011; Storelli et al., 2011) and probably humans (Blanton et al., 2016), but the mechanisms remain elusive. The purpose of my thesis work was to identify and describe mechanisms that may explain the growth promoting effect exerted on *Drosophila* larvae by its symbiotic microbes. I used a simple model of mono-association of larvae with two growth-promoting symbiotic bacteria, *Acetobacter pomorum* (Ap) and *Lactiplantibacillus plantarum* (Lp), which enabled me to manipulate the genetics of both the host and the symbiont, on a holidic diet that allowed control of the nutrition.

I worked on two distinct mechanisms, explained in the two parts of the manuscript: fulfilling of nutritional requirements by symbiotic bacteria (Chapter I) and rescue of the delay due to AA unbalance by Lp (Chapter II).

The Chapter I is an extensive study of all nutrients that compose a holidic diet for *Drosophila*. For each nutrient, we used genome-based metabolic network reconstruction to predict whether or not this nutrient can be synthesized by *Drosophila* and by the two symbionts that we study, Lp and Ap. We then monitored bacterial growth and the growth of GF larvae on HD lacking this nutrient, and found a very good correlation between predictions and observations. We noted a few exceptions; for example, Lp is auxotroph to Arg though its genome encodes all the enzymes necessary for Arg synthesis. These exceptions show the interest of *in vivo* confirmation of genome-based predictions of metabolic pathways. Moreover, we monitored the ability of larvae to grow in the absence of each nutrient, in presence of the two bacterial symbionts. We concluded that the two symbionts have different effects on their host's nutritional requirements: Ap fulfills 19 out of the 22 requirements of GF larvae, whereas Lp fulfills only 12 out of 22. In most cases, we were able to correlate the ability of symbionts to rescue the lack of a nutrient with their ability to synthesize this nutrient. This is in line with other studies that showed that symbiotic bacteria can actively provide certain nutrients to *Drosophila* (Sannino et al., 2018; Wong et al., 2014). Moreover, we identified a few situations where the rescue of nutrient deficiency cannot be explained by the provision of the nutrients. For instance, we do not know how Lp can fulfill Zn requirements, nor how Ap can fulfill choline requirements since it does not have the enzymatic capacities to produce choline. Further studies focusing on these cases may allow to discover novel beneficial symbiotic mechanisms.

One of the main interests of the Chapter I was to provide a catalogue of which nutrients may or may not be provided by bacteria to the host. We used this catalogue in the Chapter II, to focus on a surprising observation: that Lp can rescue the developmental delay caused by AA unbalance due to the limitation in certain AA, without being able to synthesize these AA *de novo* and to provide them to its host. We took advantage of the main advantage of our model, which is to be able to manipulate both the host's and the bacteria's genetics: we showed that Lp's capacity to promote growth on an AA-unbalanced diet relies on both the activation of GCN2 in larval enterocytes and on the presence of operons encoding transfer and ribosomal RNAs in Lp. Moreover, we detected a "host-symbiont epistasis" between the r/tRNAs in Lp and GCN2 in larvae: GCN2 is activated by the tRNAs, and we do not observe an effect of the r/tRNA mutation in a GCN2 knock-down background. These observations, and the mechanism of activation of GCN2, which can be stimulated by multiple kinds of double-stranded RNAs (all eukaryotic tRNAs regardless of their AA specificity, eukaryotic rRNAs, viral RNAs) (Masson, 2019), allow us to propose the following model: r/tRNAs produced by

Lp may stimulate the activity of GCN2 in the enterocytes of the anterior midgut, which supports larval growth on an AA unbalanced diet. To understand how GCN2 activation supports growth, we used RNA sequencing to identify genes in the larval midgut that are activated by Lp in a GCN2-dependent and r/tRNA operon-dependent manner. This approach allowed us to identify promising candidates: genes regulating Ecdysone signalling, and genes of glucose metabolism, which may foster gut growth and nutrient absorption.

We do not know whether other bacteria, e.g. Ap, can elicit a GCN2-dependent adaptation to AA unbalance as well. Ap can rescue Val limitation in a GCN2 knock-down background, but we know from the Chapter I that Ap can provide Valine to the larva, which makes GCN2 unnecessary (similarly, Lp does not require GCN2 in enterocytes to rescue Lysine scarcity, because Lp can provide Lysine and correct the AA unbalance). It would be interesting to generate a mutant Ap that cannot synthesize Valine, and test whether it can still rescue the effects of Valine scarcity through a GCN2-dependent mechanism. Figure 5 presents our working model of the two situations described in my thesis: when symbiotic bacteria provide the scarce nutrient, and when symbiotic bacteria cannot provide the scarce nutrient.

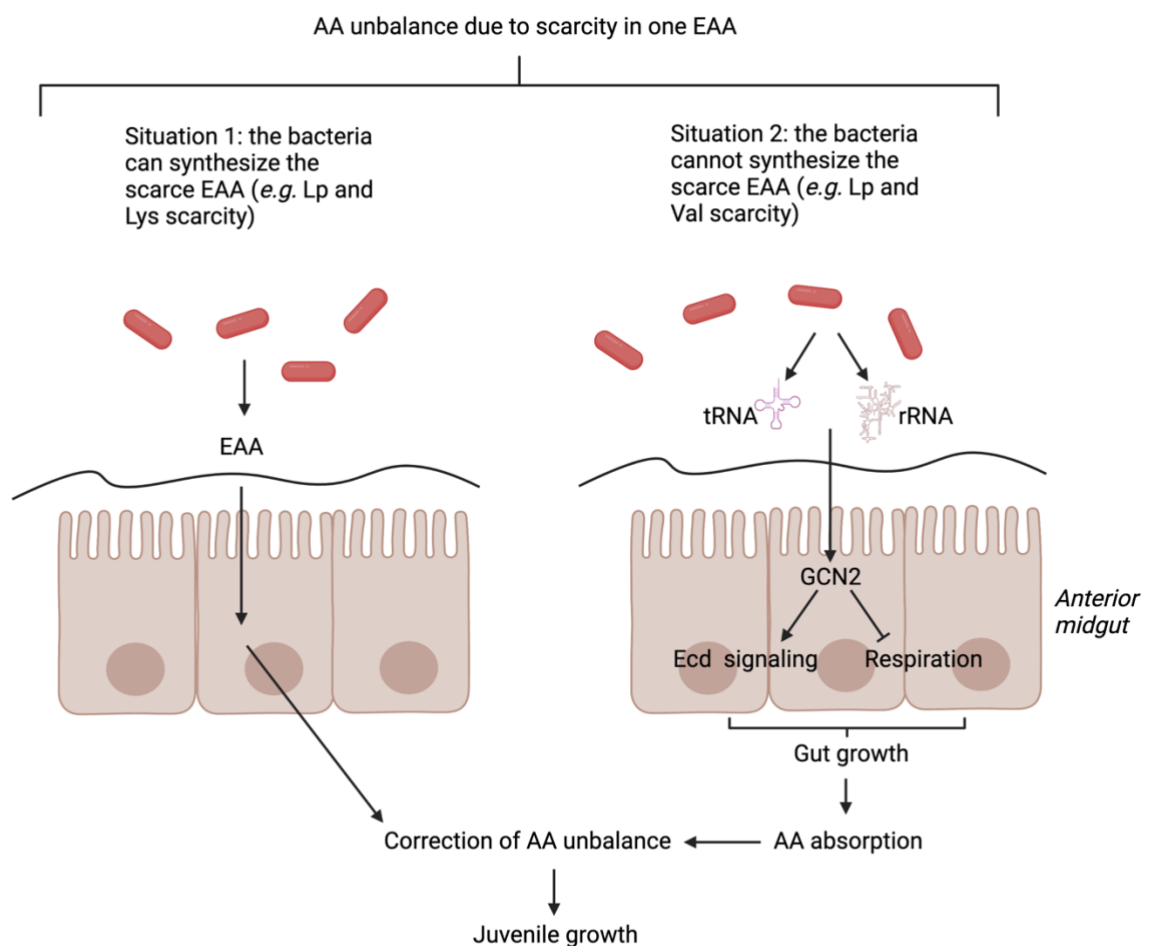


Fig 5. Model of the mechanisms underlying growth-promotion in situation of AA unbalance by symbiotic bacteria. AA: Amino acid. EAA: essential amino acid. Lp: *Lactiplantibacillus plantarum*. tRNA: transfer RNA. rRNA: ribosomal RNA. GCN2: general control nonderepressible 2. Ecd: Ecdysone.

This model suffers from several caveats. First of all, we do not know whether the metabolites at play (AA, tRNAs, rRNAs) are secreted by bacteria in the gut, or if they are produced in the diet and ingested by the larvae. Moreover, we did not formerly demonstrate that the r/tRNAs of Lp directly activate GCN2 in enterocytes. We are currently testing this hypothesis through a genetic approach: we are deleting each component of the operon (tRNA and each rRNA), as well as the full operon, to test whether one single deletion can recapitulate the loss of function of the mutant F07.08 on both rescue of AA unbalance and GCN2 activation. In parallel, we are using a complementation approach: transforming the r/tRNA operon mutant with plasmids expressing tRNAs or rRNAs, and testing whether it rescues the mutant's phenotype. We will also test whether feeding the larvae purified rRNAs, and r/tRNAs extracted from Lp, can activate GCN2. These experiments will allow us to test whether or not rRNAs and/or tRNAs produced by Lp do activate GCN2. Finally, the transcriptomics signatures identified in our RNAseq approach need to be tested functionally: does inhibiting/overexpressing these genes in the gut mimic Lp's effect?

Dobzhansky wrote "Nothing in biology makes sense, except in the light of evolution". I strongly believe that lab researchers, who work on very artificial models far away from nature, should sometimes wonder whether and how their work "makes sense in the light of evolution". In other words, what evolutionary phenomenon might explain the observations that we made?

The bacteria that I studied during my thesis, Lp and Ap, are found in multiple environments. Ap strains have been isolated from the gut of several Insects, but they are mostly known for their role in vinegar fermentation and can be found growing on fermenting fruits (Matsushita et al., 2016). Lp is even more versatile: strains of this species were isolated from environments as distinct as the guts of Insects or Mammals, fermenting fruits, dairy, sourdough, grass silage and sausages. More importantly, there is no correlation between the origin of an isolate and its phylogeny. Lp appears to be a "nomadic" bacterium: in contrast to specialized bacteria, such as *Buchnera aphidicola* that can only live inside the cells of pea aphids, Lp has adapted to be able to live in multiple environments without showing a specialization to any (Martino et al., 2016). Moreover, neither Ap nor Lp can persist in the gut of *Drosophila* larvae: they are transient bacteria, that mostly live on the food substrate even though they may be transported by flies. Applying experimental evolution on Lp in presence of *Drosophila* larvae result in the adaptation of Lp to the diet, not to its host (Martino et al., 2018). Finally, we did not find in the biosynthetic pathways of Lp or Ap any complementarity with the biosynthetic pathways of *Drosophila*, like it is the case for pea aphids and *B. aphidicola* and is a sign of co-evolution (Russell et al., 2013). For these reasons, I personally find unlikely that our observations result from an adaptation of Lp and Ap to *Drosophila*. However, I do believe that *Drosophila* has adapted to the presence of bacteria such as Ap and Lp. Wild *Drosophila melanogaster* larvae exclusively grow on decaying fruits, which are processed by microbes such as *Lactobacilli* and *Acetobacter* (Flatt, 2020); therefore, it seems reasonable to assume that *Drosophila* has adapted its nutrition to the presence of bacteria from the genera *Lactobacillus* and *Acetobacter*, and optimized its capacity to benefit from essential nutrients produced by its symbiotic microbes, such as the nutrients identified in the Chapter I. In the Chapter II, I suggested that GCN2 may have primarily evolved as a sensor of microbial r/t RNAs, before becoming a sensor of self r/tRNA and AA scarcity. If this hypothesis is correct, GCN2 might allow the larva to couple its growth with the abundance of microbes present in the environment: when microbes are abundant,

r/tRNA may activate GCN2 in the gut, triggering gut growth, optimal nutrient absorption and rapid organismal growth. When microbes are scarce, for instance on a fruit which decaying has just started or at the end of the ripening phase, low r/tRNA abundance may not activate GCN2, probing larvae to slow down their growth until microbes have proliferated and nutrition is more suited. This hypothesis does not contradict the cognate role of GCN2 as a sensor of AA scarcity in neurons (Bjordal et al., 2014): it suggests that the action of GCN2 is organ-specific. In neurons, GCN2 may sense AA scarcity and prompt the larvae to find a better food source; in the gut, GCN2 may sense microbe's abundance and boost gut growth and nutrient absorption. In Figure 6, I propose a unifying model for the roles of GCN2 in different larval organs, and how it can help larvae to couple the cues from its nutritional environment and its microbial environment.

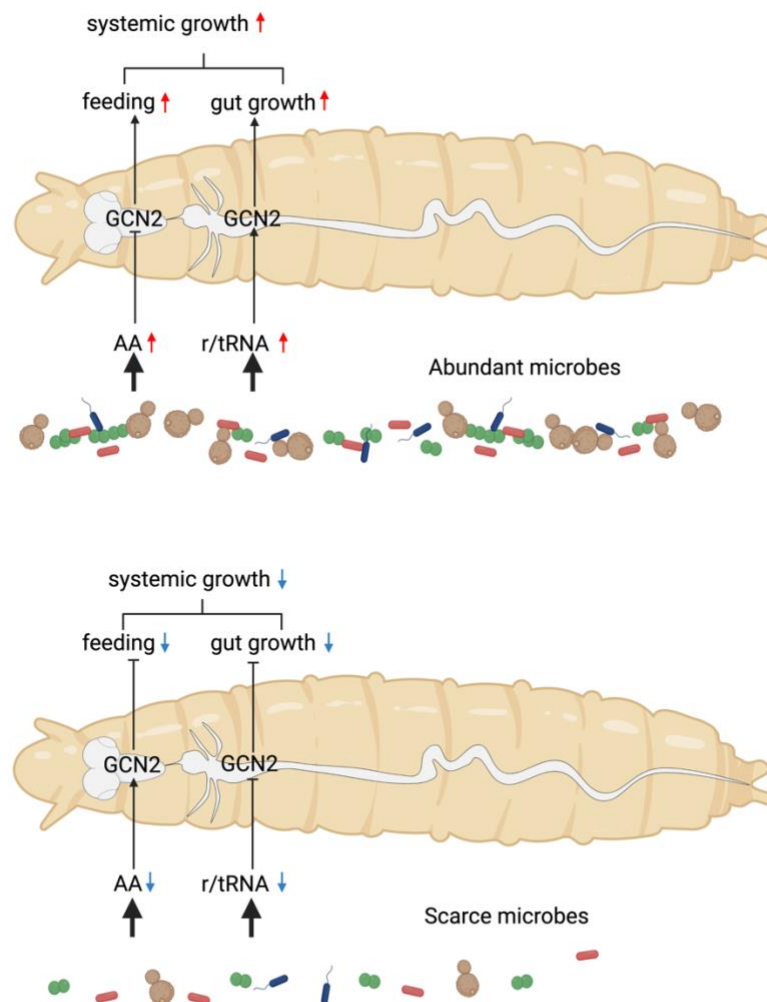


Fig 6. Complementary roles of GCN2 in the brain and the gut. When microbes are abundant (top), they inhibit GCN2 in the brain (left) through AA production and stimulate GCN2 in the gut (right) through r/tRNAs. When microbes are scarce (bottom) they provide few AA, which activates GCN2 in the brain (left), and they secrete few r/tRNAs, which represses GCN2 in the gut (right). AA: Amino acids. r/tRNAs: ribosomal/transfer RNAs. GCN2: general control nonderepressible kinase 2.

We do not know whether or not the mechanisms described here can be extrapolated to other animals. The contribution of gut bacteria to a Vertebrate host's AA requirements are unlikely to be significant; however, gut microbes may be an important source of vitamins to Vertebrates (Biesalski, 2016). It would be interesting to test whether the gut microbiome of Vertebrates can help fulfill their host's requirements in other micronutrients such as metal traces or choline. Moreover, it would be very exciting to test whether GCN2 can respond to symbiotic microbes in the gut of other Animals. There are models of GCN2 KO mice, which exhibit defects in adaptation to AA scarcity. Future studies may thus investigate whether GCN2 interacts with gut microbes in Mammals as well.

The importance of microbial symbionts for nutrition has been established a long time ago for Animals that feed on cellulose-rich diets such as ruminants (Cammack et al., 2018), or on AA-depleted plant sap such as pea aphids (Akman Gündüz and Douglas, 2009). For other animals however, the microbial contribution to nutrition has long been overlooked. Especially, the interactions between nutrition, juvenile growth and the microbiome has only recently started to be investigated in classic animal models. I believe that studying these interactions is crucial to understand growth regulation. Indeed, the guts of all Animals are a niche for symbiotic microbes that process the food, transform it and produce metabolites and signaling molecules. These microbes may or may not be resident in the gut: some simply go through the gut with food, but they can still have a profound impact on their host's nutrition. Therefore, growth regulation by juvenile animals may integrate both dietary cues, as showed by a great wealth of studies (Simpson and Raubenheimer, 2012) and microbial cues. Microbial cues may be nutrients, synthesized from dietary nutrients as described in the Chapter I, or other molecules, which may signal the presence of beneficial symbiotic microbes to the host as proposed in Chapter II. In any case, sensing of both dietary and microbial cues, nutritional or non-nutritional, may allow juvenile animals to adapt their growth to their environment.

The effect of microbes on growth is particularly spectacular because growth and nutrition are so intrinsically connected. However, as presented in the Introduction, symbiotic microbes can influence other aspects of their host's physiology: behaviour, immunity and metabolism. Like for growth, the influence of symbiotic microbes on these parameters may rely on nutritional or non-nutritional cues. Studying these mechanisms may improve our understanding of development and physiology in health and disease.

Interactions between host and symbiotic microbes are the result of a very long co-evolution. The most ancient gut-like tissue to date was identified in fossils of *Cloudina*, primitive metazoans from the terminal Ediacaran Period (~550–539 million years ago) (Schiffbauer et al., 2020). Although it is impossible to know whether or not these ancient guts contained microbes, it seems plausible that microbes from *Cloudina*'s environment and food were in contact with this primitive gut, triggering the beginning of the long co-evolution of Animals and symbiotic bacteria. The formation of a digestive cavity is a major evolutionary step in the history of Animals (Nielsen, 2008): it allowed to concentrate digestive enzymes, nutrients and absorptive cells into an enclosed space, which permitted extracellular digestion of macronutrients and considerably increased the potential nutritional influx (Steinmetz, 2019). It also created a niche for microbes to colonize, and allowed the formation of complex symbiotic interactions that

likely contributed to the explosion of animal diversity across a wide variety of environments.

References

Akman Gündüz, E., and Douglas, A.E. (2009). Symbiotic bacteria enable insect to use a nutritionally inadequate diet. *Proc Biol Sci* 276, 987–991.

Biesalski, H.K. (2016). Nutrition meets the microbiome: micronutrients and the microbiota. *Annals of the New York Academy of Sciences* 1372, 53–64.

Bjordal, M., Arquier, N., Kniazeff, J., Pin, J.P., and Léopold, P. (2014). Sensing of Amino Acids in a Dopaminergic Circuitry Promotes Rejection of an Incomplete Diet in *Drosophila*. *Cell* 156, 510–521.

Blanton, L.V., Barratt, M.J., Charbonneau, M.R., Ahmed, T., and Gordon, J.I. (2016). Childhood undernutrition, the gut microbiota, and microbiota-directed therapeutics. *Science* 352, 1533–1533.

Cammack, K.M., Austin, K.J., Lamberson, W.R., Conant, G.C., and Cunningham, H.C. (2018). Ruminant nutrition symbiosis: Tiny but mighty: the role of the rumen microbes in livestock production. *J. Anim. Sci.* 96, 752–770.

Flatt, T. (2020). Life-History Evolution and the Genetics of Fitness Components in *Drosophila melanogaster*. *Genetics* 214, 3–48.

Martino, M.E., Bayjanov, J.R., Caffrey, B.E., Wels, M., Joncour, P., Hughes, S., Gillet, B., Kleerebezem, M., van Hijum, S.A.F.T., and Leulier, F. (2016). Nomadic lifestyle of *Lactobacillus plantarum* revealed by comparative genomics of 54 strains isolated from different habitats. *Environ. Microbiol.* 18, 4974–4989.

Martino, M.E., Joncour, P., Leenay, R., Gervais, H., Shah, M., Hughes, S., Gillet, B., Beisel, C., and Leulier, F. (2018). Bacterial Adaptation to the Host's Diet Is a Key Evolutionary Force Shaping *Drosophila-Lactobacillus* Symbiosis. *Cell Host Microbe* 24, 109-119.e6.

Masson, G.R. (2019). Towards a model of GCN2 activation. *Biochem Soc Trans* 47, 1481–1488.

Matsushita, K., Toyama, H., Tonouchi, N., and Okamoto-Kainuma, A. (2016). Acetic acid bacteria: ecology and physiology (Springer Japan).

Nielsen, C. (2008). Six major steps in animal evolution: are we derived sponge larvae? *Evolution & Development* 10, 241–257.

Russell, C.W., Bouvaine, S., Newell, P.D., and Douglas, A.E. (2013). Shared metabolic pathways in a coevolved insect-bacterial symbiosis. *Appl. Environ. Microbiol.* 79, 6117–6123.

Sannino, D.R., Dobson, A.J., Edwards, K., Angert, E.R., and Buchon, N. (2018). The

Drosophila melanogaster gut microbiota provisions thiamine to its host. *MBio* 9, e00155-18.

Schiffbauer, J.D., Selly, T., Jacquet, S.M., Merz, R.A., Nelson, L.L., Strange, M.A., Cai, Y., and Smith, E.F. (2020). Discovery of bilaterian-type through-guts in cloudinomorphs from the terminal Ediacaran Period. *Nat Commun* 11, 205.

Schwarzer, M., Makki, K., Storelli, G., Machuca-Gayet, I., Srutkova, D., Hermanova, P., Martino, M.E., Balmand, S., Hudcovic, T., Heddi, A., et al. (2016). *Lactobacillus plantarum* strain maintains growth of infant mice during chronic undernutrition. *Science* 351, 854–857.

Shin, S.C., Kim, S.-H., You, H., Kim, B., Kim, A.C., Lee, K.-A., Yoon, J.-H., Ryu, J.-H., and Lee, W.-J. (2011). *Drosophila* microbiome modulates host developmental and metabolic homeostasis via insulin signaling. *Science* 334, 670–674.

Simpson, S.J., and Raubenheimer, D. (2012). The Nature of Nutrition.

Steinmetz, P.R.H. (2019). A non-bilaterian perspective on the development and evolution of animal digestive systems. *Cell Tissue Res* 377, 321–339.

Storelli, G., Defaye, A., Erkosar, B., Hols, P., Royet, J., and Leulier, F. (2011). *Lactobacillus plantarum* promotes *Drosophila* systemic growth by modulating hormonal signals through TOR-dependent nutrient sensing. *Cell Metab.* 14, 403–414.

Wong, A.C.-N., Dobson, A.J., and Douglas, A.E. (2014). Gut microbiota dictates the metabolic response of *Drosophila* to diet. *J. Exp. Biol.* 217, 1894–1901.

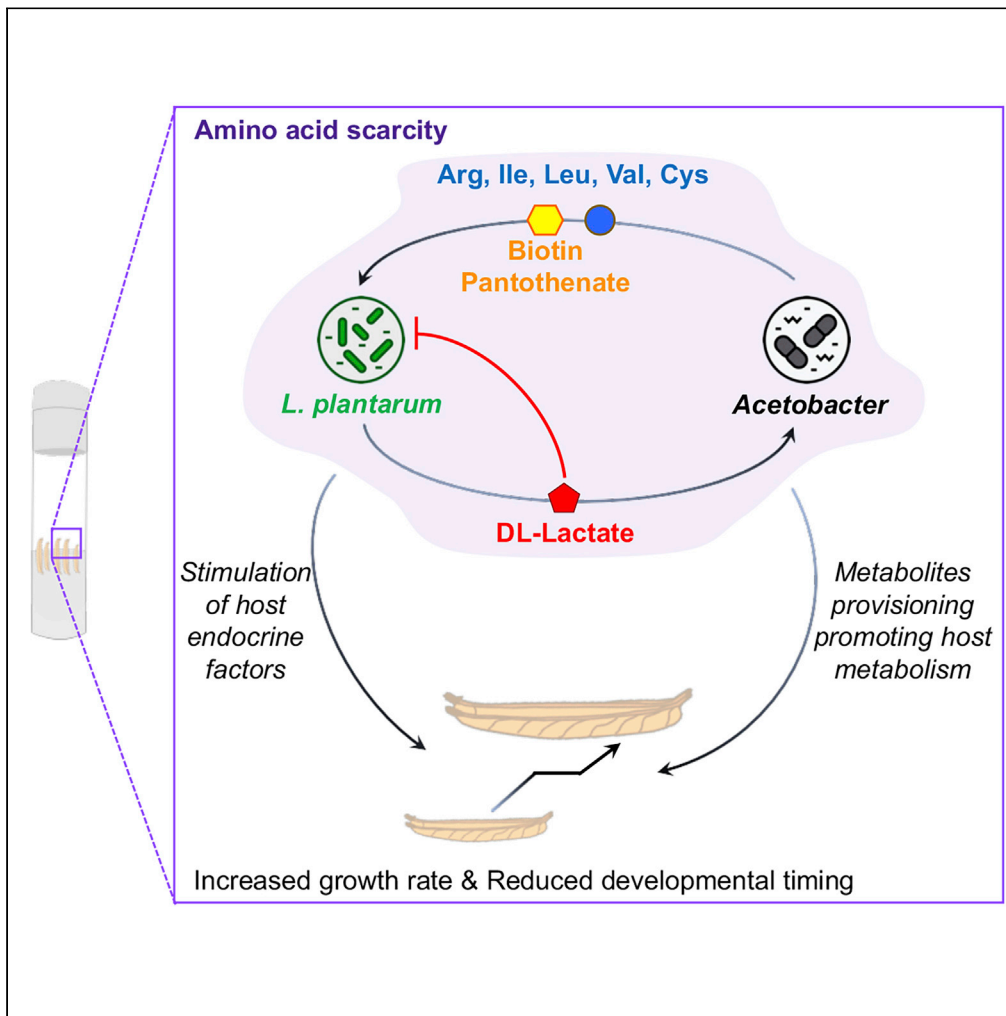
Annexes

Annex I:

Metabolic cooperation among commensal bacteria supports *Drosophila* juvenile growth under nutritional stress

Article published in *iScience* 2020 23(6), 101232.

Article

Metabolic Cooperation among Commensal Bacteria Supports *Drosophila* Juvenile Growth under Nutritional Stress

Jessika Consuegra, Théodore Grenier, Houssam Akherraz, Isabelle Rahioui, Hugo Gervais, Pedro da Silva, François Leulier

jessika.consuegra@ens-lyon.fr (J.C.)
francois.leulier@ens-lyon.fr (F.L.)

HIGHLIGHTS

L. plantarum feeds lactate to *A. pomorum*

A. pomorum supplies essential amino acids and vitamins to *L. plantarum*

Microbiota metabolic dialogue boosts *Drosophila*'s larval growth

Lactate utilization by *Acetobacter* releases anabolic metabolites to larvae

Consuegra et al., iScience 23, 101232
June 26, 2020 © 2020 The Authors.
<https://doi.org/10.1016/j.isci.2020.101232>

Article

Metabolic Cooperation among Commensal Bacteria Supports *Drosophila* Juvenile Growth under Nutritional Stress

Jessika Consuegra,^{1,*} Théodore Grenier,¹ Houssam Akherraz,¹ Isabelle Rahioui,² Hugo Gervais,¹ Pedro da Silva,² and François Leulier^{1,3,*}

SUMMARY

The gut microbiota shapes animal growth trajectory in stressful nutritional environments, but the molecular mechanisms behind such physiological benefits remain poorly understood. The gut microbiota is mostly composed of bacteria, which construct metabolic networks among themselves and with the host. Until now, how the metabolic activities of the microbiota contribute to host juvenile growth remains unknown. Here, using *Drosophila* as a host model, we report that two of its major bacterial partners, *Lactobacillus plantarum* and *Acetobacter pomorum*, engage in a beneficial metabolic dialogue that boosts host juvenile growth despite nutritional stress. We pinpoint that lactate, produced by *L. plantarum*, is utilized by *A. pomorum* as an additional carbon source, and *A. pomorum* provides essential amino acids and vitamins to *L. plantarum*. Such bacterial cross-feeding provisions a set of anabolic metabolites to the host, which may foster host systemic growth despite poor nutrition.

INTRODUCTION

In the animal kingdom, juvenile growth takes place during the post-natal stages preceding sexual maturation and ushers in the most profound physiological changes in an organism's lifetime. These changes are governed by the complex interplay between the animal's genotype and its nutritional environment. In humans, chronic undernutrition at the juvenile stage leads to severe stunting and long-term negative neurological, metabolic, and reproductive consequences (Goyal et al., 2015). Today 155 million children are plagued by childhood malnutrition worldwide (Development Initiatives, 2018).

Recent studies establish that the microbial communities colonizing the body surfaces (i.e., microbiota), especially the activities and constituents of the gut microbiota, can alter the host's growth trajectory. Both in invertebrates and in mammals, selected strains of microbiota members can buffer the deleterious impact of undernutrition on juvenile growth dynamics (Blanton et al., 2016; Schwarzer et al., 2016; Shin et al., 2011; Smith et al., 2013; Storelli et al., 2011). In humans, children suffering from malnutrition carry an "immature" gut microbiota that fails to be remedied by classical re-nutrition strategies (Subramanian et al., 2014).

Juvenile growth is marked by the exponential increase of the animals' biomass manifested as gain in weight and longitudinal size. These physical traits are governed by the host's growth hormone and growth factors (GH/IGF1 in mammals) whose production and activities are regulated by nutrients availability (Thissen et al., 1994). Recently, it was established that gut microbiota members also influence the production and activity of growth hormone and growth factors in both invertebrate and mammals (Schwarzer et al., 2016; Shin et al., 2011; Storelli et al., 2011; Yan et al., 2016).

Despite recent progress, how the gut microbiota confers such benefits to the host remains poorly understood. This is partly due to the fact that the gut microbiota is a complex ecosystem comprising up to hundreds of microbial species in mammals, mostly bacteria (Hooper and Gordon, 2018). They construct multiplex, high-order nutritional and metabolic networks among themselves and with the host such that these interactions directly influence host nutrition and metabolism (Schroeder and Bäckhed, 2016). Given

¹Institut de Génomique Fonctionnelle de Lyon, Université de Lyon, Ecole Normale Supérieure de Lyon, Centre National de la Recherche Scientifique, Université Claude Bernard Lyon 1, UMR5242, 69364 Cedex 07, Lyon, France

²Laboratoire Biologie Fonctionnelle, Insectes et Interactions, Université de Lyon, Institut National des Sciences Appliquées, Institut National de Recherche pour l'Agriculture, l'Alimentation et l'Environnement, UMR0203, 69621 Villeurbanne, France

³Lead Contact

*Correspondence: jessika.consuegra@ens-lyon.fr (J.C.), francois.leulier@ens-lyon.fr (F.L.)

<https://doi.org/10.1016/j.isci.2020.101232>



this complexity, until now no study has elucidated to what extent and how the metabolic interactions among members of the microbiota contribute to host juvenile growth.

To answer this question, we bypassed the complexity encountered in mammals and developed an experimentally tractable gnotobiotic *Drosophila* model associated with its two major bacterial partners, *Lactobacillus plantarum* and *Acetobacter pomorum*, which are frequently found to co-exist in wild flies captured on fruit-based baits (Chandler et al., 2011; Pais et al., 2018; Wong et al., 2013). Previously, using oligidic diets (i.e., a diet composed of complex ingredients such as inactivated yeast and cornmeal flour), we and others have established that association of germ-free (GF) larvae with either *A. pomorum* or *L. plantarum* stimulates juvenile growth by promoting the systemic release and activities of *Drosophila* insulin-like peptides (dILPs), the functional analogs of vertebrate insulin and IGFs (Shin et al., 2011; Storelli et al., 2011). Here, using *Drosophila* bi-associated with *A. pomorum* and *L. plantarum*, we characterized the metabolic dialogues among the three partners in a strictly controlled nutritional environment low in amino acids to mimic chronic protein undernutrition, namely, a fully chemically defined or holidic diet (HD) (Piper et al., 2017). HDs support suboptimal growth and development of *Drosophila* larvae (Jang and Lee, 2018; Piper et al., 2013; Rapport et al., 1983; Schultz et al., 1946), yet it has proved to be a useful tool to study the specific influence of individual nutrients on *Drosophila* physiology (Jang and Lee, 2018; Mishra et al., 2018; Piper et al., 2013, 2017). This experimental model grants us complete control over three key parameters in the system: the diet, the host, and its commensal partners. We defined the nutritional requirements, auxotrophies, and complementation of over 40 individual nutrients including all amino acids, vitamins, nucleic acids, lipid precursors, and minerals for each commensal and the juvenile host in the GF context or upon association with either microbial partner (Consuegra et al., 2020).

Here, we report that, when co-inoculated on a *Drosophila* HD low in amino acids, *L. plantarum* and *A. pomorum* engage in a beneficial metabolic dialogue that supports bacterial growth and buffers the deleterious impact of nutritional stress on host juvenile growth. We specifically pinpoint that lactate, the main metabolic by-product of *L. plantarum*, is utilized by *A. pomorum* as an additional carbon source, and in turn, *A. pomorum* provides various amino acids and B vitamins to complement *L. plantarum* auxotrophies. Inert microbial biomass has been reported to promote larval development (Bing et al., 2018; Storelli et al., 2011) and adult longevity (Keebaugh et al., 2018; Yamada et al., 2015) probably by acting as an additional nutritional source. Although we confirm that inert bacterial biomass slightly contributes to increased juvenile growth, we show that *Lactobacillus* provision of lactate to *Acetobacter* triggers a metabolic shift in *Acetobacter* leading to the provision of a set of anabolic metabolites to the host, which may boost host systemic growth despite poor nutrition.

RESULTS

Bi-Association Enhances the Benefit of Commensal Bacteria on Larval Development

In a Holidic Diet (HD) low in amino acids that mimics chronic protein undernutrition, we studied larval development in germ-free (GF) and upon mono or bi-association with two representative commensal strains of the *Drosophila* microbiota: *Acetobacter pomorum*^{WJL} (Ap^{WJL}) and *Lactobacillus plantarum*^{NC8} (Lp^{NC8}). In this diet, GF larvae reach metamorphosis at ~10 days. By comparison, the time from embryogenesis to metamorphosis of GF animals on rich oligidic diets (i.e., yeast, 50 g/L) is ~5 days, whereas it is increased to ~13 days on poor oligidic diet (i.e., yeast, 6 g/L) (Matos et al., 2017).

On HD, the benefit on larval development of bacterial mono-association is enhanced in larvae bi-associated with Ap^{WJL} and Lp^{NC8} (Ap^{WJL}:Lp^{NC8}; Figures 1A and 1B). Bi-associated animals always develop faster than their mono-associated siblings and reach metamorphosis in ~5.2 days (Figure 1A) or ~8.2 days (Figure 1B) according to the initial bacterial inoculum. We observed similar results using both complete HDs with optimal amino acid content (Figure S1A, HD 16 g and HD 20 g) or with a fruit-based diet (banana diet, Figure S1B) containing ~7 g/kg of protein (Oyeyinka and Afolayan, 2019) where GF larvae fail to develop (see Methods). Of note, the differential capacities of the bacteria to sustain *Drosophila* growth on the banana diet are not a consequence of differential bacteria growth on this fruit-based diet as both Ap^{WJL} and Lp^{NC8} grew to the same extent in the presence or absence of larvae (Figures S1C and S1D).

During post-embryonic development, Ap^{WJL} or Lp^{NC8} not only influences maturation rates (i.e., time to entry to metamorphosis) but also increases larval linear size gains upon nutrient scarcity (Figure 1C).

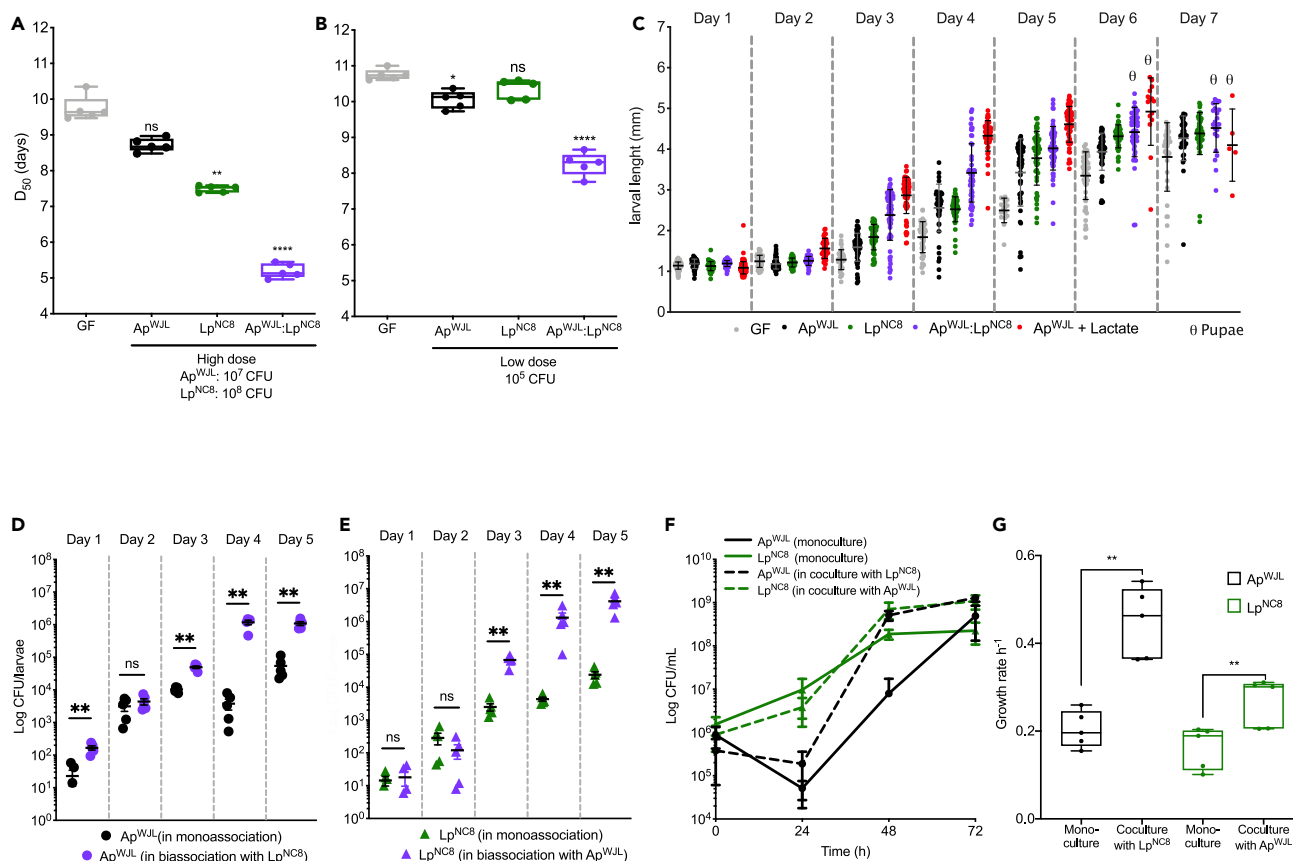


Figure 1. Bi-Association with Ap^{WJL} and Lp^{NC8} Enhances Commensal-Mediated Benefit on Larval Development

(A and B) Developmental timing (time from egg to metamorphosis) on complete holidic diet (HD) of Germ-Free (GF) larvae (gray) or GF larvae inoculated with high dose (10^7 or 10^8 CFU) respectively; (A) or low dose (10^5 CFU); (B) of Ap^{WJL} and/or Lp^{NC8} (Ap^{WJL} , black; Lp^{NC8} , green; Ap^{WJL} : Lp^{NC8} , purple). D_{50} : Day when 50% of the larvae population has entered metamorphosis.

(C) Larval length at every day post-embryogenesis of GF larvae or post-inoculation (Day 1) with 10^5 CFU of Ap^{WJL} and/or Lp^{NC8} or Ap^{WJL} mono-associated larvae supplemented with DL-lactate at a final concentration of 0.6 g/L (red). θ , pupae detected in the vial.

(D and E) Microbial load (Ap^{WJL} , D; Lp^{NC8} , E) of larvae mono- or bi-associated with 10^5 CFU of Ap^{WJL} and/or Lp^{NC8} .

(F and G) Growth in liquid HD (F) and growth rates (G) of Ap^{WJL} and Lp^{NC8} in mono- (plain lines) or cocultures (dashed lines) in liquid HD. Gray always refers to GF, black to Ap^{WJL} mono-association, green to Lp^{NC8} mono-association condition, and purple to Ap^{WJL} : Lp^{NC8} bi-association. Each symbol represents an independent replicate except in (F) where symbols represent the means \pm SEM of three biological replicates. Boxplots show minimum, maximum, and median where each point is a biological replicate. Dot plots show mean \pm SEM. (A and B) We performed Kruskal-Wallis test followed by uncorrected Dunn's tests to compare each gnotobiotic condition with GF. (D and E) Each point represents a biological replicate comprising the average microbial load of a pool of 10 larvae. We performed Mann-Whitney test to compare microbial loads in mono-association with microbial loads in bi-association for the strain of interest at each time point. (G) We performed Mann-Whitney test to compare the growth rate in monoculture to the growth rate in coculture for the strain of interest.

ns: non-significant, *: p value < 0.05, **: p value < 0.005, ***: p value < 0.0005, ****: p value < 0.0001. See also Figures S1 and S2.

Ap^{WJL} : Lp^{NC8} bi-association also enhances the benefit of commensals on this trait as early as 3 days after bi-association (Figure 1C).

Next, we wondered if each bacterium benefits from the presence of the other. To this end, we assessed the microbial load in larvae through larval development upon mono- and bi-association with Ap^{WJL} , Lp^{NC8} or Ap^{WJL} : Lp^{NC8} , respectively. Ap^{WJL} and Lp^{NC8} loads in mono- or bi-association start to differ from day 3 after egg laying and reach a two-log difference at day 5 (Figures 1D and 1E). The reciprocal benefit between Ap^{WJL} and Lp^{NC8} is also observed while bacteria grow in a liquid version of the HD (see Methods). In coculture, Ap^{WJL} and Lp^{NC8} have slightly higher final biomasses (Figure 1F) and marked higher growth rates (Figure 1G) than in mono-cultures. As previously reported in other experimental settings, the enhanced benefit of commensals on fly's lifespan (Yamada et al., 2015) or larval development (Bing et al., 2018; Storelli et al., 2011) is mediated at least partly by the trophic effect of providing inert microbial biomass as nutrients to the

host. Since we detected a slightly increased bacterial biomass in the diet and the host upon bi-association, we investigated the contribution of such inert biomass to the observed growth promotion phenotype. To this end, we inoculated GF larvae with Heat Killed (HK) Ap^{WJL} or Lp^{NC8} at high dose (10⁹ CFU) in mono- and bi-associated conditions (Figure S2A). Mono-association with HK bacteria at high or low doses fails to accelerate larval development (Figures S2A and S2B), yet bi-association with HK bacteria at high doses slightly contribute to host development by accelerating larval development by ~1 day compared with GF animals (Figure S2A). However, this effect is very mild when compared with the effect of live and metabolically active bacteria bi-association at high or low doses (Figures 1A and 1B), which, respectively, led to larval development accelerations of ~5.5 or ~2.5 days compared with GF conditions. Of note, in contrast to live bacteria bi-association, bi-association with HK bacteria on HDs with an increased amino acid content or a banana diet did not rescue or accelerate larval development (Figures S1A and S1B). Moreover, the enhanced *Drosophila* growth observed upon bi-association requires both bacteria to be metabolically active and associated to the host from early stages of development, since bi-association where one of the bacteria is HK (Figure S2B) or delayed bi-association (Figures S2C and S2D) fails to accelerate larvae development.

Collectively, our results show that microbial bi-association of larvae developing in a suboptimal nutritional context results in increased host's maturation rates and size gains compared with mono-associations. This beneficial effect partially results from a trophic effect of increased bacterial biomass provision to the host but mostly relies on the functional impact of alive and metabolically active microbes.

Ap^{WJL} Benefits Lp^{NC8} via Essential Amino Acid and Vitamins Provision

Recently, we showed that Ap^{WJL} and Lp^{NC8} differentially fulfil the nutritional requirements of the ex-GF larva thanks to their individual genetic repertoires. In this context, the positive impact of Ap^{WJL} or Lp^{NC8} on host development requires metabolically active bacteria and is independent of bacterial loads in the depleted diets or in the larval gut (Consuegra et al., 2020). Specifically, we identified the nutritional auxotrophies of both Ap^{WJL} and Lp^{NC8} in HD. Ap^{WJL} is completely prototroph, whereas Lp^{NC8} is auxotroph for Arg, Ile, Leu, Val, Cys, biotin, and pantothenate. Such differences between Ap^{WJL} and Lp^{NC8} were expected. Indeed, *L. plantarum* is a fastidious bacterium with complex metabolic requirements including amino acids and vitamins (Martino et al., 2016; Vos et al., 2009). Therefore, in a simple microbial community like the one studied here, a prototrophic bacterium like *A. pomorum* may support *L. plantarum* growth by providing essential amino acids and vitamins.

To directly test this hypothesis, we studied the growth of Lp^{NC8} in the presence of Ap^{WJL} in liquid HD lacking each of the amino acids and vitamins for which it is auxotroph. We set monocultures of Ap^{WJL} and Lp^{NC8} and a coculture of Ap^{WJL}:Lp^{NC8} in liquid HDΔArg, ΔIle, ΔLeu, ΔVal, ΔCys, ΔBiotin, or ΔPantothenate and assessed the bacterial counts in mono and cocultures during 72 h. As expected, Ap^{WJL} grows in these media to the same extent as in the complete HD, whereas Lp^{NC8} is unable to grow as a monoculture (Figures 2A–2G). Interestingly, Lp^{NC8} grows in the deficient media only when cocultured with Ap^{WJL} (Figures 2A–2G). From the HDΔArg, HDΔIle, and HDΔLeu mono- and cocultures, we also recovered supernatants and quantified Arg, Ile, and Leu release in the media using high-performance liquid chromatography (HPLC). In Ap^{WJL} monocultures, we observe an accumulation of these amino acids that correlates with Ap^{WJL} growth (Figures 2H–2J). As expected, they are not detected in the Lp^{NC8} monocultures (Figures 2H–2J). In Ap^{WJL}:Lp^{NC8} coculture, we do not detect any accumulation of Arg or Leu and a reduction in Ile accumulation, which suggests that the amino acids released by Ap^{WJL} are immediately consumed by Lp^{NC8} to support its growth and thus do not accumulate in the media (Figures 2H–2J). These results therefore establish that Ap^{WJL} provides amino acids, and probably B vitamins to Lp^{NC8}.

Ap^{WJL} to Lp^{NC8} Nutrient Provision Potentiates Commensal-Mediated Larval Auxotrophies Compensation

Next, we sought to determine if these metabolic interactions among *Drosophila* commensals could be translated into a further benefit to larvae developing on media lacking each of the amino acids and vitamins for which Lp^{NC8} is auxotrophic. We therefore assessed the developmental time in HDΔArg, ΔIle, ΔLeu, ΔVal, ΔCys, ΔBiotin, and ΔPantothenate of mono- (Ap^{WJL} or Lp^{NC8}) or bi-associated (Ap^{WJL}:Lp^{NC8}) larvae (Figure 2K). Association of the larval host with Ap^{WJL} compensates all nutrient depletions except for pantothenate, whereas Lp^{NC8} fails to compensate the lack of any nutrient for the host because of its own

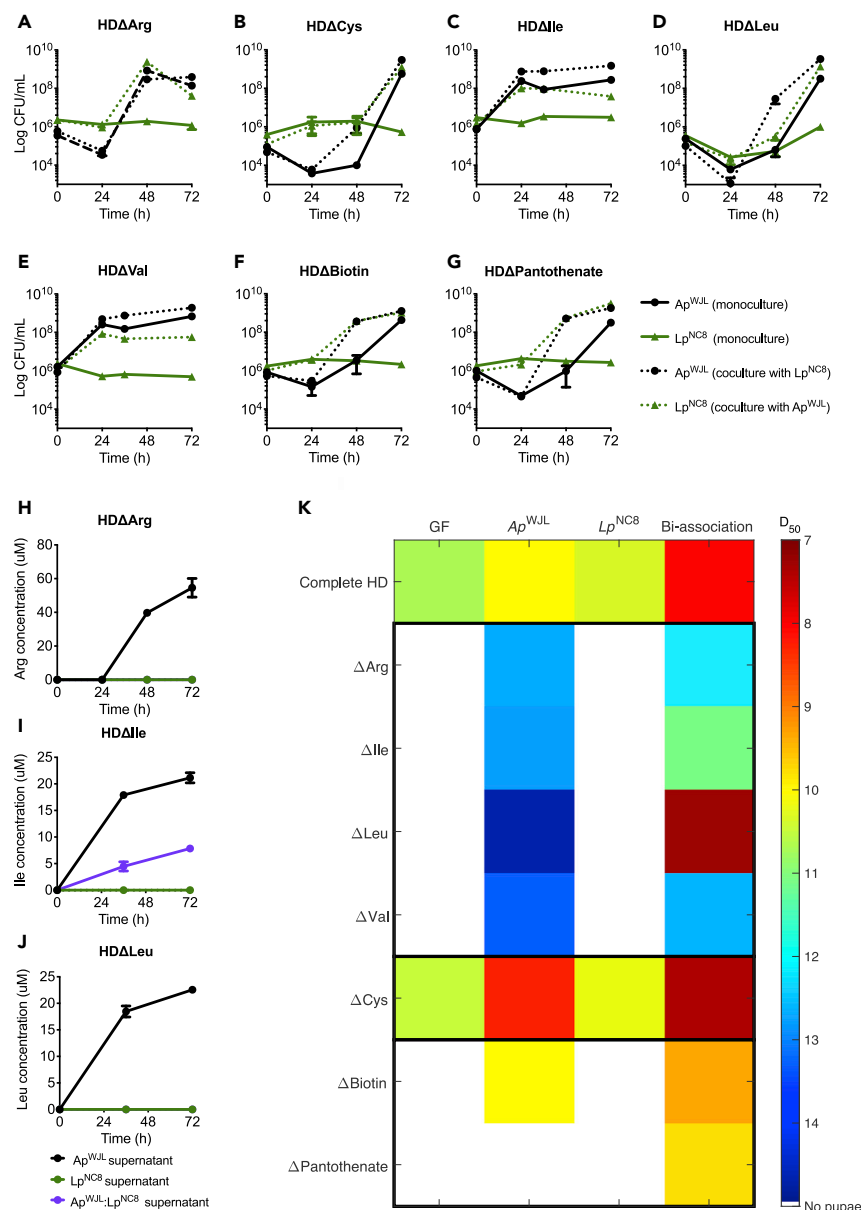


Figure 2. Ap^{WJL} Benefits Lp^{NC8} via Essential Amino Acid and Vitamins Provision

(A–G) Growth curves of Ap^{WJL} and Lp^{NC8} in mono- (plain lines) or cocultures (dotted lines) in liquid holidic diets (HD) lacking Arg (HD Δ Arg) (A), Cys (HD Δ Cys) (B), Ile (HD Δ Ile) (C), Leu (HD Δ Leu) (D), Val (HD Δ Val) (E), Biotin (HD Δ Biotin) (F) or Pantothenate (HD Δ Pantothenate) (G). Black refers to Ap^{WJL} , green the Lp^{NC8} .

(H–J) HPLC quantification of Arg, Ile, and Leu in Ap^{WJL} or Lp^{NC8} mono-culture supernatants (black and green lines, respectively) or Ap^{WJL} : Lp^{NC8} coculture (purple line) in HD Δ Arg, HD Δ Ile, HD Δ Leu, respectively. (A–J) Symbols represent the means \pm SEM of three biological replicates.

(K) Heatmap representing the mean D_{50} (day when 50% of the larvae population has entered metamorphosis) of GF larvae (first column) and larvae mono-associated with Ap^{WJL} or Lp^{NC8} or bi-associated with Ap^{WJL} : Lp^{NC8} (columns 2, 3, and 4, respectively). Each row shows D_{50} in a different version of the HD: complete HD or HDs each lacking a specific nutrient HD Δ Arg, HD Δ Ile, HD Δ Leu, HD Δ Val, HD Δ Cys, HD Δ Biotin, HD Δ Pantothenate. White color code means that larvae did not reach pupariation.

auxotrophies. Interestingly, bi-association with Ap^{WJL} : Lp^{NC8} systematically exceeds the benefit provided to the host by mono-association with Ap^{WJL} , and in HD Δ Pantothenate even rescues host viability (Figure 2K).

Taken together, these results establish that upon bi-association, Ap^{WJL} supplies Arg, Ile, Leu, Val, Cys, biotin, and pantothenate to Lp^{NC8}, thus allowing both commensals to thrive on these depleted media. This nutritional cooperation then potentiates the commensal-mediated promotion of larval development in depleted diets via the bacterial provision of the missing essential nutrients to the host.

Lp^{NC8}-Derived Lactate Benefits Ap^{WJL} and Enhances Ap^{WJL}-Mediated Larval Growth Promotion

Next, we wondered how Ap^{WJL} benefits from Lp^{NC8} (Figures 1F and 1G). We hypothesize that Lp^{NC8} metabolic by-products enhance the ability of Ap^{WJL} to promote larval development. To test this, we mono-associated GF embryos with Ap^{WJL} and added either sterile PBS or the supernatant of a culture of Lp^{NC8} grown on liquid HD for 3 days. The addition of an Lp^{NC8} supernatant on embryos mono-associated with Ap^{WJL} is sufficient to accelerate larval development by ~4 days compared with GF animals, whereas Ap^{WJL} mono-association only triggers a single day acceleration. However, addition of Lp^{NC8} supernatant did not improve larval development in GF condition or in mono-association with Lp^{NC8} (Figure 3A).

L. plantarum is a homolactic fermentative microorganism that secretes its principal metabolic by-products D- and L-lactate into the nutritional substrate. We next assayed if an equimolar solution of DL-lactate could reproduce the benefit of Lp^{NC8} supernatant on embryos mono-associated with Ap^{WJL}. When DL-lactate is added at a final concentration of 0.6 g/L, larvae mono-associated with Ap^{WJL} exhibit strong developmental acceleration and linear size gain (Figures 3B and 1C). However, DL-lactate is deleterious to GF larvae as it delays development by ~2 days (Figure 3B). Furthermore, in HD lacking each of the fly essential amino acids (Figure 3C) or in complete HDs with optimal amino acid content (Figure S1A, HD 16g and HD 20g), the DL-lactate supplementation to larvae mono-associated with Ap^{WJL} reproduces and even exceeds the benefit of the bi-association.

A. pomorum is an acetic acid bacterium that produces acetic acid by aerobic fermentation. We first confirmed that Ap^{WJL} does not produce lactate during growth on liquid HD (Figure 3D) but is capable of consuming exogenous sources of lactate in the cultured media, without a preference of either chiral form (Figure 3E). Consumption of DL-lactate by Ap^{WJL} slightly increases its final biomass in solid HD (Figures S3A and S3B), reaching an average ~4x10⁷ CFU/tube (instead of ~1x10⁷ CFU/tube when lactate was omitted) and markedly enhances bacterial growth rate in both liquid (Figure 3F) and solid HD with or without larvae (Figures 3G, 3H, S3A, and S3B). In liquid HD, we quantified that Lp^{NC8} releases ~8 g/L of DL-lactate (3:1 ratio, D:L; Figure 3I). Finally, in an Ap^{WJL}:Lp^{NC8} coculture, we observed that the lactate released by Lp^{NC8} is immediately consumed by Ap^{WJL}, preventing its accumulation in the media (Figure 3J).

Next, we wondered if the beneficial effect on larval development we observed upon supplementation with DL-lactate of Ap^{WJL} mono-associated larvae is due to the mere increase of Ap^{WJL} biomass. To test this hypothesis, we assessed the development of larvae mono-associated with Ap^{WJL} in two conditions: first, with a high dose of Ap^{WJL} biomass (~10⁸ CFU) so it matches the final bacterial count at stationary phase in solid HD supplemented with lactate in the presence of larvae. Second, live Ap^{WJL} biomass associated to *Drosophila* larvae was corrected daily to match the biomass reached when Ap^{WJL} mono-associated animals are supplemented with lactate, according to the bacterial growth dynamics established in Figures S3B–S3D. Mono-association with a higher dose of Ap^{WJL} (10⁸ CFU) was deleterious to larval development (Figure S3D); this also justifies our choice of 10⁷ CFU Ap^{WJL} inoculum in Figure 1A. Indeed, in two of five replicates, flies did not reach pupariation (egg-to-pupae survival <20%, Figure S3E). In the other three replicates, egg-to-pupae survival was higher (~80%) as well as variability among replicates (coefficient of variation [CV] = 17.4%). In the Ap^{WJL} lactate-matched biomass condition, larval development was not faster than larvae mono-associated with Ap^{WJL}, yet lactate supplementation triggered the expected enhanced larval development of Ap^{WJL} mono-associated animals (Figure S3D). Thus, we conclude that the enhanced host growth observed upon lactate supplementation to Ap^{WJL} is not due to the mere increase in Ap^{WJL} biomass and growth rate upon lactate consumption.

The lactate produced by Lp^{NC8} seems to be the key metabolite altering Ap^{WJL} metabolism and its influence on host growth. To directly test this hypothesis, we recovered supernatants of 3-day cultures in liquid HD of an *L. plantarum* strain lacking the *ldh* genes (Lp^{WCF51}Δ*ldhDL*) and its wild-type counterpart (Lp^{WCF51}) and assessed their effects on the development of larvae mono-associated with Ap^{WJL}. Lp^{WCF51}Δ*ldhDL* has

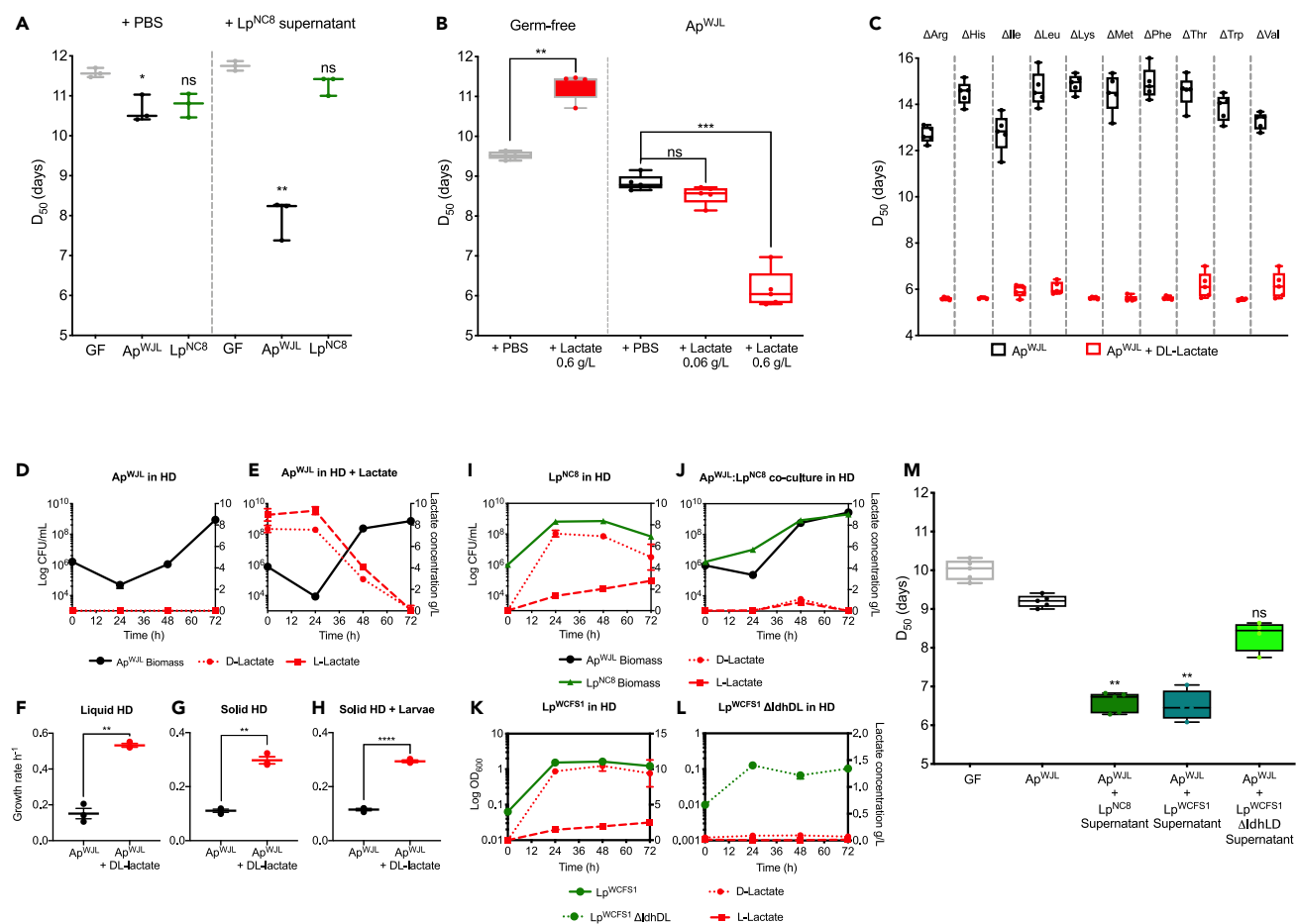


Figure 3. *Lp*^{NC8}-Derived Lactate Benefits *Ap*^{WJL} and Enhances *Ap*^{WJL}-Mediated Larval Growth Promotion

(A and M) Developmental timing of Germ-Free (GF) larvae or GF larvae inoculated with 10^5 CFU of *Ap*^{WJL} (A, M black) or *Lp*^{NC8} (A, green) supplemented with either sterile PBS (A) or the supernatant from a 72-h culture of *Lp*^{NC8} (A, M), *Lp*^{WCF51} (M, turquoise), or *Lp*^{WCF51} Δ ldhDL (M, light green) in complete holidic diet (HD).

(B) Developmental timing on HD of GF larvae (gray) or GF larvae inoculated with 10^5 CFU of *Ap*^{WJL} supplemented with either sterile PBS (black) or DL-lactate solutions (red) at inoculation (final concentration in the diet 0.06 or 0.6 g/L). (A, B, and M) Each dot represents an independent biological replicate. Boxplots show minimum, maximum, and median. We performed Kruskal-Wallis test followed by uncorrected Dunn's tests to compare each condition with GF. ns: non-significant, *: p value < 0.05, **: p value < 0.005, ***: p value < 0.0005.

(C–H) (C) Developmental timing of GF larvae inoculated with 10^5 CFU of *Ap*^{WJL} supplemented at inoculation with either sterile PBS (black) or DL-lactate at final concentration of 0.6 g/L in HDs lacking each an essential amino acid for *Drosophila*: from left to right, HD Δ Arg, HD Δ His, HD Δ Ile, HD Δ Leu, HD Δ Lys, HD Δ Met, HD Δ Phe, HD Δ Thr, and HD Δ Val. Boxplots show minimum, maximum, and median, and each dot represents an independent biological replicate. Growth curves (D and E) and growth rates (F) of *Ap*^{WJL} in liquid HD supplemented (E) or not (D) with DL-lactate solution. D- (dotted line) and L-lactate (dashed line) levels (red) were quantified in both conditions. Growth rates of *Ap*^{WJL} in solid HD and HD + DL-lactate with (H) or without (G) larvae.

(I–L) Growth curves in liquid HD of *Lp*^{NC8} (green) or *Ap*^{WJL} (black) in mono- (I) or coculture (J), or *Lp*^{WCF51} (K, green) or *Lp*^{WCF51} Δ ldhDL (L, dotted green) with the respective D- (dotted line) or L-lactate (dashed line) levels (red). Note the low OD₆₀₀ of *Lp*^{WCF51} Δ ldhDL versus *Lp*^{WCF51} but similar CFU counts (Figures S4A and S4B). Symbols represent the means \pm SEM of three biological replicates except for (F)–(H) where each symbol represents an independent replicate \pm SEM.

See also Figures S1, S3, and S4.

been reported to produce only trace amounts of D- and L-lactate (Ferain et al., 1996). We confirmed these findings in liquid HD by monitoring bacterial growth and DL-lactate production by both strains for 72 h (Figures 3K and 3L). Both strains grow in MRS and liquid HD to the same extent without any difference in their final biomass (CFU/mL) despite the observed reduced OD₆₀₀ of *Lp*^{WCF51} Δ ldhDL (Figures S4A and S4B). *Lp*^{WCF51} supernatant at 72 h contains \sim 9.4 g/L of D-lactate and \sim 2.5 g/L of L-lactate (Figure 3K). *Lp*^{WCF51} Δ ldhDL, on the other hand, only accumulates a total of \sim 0.09 g/L of DL-lactate (Figure 3L). Importantly, as in an HD + DL-lactate, *Ap*^{WJL} growth rate is higher when growing on *Lp*^{NC8} or *Lp*^{WCF51} supernatants but not on *Lp*^{WCF51} Δ ldhDL supernatant (Figure S4C). Also, lactate or lactate-containing supernatants

from Lp^{NC8} or Lp^{WCFS1} sustain increased Ap^{WJL} larval loads during development (Figure S4D), as does bi-association with Lp^{NC8} (Figure 1D). Finally, the addition of a supernatant from Lp^{WCFS1} culture on larvae mono-associated with Ap^{WJL} boosts larval growth and maturation to a degree comparable with Lp^{NC8} 's supernatant (Figure 3M). The effect of these supernatants on host development is not due to secreted bacterial peptides since the total amino acid concentration of Lp^{NC8} culture supernatants remains stable during growth on liquid HD (Figure S4E) and the addition of an equal volume of sterile liquid HD (containing an amount of amino acids similar to the culture supernatant) on larvae mono-associated with Ap^{WJL} does not accelerate development (Figure S4F). Instead, the impact of the tested supernatants on larval development is most likely due to the lactate produced by Lp^{NC8} and Lp^{WCFS1} (Figures 3I and 3K) since a supernatant from $Lp^{WCFS1} \Delta dhDL$ culture fails to accelerate development of larvae mono-associated with Ap^{WJL} (Figure 3M).

So far, we demonstrated that the positive effect of *L. plantarum* supernatant on larva mono-associated with Ap^{WJL} is based on its lactate content. Importantly, treatment of GF larvae with the supernatants of either Lp^{WCFS1} or $Lp^{WCFS1} \Delta dhDL$ has no effect on GF larvae development, neither does treatment with a supernatant of Ap^{WJL} grown either in the presence of these filtrates or with filtrates of Ap^{WJL} cocultured with any of the test *L. plantarum* strains (Figure S4G). Therefore, we first conclude that DL-lactate does not directly benefit the larval host, rather DL-lactate may trigger a switch of carbon utilization in Ap^{WJL} , which in turn reconfigures the metabolic by-products it releases, which the host utilizes to fuel its anabolic growth.

Lactate-Mediated Enhanced Ap^{WJL} Larval Growth Promotion Does Not Rely on Amino Acid Provision to the Host

To test our proposal, we focused on lactate metabolism in *A. pomorum*. Unfortunately, little is known about the core metabolism of this *Acetobacter* species. Most metabolic and genetic studies on *Acetobacter* have been performed on *A. aceti* because of its industrial use in vinegar production (Sakurai et al., 2010) or on *A. pasteurianus* as a core member of the fermenting microbiota of cocoa (Adler et al., 2014), which shares ~90% nucleotide identity with *A. pomorum* (Sannino et al., 2018). *A. pasteurianus* oxidizes lactate to pyruvate and converts it to (1) acetoin, which is released into the surrounding media, to (2) acetyl-CoA, which is directed to the TCA cycle, or (3) to phosphoenolpyruvate (PEP) for gluconeogenesis. In the two last cases, lactate consumption is accompanied by higher metabolic fluxes through biosynthetic pathways for biomass production including *de novo* amino acid biosynthesis (Adler et al., 2014).

We thus wondered if lactate consumption by Ap^{WJL} triggers an increased production and release of amino acids that would be consumed by the host and would stimulate larval growth. To test this hypothesis, we set cultures in liquid HD with or without DL-lactate supplementation, followed bacterial counts, and sampled supernatants every 24 h for 72 h for quantification of amino acids. We calculated the net amino acid release in each condition at 24, 48, and 72 h by subtracting the amino acid concentration quantified at 0 h from each incremental time points (Figures 4A and 4B). First, we observed a distinct release of amino acids at 24 and 48 h in both conditions. In the absence of lactate, we focused on the amino acid release by Ap^{WJL} at 48 h, while in the middle of its exponential phase (Figure 4A inner panel). With DL-lactate addition (Figure 4B), we observed a distinct release of amino acids at 24 (early exponential phase) and 48 h (late exponential phase, Figure 4B inner panel). Unexpectedly, during the stationary phase at 72 h, amino acids are depleted instead of accumulating.

Based on these observations, we prepared solid HDs each supplemented with the specific concentration of amino acid mixtures from each specific time points (Table S1; See Methods). These include a mixture of the amino acids representative of those released by Ap^{WJL} in liquid HD at 48 h (AA mix Ap @48h) and the mixtures of the amino acids released by Ap^{WJL} at 24 and 48 h in liquid HD supplemented with DL-lactate (AA mix Ap + lactate @24h and AA mix Ap + lactate @48h, respectively) (Figure 4B and inner panel). We then assessed the maturation time of GF and Ap^{WJL} mono-associated larvae on these three supplemented diets. We observe no enhanced benefit of the different amino acid mixes on GF or Ap^{WJL} mono-associated larvae maturation time (Figures 4C and 4D).

These results suggest that amino acid release by Ap^{WJL} is not a key mechanism by which Ap^{WJL} promotes host growth on complete HD, but we cannot rule out the contribution of amino acid precursors or derivatives to host growth promotion in this setting. However, our results indicate that the enhanced beneficial effect of Ap^{WJL} on larval development upon DL-lactate metabolism is not mediated by *de novo* amino acid biosynthesis and release.

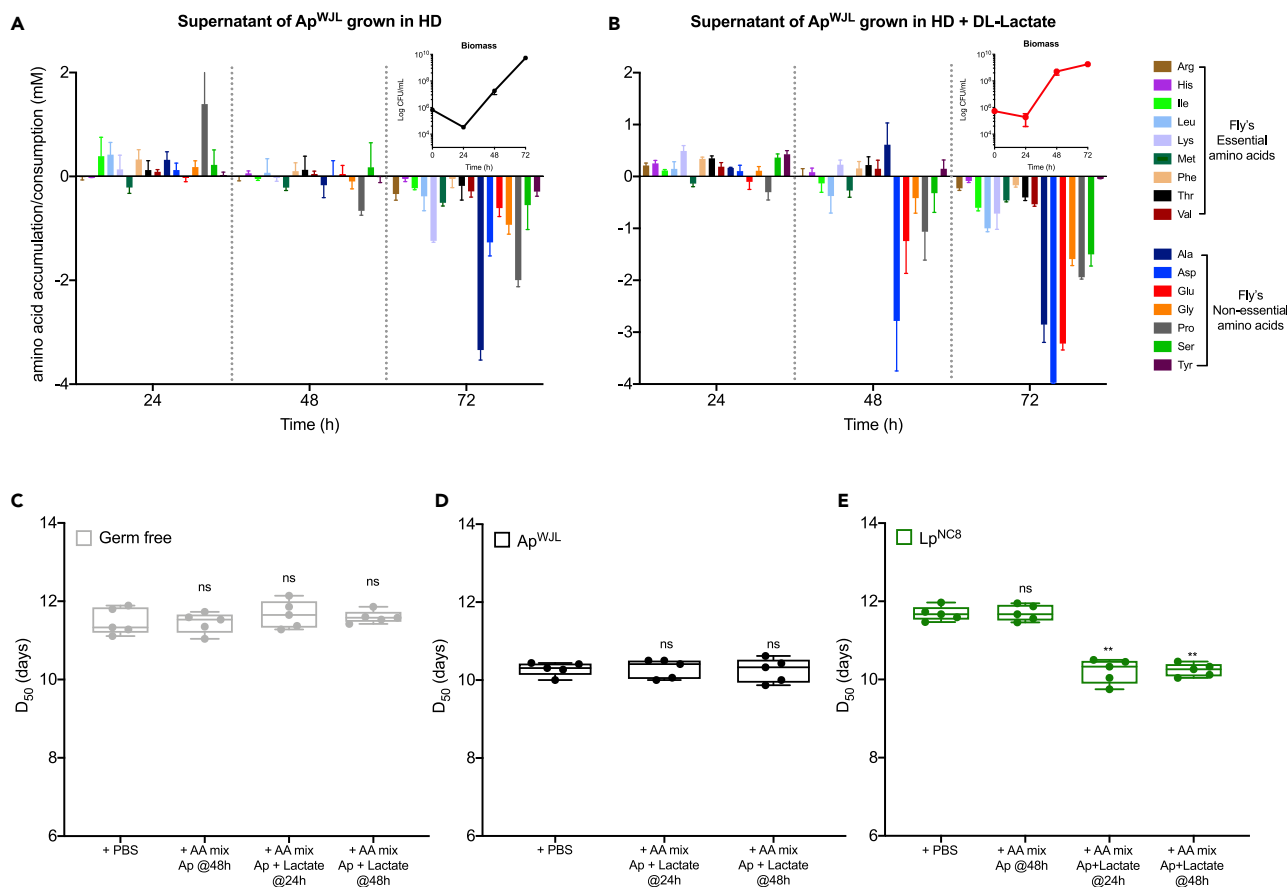


Figure 4. Upon Lactate Consumption Ap^{WJL} Produces an Amino Acid Cocktail that Enhances the Growth-Promoting Ability of Lp^{NC8}

(A and B) Net production of essential and non-essential fly amino acids at 24, 48, and 72 h. Net production was calculated from HPLC quantification data by subtracting the amino acid concentration quantified at 0 h from each incremental time point. Conditions included the supernatant of Ap^{WJL} cultures (inner panels) in complete HD supplemented (B) or not (A) with DL-lactate. Symbols in inner panels represent the means \pm SEM of three biological replicates. Bars represent the means \pm SEM of three biological replicates.

(C–E) Developmental timing of GF larvae (C) inoculated with 10^5 CFU of Ap^{WJL} (D) or 10^5 CFU of Lp^{NC8} (E) supplemented with either sterile PBS, the amino acid mix produced by Ap^{WJL} in liquid culture at 48 h (+AA mix Ap @48h), the amino acid mix produced by Ap^{WJL} in liquid culture supplemented with DL-lactate at 24 h (+AA mix Ap + Lactate @24h) or the amino acid mix produced by Ap^{WJL} in liquid culture supplemented with DL-lactate at 48 h (+AA mix Ap + Lactate @48h). See Table S1 for detailed information on the amino acid mixes. Boxplots show minimum, maximum, and median; each point represents a biological replicate. We performed Kruskal-Wallis test followed by uncorrected Dunn's tests to compare each condition with the PBS-treated condition. ns: non-significant, **: p value < 0.005.

Upon Lactate Consumption Ap^{WJL} Produces Amino Acids that Enhance the Growth-Promoting Ability of Lp^{NC8}

We previously established that Ap^{WJL} cross-feeds amino acids and B vitamins to Lp^{NC8} (Figure 2). Therefore, we wonder if the amino acid mix produced by Ap^{WJL} while growing on HD supplemented with DL-lactate would further enhance the larval growth promotion ability of Lp^{NC8}. We tested this hypothesis in the same set-up described above (Figures 4A–4D). We prepared solid HDs supplemented with the three different mixtures of amino acids (AA mix Ap @48h; AA mix Ap + lactate @24h, and AA mix Ap + lactate @48h; Table S1). On these three supplemented media, the development of Lp^{NC8} mono-associated larvae is significantly accelerated with either the AA mix Ap + lactate @24h or AA mix Ap + lactate @48h but not with the AA mix Ap @48h (Figure 4E).

Together our results indicate that, upon consumption of the DL-lactate secreted by Lp^{NC8}, Ap^{WJL} releases amino acids that are now accessible to Lp^{NC8}. As a result, these amino acids further benefit Lp^{NC8} and enhance Lp^{NC8}-mediated larval growth promotion in complete HD. However, the amino acids released by Ap^{WJL} in response to lactate do not directly influence the host. This is therefore the metabolic cooperation between the two

commensals that results in increased host juvenile growth, higher microbial larval loads (Figures 1D and 1E), and improved growth rate of Ap^{WJL} and Lp^{NC8} in the HD (Figures 1F and 1G). These results establish that the metabolic cooperation occurring between the two major commensal bacteria of *Drosophila* supports an optimal nutritional mutualism among all the partners while facing amino acid scarcity.

Lactate Utilization by *Acetobacter* Is Necessary to Its Physiological Response to Lp^{NC8} and Enhanced Benefit on Host Growth

We aimed to elucidate the mechanisms underpinning the *Lactobacillus*-derived lactate influence on *Acetobacter* in relation to its increased potential to mediate larval growth. First, we focused on lactate utilization by *Acetobacter*. As mentioned previously, DL-lactate consumption by *A. pastorianus* generates acetoin and an increased carbon flux toward gluconeogenic pathways. These metabolic features seem to be shared among other *Acetobacter* species such as *A. fabarum*^{DsW_054} (Af), a strain isolated from wild-caught *Drosophila suzukii* (Winans et al., 2017). Indeed, Sommer and Newell recently reported that lactate produced by *L. brevis* is metabolized by Af through gluconeogenesis pathways via lactate dehydrogenase (LDH) and pyruvate phosphate dikinase (PPDK), whereas pyruvate is converted to acetoin by α -acetolactate synthase (ALS) and α -acetolactate decarboxylase (ALDC) (Sommer and Newell, 2018) (Figure 5A). Based on this information, we hypothesized that the effect of DL-lactate on Ap^{WJL} and the development of Ap^{WJL} mono-associated larvae relies on the lactate utilization by Ap^{WJL} and its conversion to acetoin or to an increased flux toward gluconeogenic pathways (Figure 5A). To test these hypotheses, we use a set of Af mutants affecting key enzymes of the lactate metabolism from the Af's transposon insertion mutant library generated by White et al. (2018) (Figure 5A). First, we confirmed that in HD Af behaves like Ap^{WJL} . As Ap^{WJL} , Af tends to accelerate larval development and Lp^{NC8} supernatant or DL-lactate supplementation enhances the influence of Af on larval growth (Figures 5B and 5C). As Ap^{WJL} , Af also consumes exogenous sources of DL-lactate, without a preference for either chiral form (Figure S5A). Af prevents the accumulation of DL-lactate produced by Lp^{NC8} when cocultured with this strain in liquid HD (Figure S5B). The first step of lactate metabolism is its oxidation by the enzyme LDH to produce two H^+ and pyruvate (Figure 5A). We tested two independent Af mutants in the *ldh* gene, Af::Tn*ldh*, clones 10B7 and 92G1 (Sommer and Newell, 2018; White et al., 2018). These mutants grow in liquid HD to the same extent as that of the Af wild-type strain (Figure S5C). On an HD supplemented with DL-lactate, Af::Tn*ldh* mutants consume the D chiral form of lactate (D-lactate) (Figures S5D and S5E) and still confer a significant benefit to larvae development upon addition of either DL-lactate or D-lactate, albeit with a slight reduction as compared with the WT strain (Figure 5C). However, both Af::Tn*ldh* mutants fail to consume L-lactate (Figures S5D and S5E) and accordingly completely fail to enhance larvae development upon addition of L-lactate (Figure 5C). These results therefore establish that the positive effect of lactate on the development of *Acetobacter* mono-associated larvae relies on lactate utilization by *Acetobacter* strains.

Acetobacter Acetoin Pathway Is Not Limiting for Lactate-Mediated Enhancement of *Acetobacter* Larval Growth Promotion

After LDH conversion of lactate to pyruvate, acetoin can be produced from pyruvate either directly through pyruvate decarboxylase (PDC) or by the successive action of ALS and ALDC with acetolactate as the intermediate product (Figure 5A). To investigate if the acetoin production pathway is necessary for the lactate-mediated enhancement of *Acetobacter* benefit to larvae development, we assessed the development of larvae mono-associated with each of the acetoin pathway mutants, Af::Tn*pdc*, Af::Tn*als*, and Af::Tn*aldc*, supplemented with DL-lactate. Of note, the mutants do not show any growth impairment on liquid HD (Figure S5F), and previous analyses of these mutants showed that, even if acetoin production is significantly reduced, it is not fully inhibited; the Af::Tn*als* and Af::Tn*aldc* mutants produce three times less acetoin than Af and Af::Tn*pdc* in rich liquid media (Sommer and Newell, 2018). However, all the mutants in the genes responsible for acetoin production enhance larval development upon addition of DL-lactate to the same extent as the WT strain (Figure 5D). Therefore, we conclude that acetoin production is not a limiting metabolic step in Af for the positive effect of lactate on the development of Af mono-associated larvae.

Another possible utilization of lactate by *Acetobacter* strains is the conversion from pyruvate to phosphoenolpyruvate (PEP) by the enzyme PDK (Figure 5A). PEP is a precursor for the synthesis of many cellular building blocks through the gluconeogenesis and the pentose phosphate pathways. We hypothesize that DL-lactate consumption by Af results in a higher flux toward biosynthetic pathways. However, Tn disruption of the *ppdk* gene has a strong effect on Af fitness in HD, completely precluding the growth of the mutant strains in this media (Figure S5G) making it impossible to test them in our setting to obtain a complete genetic characterization of the phenotype.

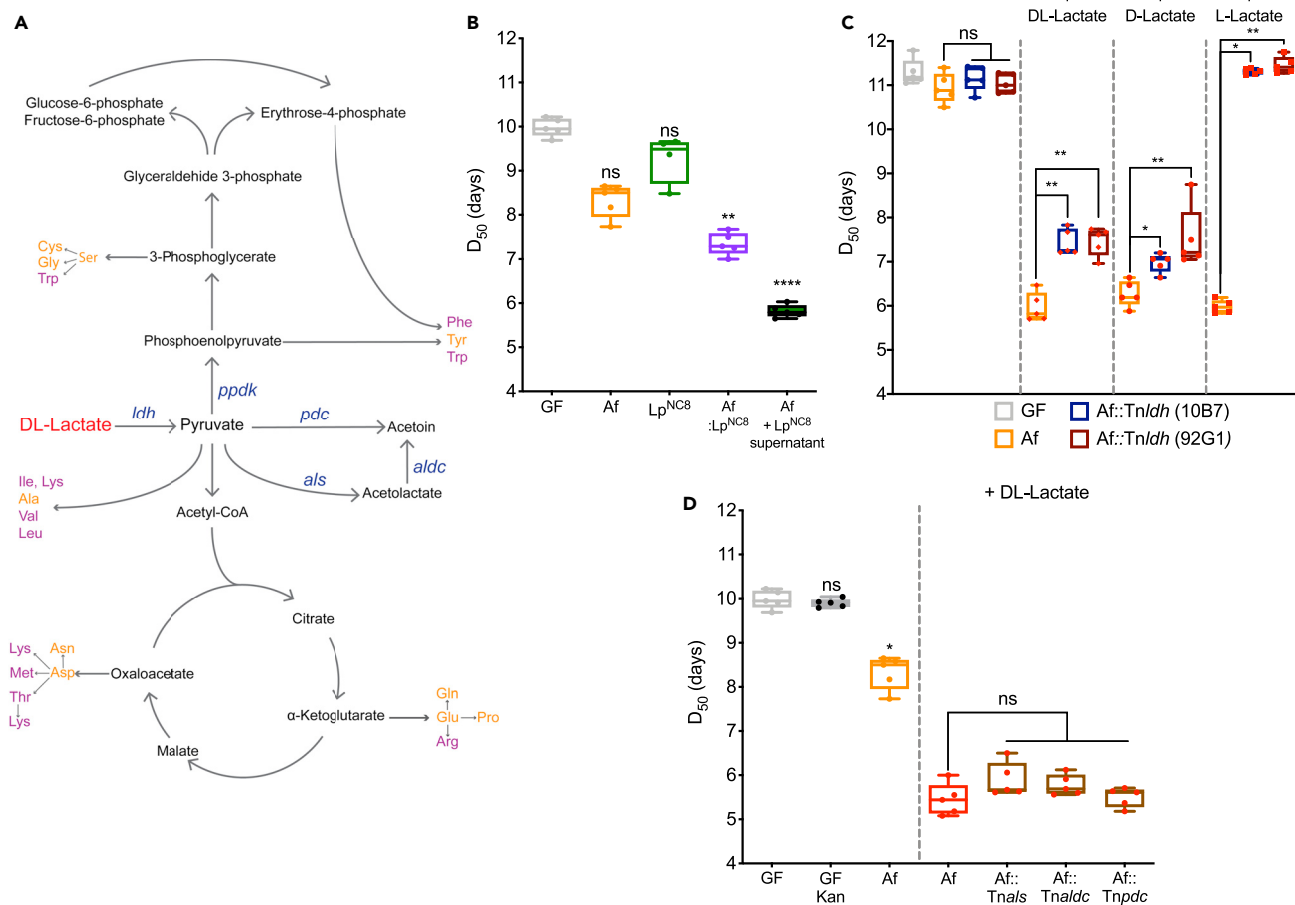


Figure 5. Lactate Utilization by *Acetobacter* Is Central to Its Physiological Response to Lp^{NC8} and Enhanced Benefit on Host Growth

(A) Schematic representation of the main metabolic routes of DL-lactate utilization by *Acetobacter* species. Purple: Fly's essential amino acids. Yellow: Fly's non-essential amino acids. Blue: genes related with lactate consumption.

(B) Developmental timing of Germ-Free (GF, gray) larvae or GF larvae inoculated with 10^5 CFU of *A. fabarum*^{D_{5W}_054} (Af, orange), Lp^{NC8} (green), both strains (Af: Lp^{NC8} , purple), or Af supplemented with the supernatant from 72-h culture of Lp^{NC8} (black, filled green) in complete HD.

(C) Developmental timing of GF (gray) larvae or GF larvae inoculated with 10^5 CFU of Af (orange), Af::Tnldh (10B7) (blue) or Af::Tnldh (92G1) (brown) supplemented with sterile PBS, DL-lactate, D-lactate, or L-lactate in complete HD.

(D) Developmental timing of GF (gray) larvae or GF larvae inoculated with 10^5 CFU of Af (orange) or Af (red), Af::Tnals (brown), Af::Tnaldc (brown), Af::Tnpdc (brown) supplemented with DL-lactate in complete HD or complete HD supplemented with 50 μ g/mL of kanamycin (GF and Af mutants). Boxplots show minimum, maximum, and median; each point represents a biological replicate. We performed Kruskal-Wallis test followed by uncorrected Dunn's tests to compare each condition with the GF treated condition or the Af condition when indicated. ns: non-significant, *: p value < 0.05, **: p value < 0.005, ****: p value < 0.0001.

See also Figure S5.

Lactate-Dependent *Acetobacter* Stimulation of Larval Growth Evokes Metabolites Release Enhancing Host Anabolic Metabolism and Resistance to Oxidative Stress

We next sought to characterize the molecular mechanisms involved in the enhancement of the growth promoting effect of *Acetobacter* strains upon lactate supplementation by a metabolic approach, using untargeted metabolomics (Figure 6). To this end, we used Af as a model bacterium since it reproduces the phenotype of Ap^{WJL} and Af's loss-of-function mutant Af::Tnldh (clone 10B7). We capitalized on these two strains to characterize the bacterial metabolites produced at day 3 upon L-lactate supplementation in the absence or presence of *Drosophila* larvae on HD (Figure 6A and see Methods). We chose this time point to collect the samples because at day 3 post mono-association and lactate supplementation, we start observing significant larval size gains when compared with GF or *Acetobacter* mono-associated larvae. Also, at this time point larvae are actively increasing their size and mass and have not yet reached the critical weight to enter metamorphosis (Figure 1B).

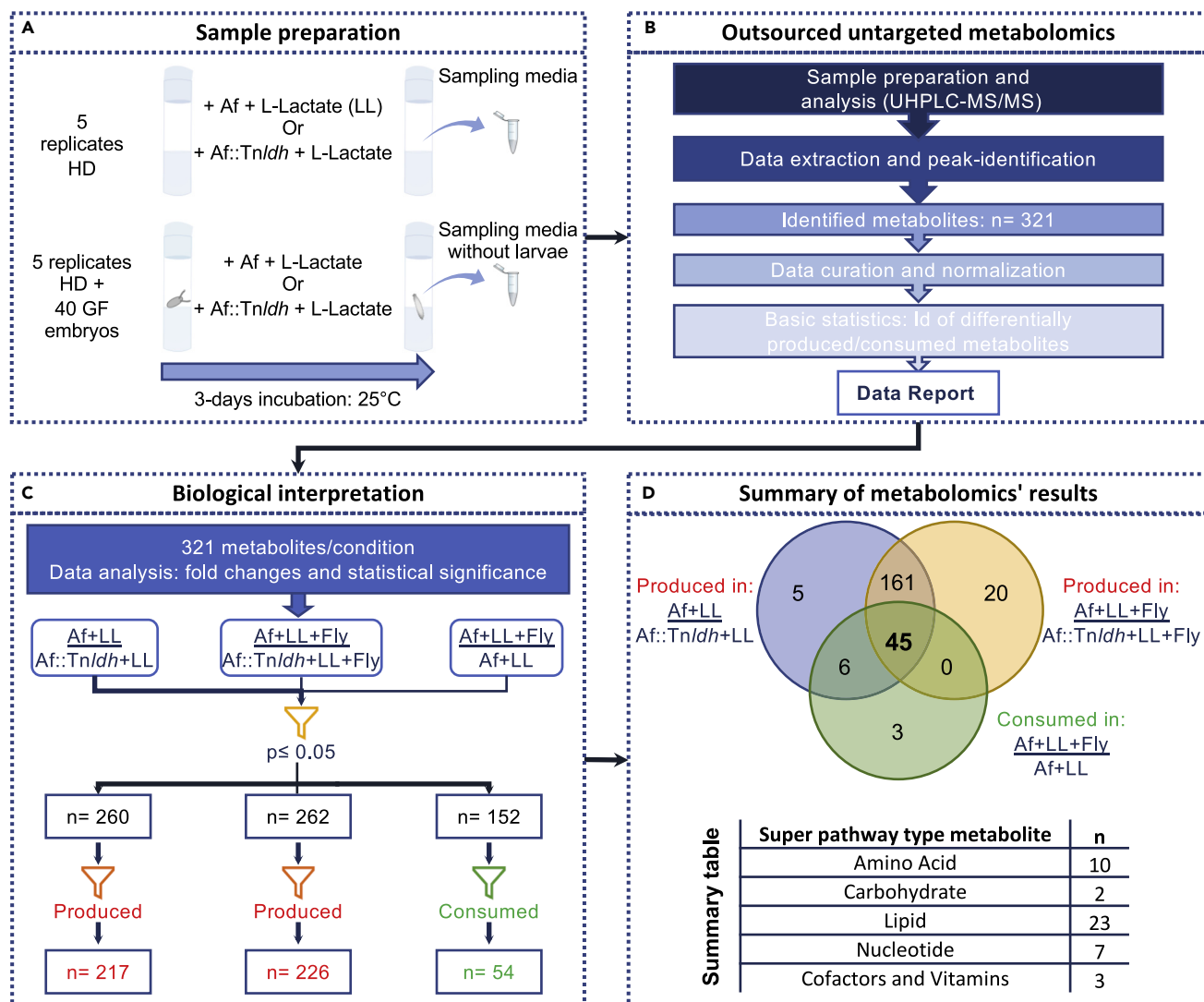


Figure 6. Lactate-Dependent Acetobacter Stimulation of Larval Growth Evokes Metabolites Release Enhancing Host Anabolic Metabolism and Resistance to Oxidative Stress

(A) Schematic representation of sample preparation for metabolomic analysis.

(B) Outsourced untargeted metabolomics and data analysis pipeline.

(C) Investigator-driven data analysis and biological interpretation.

(D) Venn diagram of the identified metabolites in the three test conditions. Our analysis points to 45 metabolites of interest belonging to all major metabolite families. See [Table 1](#) for a detailed list of metabolites.

Untargeted metabolomic analyses based on ultrahigh-performance liquid chromatography coupled to tandem mass spectrometry (UHPLC-MS/MS) identified 321 different metabolites (Figure 6B). We first calculated the fold changes of the metabolites among four conditions: Af + LL/Af::Tn/dh + LL, Af + LL + Fly/Af::Tn/dh + LL + Fly, and Af + LL + Fly/Af + LL (Figure 6C and Table S2). As shown above, Af::Tn/dh fails to consume L-lactate and does not accelerate larval development (Figures 5C, 5D, and 5E). Thus, the first two comparisons allow us to identify the differentially produced/consumed metabolites by Af upon L-lactate supplementation in the absence or presence of the larvae, respectively. The third comparison, Af + LL + Fly/Af + LL, allows us to identify the metabolites that are produced/consumed by the larvae when they are mono-associated with Af and supplemented with L-lactate. From the three different sets of differentially produced/consumed metabolites, we selected only the metabolites that differed with statistical significance between experimental groups (Welch's two-sample t test, $p \leq 0.05$, Figure 6C and Table S2). Next, we filtered the datasets in order to retain only the metabolites differentially produced by Af in

Super Pathway	Sub Pathway	Biochemical Name	Fold Change (p < 0.05)		
			Af + LL Af::Tnldh + LL	Af + LL + Fly Af::Tnldh + LL + Fly	Af + LL + Fly Af + LL
Amino acid	Lysine metabolism	Pipecolate	228.86	1119.99	0.79
	Tryptophan metabolism	Indoleacetate	5.85	6.22	0.86
	Methionine, cysteine, SAM and taurine metabolism	S-adenosylmethionine (SAM)	2.94	1.64	0.56
		S-adenosylhomocysteine (SAH)	3.26	2.11	0.65
		Homocysteine	9.84	7.28	0.65
		Cysteine	8.31	5.87	0.85
		S-methylcysteine	14.10	7.95	0.54
	Polyamine metabolism	Spermidine	373.79	92.21	0.25
	Glutathione metabolism	Cysteinylglycine	4.22	1.43	0.34
Cys-gly, oxidized		15.23	1.92	0.13	
Carbohydrate	Glycolysis, gluconeogenesis, and pyruvate metabolism	Dihydroxyacetone phosphate (DHAP)	19.84	11.46	0.71
	Nucleotide sugar	UDP-glucuronate	3.86	1.94	0.50
Lipid	Long-chain monounsaturated fatty acid	Eicosenoate (20:1)	12.07	3.27	0.48
		Fatty acid, monohydroxy	2-Hydroxypalmitate	9.68	4.99
		2-Hydroxystearate	31.57	13.87	0.38
		3-Hydroxylaurate	12.74	5.64	0.45
		3-hydroxymyristate	48.30	7.43	0.22
		3-Hydroxypalmitate	105.93	34.11	0.25
		3-Hydroxystearate	97.11	46.57	0.30
	Phosphatidylcholine (PC)	1-Palmitoyl-2-palmitoleoyl-GPC	8.34	2.33	0.28
		1-Palmitoyl-2-oleoyl-GPC	38.40	33.83	0.26
		1-Palmitoleoyl-2-oleoyl-GPC	8.79	1.62	0.18
		1-Stearoyl-2-oleoyl-GPC	67.53	17.79	0.26
		1,2-Dioleoyl-GPC	135.60	276.71	0.32
	Phosphatidylethanolamine (PE)	1,2-Dipalmitoyl-GPE	6.14	1.63	0.27
		1-Palmitoyl-2-oleoyl-GPE	100.32	84.04	0.27
		1-Palmitoyl-2-linoleoyl-GPE	10.83	1.91	0.18
		1-Stearoyl-2-oleoyl-GPE	5.66	1.49	0.26
		1,2-Dioleoyl-GPE	156.95	77.19	0.29
	Phosphatidylglycerol (PG)	1,2-Dipalmitoyl-GPG	13.29	2.55	0.19

Table 1. Final Metabolite Candidate Set

(Continued on next page)

Super Pathway	Sub Pathway	Biochemical Name	Fold Change ($p < 0.05$)		
			Af + LL Af::Tnldh + LL	Af + LL + Fly Af::Tnldh + LL + Fly	Af + LL + Fly Af + LL
		1-Palmitoyl-2-oleoyl-GPG	4.75	1.43	0.30
		1-Stearoyl-2-oleoyl-GPG	4.10	1.38	0.34
		1,2-Dioleoyl-GPG	3.55	1.35	0.38
	Sphingolipid synthesis	Sphinganine	236.83	651.75	0.36
		Hexadecaspheinganine	676.50	312.83	0.37
Nucleotide	Purine metabolism, adenine containing	Adenosine 5'-monophosphate (AMP)	264.58	146.97	0.32
		N6-methyladenosine	16.48	8.33	0.63
		guanosine 5'-monophosphate (5'-GMP)	12.58	4.64	0.37
	Pyrimidine metabolism, orotate containing	Dihydroorotate	17.16	10.60	0.65
		Uridine 5'-monophosphate (UMP)	11.18	2.82	0.25
		2'-Deoxyuridine	8.17	3.80	0.47
	Purine and pyrimidine metabolism	Methylphosphate	10.28	6.04	0.36
Cofactors and vitamins	Nicotinate and nicotinamide metabolism	Nicotinamide adenine dinucleotide (NAD ⁺)	5.32	1.53	0.29
	Riboflavin metabolism	Flavin mononucleotide (FMN)	3.24	1.42	0.44
	Vitamin B6 metabolism	Pyridoxamine phosphate	5.02	1.93	0.38

Table 1. Continued

the absence or presence of the larvae upon L-lactate supplementation and the metabolites differentially consumed by the larvae in these conditions. The filtering generated three different sets of metabolites. The first is composed of 217 metabolites that are produced by Af upon L-lactate supplementation when growing on HD. The second comprises 226 metabolites that are produced by Af upon L-lactate supplementation when growing on HD in the presence of larvae. The third includes 54 metabolites that are consumed by larvae when mono-associated with Af and supplemented with L-lactate (Figure 6C and Table S2). Finally, we crossed the three sets of metabolites in order to retain only the metabolites that are produced by Af upon L-lactate supplementation in the presence or absence of larvae and that at the same time are consumed by the larvae (Figure 6D, Venn diagram). These analyses provide us with a set of 45 metabolites encompassing all main metabolite families such as amino acids, carbohydrates, lipids, nucleotides, co-enzymes, cofactors, and vitamins with a clear overrepresentation of amino acid derivatives and phospholipids (Figure 6D, summary table and Table 1).

The 45 differentially produced metabolites constitute a large repertoire of molecules produced by *Acetobacter* upon lactate utilization and are potentially accessible to the developing larvae. This particular combination of metabolites contains essential building blocks and regulators for the host's core anabolic process (nucleotides: AMP, GMP, UMP and cofactors/vitamins: NAD⁺, FMN, pyridoxamine phosphate) as well as regulator or intermediates of metabolic and developmental pathways (co-enzymes: SAM and SAH; phospholipids: biosynthetic intermediates of phosphatidylcholine, phosphatidylethanolamine, and phosphatidylglycerol pathways; and sphingolipids: sphinganine) and effectors of oxidative stress resistance (spermidine, cysteinylglycine). The collective action of these metabolites may converge to sustain linear larval growth and development despite a suboptimal nutritional environment. Altogether our work

identifies a fruitful metabolic cooperation among commensal bacteria that support their physiology and would boost host juvenile growth while facing amino acids scarcity.

DISCUSSION

Here, we identify a beneficial metabolic dialogue among frequently co-habiting species of *Drosophila*'s commensal bacteria that optimizes host juvenile growth and enables cross-feeding and nutrient provision upon chronic amino acid scarcity. Such benefit is also observed in full HDs containing optimal amino acid content as well as in fruit-based diets indicating that the metabolic cooperation among commensal bacteria and their influence on host growth is not restricted to artificial or poor nutritional conditions.

Using low amino acids-containing HDs as an experimental model, we show that *L. plantarum* captures the essential amino acids and B vitamins synthesized by the *Acetobacter* species to fulfill its auxotrophic requirements. In parallel, *Acetobacter* species exploit the lactate produced by *L. plantarum* as an additional carbon source that alters its metabolic state and physiology. Such metabolic interactions support an optimized growth of both commensal species in the diet and an increased colonization of the host.

Previous work has shown a positive correlation between host-associated microbial counts and linear larval growth in *Drosophila* (Keebaugh et al., 2019). Moreover, inert microbial biomass (heat-killed microbes) can accelerate larval development (Bing et al., 2018; Storelli et al., 2011) and impact *Drosophila* lifespan (Yamada et al., 2015). Here, we show that the metabolic cooperation between Ap^{WJL} and Lp^{NC8} increases bacterial biomass in the nutritional substrate, which slightly increases larval growth. However, the bacterial biomass alone never reproduces to the same extent as the positive impact of live Ap^{WJL}:Lp^{NC8} bi-association or lactate supplemented Ap^{WJL} mono-association on host growth. Instead, we show that lactate utilization by *Acetobacter* species rewires its carbon metabolism resulting in the enhanced and *de novo* production of a panoply of anabolic metabolites that would support enhanced host systemic growth.

Studies have previously shown that cooperation among the gut microbes can influence other aspects of *Drosophila* physiology. For example, multiple fermentation products of *L. brevis* foster the growth of *A. fabarum* on a fly diet leading to depletion of dietary glucose, consequently triggering reduced TAG levels in the adult host (Newell and Douglas, 2014; Sommer and Newell, 2018). Moreover, multi-microbe interactions among the *Acetobacter* and *Lactobacillus* species and yeast were shown to influence additional adult traits such as olfaction and egg laying behavior (Fischer et al., 2017), food choice behavior (Leitão-Gonçalves et al., 2017), lifespan and fecundity (Gould et al., 2018), and immunity (Fast et al., 2020). Therefore, along with these studies, our work provides an entry point to further deepen the understanding of how metabolites originating from microbial metabolic networks shape the biology of their host.

In this study, we confirm that lactate is a key metabolite supporting the metabolic cross talk between different microbial species. Lactate supplementation to *Acetobacter* species triggers the release of metabolic by-products that include ribonucleotides AMP, GMP, and UMP and vitamin and amino acid derivatives SAM, SAH, NAD⁺, FMN, and pyridoxamine phosphate, which are co-factors for enzymes involved in multiple host metabolic pathways. These metabolites are essential for optimal larval growth and survival (Consuegra et al., 2020; Mishra et al., 2018; Sang, 1956). Fatty acids and membrane lipids are another group of metabolites whose production is enhanced by lactate presence. Among this group, we found mostly phospholipids such as phosphatidylcholine (PC), phosphatidylethanolamine (PE), and phosphatidylglycerol (PG) and a sphingolipid precursor, sphinganine. In *Drosophila*, PE, PC, PG, and sphingolipids are part of the membrane phospholipids repertoire, with PE being the largely dominating species (Carvalho et al., 2012). Previously, it was established that the total content of membrane lipids increases during larval growth, until a clear pause that occurs in the third instar just prior to the time when larvae stop feeding and enter the wandering stage. This indicates that feeding larvae favor new membrane synthesis and tissue growth over lipid storage (Carvalho et al., 2012). In the same study, it was shown that dietary lipids directly influence membrane lipids proportions, including phospholipids and sphingolipids. In mammals, sphingolipid balance has a central role in controlling nutrient utilization and growth (Holland et al., 2007). Sphingolipids are also activators of serum response element binding protein signaling, which controls biosynthesis of fats (Worgall, 2008). Despite a relatively smaller literature on *Drosophila* sphingolipids, these lipids seem as critical to developmental and metabolic processes in the fly as they are to mammals (Kraut, 2011). Although *Drosophila* cells can synthesize *de novo* all the fatty acids for survival, they incorporate different dietary lipids into the membrane lipids if found in the diet (Carvalho et al., 2012). Therefore, we propose that larvae preferentially utilize the PC, PE, PG, and sphingolipids intermediates produced by *Acetobacter*

species upon lactate utilization to foster membrane synthesis, tissue growth, and metabolic processes such as lipid storage and response to nutrient availability.

Lactate utilization also triggers another major class of metabolites released by *Acetobacter* species that confers oxidative stress resistance. Specifically, we found cysteinylglycine and spermidine. Cysteinylglycine is an intermediate of glutathione (GSH) metabolism, the most abundant cellular antioxidant (Forman et al., 2009). It is produced by GSH hydrolysis or by action of the enzyme γ -L-glutamyl-transpeptidase (GGT). GGT transfers the γ -glutamyl group of GSH onto amino acids forming γ -glutamyl peptides and cysteinylglycine. These intermediaries can be recycled and used to resynthesize GSH and maintain its cellular pool, which protects cells from oxidative damage and maintains redox homeostasis (Ursini et al., 2016). Of note, during *Drosophila* larval development, in addition to its antioxidant role, GSH also contributes to ecdysteroid biosynthesis including the biologically active hormone 20-hydroxyecdysone, which plays an essential role in promoting juvenile growth and maturation (Enya et al., 2017). Spermidine is a natural polyamine widely found in both prokaryotes and eukaryotes including flies and mammals. Nutritional supplementation of spermidine increases the lifespan of yeast, worms, flies, and human cells through inhibition of oxidative stress (Eisenberg et al., 2009). The mode of action of spermidine, mainly through autophagy regulation, is emerging, but evidence for other mechanisms exist such as inflammation reduction, lipid metabolism, and regulation of cell growth, proliferation, and death (Minois, 2014; Minois et al., 2012). Oxidative stress resistance in *Drosophila* has been largely reported to improve adult physiology including lifespan extension. We therefore posit that larvae's physiology and growth potential are also supported by such metabolites obtained from their microbial partners, especially during development on a suboptimal diet. Further work, including testing individual metabolites and their combinations, will be required to identify the specific compounds or cocktails produced by *Acetobacter* upon lactate utilization supporting acceleration of larval development.

Beyond essential nutrient provision and metabolic cooperation between commensals and their host, we posit that other bacteria-mediated mechanisms would also contribute to enhanced host growth. Indeed, upon lactate utilization *Acetobacter* may release molecules that would activate host endocrine signals and promote anabolism. Accordingly, it was recently shown that acetate produced by *Acetobacter* improves larval growth by impacting host lipid metabolism through the activation of the IMD signaling pathway in entero-endocrine cells and the release of the endocrine peptide tachykinin (Kamareddine et al., 2018). However, this mechanism is unlikely to be at play here owing to the high content of acetate in our fly diet.

Collectively our results deconstruct the intertwined metabolic networks forged between commensal bacteria that support juvenile growth of the host. This work contributes to the understanding of how the microbiota activities as a whole influence host nutritional and metabolic processes supporting host juvenile growth despite a stressful nutritional environment.

Limitations of the Study

The complete genetic characterization of Lactate-dependent *Acetobacter* stimulation of larval growth was hampered by the lethality of *Acetobacter* mutants affecting the central metabolic pathways while growing in complete HD. Instead, using metabolomics, we pinpoint a large repertoire of molecules produced by *Acetobacter* upon lactate utilization and accessible to the developing larvae. Further studies will be necessary to test the 45 candidate metabolites, individually or in combinations, to identify the minimal metabolite cocktail enhancing the development of GF larvae or larvae mono-associated with *Acetobacter*. Moreover, functional analyses in the host would be required to identify the metabolic pathways sustained by commensal bacteria and involved in the anabolic growth of the host.

Resource Availability

Lead Contact

Further information and requests for resources should be addressed to the Lead Contact, François Leulier (francois.leulier@ens-lyon.fr).

Materials Availability

This study did not generate new unique reagents.

Data and Code Availability

Tables 1 and S2 provide the main results derived from the metabolomic analysis presented in this study.

METHODS

All methods can be found in the accompanying [Transparent Methods supplemental file](#).

SUPPLEMENTAL INFORMATION

Supplemental Information can be found online at <https://doi.org/10.1016/j.isci.2020.101232>.

ACKNOWLEDGMENTS

We would like to thank Dali Ma for critical reading and editing of the manuscript and valuable suggestions, John Chaston and Peter Newell for *Acetobacter fabarum* strains and mutants, and the ArthroTools platform of the SFR Biosciences (UMS3444/US8) for fly equipment and facility. Research in F.L.'s lab is supported by the ENS de Lyon, CNRS, and the Finovi foundation. Research in P.d.S.' lab is supported by INRA and INSA Lyon. J.C. is funded by a postdoctoral fellowship from the "Fondation pour la Recherche Médicale" (FRM, SPF20170938612). T.G. is funded by a PhD fellowship from ENS de Lyon.

AUTHOR CONTRIBUTIONS

Conceptualization, J.C. and F.L.; Methodology, J.C. and F.L.; Validation, J.C. and F.L.; Formal Analysis, J.C.; Investigation, J.C., T.G., H.A., H.G., I.R., and P.d.S.; Data Curation, J.C.; Writing – Original Draft, J.C. and F.L.; Writing – Review & Editing, J.C. T.G., P.d.S., and F.L.; Visualization, J.C.; Supervision, J.C. and F.L.; Project Administration, J.C. and F.L.; Funding Acquisition, F.L.

DECLARATION OF INTERESTS

The authors declare no competing financial interests.

Received: November 12, 2019

Revised: March 13, 2020

Accepted: June 1, 2020

Published: June 26, 2020

REFERENCES

- Adler, P., Frey, L., Berger, A., Bolten, C., Hansen, C., and Wittmann, C. (2014). The key to acetate: metabolic fluxes of acetic acid bacteria under cocoa pulp fermentation-simulating conditions. *Appl. Environ. Microbiol.* *80*, 4702–4716.
- Bing, X., Gerlach, J., Loeb, G., and Buchon, N. (2018). Nutrient-dependent impact of microbes on *Drosophila suzukii* development. *mBio* *9*, e02199–17.
- Blanton, L.V., Charbonneau, M.R., Salih, T., Barratt, M.J., Venkatesh, S., Ilkaveya, O., Subramanian, S., Manary, M.J., Trehan, I., Jorgensen, J.M., et al. (2016). Gut bacteria that prevent growth impairments transmitted by microbiota from malnourished children. *Science* *351*, aad3311-1–aad3311-7.
- Carvalho, M., Sampaio, J.L., Palm, W., Brankatschk, M., Eaton, S., and Shevchenko, A. (2012). Effects of diet and development on the *Drosophila* lipidome. *Mol. Syst. Biol.* *8*, 600.
- Chandler, J.A., Lang, J.M., Bhatnagar, S., Eisen, J.A., and Kopp, A. (2011). Bacterial communities of diverse *Drosophila* species: ecological context of a host–microbe model system. *PLoS Genet.* *7*, e1002272.
- Consuegra, J., Grenier, T., Baa-Puyoulet, P., Rahioui, I., Akherraz, H., Gervais, H., Parisot, N., Silva, P., Charles, H., Calevro, F., et al. (2020). *Drosophila*-associated bacteria differentially shape the nutritional requirements of their host during juvenile growth. *Plos Biol.* *18*, e3000681.
- Development Initiatives (2018). 2018 Global Nutrition Report: Shining a light to spur action on nutrition (Development Initiatives).
- Eisenberg, T., Knauer, H., Schauer, A., Büttner, S., Ruckstuhl, C., Carmona-Gutierrez, D., Ring, J., Schroeder, S., Magnes, C., Antonacci, L., et al. (2009). Induction of autophagy by spermidine promotes longevity. *Nat. Cell. Biol.* *11*, ncb1975.
- Enya, S., Yamamoto, C., Mizuno, H., Esaki, T., Lin, H.-K., Iga, M., Morohashi, K., Hirano, Y., Kataoka, H., Masujima, T., et al. (2017). Dual roles of glutathione in ecdysone biosynthesis and antioxidant function during the larval development in *Drosophila*. *Genetics* *207*, 1519–1532.
- Fast, D., Petkau, K., Ferguson, M., Shin, M., Galenza, A., Kostiuik, B., Pukatzki, S., and Foley, E. (2020). *Vibrio cholerae*-symbiont interactions inhibit intestinal repair in *Drosophila*. *Cell Rep.* *30*, 1088–1100.
- Ferain, T., Hobbs, J.N., Richardson, J., Bernard, N., Garmyn, D., Hols, P., Allen, N.E., and Delcour, J. (1996). Knockout of the two *ldh* genes has a major impact on peptidoglycan precursor synthesis in *Lactobacillus plantarum*. *J. Bacteriol.* *178*, 5431–5437.
- Fischer, C., Trautman, E.P., Crawford, J.M., Stabb, E.V., Handelsman, J., and Broderick, N.A. (2017). Metabolite exchange between microbiome members produces compounds that influence *Drosophila* behavior. *Elife* *6*, e18855.
- Forman, H.J., Zhang, H., and Rinna, A. (2009). Glutathione: overview of its protective roles, measurement, and biosynthesis. *Mol. Aspects. Med.* *30*, 1–12.
- Gould, A.L., Zhang, V., Lamberti, L., Jones, E.W., Obadia, B., Korasidis, N., Gavryushkin, A., Carlson, J.M., Beerenwinkel, N., and Ludington, W.B. (2018). Microbiome interactions shape host fitness. *Proc. Natl. Acad. Sci. U S A* *115*, E11951–E11960.
- Goyal, M.S., Venkatesh, S., Milbrandt, J., Gordon, J.I., and Raichle, M.E. (2015). Feeding the brain and nurturing the mind: linking nutrition and the gut microbiota to brain development. *Proc. Natl. Acad. Sci. U S A* *112*, 14105–14112.
- Holland, W.L., Brozinick, J.T., Wang, L.-P., Hawkins, E.D., Sargent, K.M., Liu, Y., Narra, K., Hoehn, K.L., Knotts, T.A., Siesky, A., et al. (2007). Inhibition of ceramide synthesis ameliorates glucocorticoid-, saturated-fat-, and obesity-induced insulin resistance. *Cell Metab* *5*, 167–179.
- Hooper, L.V., and Gordon, J.I. (2018). Commensal host-bacterial relationships in the gut. *Science* *292*, 1115–1118.

- Jang, T., and Lee, K.P. (2018). Comparing the impacts of macronutrients on life-history traits in larval and adult *Drosophila melanogaster*: the use of nutritional geometry and chemically defined diets. *J. Exp. Biol.* 221, jeb181115.
- Kamareddine, L., Robins, W.P., Berkey, C.D., Mekalanos, J.J., and Watnick, P.I. (2018). The *Drosophila* immune deficiency pathway modulates enteroendocrine function and host metabolism. *Cell Metab.* 28, 1–14.
- Keebaugh, E.S., Yamada, R., Obadia, B., Ludington, W.B., and Ja, W.W. (2018). Microbial quantity impacts *Drosophila* nutrition, development, and lifespan. *iScience* 4, 247–259.
- Keebaugh, E.S., Yamada, R., and Ja, W.W. (2019). The nutritional environment influences the impact of microbes on *Drosophila melanogaster* life span. *mBio* 10, e00885–19.
- Kraut, R. (2011). Roles of sphingolipids in *Drosophila* development and disease. *J. Neurochem.* 116, 764–778.
- Leitão-Gonçalves, R., Carvalho-Santos, Z., Francisco, A.P., Fioreze, G.T., Anjos, M., Baltazar, C., Elias, A.P., Itskov, P.M., Piper, M.D.W., and Ribeiro, C. (2017). Commensal bacteria and essential amino acids control food choice behavior and reproduction. *Plos Biol.* 15, e2000862.
- Martino, M.E., Bayjanov, J.R., Caffrey, B.E., Wels, M., Joncour, P., Hughes, S., Gillet, B., Kleerebezem, M., van Hijum, S.A.F.T., and Leulier, F. (2016). Nomadic lifestyle of *Lactobacillus plantarum* revealed by comparative genomics of 54 strains isolated from different habitats. *Environ. Microbiol.* 18, 4974–4989.
- Matos, R.C., Schwarzer, M., Gervais, H., Courtin, P., Joncour, P., Gillet, B., Ma, D., Bulteau, A.-L., Martino, M., Hughes, S., et al. (2017). D-alanine esterification of teichoic acids contributes to *Lactobacillus plantarum* mediated *Drosophila* growth promotion upon chronic undernutrition. *Nat. Microbiol.* 2, 1635–1647.
- Minois, N. (2014). Molecular basis of the “anti-aging” effect of spermidine and other natural polyamines - a mini-review. *Gerontology* 60, 319–326.
- Minois, N., Carmona-Gutierrez, D., Bauer, M.A., Rockenfeller, P., Eisenberg, T., Brandhorst, S., Sigrist, S.J., Kroemer, G., and Madeo, F. (2012). Spermidine promotes stress resistance in *Drosophila melanogaster* through autophagy-dependent and -independent pathways. *Cell. Death Dis.* 3, e401.
- Mishra, D., Thorne, N., Miyamoto, C., Jagge, C., and Amrein, H. (2018). The taste of ribonucleosides: novel macronutrients essential for larval growth are sensed by *Drosophila* gustatory receptor proteins. *PLoS Biol.* 16, e2005570.
- Newell, P.D., and Douglas, A.E. (2014). Interspecies interactions determine the impact of the gut Microbiota on nutrient allocation in *Drosophila melanogaster*. *Appl. Environ. Microbiol.* 80, 788–796.
- Oyeyinka, B.O., and Afolayan, A.J. (2019). Comparative evaluation of the nutritive, mineral, and antinutritive composition of *Musa sinensis* L. (Banana) and *Musa paradisiaca* L. (Plantain) fruit compartments. *Plants* 8, 598.
- Pais, I.S., Valente, R.S., Sporniak, M., and Teixeira, L. (2018). *Drosophila melanogaster* establishes a species-specific mutualistic interaction with stable gut-colonizing bacteria. *PLoS Biol.* 16, e2005710.
- Piper, M.D.W., Blanc, E., Leitão-Gonçalves, R., Yang, M., He, X., Linford, N.J., Hoddinott, M.P., Hopfen, C., Soultoukis, G.A., Niemeier, C., et al. (2013). A holidic medium for *Drosophila melanogaster*. *Nat. Methods* 11, 100–105.
- Piper, M.D.W., Soultoukis, G.A., Blanc, E., Mesaros, A., Herbert, S.L., Juricic, P., He, X., Atanassov, I., Salmonowicz, H., Yang, M., et al. (2017). Matching dietary amino acid balance to the in Silico-translated exome optimizes growth and reproduction without cost to lifespan. *Cell Metab.* 25, 610–621.
- Rapport, E.W., Stanley-Samuelson, D., and Dadd, R.H. (1983). Ten generations of *Drosophila melanogaster* reared asexually on a fatty acid-free holidic diet. *Arch. Insect Biochem.* 1, 243–250.
- Sakurai, K., Arai, H., Ishii, M., and Igarashi, Y. (2010). Transcriptome response to different carbon sources in *Acetobacter acetii*. *Microbiology* 157, 899–910.
- Sang, J.H. (1956). The quantitative nutritional requirements of *Drosophila melanogaster*. *J. Exp. Biol.* 33, 45–72.
- Sannino, D.R., Dobson, A.J., Edwards, K., Angert, E.R., and Buchon, N. (2018). The *Drosophila melanogaster* gut microbiota provisions thiamine to its host. *mBio* 9, e00155–18.
- Schroeder, B.O., and Bäckhed, F. (2016). Signals from the gut microbiota to distant organs in physiology and disease. *Nat. Med.* 22, 1079–1089.
- Schultz, J., Lawrence, P.S., and Newmeyer, D. (1946). A chemically defined medium for the growth of *Drosophila melanogaster*. *Anatomical Rec.* 96, 540.
- Schwarzer, M., Makki, K., Storelli, G., Machuca-Gayet, I., Srutkova, D., Hermanova, P., Martino, M.E., Balmund, S., Hudcovic, T., Heddi, A., et al. (2016). *Lactobacillus plantarum* strain maintains growth of infant mice during chronic undernutrition. *Science* 351, 854–857.
- Shin, S., Kim, S.-H., You, H., Kim, B., Kim, A.C., Lee, K.-A., Yoon, J.-H., Ryu, J.-H., and Lee, W.-J. (2011). *Drosophila* microbiome modulates host developmental and metabolic homeostasis via insulin signaling. *Science* 334, 670–674.
- Smith, M.I., Yatsunenko, T., Manary, M.J., Trehan, I., Mkakosya, R., Cheng, J., Kau, A.L., Rich, S.S., Concannon, P., Mychaleckyj, J.C., et al. (2013). Gut microbiomes of Malawian twin pairs discordant for kwashiorkor. *Science* 339, 548–554.
- Sommer, A.J., and Newell, P.D. (2018). Metabolic basis for mutualism between gut bacteria and its impact on their host *Drosophila melanogaster*. *Appl. Environ. Microb.* 85, e01882–18.
- Storelli, G., Defaye, A., Erkosar, B., Hols, P., Royet, J., and Leulier, F. (2011). *Lactobacillus plantarum* promotes *Drosophila* systemic growth by modulating hormonal signals through TOR-dependent nutrient sensing. *Cell Metab.* 14, 403–414.
- Subramanian, S., Huq, S., Yatsunenko, T., Haque, R., Mahfuz, M., Alam, M., Benezra, A., DeStefano, J., Meier, M., Muegge, B., et al. (2014). Persistent gut microbiota immaturity in malnourished Bangladeshi children. *Nature* 510, 417–421.
- Thissen, J.-P., Ketelslegers, J.-M., and Underwood, L.E. (1994). Nutritional regulation of the insulin-like growth factors. *Endocr. Rev.* 15, 80–101.
- Ursini, F., Maiorino, M., and Forman, H.J. (2016). Redox homeostasis: the Golden Mean of healthy living. *Redox Biol.* 8, 205–215.
- P. Vos, G. Garrity, D. Jones, N.R. Krieg, W. Ludwig, F.A. Rainey, K.-H. Schleifer, and W. Whitman, eds (2009). *Bergey’s Manual of Systematic Bacteriology*, 2nd ed. The Firmicutes, Volume 3 (Springer-Verlag).
- White, K.M., Matthews, M.K., Hughes, R., Sommer, A.J., Griffiths, J.S., Newell, P.D., and Chaston, J.M. (2018). A metagenome-wide association study and arrayed mutant library confirm *Acetobacter* lipopolysaccharide genes are necessary for association with *Drosophila melanogaster*. *G3 (Bethesda)* 8, 1119–1127.
- Winans, N.J., Walter, A., Chouaib, B., Chaston, J.M., Douglas, A.E., and Newell, P.D. (2017). A genomic investigation of ecological differentiation between free-living and *Drosophila*-associated bacteria. *Mol. Ecol.* 26, 4536–4550.
- Wong, A.C.-N., Chaston, J.M., and Douglas, A.E. (2013). The inconstant gut microbiota of *Drosophila* species revealed by 16S rRNA gene analysis. *ISME J.* 7, 1922–1932.
- Worgall, T.S. (2008). Regulation of lipid metabolism by sphingolipids. *Subcell. Biochem.* 49, 371–385.
- Yamada, R., Deshpande, S.A., Bruce, K.D., Mak, E.M., and Ja, W.W. (2015). Microbes promote amino acid harvest to rescue undernutrition in *Drosophila*. *Cell Rep.* 10, 865–872.
- Yan, J., Herzog, J.W., Tsang, K., Brennan, C.A., Bower, M.A., Garrett, W.S., Sartor, B.R., Aliprantis, A.O., and Charles, J.F. (2016). Gut microbiota induce IGF-1 and promote bone formation and growth. *Proc. Natl. Acad. Sci. U S A* 113, E7554–E7563.

iScience, Volume 23

Supplemental Information

Metabolic Cooperation among Commensal Bacteria

Supports *Drosophila* Juvenile Growth

under Nutritional Stress

Jessika Consuegra, Théodore Grenier, Houssam Akherraz, Isabelle Rahioui, Hugo Gervais, Pedro da Silva, and François Leulier

SUPPLEMENTAL FIGURES

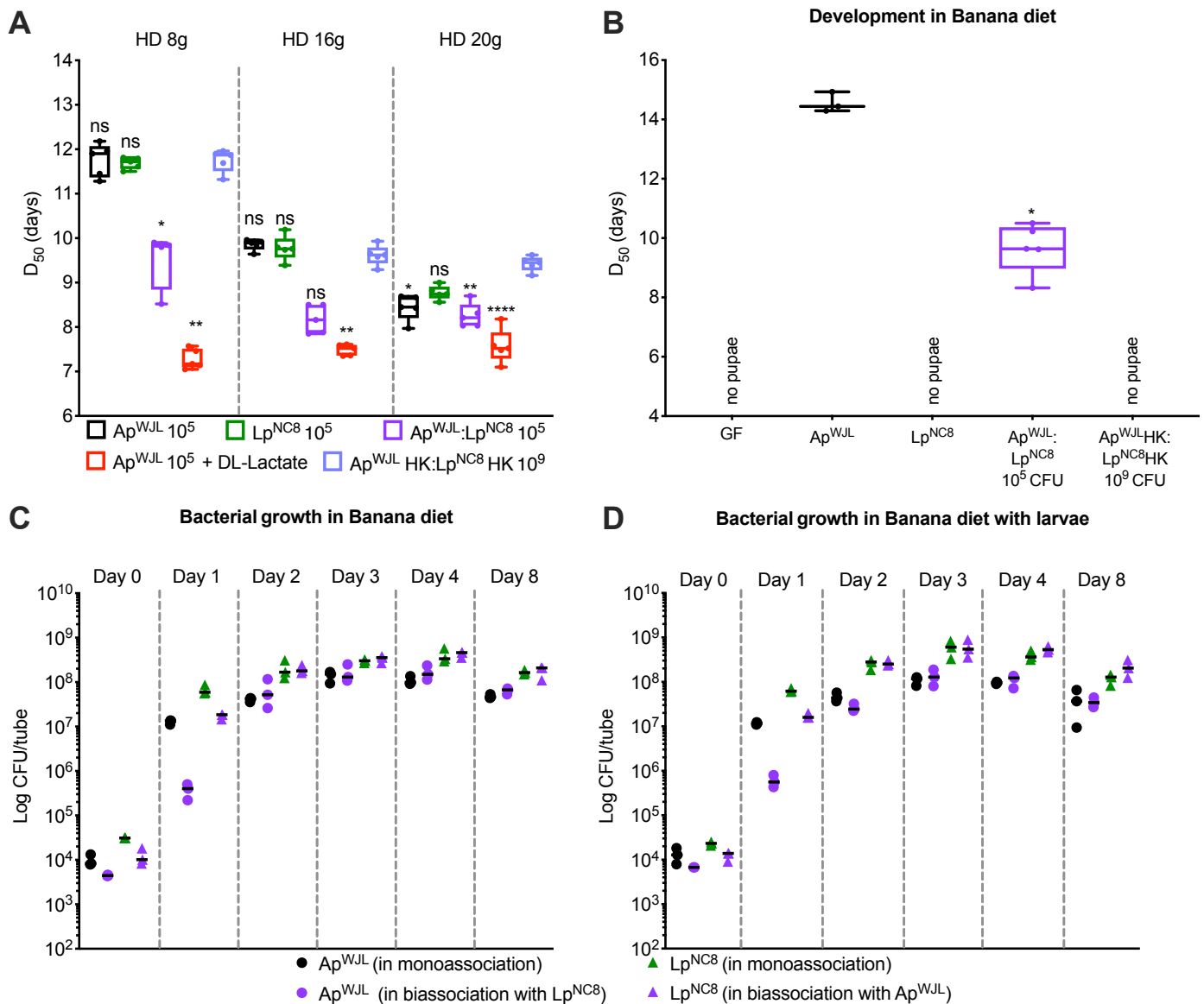


Figure S1. Related to Figure 1 and Figure 3: (A-B) Developmental timing of Germ Free (GF, grey) larvae or GF larvae inoculated with 10^5 CFU of live Ap^{WJL} (black), Lp^{NC8} (green), $Ap^{WJL}:Lp^{NC8}$ bi-association (purple) or 10^9 CFU heat-killed $Ap^{WJL}:Lp^{NC8}$ bi-association (light purple) in HD with a total amino acid content of 8 g/L, 16 g/L, or 20 g/L (A) or Banana-diet (B). (C-D) Load of Ap^{WJL} and Lp^{NC8} in mono- (black and green, respectively), bi-association (purple) or Ap^{WJL} mono-association supplemented with DL-lactate at a final concentration of 0.6 g/L (red) in solid Banana-diet with (D) and

without (C) larvae, from day 0 to 4 days and 8 days after inoculation. Boxplots show minimum, maximum and median. Points represent biological replicates. We performed Kruskal-Wallis test followed by uncorrected Dunn's tests to compare each condition to the GF treated condition. ns: non-significant, *: p-value<0,05, **: p-value<0,005, ***: p-value<0,0005 ****: p-value<0,0001. Dot plots shows mean and each dot represents an independent biological replicate.

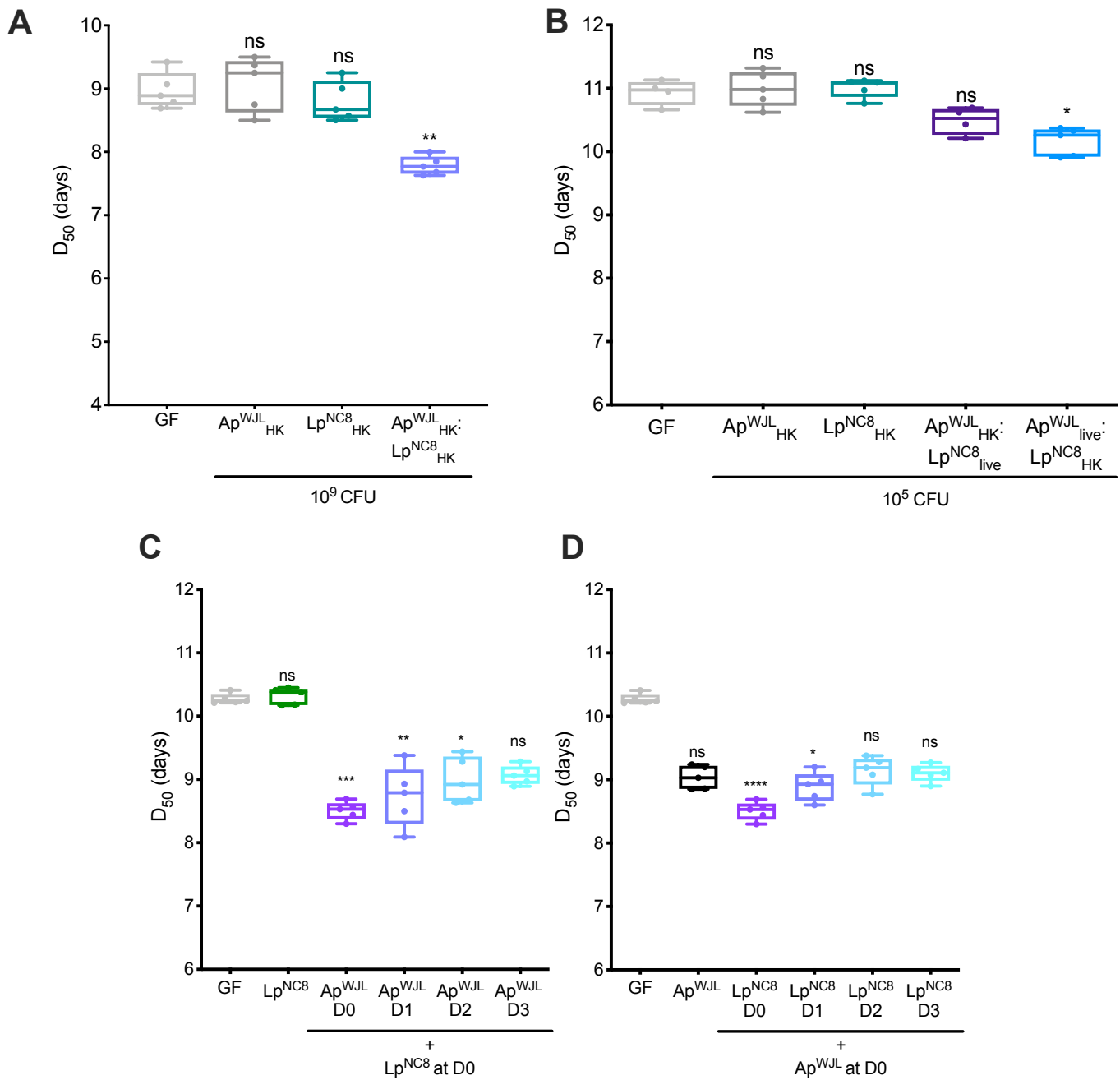


Figure S2. Related to Figure 1: (A) Developmental timing of Germ Free (GF, light grey) larvae or GF larvae inoculated with 10^9 CFU of Ap^{WJL} Heat-Killed (Ap^{WJL}_{HK} , dark grey), Lp^{NC8}_{HK} (turquoise) or $Ap^{WJL}_{HK}:Lp^{NC8}_{HK}$ bi-association (light purple). (B) Developmental timing of GF (light grey) larvae or GF larvae inoculated with 10^5 CFU of Ap^{WJL}_{HK} (dark grey), Lp^{NC8}_{HK} (turquoise), Ap^{WJL}_{HK} plus live Lp^{NC8} ($Ap^{WJL}_{HK}:Lp^{NC8}_{live}$, dark purple) or $Ap^{WJL}_{live}:Lp^{NC8}_{HK}$, light blue). (C) Developmental timing of GF (grey)

larvae or GF larvae inoculated with 10^5 CFU of Lp^{NC8} at D0 and subsequently at D0/1/2/3 with $\sim 10^5$ CFU of Ap^{WJL} . (D) Developmental timing of GF (grey) larvae or GF larvae inoculated with 10^5 CFU of Ap^{WJL} at D0 and subsequently at D0/1/2/3 with 10^5 CFU of Lp^{NC8} . Boxplots show minimum, maximum and median. Points represent biological replicates. We performed Kruskal-Wallis test followed by uncorrected Dunn's tests to compare each condition to the GF treated condition. ns: non-significant, *: p-value<0,05, **: p-value<0,005, ***: p-value<0,0005 ****: p-value<0,0001.

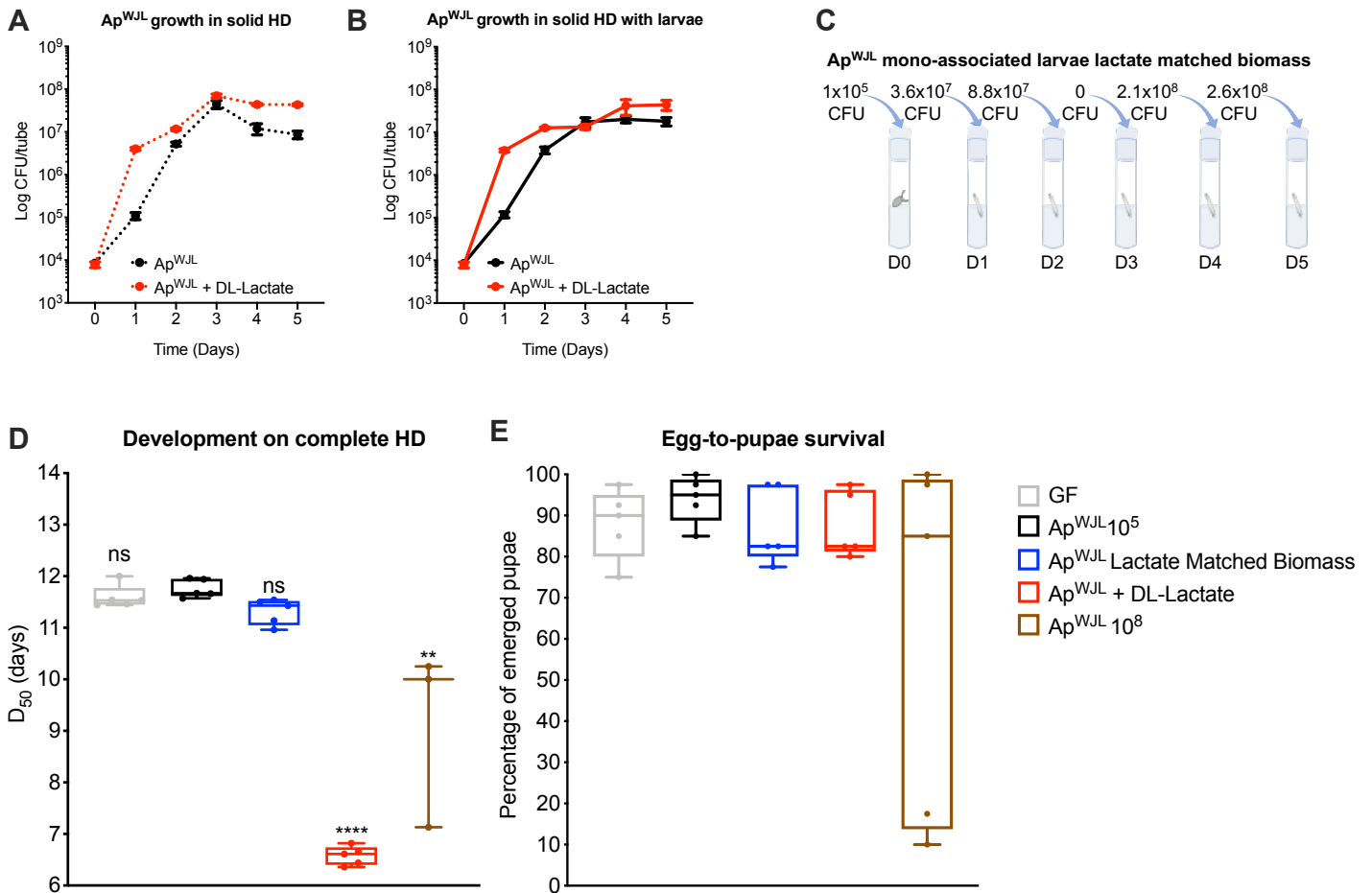


Figure S3. Related to Figure 3: (A-B) Load of Ap^{WJL} in solid HD supplemented (red) or not (black) with DL-lactate at a final concentration of 0.6 g/L with (B) and without (A) larvae, from day 0 to 5 days after inoculation. (C) Graphical representation of the daily Ap^{WJL} biomass supplementation to Ap^{WJL} mono-associated larvae in order to match the biomass reached upon DL-lactate supplementation, according with Fig. S3B. (D) Developmental timing of Germ Free (GF, light grey) larvae or GF larvae inoculated with 10⁵ CFU of Ap^{WJL} (black) or Ap^{WJL} mono-associated larvae supplemented daily with live Ap^{WJL} biomass (blue) or DL-lactate (red) and GF larvae inoculated with 10⁸ CFU of Ap^{WJL} (brown). (E) Percentage of the emerged pupae from the developmental timing experiment of Fig. S3D. Symbols represent the means \pm SEM of three biological replicates except for panel (A-B). Boxplots show minimum, maximum and median. Points represent biological replicates. We performed Kruskal-Wallis test followed by

uncorrected Dunn's tests to compare each condition to the GF treated condition. ns: non-significant, *: p-value<0,05, **: p-value<0,005, ***: p-value<0,0005 ****: p-value<0,0001.

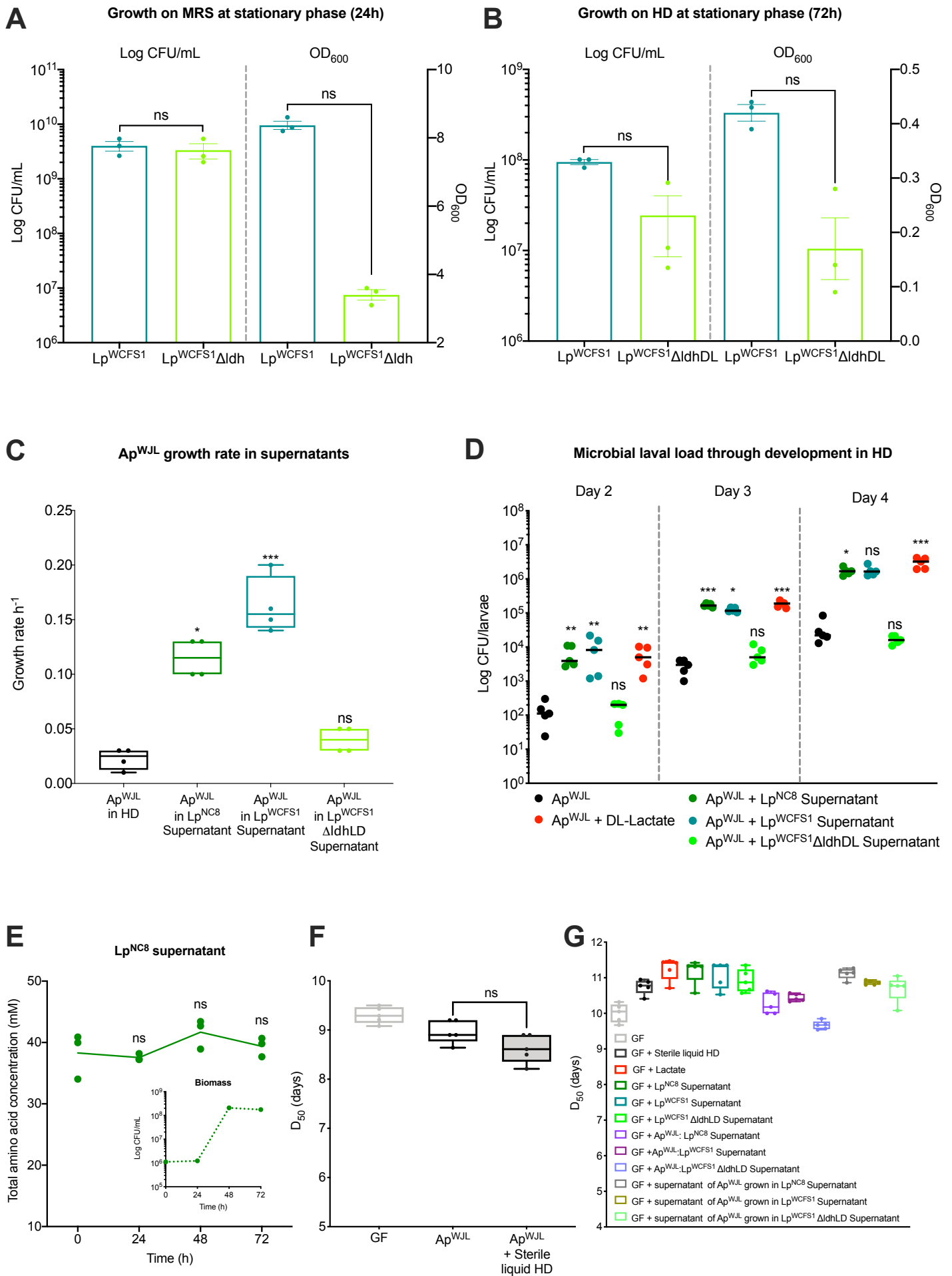


Figure S4. Related to Figure 3: (A-B) CFU count and OD₆₀₀ of *Lp*^{WCFS1} (turquoise) or *Lp*^{WCFS1} Δ *ldhDL* (light green) cultures at stationary phase in MRS (24h, A) or complete holidic diet (72h, B). Bars represent mean \pm SEM. We performed Mann-Whitney test to compare OD and CFU counts of *Lp*^{WCFS1} to *Lp*^{WCFS1} Δ *ldhDL*. (C) Growth rate of *Ap*^{WJL} on complete HD (black), *Lp*^{NC8} supernatant (green), *Lp*^{WCFS1} supernatant (turquoise) or *Lp*^{WCFS1} Δ *ldhDL* supernatant (light green). We performed Mann-Whitney test to compare the growth rate of *Ap*^{WJL} monoculture in HD to to the growth rate of *Ap*^{WJL} growing in the supernatant of interest. (D) *Ap*^{WJL} larval loads on complete HD (black) or complete HD supplemented with *Lp*^{NC8} supernatant (green), *Lp*^{WCFS1} supernatant (turquoise), *Lp*^{WCFS1} Δ *ldhDL* supernatant (light green) or DL-lactate at a final concentration of 0.6 g/L (red). We performed Kruskal-Wallis test followed by uncorrected Dunn's tests to compare each condition to the *Ap*^{WJL} condition (E) HPLC quantification of total amino acid concentration (μ M) in *Lp*^{NC8} supernatant during growth in liquid HD. Inner panel: *Lp*^{NC8} growth. Dot plots show mean and each point represent a biological replicate. We performed Kruskal-Wallis test followed by uncorrected Dunn's tests to compare each time point to T0. (F) Developmental timing of Germ Free (GF, light grey) larvae or GF larvae inoculated with 10⁵ CFU of *Ap*^{WJL} supplemented (black, grey filling) or not (black) with 300 μ L of sterile liquid HD. We performed Mann-Whitney test to compare the D₅₀ of *Ap*^{WJL} to *Ap*^{WJL} supplemented with steril HD. (G) Developmental timing of GF (grey) larvae or GF larvae supplemented with pure lactate (red), 300 μ L of sterile liquid HD (black) or 300 μ L of the different culture supernatants. ns: non-significant, *: p-value<0,05, **: p-value<0,005, ***: p-value<0,0005.

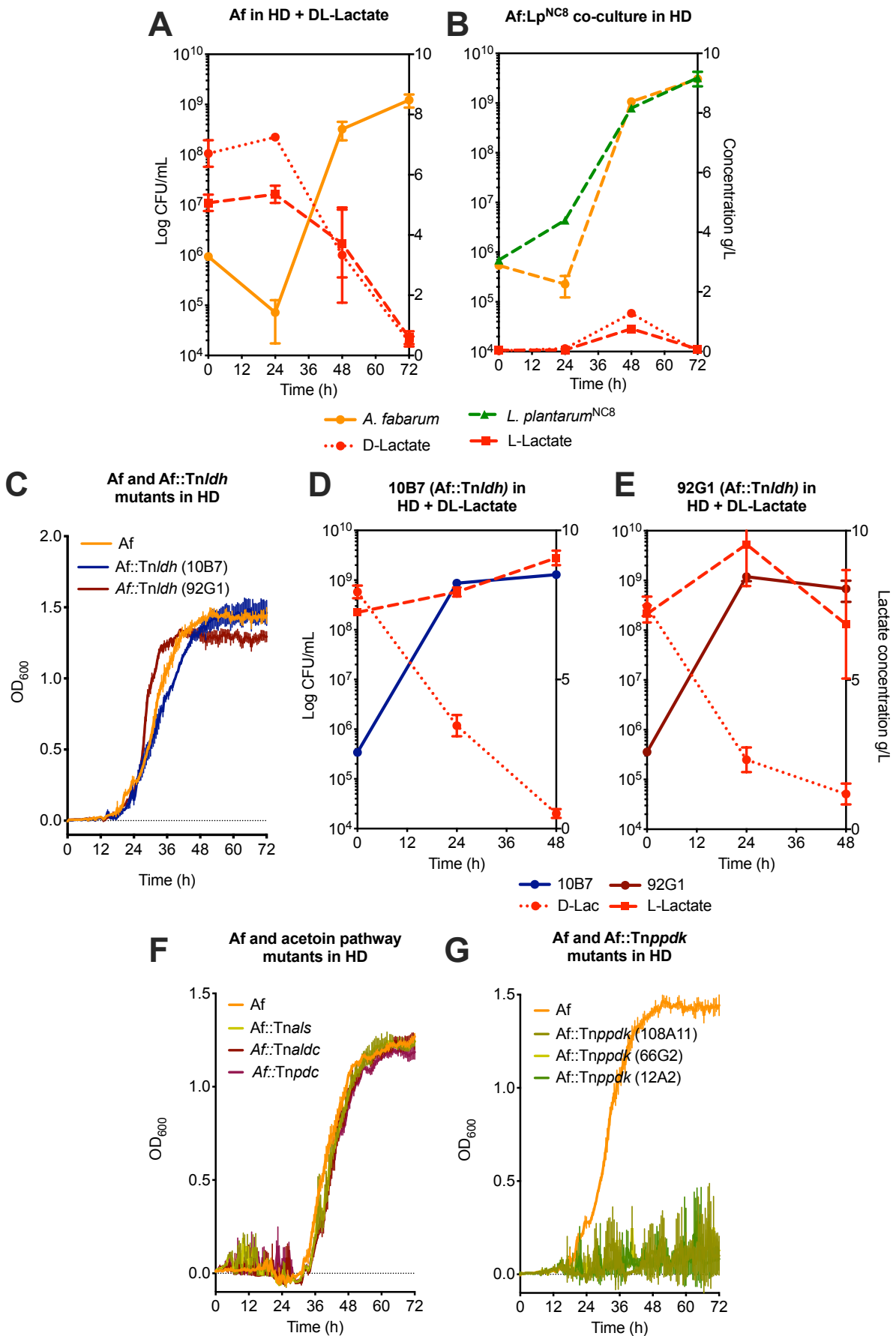


Figure S5. Related to Fig. 5: (A) Growth curve of *A. fabarum* (orange) in liquid HD

supplemented with DL-lactate. D- (dotted line) and L-lactate (dashed line) consumption (red) was quantified. (B) Growth curves in liquid HD of *Lp*^{NC8} (dashed green line) or *Af* (dashed orange line) in co-culture with the respective D- (dotted red line) or L-lactate (dashed red line) levels (red). (C) Growth curve of *A. fabarum* (orange), *Af::Tnldh* (10B7) (blue) or *Af::Tnldh* (92G1) (brown) in liquid HD. (D-E) Growth curves in liquid HD supplemented with DL-lactate of *Af::Tnldh* (10B7) (D) (blue line) or *Af::Tnldh* (92G1) (E) (brown line) with the respective D- (dotted red line) or L-lactate (dashed red line) levels (red). (F) Growth curves of *A. fabarum* (orange), *Af::Tnals* (light green), *Af::Tnaldc* (brown) or *Af::Tnfdc* (dark red) in liquid HD. (G) Growth curves of *A. fabarum* (orange), *Af::Tnppdk* (108A11) (green), *Af::Tnppdk* (66G2) (light green) or *Af::Tnppdk* (12A2) (dark green) in liquid HD. Symbols represent the means \pm SEM of three biological replicates.

SUPPLEMENTAL TABLES

Table S1: Final amino acid concentration supplemented to complete HD in the amino acid cocktail supplementation experiment. Related to Figure 4.

Amino acid	AA Mix (mg/L)		
	Ap @48h	Ap + Lactate @24h	Ap + Lactate @48h
Arg	-	36.802	1.337
His	7.467	39.088	12.911
Ile	-	14.913	-
Leu	9.091	19.230	-
Lys	-	71.720	33.243
Met	-	-	-
Phe	16.911	56.140	25.482
Thr	15.223	41.586	26.157
Val	5.115	22.169	17.314
Ala	-	21.621	80.409
Asp	0.241	13.920	-
Glu	4.703	-	-
Gly	-	8.284	-
Pro	-	-	-
Ser	18.407	38.394	-
Tyr	-	77.555	26.883
Total	77.160	461.428	223.740

Table S3. Strains used in this study. Related with Methods and all Figures.

Strain	Abbreviation	Genotype	Reference
<i>Acetobacter pomorum</i> ^{WJL}	Ap ^{WJL}	WT	Shin et al. 2011
<i>Lactobacillus plantarum</i> ^{NC8}	Lp ^{NC8}	WT	Axelsson L et al. 2012
<i>L. plantarum</i> ^{WCFS1}	Lp ^{WCFS1}	WT	Ferain et al. 1996
<i>L. plantarum</i> ^{WCFS1} Δ ldhDL	Lp ^{WCFS1} Δ ldhDL	Δ ldhDL	
<i>A. fabarum</i> ^{DsW_054}	Af	WT	Winans et al. 2017
<i>A. fabarum</i> ^{DsW_054} Tn:: <i>ldh</i> (10B7)	Af::Tn <i>ldh</i> (10B7)	Tn:: <i>ldh</i>	Winans et al. 2017 and Sommer & Newell 2018
<i>A. fabarum</i> ^{DsW_054} Tn:: <i>ldh</i> (92G1)	Af::Tn <i>ldh</i> (92G1)	Tn:: <i>ldh</i>	
<i>A. fabarum</i> ^{DsW_054} Tn:: <i>als</i>	Af::Tn <i>als</i>	Tn:: <i>als</i>	
<i>A. fabarum</i> ^{DsW_054} Tn:: <i>aldc</i>	Af::Tn <i>aldc</i>	Tn:: <i>aldc</i>	
<i>A. fabarum</i> ^{DsW_054} Tn:: <i>pdh</i>	Af::Tn <i>pdh</i>	Tn:: <i>pdh</i>	
<i>A. fabarum</i> ^{DsW_054} Tn:: <i>ppdk</i> (108A11)	Af::Tn <i>ppdk</i> (108A11)	Tn:: <i>ppdk</i>	
<i>A. fabarum</i> ^{DsW_054} Tn:: <i>ppdk</i> (66G2)	Af::Tn <i>ppdk</i> (66G2)	Tn:: <i>ppdk</i>	
<i>A. fabarum</i> ^{DsW_054} Tn:: <i>ppdk</i> (12A2)	Af::Tn <i>ppdk</i> (12A2)	Tn:: <i>ppdk</i>	

TRANSPARENT METHODS

***Drosophila* diets, stocks and breeding**

Drosophila stocks were reared as described previously (Erkosar et al., 2015). Briefly, flies were kept at 25°C with 12/12-hour dark/light cycles on a yeast/cornmeal medium containing 50 g/L of inactivated yeast, 80 g/L of cornmeal, 7.4 g/L of agar, 4 mL/L of propionic acid and 5.2 g/L of nipagin. Germ-free stocks were established as described previously (Erkosar et al., 2014) and maintained in yeast/cornmeal medium supplemented with an antibiotic cocktail composed of kanamycin (50 µg/mL), ampicillin (50 µg/mL), tetracycline (10 µg/mL) and erythromycin (5 µg/mL). Axenicity was tested by plating fly media on nutrient agar plates. *Drosophila yw* flies were used as the reference strain in this work.

Experiments were performed on Holidic Diet (HD) without preservatives. Complete HD, with a total of 8 g/L, 16 g/L or 20 g/L of amino acids, were prepared as described by Piper et al. using the fly's exome matched amino acid ratios (FLYAA) (Piper et al., 2017). Briefly, sucrose, agar, amino acids with low solubility (Ile, Leu and Tyr) as well as stock solutions of metal ions and cholesterol were combined in an autoclavable bottle with milli-Q water up to the desired volume, minus the volume of solutions to be added after autoclaving. After autoclaving at 120°C for 15 min, the solution was allowed to cool down at room temperature to ~60 °C. Acetic acid buffer and stock solutions for the essential and non-essential amino acids, vitamins, nucleic acids and lipids precursors were added. Single nutrient deficient HD (Fig. 2 and Fig. 3C) were prepared following the same recipe excluding the nutrient of interest (named HD Δ X, X being the nutrient omitted) as described in (Consuegra et al., 2020). Tubes used

to pour the HD were sterilized under UV for 20 min. HD was stored at 4°C until use, for no longer than one week.

Banana diet was prepared with 200 mL of mixed banana, 300 mL of water and 3.5 g of agar. After autoclaving at 120°C for 15 min, 10 mL of diet were poured into UV-sterilized tubes. Banana diet was stored at 4°C and used the next day.

Bacterial strains and growth conditions

Strains used in this study are listed in Table S3. *A. pomorum* was cultured in 10 mL of Mannitol Broth (Bacto peptone 3 g/L, yeast extract 5 g/L, D-mannitol 25 g/L) in 50 mL flask at 30°C under 180 rpm agitation during 24h. *A. fabarum* strains were cultured in 10 mL of YPD (yeast extract 10 g/L, Bacto peptone 10 g/L, Glucose 8 g/L) in 50 mL flask at 30°C under 180 rpm agitation during 24h. *L. plantarum* strains were cultured in 10 mL of MRS broth (Carl Roth, Germany) in 15 mL culture tubes at 37°C, without agitation, overnight. Liquid or solid cultures of Af::Tn were supplemented with kanamycin (Sigma-Aldrich, Germany) at a final concentration of 50 µg/mL. CFU counts were performed for all strains on MRS agar (Carl Roth, Germany). For selective isolation of *Acetobacter* or *Lactobacillus* during cocultures or bi-association, MRS plates were supplemented with ampiciline (10 µg/mL) or kanamycin (50 µg/mL), respectively. Appropriated dilutions were plated using the Easyspiral automatic plater (Intersciences, Saint Nom, France). The MRS agar plates were then incubated for 24-48h at 30°C for *Acetobacter* strains or 37°C for *Lactobacillus*. CFU counts were done using the automatic colony counter Scan1200 (Intersciences, Saint Nom, France) and its counting software.

Bacterial growth in liquid HD

To assess bacterial growth in the fly nutritional environment we used a recently developed liquid HD comprising all HD components except agar and cholesterol (Consuegra et al., 2020). Liquid HD was prepared as described for solid HD. Single nutrient deficient liquid HD was prepared following the same recipe excluding the nutrient of interest. After growth in rich media, the strain to be tested was washed with PBS twice and inoculated at a final concentration of $\sim 10^6$ CFU/mL. For cocultures, the strains were inoculated in a 1:1 ratio. For growth assessment in microplates, 200 μ L of media were inoculated in triplicate. Cultures were incubated in 96-well microtiter plates (Nunc™ Edge 2.0. Thermo Fisher Scientific) at 30°C for 72h. Growth was monitored using an SPECTROstar^{Nano} (BMG Labtech GmbH, Germany) by measuring the optical density at 600 nm (OD_{600}) every 30 minutes. For growth assessment in flasks, 10mL of complete or single nutrient deficient HD were inoculated in triplicate. Cultures were incubated in 50 mL flasks at 30°C under 180 rpm during 72h. Bacterial growth was assessed by plating appropriated dilutions of the cultures every 24h on MRS agar as described above. In figures representing growth in flasks the symbols represent the means with standard error based on three biological replicates. Growth rates were computed by calculating the slope of the curve during exponential growth using SPECTROstar^{Nano} custom analysis software, (BMG Labtech GmbH, Germany). We performed Mann-Whitney test to compare the growth rate among conditions.

Bacterial growth in solid HD

Bacterial CFUs in HD were assessed in microtubes containing 400 μ L of the diet of interest and 0.75–1 mm glass microbeads. Microtubes were inoculated with $\sim 10^4$ CFU of Ap^{WJL} or Lp^{NC8} or a $\sim 10^4$ CFU of a 1:1 mixture of Ap^{WJL} and Lp^{NC8} for coculture. To

assess grow with larvae, 5 first-instar larvae, were added. The tubes were incubated at 25°C. After incubation, 600µL of PBS were added directly into the microtubes. Samples were homogenized with the Precellys 24 tissue homogenizer (Bertin Technologies, Montigny-le-Bretonneux, France). Lysates were diluted in PBS and plated on MRS. CFU counts were assessed as described above.

Developmental timing determination

Axenic adults were placed in sterile breeding cages overnight to lay eggs on sterile HD. The HD used to collect embryos always matched the experimental condition. Fresh axenic embryos were collected the next morning and seeded by pools of 40 in tubes containing 10mL of the HD to test. Unless otherwise stated, in mono-associated conditions a total of $\sim 10^5$ CFU of the strain of interest, washed on PBS, was inoculated on the substrate and the eggs. For bi-association $\sim 10^5$ CFU of a 1:1 mixture of Ap^{WJL} and Lp^{NC8} were inoculated. For heat killed (HK) conditions, washed cells of Ap^{WJL} or Lp^{NC8} were incubated 3h at 65°C. Once at room temperature, embryos were inoculated with $\sim 10^5$ or $\sim 10^9$ CFU. In the germ-free conditions, bacterial suspensions were replaced with sterile PBS. When testing the effect of bacterial by-products on developmental timing, 300 µL of supernatants of a 72h culture on complete HD of the strain of interest was added to the GF or mono-associated embryos. For the lactate supplementation experiments, DL-lactate, D-lactate or L-lactate (Sigma-Aldrich, Germany) were added to a final concentration of 0.6 g/L on GF or mono-associated eggs. For the amino acid cocktail supplementation experiment (Fig. 4), solid complete HD was supplemented with a solution containing the amino acid mixes described in Table S1.

After inoculation, the tubes were incubated at 25°C with 12/12-hour dark/light cycles. The emergence of pupae was scored every day until all pupae had emerged. The experiment was stopped when no pupae emerged after 30 days. Each gnotobiotic or nutritional condition was inoculated in five replicates. D_{50} was determined using D50App (<http://paulinejoncour.shinyapps.io/D50App>) as described previously (Matos et al., 2017). D_{50} heatmap represent the average of the five replicates of each gnotobiotic and nutritional condition. Fig 2K was done using the `imagesc` function on MATLAB (version 2016b. MathWorks, Natick, Massachusetts). Developmental timings are represented as boxplots showing the minimum, maximum and median where each point is a biological replicate. We performed Kruskal-Wallis test followed by uncorrected Dunn's tests to compare each gnotobiotic condition to GF or the condition indicated on the figure.

Larval size measurements

Axenic adults were placed in sterile breeding cages overnight to lay eggs on sterile HD. Fresh axenic embryos were collected the next morning and seeded by pools of 40 in tubes containing 10mL of complete HD. For the mono-associated conditions a total of $\sim 10^5$ CFU Ap^{WJL} or Lp^{NC8}, washed on PBS, was inoculated on the substrate and the eggs. For biassociation $\sim 10^5$ CFU of a 1:1 mixture of Ap^{WJL} and Lp^{NC8} were inoculated. For the lactate supplementation experiments, DL-lactate was added to a final concentration of 0.6 g/L on Ap^{WJL} mono-associated eggs. After inoculation, the tubes were incubated at 25°C with 12/12-hour dark/light cycles until collection of larvae. *Drosophila* larvae were randomly collected every day until day seven after inoculation and processed as described previously (Erkosar, 2015). Larval longitudinal length of individual larvae was quantified using ImageJ software.

Microbial larval load in solid HD

Axenic adults were placed in sterile breeding cages overnight to lay eggs on sterile HD. Fresh axenic embryos were collected the next morning and seeded by pools of 40 in tubes containing 10mL of complete HD supplemented with 0.08% of erioglucine disodium salt (Sigma-Aldrich, Germany). For the mono-associated conditions a total of $\sim 10^5$ CFU Ap^{WJL} or Lp^{NC8}, washed on PBS, were inoculated on the substrate and the eggs. For biassociation $\sim 10^5$ CFU of a 1:1 mixture of Ap^{WJL} and Lp^{NC8} were inoculated. When testing the effect of bacterial by-products on Ap^{WJL} larval load, 300 μ L of supernatants of a 72h culture on complete HD of the strain of interest was added to mono-associated embryos. After inoculation, the tubes were incubated at 25°C with 12/12-hour dark/light cycles until collection of larvae. *Drosophila* larvae were collected every day until five days after inoculation. We selected larvae with a blue gut to eliminate non-feeding individuals. Larvae were surface sterilize by rinsing once in ethanol 70% and twice in sterile PBS and placed in pools of 10 larvae/replicate/condition in 1.5 mL microtubes containing 500 μ L of sterile PBS and 0.75–1 mm glass microbeads. Samples were homogenized with the Precellys 24 tissue homogenizer (Bertin Technologies, Montigny-le-Bretonneux, France). Lysates dilutions (in PBS) were plated on MRS and CFU counts were assessed as described above. Microbial larval loads are represented as dot plots where each point represents a biological replicate comprising the average microbial load of a pool of 10 larvae. We performed Mann-Whitney test to compare microbial loads in mono-association to microbial loads in biassociation for the strain of interest at each time point.

DL-Lactate quantification

Mono-cultures of Ap^{WJL}, Lp^{NC8}, Lp^{WCFS1}, Lp^{WCFS1}ΔldhDL, Af and co-cultures of Ap^{WJL}:Lp^{NC8} and Af:Lp^{NC8} were grown in liquid complete HD as described above. Samples were taken at time 0h and every 24h for 72 h. After centrifugation (5000 rpm, 5 min) to remove cells, D and L lactate concentrations were measured in the supernatants using the D-Lactate and L-Lactate Assay Kit, respectively (Megazyme, Pontcharra-sur-Turdine, France), following the manufacturers' recommendations.

Amino acid quantification by HPLC

In order to quantify Arg, Ile and Leu production in depleted media (Fig. 2H-J), PBS washed Ap^{WJL}, Lp^{NC8} or Ap^{WJL}:Lp^{NC8} were grown in liquid HDΔArg, HDΔIle or HDΔLeu as described above. Samples were collected every 24h for 72h. CFU counts were assessed as described above and supernatants were stored at -20°C until use. To test total protein production by Lp^{NC8} (Fig. S4E) PBS washed Lp^{NC8} was grown in complete HD as described above. Supernatants were collected every 24h for 72h and stored at -20°C until use.

To test Ap^{WJL} amino acid production upon DL-lactate supplementation (Fig. 4A-B), PBS washed Ap^{WJL} was grown in complete HD supplemented or not with DL-lactate at final concentration of 20 g/L as described above. Supernatants were collected every 24h for 72h. CFU counts were assessed as described previously and supernatants were stored at -20°C until use.

Amino acid quantification was performed by HPLC from the supernatants. All proteinogenic amino acids were quantified except Cysteine, Tryptophan, Glutamine and Asparagine. Samples were crushed in 320 μl of ultra-pure water with a known quantity of norvaline used as the internal standard. Each sample was submitted to a

classical protein hydrolysis in sealed glass tubes with Teflon-lined screw caps (6N HCl, 115°C, during 22h). After air vacuum removal, tubes were purged with nitrogen. All samples were stored at -20°C, and then mixed with 50 µL of ultra-pure water for amino acids analyses. Amino acid analysis was performed by HPLC (Agilent 1100; Agilent Technologies, Massy, France) with a guard cartridge and a reverse phase C18 column (Zorbax Eclipse-AAA 3.5 µm, 150 × 4.6 mm, Agilent Technologies). Prior to injection, the sample was buffered with borate at pH 10.2, and primary or secondary amino acids were derivatized with ortho-phthalaldehyde (OPA) or 9-fluorenylmethyl chloroformate (FMOC), respectively. The derivatization process, at room temperature, was automated using the Agilent 1313A autosampler. Separation was carried out at 40°C, with a flow rate of 2 mL/min, using 40 mM NaH₂PO₄ (eluent A, pH 7.8, adjusted with NaOH) as the polar phase and an acetonitrile/methanol/water mixture (45/45/10, v/v/v) as the non-polar phase (eluent B). A gradient was applied during chromatography, starting with 20% of B and increasing to 80% at the end. Detection was performed by a fluorescence detector set at 340 and 450 nm of excitation and emission wavelengths, respectively (266/305 nm for proline). These conditions do not allow for the detection and quantification of cysteine and tryptophan, so only 18 amino acids were quantified. For this quantification, norvaline was used as the internal standard and the response factor of each amino acid was determined using a 250 pmol/µl standard mix of amino acids. The software used was the ChemStation for LC 3D Systems (Agilent Technologies).

Metabolite Profiling

Samples were prepared from tubes inoculated as a DT experiment (see above) comprising 5 biological replicates per condition. Conditions included GF, Af and Af::Tn*ldh* (10B7) inoculated at $\sim 10^5$ CFU on complete HD in presence or not of a pool of 40 GF-eggs. For the lactate supplemented conditions, L-lactate (Sigma-Aldrich, Germany) was added to a final concentration of 0.6 g/L on mono-inoculated tubes (Fig. 6A). Tubes were incubated at 25°C with 12/12-hour dark/light cycles during 3 days. After incubation, a sample of minimum 100 mg was taken from the tubes. In the conditions including embryos, larvae were completely removed. Samples were stored at -80°C before sending to Metabolon Inc. (www.metabolon.com). Samples were extracted and prepared for analysis by Metabolon using standard solvent extraction method. The extracted samples were analysed using UltraHigh Performance Liquid Chromatography coupled to Tandem Mass Spectrometry. 321 compounds were identified by comparison to library entries of purified standards or recurrent unknown entities. Following log transformation and imputation of missing values, if any, with the minimum observed value for each compound, Welch's two-sample *t*-test was used to identify biochemicals that differed significantly between experimental groups.

SUPPLEMENTAL REFERENCES

Consuegra, J., Grenier, T., Baa-Puyoulet, P., Rahioui, I., Akherraz, H., Gervais, H., Parisot, N., Silva, P. da, Charles, H., Calevro, F., et al. (2020). *Drosophila*-associated bacteria differentially shape the nutritional requirements of their host during juvenile growth. *Plos Biol* 18, e3000681.

Erkosar, B., Combe, B., Defaye, A., Bozonnet, N., Puthier, D., Royet, J., and Leulier, F. (2014). *Drosophila* microbiota modulates host metabolic gene expression via IMD/NF- κ B signaling. *PLoS ONE* 9, e94729.

Erkosar, B., Storelli, G., Mitchell, M., Bozonnet, L., Bozonnet, N., and Leulier, F. (2015). Pathogen virulence impedes mutualist-mediated enhancement of host juvenile growth via inhibition of protein digestion. *Cell Host Microbe* 18, 445–455.

Matos, R.C., Schwarzer, M., Gervais, H., Courtin, P., Joncour, P., Gillet, B., Ma, D., Bulteau, A.-L., Martino, M., Hughes, S., et al. (2017). D-alanine esterification of teichoic acids contributes to *Lactobacillus plantarum* mediated *Drosophila* growth promotion upon chronic undernutrition. *Nat. Microbiol.* 2, 1635–1647.

Piper, M.D.W., Soultoukis, G.A., Blanc, E., Mesaros, A., Herbert, S.L., Juricic, P., He, X., Atanassov, I., Salmonowicz, H., Yang, M., et al. (2017). Matching dietary amino acid balance to the In Silico-translated exome optimizes growth and reproduction without cost to lifespan. *Cell. Metab.* 25, 610–621.

Annex II:

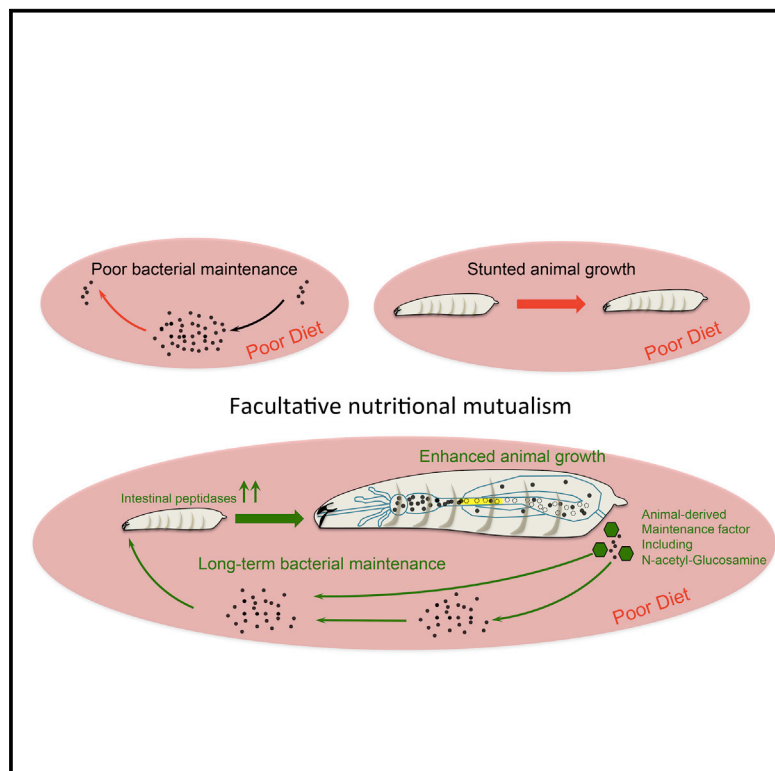
Drosophila perpetuates nutritional mutualism by promoting the fitness of its intestinal symbiont
Lactobacillus plantarum

Article published in Cell Metab. 2018 27(2), 362-377.e8.

Cell Metabolism

Drosophila Perpetuates Nutritional Mutualism by Promoting the Fitness of Its Intestinal Symbiont *Lactobacillus plantarum*

Graphical Abstract



Authors

Gilles Storelli, Maura Strigini, Théodore Grenier, ..., Catherine Daniel, Renata Matos, François Leulier

Correspondence

gstorelli@genetics.utah.edu (G.S.), francois.leulier@ens-lyon.fr (F.L.)

In Brief

Storelli et al. describe a mechanism whereby *Drosophila* larvae maintain their association with beneficial symbiotic bacteria. Symbiotic bacteria hasten the growth of undernourished larvae, while larvae secrete maintenance factors allowing bacteria to persist despite the shortage of their nutritional resources. Thus, *Drosophila*/bacteria symbiosis is a case of facultative nutritional mutualism.

Highlights

- Symbiotic bacteria hasten the growth of undernourished *Drosophila* larvae
- Without larvae, bacteria rapidly exhaust their nutritional resources and collapse
- Larvae secrete maintenance factors allowing bacteria to overcome nutrient shortage
- *Drosophila* larvae/bacteria symbiosis is a case of facultative nutritional mutualism



Drosophila Perpetuates Nutritional Mutualism by Promoting the Fitness of Its Intestinal Symbiont *Lactobacillus plantarum*

Gilles Storelli,^{1,3,*} Maura Strigini,^{1,4,5} Théodore Grenier,^{1,5} Loan Bozonnet,¹ Martin Schwarzer,¹ Catherine Daniel,² Renata Matos,¹ and François Leulier^{1,6,*}

¹Institut de Génomique Fonctionnelle de Lyon (IGFL), Université de Lyon, Ecole Normale Supérieure de Lyon, CNRS UMR 5242, Université Claude Bernard Lyon 1, 69364 Lyon Cedex 07, France

²Lactic Acid Bacteria and Mucosal Immunity Team, Institut Pasteur de Lille, Center for Infection and Immunity of Lille, CNRS UMR 8204, Université de Lille, 59019 Lille, France

³Present address: Department of Human Genetics, University of Utah School of Medicine, Salt Lake City, UT 84112, USA

⁴Present address: Laboratoire de Biologie des Tissus Ostéoarticulaires, INSERM U1059 Sainbiose, Université de Lyon - Université Jean Monnet, Faculté de Médecine, Campus Santé Innovation, 42023, Saint-Étienne, France

⁵These authors contributed equally

⁶Lead Contact

*Correspondence: gstorelli@genetics.utah.edu (G.S.), francois.leulier@ens-lyon.fr (F.L.)

<https://doi.org/10.1016/j.cmet.2017.11.011>

SUMMARY

Facultative animal-bacteria symbioses, which are critical determinants of animal fitness, are largely assumed to be mutualistic. However, whether commensal bacteria benefit from the association has not been rigorously assessed. Using a simple and tractable gnotobiotic model—*Drosophila* mono-associated with one of its dominant commensals, *Lactobacillus plantarum*—we reveal that in addition to benefiting animal growth, this facultative symbiosis has a positive impact on commensal bacteria fitness. We find that bacteria encounter a strong cost during gut transit, yet larvae-derived maintenance factors override this cost and increase bacterial population fitness, thus perpetuating symbiosis. In addition, we demonstrate that the maintenance of the association is required for achieving maximum animal growth benefits upon chronic undernutrition. Taken together, our study establishes a prototypical case of facultative nutritional mutualism, whereby a farming mechanism perpetuates animal-bacteria symbiosis, which bolsters fitness gains for both partners upon poor nutritional conditions.

INTRODUCTION

Animals live in constant association with bacteria. While sharing common niches, they frequently engage in complex symbiotic interactions that influence animal fitness (McFall-Ngai et al., 2013). Bacterial symbionts shape many animal traits, such as growth, fecundity, lifespan, and behavior (Collins et al., 2012; Sommer and Backhed, 2013). Compelling evidence suggests that it occurs primarily via the modulation of host nutrition, a

phenomenon referred to as nutritional symbiosis (Hooper et al., 2002). Thanks to their large enzymatic toolset and biosynthetic capabilities, symbiotic bacteria help their animal partners digest, take up, and metabolize complex nutrients (Flint et al., 2012). In addition, they can synthesize organic molecules that cannot be produced by animals or are limiting in their diets, and thus are strictly required to sustain animal metabolism and growth (Nicholson et al., 2012). Hence, through nutritional symbiosis, bacterial symbionts are critical determinants of animal fitness.

Studies of insects/bacteria endosymbiosis have provided seminal insights into the mechanisms of nutritional symbiosis. Some bacterial endosymbionts enable the insect to survive in extremely poor nutritional niches by producing vitamins and/or essential amino acids (EAAs) (Douglas, 2010). In return, the insect host provides shelter and supplies a continuous flux of nutrients, or complements the metabolic capabilities of its bacterial partner (Wilson et al., 2010). Such endosymbioses are cases of obligate mutualism, as both the insect and its symbionts suffer and even perish in the absence of their partner. Importantly, confinement in this stable and nutrient-rich niche is thought to have led endosymbionts to a state of strict dependency toward their host, due to the sequential loss of genomic potential required for their independence (Douglas, 2010). Obligate endosymbiosis in insects illustrates a classic trade-off concept: even though symbiosis confers tangible benefits to endosymbionts, there is also a strong cost associated with it.

Besides obligate symbiosis, facultative symbioses between bacteria and animals are also widespread. In facultative symbiosis, both partners are dispensable for each other's survival. A typical form of facultative symbiosis exists between most animals and their luminal intestinal bacteria, or "intestinal microbiota": the host can survive without these gut commensals, which, in turn, can also persist in various niches in the absence of their hosts (Gilbert and Neufeld, 2014). Facultative symbioses are largely assumed as mutualistic, and many studies have provided convincing evidence that commensal bacteria, despite



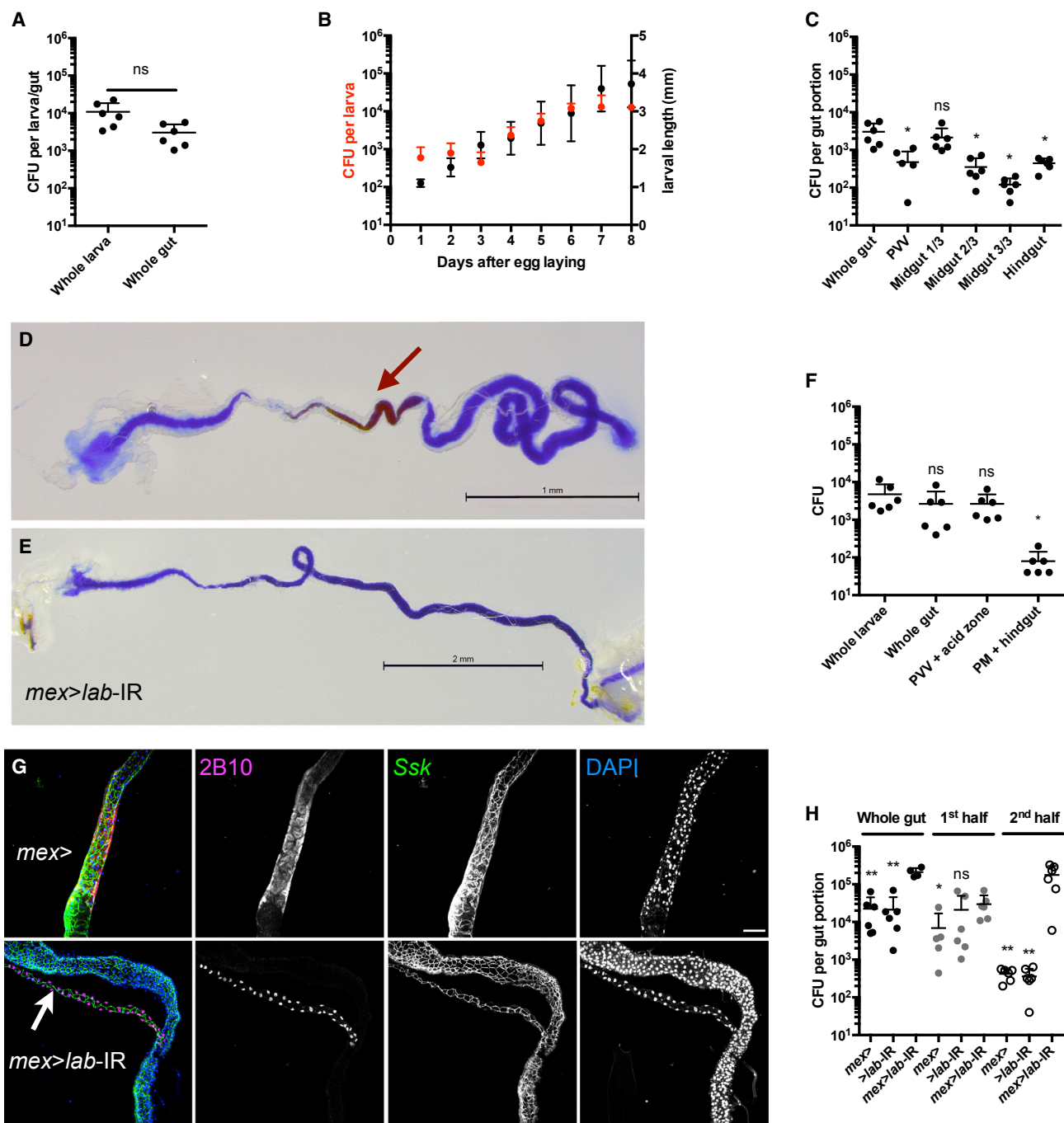


Figure 1. Viable *L. plantarum* Cells Accumulate Anteriorly to the Midgut Acidic Region

(A) Bacterial loads of surface-sterilized larvae and dissected guts after 6 days of mono-association with *Lp*^{WJL} on PYD.

(B) Larva bacterial loads (red closed circles) and larva longitudinal length (black closed circles) over time after mono-association on PYD.

(C) Bacterial loads of whole gut and dissected gut portions from 6DAEL mono-associated larvae. PVV, proventriculus and ventriculus. Midgut 1/3: first third of the midgut, minus the ventriculus. See Figure S1. Asterisks indicate significant difference compared with whole-gut values.

(D and E) Representative guts of 2-day-old wild-type larva (*y,w*) (D) or 3-day-old *mex>lab-IR* larva (E) reared on rich yeast diet (RYD) supplemented with bromophenol blue (BB). The brown arrow points to the acidic region, which is missing in *mex>lab-IR* larva. Scale bars, 1 mm (D) and 2 mm (E).

(F) Bacterial load of dissected gut portions from larvae reared on PYD-BB diet. PVV + acid zone, proventriculus, ventriculus, anterior midgut, and the acidic zone. PM + hindgut, posterior midgut + hindgut.

(G) Knockdown of *labial* expression in the midgut prevents the differentiation of the copper cells. Control *mex>*-Gal4; + larvae (top panel, *mex>*) and *mex>*-Gal4; UAS-*lab-IR* acidic zone depleted larvae (lower panel, *mex>lab-IR*) stained with 2B10 monoclonal antibody highlighting the copper cell region, anti-Ssk marking

(legend continued on next page)

being dispensable for the host survival, are critical determinants of their host's biology (Sommer and Backhed, 2013). Whether bacteria benefit from the association is generally inferred but has not been rigorously assessed (Mushegian and Ebert, 2016). Here we aimed at determining if commensal bacteria benefit from facultative symbioses.

Most insects engage in facultative symbioses. A handful of aerotolerant bacteria, including species of the *Acetobacter* and *Lactobacillus* genera, are commonly associated with the intestinal tract of the model organism *Drosophila melanogaster* in both the wild and in the laboratory (Erkosar et al., 2013). Axenic larvae can develop normally into adulthood in standard rearing conditions, and microbiota members can also persist in different niches in the absence of the fruit fly. However, numerous *Drosophila* life-history traits are modulated by symbionts, such as juvenile growth, lifespan, and behavior (Erkosar et al., 2013; Lee and Brey, 2013; Strigini and Leulier, 2016). Studies with simple and tractable gnotobiotic fly models have begun to unravel the molecular underpinnings of these effects (Ma et al., 2015). We previously demonstrated that the *Drosophila* symbiont *Lactobacillus plantarum*^{WJL} (*Lp*^{WJL}) positively impacts juvenile growth rate and maturation when *Drosophila* larvae are raised under chronic undernutrition. *Lp*^{WJL} induces the expression of larval intestinal peptidases, thereby enhancing dietary protein assimilation and sustaining the host's amino acid sensing target of rapamycin (TOR) signaling pathway (Storelli et al., 2011; Erkosar et al., 2015; Matos et al., 2017). Sustained TOR activity leads to increased insulin-like peptide and steroid hormone signaling, accelerating growth and maturation.

Here we aimed at defining whether *Drosophila* and its commensal partner *Lp*^{WJL} engage in a truly mutualistic interaction, where bacteria also benefit from the association. In this regard, we describe in detail the mode of *Lp*^{WJL} association with *Drosophila* through the entire course of symbiosis. We discover that *Lp*^{WJL} encounters a cost associated with symbiosis, as a large fraction of ingested bacteria get killed while passing through the stomach-like region of the *Drosophila* gut. Yet, despite the loss in numbers, *Lp*^{WJL} cells fare better and persist longer in the niche when in the presence of larvae. We further found that larvae secrete a complex blend of metabolites, including N-acetyl-glucosamine (NAG), which act in synergy to support the long-term persistence of *Lp*^{WJL} in the shared habitat, and consequently maintain symbiosis. In parallel, we show that constant association between *Drosophila* and *Lp*^{WJL} is required for maximum growth benefit for *Drosophila* larvae. Thus, our study unravels an elegant farming mechanism by which an animal actively cultivates a mutually beneficial partnership with its bacterial symbiont through facultative nutritional symbiosis. This mode of symbiosis ensures fitness gains for both partners while facing poor dietary conditions.

RESULTS

L. plantarum Occupies the Endoperitrophic Space, and Live Bacterial Cells Are Concentrated Anteriorly to the Midgut Acidic Region

We previously identified *Lp*^{WJL} as a symbiotic bacteria associated with *Drosophila* during its entire life cycle, and promoting the growth of undernourished *Drosophila* larvae (Storelli et al., 2011). *Lp*^{WJL} is mostly found in the gut (Figure 1A), and its load increases steadily as the larvae grow (Figure 1B). To analyze in detail *Lp*^{WJL} localization in the larval gut, we quantified *Lp*^{WJL}'s loads in different regions of the intestine (Figure S1). Viable *Lp*^{WJL} cells are present all along the intestinal tract, but the anterior part of the midgut harbors 10–100 more bacteria than the middle or posterior midgut sections (Figures 1C and S1A). While the pH in most parts of the midgut is neutral and the posterior-most part is alkaline, the middle section of the larval midgut encompasses the copper cells region, which is marked by luminal acidic pH (Figure 1D) (Overend et al., 2016; Shanbhag and Tripathi, 2009). We hypothesized that this acidic region forms a biological barrier regionalizing *Lp*^{WJL} accumulation in the gut. Accordingly, when we quantified the number of live *Lp*^{WJL} cells in two dissected gut sections delimited by the acidic region (Figures 1F and S1B), we found that live *Lp*^{WJL} cells accumulate in the anterior section that includes the proventriculus, the ventriculus, and the copper cell region. More than 95% of viable *Lp*^{WJL} cells were found in this section (Figure 1F).

The copper cells are functionally and morphologically analogous to the acid-producing gastric parietal cells of the mammalian stomach (Dubreuil, 2004). *labial* is a homeotic gene that specifies and maintains the larval copper cell fate in the embryonic and post-embryonic tissue (Hoppler and Bienz, 1994). By lowering the expression of *labial* in the larval midgut through midgut-specific RNAi (*mex*-GAL4>UAS-*labial*-IR), we altered the larval acidic region. Specifically, the pH in this region is raised (Figure 1E), and 2B10 monoclonal antibody stain, a specific cytoplasmic marker of copper cell fate, disappeared (Strand and Micchelli, 2011) (Figure 1G). In these “acid-less” guts, *Lp*^{WJL} load is increased approximately 10 times compared with control guts (Figure 1H). Furthermore, 100 times more viable *Lp*^{WJL} cells are found in the posterior midgut region next to the would-be acidic domain, compared with control guts (Figures 1H, S1B, and S1C). Based on these observations, we conclude that, under physiological conditions, most viable *Lp*^{WJL} cells are found in the larval gut between the ventriculus and the middle midgut, and that the acidic region acts as a biological barrier shaping *Lp*^{WJL} distribution in the intestines.

In adult *Drosophila*, commensal bacteria are transiently associated with their host (Blum et al., 2013; Broderick et al., 2014). Since the presence of *Lp*^{WJL} is highly regionalized in the larval gut, we wondered if *Lp*^{WJL} persists there or only transits through, in association with ingested food. To answer this question, we designed experiments to “pulse-chase” gut-associated bacteria. We

midgut septate junction and DAPI for nuclei. The 2B10 antibody stains nuclei in Malpighian tubules (white arrow) and the cytoplasm of copper cells. The latter stain is missing in guts of *mex>lab*-IR larvae. Scale bar, 100 μ m.

(H) Bacterial load of whole guts and gut portions of 7DAEL *mex*-Gal4>, >*lab*-IR and *mex>lab*-IR larvae reared on PYD-BB. Black dots, whole guts; dark gray dots, gut portions including PVV and the acid zone (for *mex*-Gal4 and UAS-*lab*-IR larvae) or approximate first half of the gut (for *mex>lab*-IR larvae). Open white dots, gut portions from the end of the acid region to the middle of the hindgut (for *mex*-Gal4 and UAS-*lab*-IR larvae) or the second half of the gut (*mex>lab*-IR larvae). Asterisks indicate a statistically significant difference with the respective *mex>lab*-IR guts/gut portions. **0.001 < p < 0.01, *p < 0.05, ns, not significant (p > 0.05).

transferred surface-sterilized third-instar larvae previously grown on bacteria-associated diet onto fresh axenic food, and transferred them again twice, at 2-hr intervals. We measured gut bacterial loads at each step (Figure 2A). Two hours after the first transfer onto axenic food, the mono-associated larvae have lost 95% of the viable Lp^{WJL} cells that they initially carried at the beginning of the experiment. In fact, a quarter of sampled larvae harbored no detectable colony-forming units (CFUs) ($n = 5/20$). This observation holds true at the second and third transfers ($n = 6/14$ and $n = 8/18$, respectively). This demonstrates that Lp^{WJL} cells do not persist in larvae, as they can be completely lost upon ingestion of new axenic food and excretion of previous gut content.

We next studied the localization of Lp^{WJL} cells in the anterior midgut. To this end, we engineered a fluorescent Lp^{WJL} strain, and associated it with larvae expressing A142::GFP, an enterocyte brush-border marker (Buchon et al., 2013b). Lp^{WJL} cells expressing mCherry localize exclusively with food in the luminal compartment and are physically separated from the enterocytes (Figures 2B and S2A–S2D). The *Drosophila* midgut harbors a chitinous matrix called the peritrophic membrane, which wraps around the ingested food and protects the epithelium from mechanical, chemical, and microbial insults (Figure 2D) (Lemaitre and Miguel-Aliaga, 2013). Confocal microscopy analysis suggests that Lp^{WJL} cells may be secluded within the peritrophic membrane, in the endoperitrophic space (Figures 2B and 2C). To confirm this, we analyzed the anterior region of Lp^{WJL} mono-associated midguts by transmission electron microscopy and detected Lp^{WJL} cells exclusively in the endoperitrophic space of the luminal compartment (Figure 2D), indicating that Lp^{WJL} cells remain associated with the alimentary bolus in the intestinal lumen.

Stable *Drosophila/L. plantarum* Symbiosis by Constant Ingestion and/or Re-ingestion

Despite the transient nature of the association between *Drosophila* and Lp^{WJL} , we observed that the internal bacterial loads of mono-associated larvae constantly increased during development (Figure 1B), therefore Lp^{WJL} cells must be continuously re-associated with larvae, probably by constant ingestion of contaminated food. To test this hypothesis, we surface-sterilized Lp^{WJL} mono-associated third-instar larvae and transferred them individually into tubes containing fresh axenic food. At 0, 4, and 24 hr post-transfer, we quantified the bacterial load of the entire niche (i.e., the food matrix plus the larvae dwelling on it), the larvae (removed from the food), and the food matrix (from which the larvae had been removed) (Figures 3A–3C). In this setup, the only bacteria introduced into the fresh niche at 0 hr are those carried in the guts of transferred larvae. We first observed a significant decrease of the bacterial number in the entire niche 4 hr post-transfer, when >90% of Lp^{WJL} cells present at 0 hr were eliminated (Figure 3A). However, the niche load rebounded dramatically within the next 20 hr and reached a number beyond the initial bacterial burden carried by the larvae. Consistent with the data presented in Figure 2A, we also observed an initial sharp decrease in Lp^{WJL} loads in individual larvae 4 hr post-transfer (Figure 3B). Importantly, bacteria could be recovered in the previously axenic food matrix at the same time point, showing that larvae release live Lp^{WJL} onto the food (Figure 3C). Interestingly, an increase in the bacterial load in the food and in the larvae was readily detectable in the

next 20 hr (Figures 3B and 3C). This indicates that, while many bacterial cells die while transiting in the gut, the bacteria released alive by larvae can proliferate on the food matrix and gradually colonize it. These bacteria could then be re-ingested by larvae.

Since the midgut acidic region acts as a biological barrier shaping Lp^{WJL} accumulation and distribution in the midgut (Figure 1H), we wondered if the acidic region eliminates some of the Lp^{WJL} cells when they transit through the gut, thus explaining the drop in the bacterial load in the niche upon larvae transfer onto axenic food (Figure 3A). To address this question, we surface-sterilized and transferred larvae lacking the acidic region ("acid-less" larvae, $mex>lab-IR$) associated with Lp^{WJL} onto new axenic food and monitored the bacterial load of the entire niche (Figure 3D), the transferred larvae (Figure 3E), or the food matrix (Figure 3F) 4 and 24 hr post larvae transfer. In contrast to the control larvae, Lp^{WJL} load remained constant in the niche colonized by larvae with acid-less guts (Figure 3D). In addition, the decrease in Lp^{WJL} loads in acid-less larvae is delayed compared with $mex>$ controls at 4 hr post-transfer (Figure 3E). One explanation could be that acid-less larvae need more time to purge the initially higher bacterial burden held in their guts (Figure 1H). However, $mex>$ and acid-less larvae do not show a rebound in gut bacterial load 24 hr after transfer, as observed with yw larvae (Figure 3B). Thus, besides the function of copper cells, we cannot rule out the implication of physiological features that could vary between genotypes, such as ingestion and defecation rates, in modulating the evolution of gut bacterial load after transfer on a fresh axenic substrate. Finally, we did not detect differences in bacterial proliferation rates in the niche in a 20 hr period when larvae of the different genotypes, with or without copper cells, were present and when the initial bacterial inoculum was kept identical among conditions (Figure 3G). Therefore, the initial bacterial inoculum (or the quantity of bacteria defecated alive by larvae on a fresh substrate) is the main parameter dictating the evolution of the bacterial population in the niche in a 20 hr period. This demonstrates that the higher number of bacterial cells found alive on the food matrix 4 hr post-transfer of monoassociated acid-less larvae is directly responsible for the higher titer observed at 24 hr post-transfer (Figure 3F). These results indicate that removing the acidic region in the host's midgut preserves more live Lp^{WJL} cells during gut transit and, as a consequence, the excretion of Lp^{WJL} cells onto the food matrix is increased and substrate colonization is accelerated.

To refine our analysis, we used live/dead bacteria stains to probe bacterial survival throughout the intestine. In control animals, while most bacteria are alive in a portion anterior to the copper cells region, they are dead in a more posterior gut portion (Figure 3H, upper panels). This clear live/dead distribution is lost in animals devoid of copper cells, as most bacteria are alive throughout the midgut (Figure 3H, lower panels). Thus, most bacteria are killed when they transit through the acidic region of the gut.

Collectively, our results demonstrate that *Drosophila* and Lp^{WJL} maintain a stable symbiosis through a reiterated cycle: ingestion of Lp^{WJL} cells by larvae, which transit with food through the midgut; while a major portion of the bacteria are killed in the acidic region, the surviving Lp^{WJL} cells are excreted by larvae and can repopulate the food matrix before being re-ingested.

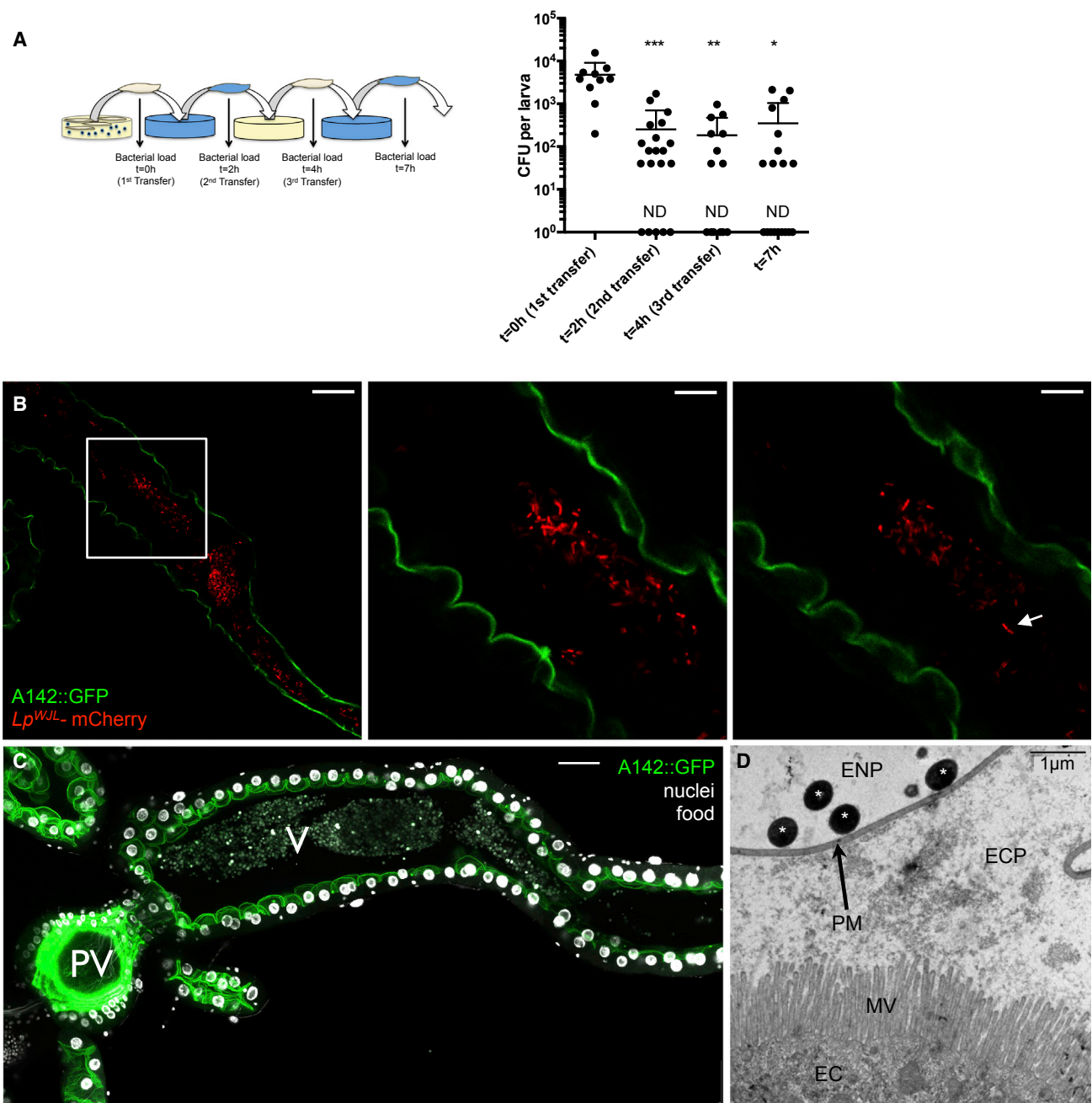


Figure 2. *L. plantarum* Transits in the Endoperitrophic Space with the Food Bolus

(A) Evolution of the larval bacterial load after repeated transfers on axenic food. Left panel: experimental setup. Right panel: bacterial load quantification. To plot all data points on a log scale, a value of "1" was attributed to samples with no detectable CFUs and these have been marked "ND" (not detected). Asterisks represent a statistically significant difference with the initial bacterial burden ($t = 0$ hr).

(B) Ingested bacteria occupy the central part of the gut lumen. Anterior midgut of an A142::GFP larva fed on food containing *Lp*^{WJL} expressing mCherry. GFP localizes to the brush border and thus the apical side of the enterocytes. Individual mCherry-expressing bacteria or pairs of bacilli (arrow) can be seen in the lumen. The samples were mounted unfixed. Single confocal sections are shown. Images for the center and right panels were taken at higher magnification (zoom 3×) than for the left panels (white square) and they are distinct sections of one z stack. Scale bars, 50 μ m (left), 16.67 μ m (center and right).

(C) A142::GFP gut fixed and stained with DAPI to mark nuclei. Autofluorescence highlights the food bolus. PV, the proventriculus; V, the ventriculus. Scale bars, 50 μ m (B and C). Note the apparent gap between the larval tissue (enterocyte epithelium) and the mass of fluorescent bacteria or food, both seem to occupy the endoperitrophic space.

(D) Transmission electron microscopy of anterior midgut transversal sections of 6DAEL *Lp*^{WJL}-mono-associated larvae reared on PYD. White asterisks, bacteria; PM, peritrophic matrix; ECP, ectoperitrophic space; ENP, endoperitrophic space; MV, microvilli; EC, enterocyte. Scale bar, 1 μ m.

Asterisks represent a statistically significant difference with the initial bacterial burden ($t = 0$ hr): ***0.0001 < p < 0.001, **0.001 < p < 0.01, * p < 0.05.

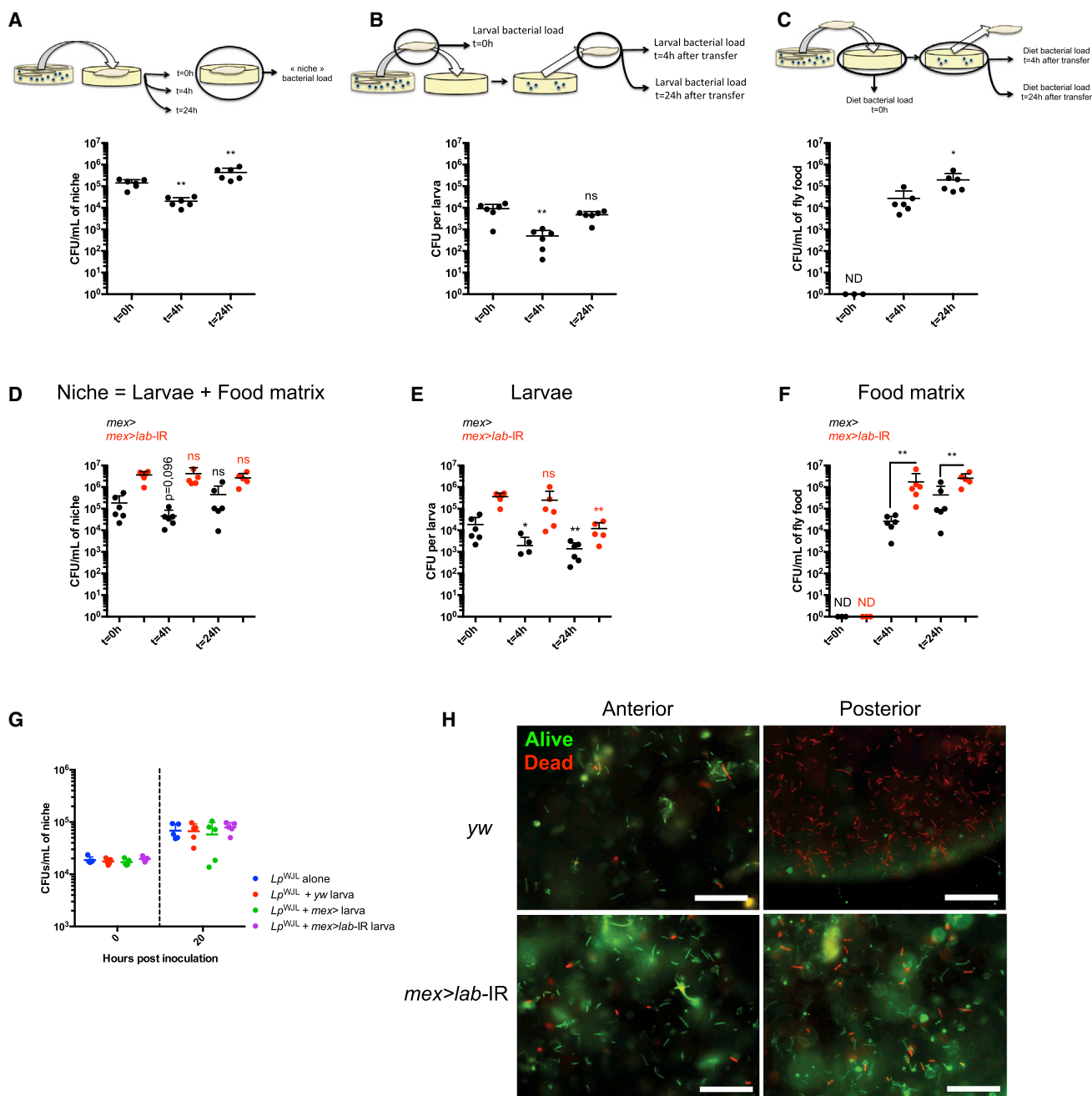


Figure 3. Stable *Drosophila/L. plantarum* Symbiosis by Constant Reingestion

(A–C) Evolution of bacterial load after larvae transfer on axenic food. Upper panels: experimental setup. Lower panels: individual bacterial loads. Single 7DAEL mono-associated larvae were transferred on axenic PYD and the niche (food + larva) (A), the larval (B), or the food matrix (C). Bacterial loads were processed immediately ($t = 0$ hr) or at $t = 4$ hr and $t = 24$ hr post-transfer. Asterisks represent a statistically significant difference with initial burden, at the time of transfer ($t = 0$ hr) (A and B) or between the food matrix bacterial burden at $t = 4$ hr and $t = 24$ hr post-transfer (C). To plot all data points on a log scale, a value of “1” was attributed to samples with no detectable CFU and these have been marked “ND” (not detected).

(D–F) Evolution of bacterial loads after transfer of mono-associated larvae with guts depleted of their acidic region. Single mono-associated larvae from *mex>* (black dots) and *mex>lab-IR* genotypes (red dots) were transferred on axenic food, and substrate and larvae were processed independently, immediately ($t = 0$ hr) or at $t = 4$ hr and $t = 24$ hr post-transfer. The niche bacterial load (D) was calculated by adding larval load values (E) to the associated substrate load values (F). In (D), lettering above dot plots represent statistically significant differences between the niche burden at a given time point and the initial niche burden at the time of transfer ($t = 0$ hr) obtained with larvae of the same genotype (black asterisks for *mex>* niches and red asterisks for *mex>lab-IR* niches). The initial niche burden is considered as equal to the initial larval load since the food is axenic before larva transfer. In (E), asterisks represent statistically significant differences between the larval bacterial load at a given time point and the bacterial burden at the time of transfer ($t = 0$ hr) of larvae of the same genotype (black asterisks for *mex>* larvae

(legend continued on next page)

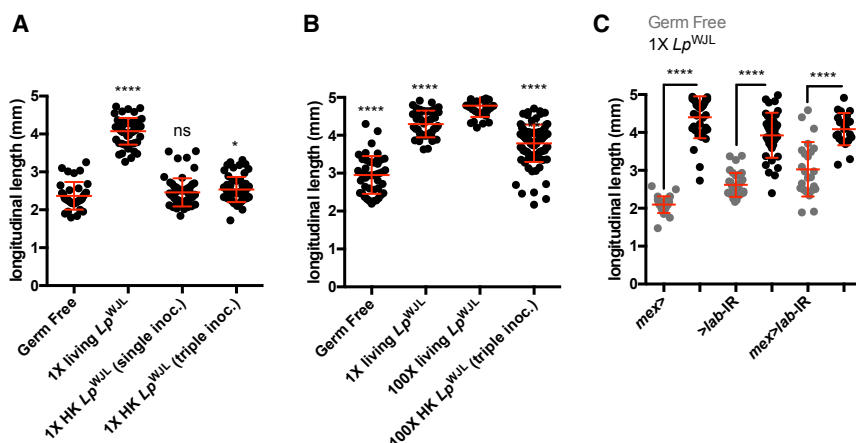


Figure 4. *L. plantarum* Has to Be Alive to Express Its Full Potential to Sustain *Drosophila* Growth

(A and B) Larval longitudinal length at D7 AEL after dead/live bacteria inoculation on PYD. Live bacteria (1× living *Lp*^{WJL} or 100× living *Lp*^{WJL}) were inoculated once at D0 AEL. Heat-killed (HK) bacteria (1× HK *Lp*^{WJL} or 100× HK *Lp*^{WJL}) were inoculated once (single inoc., at D0 AEL) or three times (triple inoc., at D0, D3, and D5 AEL). (A) Asterisks represent statistically significant differences with GF larvae. (B) Asterisks above dot plots represent statistically significant differences with larvae inoculated once with 100× living *Lp*^{WJL}.

(C) Larval longitudinal length at D7 AEL of *mex*-GAL4 (*mex*>), UAS-*labial-IR* (>*lab-IR*) and *mex*-GAL4/UAS-*labial-IR* (*mex*>*lab-IR*) animals after bacterial association on PYD. Gray dot

plots represent measurements of GF larvae; black dot plots represent measurements of mono-associated larvae. Asterisks represent statistically significant difference between GF and mono-associated larvae from the same genotype.

Asterisks illustrate statistical significance between conditions: ****p < 0.0001, *p < 0.05, ns, not significant (p > 0.1).

***L. plantarum* Has to Be Alive and Constantly Associated with Larvae to Sustain *Drosophila* Growth**

The question arises whether dead *Lp*^{WJL} cells may be digested and become an additional food source that is sufficient to promote larval growth upon undernutrition. First, even though bacteria are killed during their transit through the acidic region, they are not completely lysed: they can be visualized with live/dead stains and their coarse morphology does not seem altered (Figure 3H). To further challenge the hypothesis that dead bacterial cell constituents contribute to larval growth, we added, once or repeatedly, heat-killed *Lp*^{WJL} cells to axenic diets containing freshly laid GF eggs. We then assessed larval growth by quantifying the length of the associated larvae at day 7 (D7) after egg laying (AEL) as described previously (Erkosar et al., 2015). Strikingly, the larvae once- or thrice-inoculated with dead *Lp*^{WJL} cells did not grow more than GF siblings (Figure 4A). We detected an increase in larval growth when GF larvae were repeatedly inoculated with 100× dead *Lp*^{WJL} cells, yet the larvae once inoculated with the same amount of viable *Lp*^{WJL} cells still grew longer (Figure 4B). These results clearly demonstrate that, unless in massive excess, dead *Lp*^{WJL} cells fail to promote larval growth to the extent of live bacteria.

In parallel, we tested the growth performance of the acid-less larvae, in which midgut inactivation of *Lp*^{WJL} cells is greatly impaired (Figure 1H). In these animals, *Lp*^{WJL}-mediated growth promotion is still strongly detected (Figure 4C). Therefore, *Lp*^{WJL} inactivation in the midgut is not required for *Lp*^{WJL}-mediated growth promotion, and even though constituents of dead bacteria may serve as a limited trophic source, it is not sufficient to

explain the maximum growth benefit that live *Lp*^{WJL} provides to its animal partner in a low nutritional condition. In conclusion, our results establish that *Lp*^{WJL} cells have to be alive and presumably metabolically active to express their full potential to sustain larval growth.

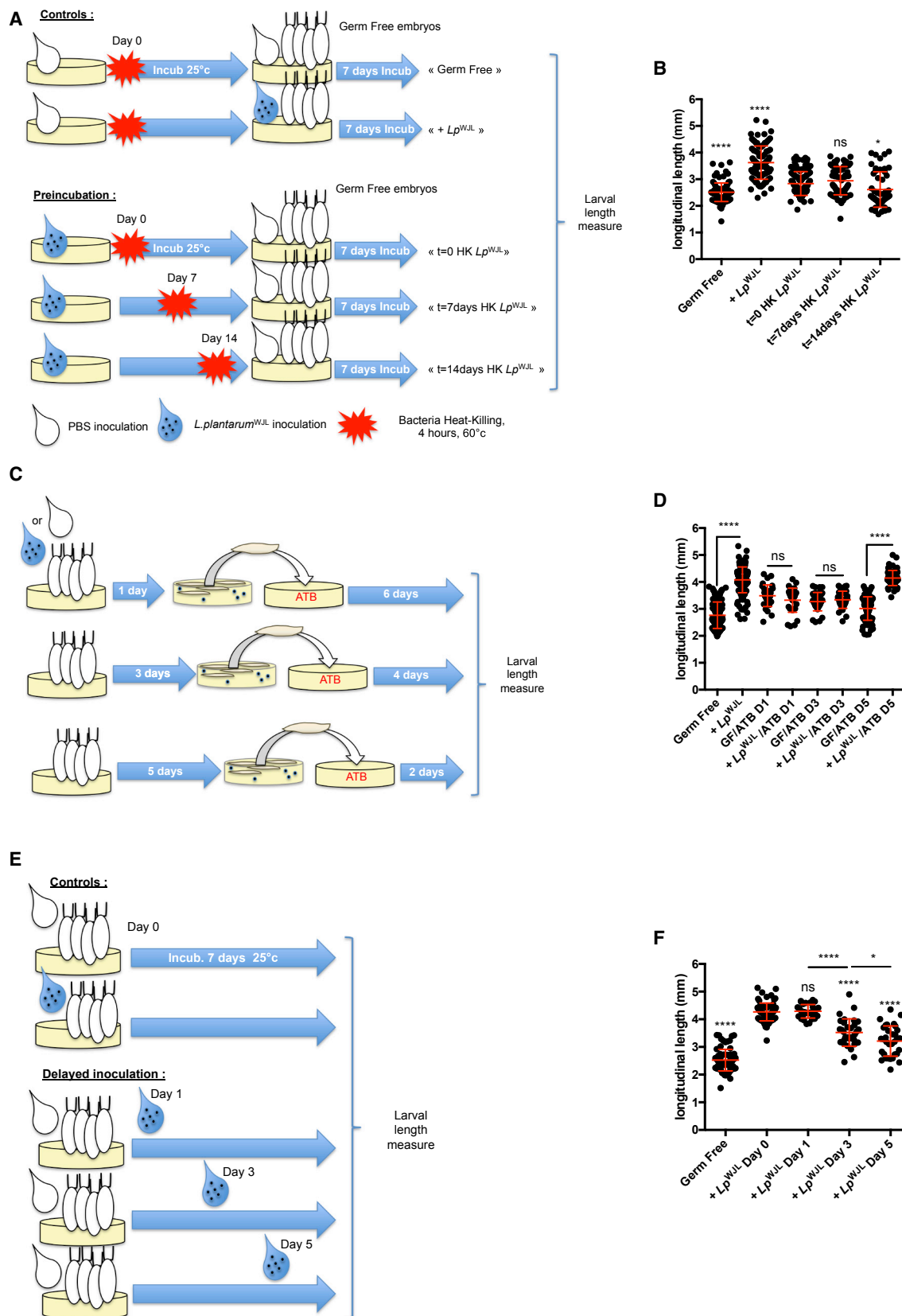
Previous studies suggest that commensal bacteria can confer increased metabolic fitness to *Drosophila* adults through direct modification of the food (Chaston et al., 2014; Huang and Douglas, 2015). We thus tested if diet modification by *Lp*^{WJL} confers larval growth benefit. To this end, we pre-incubated the diet with *Lp*^{WJL} for different lengths of time (0, 7, or 14 days) followed by a mild heat treatment (60°C for 4 hr) that is sufficient to completely kill *Lp*^{WJL} in this setting (data not shown). We then seeded GF embryos onto the “modified” diet (Figure 5A). We found that such pre-inoculation of the diet with *Lp*^{WJL} barely promoted growth of GF larvae; in fact, the longest incubation period even hampered growth (Figure 5B). We then tested if the constant association between *Drosophila* and *Lp*^{WJL} cells is necessary to sustain *Lp*^{WJL}-mediated larval growth promotion. We also wished to define if there is a critical period during larval development when such association is needed for maximal growth gain. To this end, we did the following two experiments: we associated GF embryos with *Lp*^{WJL} and transferred the mono-associated larvae at different time points onto food containing a cocktail of antibiotics that efficiently depletes *Lp*^{WJL} from the niche (Figure 5C and data not shown). In parallel, we mono-associated GF individuals with *Lp*^{WJL} at different time points during larval development (Figure 5E). Removing *Lp*^{WJL} from the niche with antibiotics at D1 or D3 markedly diminished

and red asterisks for *mex*>*lab-IR* larvae. In (F), asterisks represent statistically significant differences between the bacterial loads of food matrixes having hosted *mex*> and *mex*>*lab-IR* larvae at t = 4 hr and t = 24 hr post-transfer.

(G) Bacterial load after 20 hr incubation of PYD initially inoculated with 10⁴ CFU/mL of *Lp*^{WJL} alone or in presence of a single y,w *mex*> or *mex*>*lab-IR* larva.

(H) Live/dead bacteria stain in the endoperitrophic compartment, in different gut portions. Upper panels: stain in control (yw) animals. Lower panels: stain in animals devoid of copper cells (*mex*>*lab-IR*). Left panels show stain in portions of the midgut anterior to the copper cells region (Anterior). Right panels show stain in posterior parts of the midgut (Posterior). Live bacteria stain green, dead bacteria stain red. Scale bars, 30 μm. Note that while bacteria are dead in the posterior part of the gut of control animals, they are not completely lysed: they are efficiently stained by the dye, and their coarse morphology is not altered.

Asterisks illustrate statistical significance between conditions: **0.001 < p < 0.01, *p < 0.05, ns, not significant (p > 0.1). The p value is indicated when approaching statistical significance (0.05 < p < 0.1).



(legend on next page)

Lp^{WJL} -mediated larval growth promotion, while removal on D5 resulted in a partial (if any) alteration of Lp^{WJL} -mediated larval growth promotion (Figure 5D). Moreover, varying the duration of Lp^{WJL} association to GF animals yielded consistent result: the earlier the inoculation, the more visible the Lp^{WJL} -mediated enhanced growth phenotype (Figure 5F). Taken together, our results demonstrate that to express its full benefit toward juvenile growth, Lp^{WJL} has to be alive and constantly provided to its partner.

Drosophila Larvae Sustain *L. plantarum* Long-Term Maintenance in Their Shared Niche

The benefit of Lp^{WJL} to *Drosophila* growth performance upon chronic undernutrition is well established (Erkosar et al., 2015; Storelli et al., 2011). We now show that this beneficial partnership relies on constant association, probably through constant larval feeding activity (Figure 5). Importantly, we have identified a cost to Lp^{WJL} during symbiosis with *Drosophila*, as the majority of the ingested bacteria are killed while transiting through the gut. This observation raises the question whether such symbiosis is actually mutualistic. We thus evaluated how this cost impacts bacterial fitness in the niche in the long term. To this end, we measured the evolution of bacterial titers (CFU counts) in the food matrix over a defined period of time, in the presence or absence of larvae. Specifically, we inoculated 10^8 Lp^{WJL} CFUs/mL onto axenic food and followed the titers over a period of 12 days (larvae enter metamorphosis around days 8–10 AEL). In the absence of larvae, we observed that Lp^{WJL} titers maintain at a plateau at around 10^8 CFUs/mL of fly food until D2 post-inoculation and markedly decrease by about 1–2 logs in the following days (Figure 6A). In contrast, when larvae are present, Lp^{WJL} titers maintain the same plateau over the 12 days (Figure 6A). These observations establish that *Drosophila* and Lp^{WJL} engage in a reciprocal long-term beneficial association whereby larvae presence sustains higher titers of Lp^{WJL} in the niche, despite death of many bacteria cells during the intestinal transit.

Presence of *Drosophila* Larvae Spares Essential Nutrients and Modifies the Diet Ensuring *L. plantarum* Maintenance in the Niche

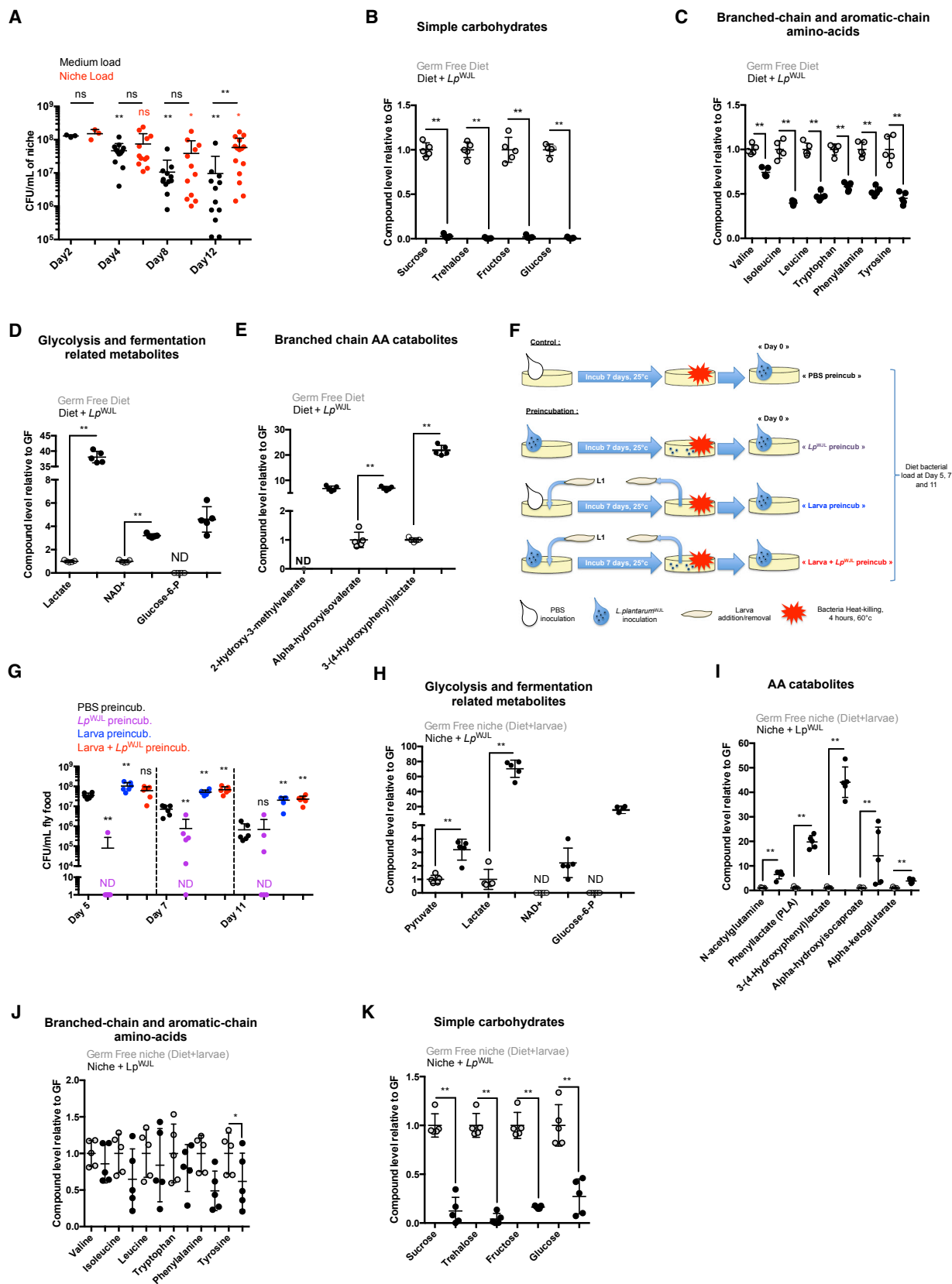
Since Lp^{WJL} maintenance in the diet benefits from the presence of larvae, we reasoned that bacterial metabolism might be altered during symbiosis. To identify potential alterations of Lp^{WJL} metabolism upon symbiosis, we compared profiles of nutrients and metabolites present in axenic diet and diet inoculated

with bacteria (Table S1). In the absence of larvae, Lp^{WJL} cells maintain a high titer for 2–4 days after inoculation and then plunge (Figure 6A, black dots). We therefore analyzed samples 3 days post Lp^{WJL} inoculation. Macronutrients such as simple sugars (sucrose, trehalose, fructose, and glucose) and most EAAs were depleted from the diet (Figures 6B and 6C). This depletion is accompanied by signatures of intense glycolytic activity, homolactic fermentation (increased glucose-6-phosphate, lactate and NAD⁺; Figure 6D), and catabolism of EAAs (increased 2-hydroxy-3-methylvalerate, α -hydroxyisovalerate, and 3,4-hydroxyphenyl lactate; Figure 6E). To see if macronutrient depletion directly impacts the maintenance of Lp^{WJL} cells, we inoculated Lp^{WJL} cells onto axenic diets, incubated them for 7 days, heat killed them, re-inoculated the modified (spent) diet with fresh Lp^{WJL} cells and followed the Lp^{WJL} titers over time (Figures 6F and 6G). The fresh Lp^{WJL} population performed poorly on the Lp^{WJL} pre-incubated diet, while it performed optimally on an unspent diet (Figure 6G, black versus purple). In summary, when inoculated alone onto the poor yeast diet, Lp^{WJL} cells deplete essential nutrients, including simple sugars and EAAs. Nutrient depletion then likely triggers a reduction in Lp^{WJL} titers over time.

To study the bacterial metabolic activity in symbiosis, we next profiled metabolites of the niche, i.e., the food containing *Drosophila* larvae with or without Lp^{WJL} inoculation (Table S2; Figures 6H–6K). Interestingly, we again detected clear signatures of heightened glycolytic activity and homolactic fermentation (Figure 6H), along with EAA catabolism (Figure 6I) in presence of bacteria, suggesting that the core metabolism of Lp^{WJL} cells is not altered upon symbiosis (compare Figures 6H and 6I with Figures 6D and 6E). Yet, the amounts of EAAs and simple sugars were spared (compare Figures 6B and 6C with Figures 6J and 6K). We thus hypothesized that *Drosophila* larvae modify the nutritional substrate, allowing its bacterial partner to sustain its core metabolic activity and maintenance on the diet. Consistent with this hypothesis, pre-incubation of the diet with GF larvae improved maintenance of Lp^{WJL} CFUs (Figures 6F and 6G, black versus blue). Moreover, incubation with both Lp^{WJL} and larvae (a condition that spares simple sugars and EAAs; Figures 6J and 6K), followed by removal of larvae and heat inactivation of Lp^{WJL} (Figure 6F), delivered a suitable substrate for the maintenance of fresh Lp^{WJL} upon re-inoculation (Figure 6G, black versus red). Based on these results, we reasoned that larvae, even when axenic, modify and/or fortify the diet in a way that it becomes more suitable for Lp^{WJL} long-term maintenance.

Figure 5. Constant Association Is Necessary for *L. plantarum*-Mediated *Drosophila* Growth

- (A) Experimental setup to assess the impact of diet pre-incubation with bacteria on larval growth.
 (B) Larval longitudinal length at D7 AEL after rearing on pre-incubated diets. Asterisks represent statistically significant differences with the pool of larvae reared on PYD where bacteria were immediately killed after inoculation ($t = 0$ HK Lp^{WJL}).
 (C) Experimental setup to assess the impact of the timing of bacterial ablation on larval length gain after mono-association.
 (D) Larval longitudinal length at D7 AEL after transfer on ATB-containing PYD. Efficient bacterial inactivation by ATB was assessed by plating larval homogenates at the time of collection on Man, Rogosa, and Sharpe (MRS) agar plates. Larval bacterial loads were evaluated to 0 CFU per larva for + Lp^{WJL} /ATB D1 and + Lp^{WJL} /ATB D3 and 19.3 CFU/larva for + Lp^{WJL} /ATB D5. Asterisks represent statistically significant differences between GF and mono-associated larvae pools transferred at the same time on ATB-containing PYD.
 (E) Experimental setup to assess the impact of delayed mono-association on larval length gain.
 (F) Larval longitudinal length at D7 AEL on PYD. Axenic embryos were mono-associated following the standard procedure (+ Lp^{WJL} D0), or mono-association was delayed (D1, D3, and D5 AEL). Asterisks represent statistically significant differences with the pool of larvae mono-associated at D0 AEL. Asterisks above horizontal bars represent statistically significant differences between two conditions. Asterisks illustrate statistical significance between conditions: **** $p < 0.0001$, * $p < 0.05$, ns, not significant ($p > 0.1$).



(legend on next page)

Drosophila Intestinal Excreta Fortifies the Diet and Ensures *L. plantarum* Long-Term Maintenance in the Niche

Drosophila larvae utilize nutrients from the diet to sustain their own growth, making it a likely competitor of *Lp^{WJL}* on the poor yeast diet. Yet, larval presence in the niche benefits the long-term maintenance of bacteria. Proteins and starch are the major macronutrients in our experimental diet, and a recent genomic survey implies that necessary enzymes required for the processing and utilization of long polypeptides and starch are lacking in *Lp^{WJL}* (Martino et al., 2016). *Drosophila* enterocytes express several intestinal digestive enzymes including peptidases and amylases, which may fulfill the proposed processing activities (Lemaitre and Miguel-Aliaga, 2013). It is conceivable that the digestive activities of the larvae help *Lp^{WJL}* persist in the niche. However, we found no accumulation of starch degradation products, such as maltose, while comparing the metabolites and nutrients of axenic diets versus diets containing larvae (i.e., germ-free niches) (Table S2), and *amy^{null}* larvae, which lack amylase activity (Hickey et al., 1988), promote *Lp^{WJL}* long-term maintenance in the niche as well as control larvae (Figure S3A). Therefore, starch digestion by *Drosophila* larvae is unlikely to be implicated in the bacterial long-term maintenance during symbiosis. We next postulated that *Lp^{WJL}* may benefit from larval proteolytic activities, as they would break down dietary proteins, rendering small peptides and amino acids accessible to *Lp^{WJL}* cells. We thus altered the capacity of *Drosophila* larvae to process dietary proteins by adding to the diet a cocktail of protease inhibitors (PICs). PIC addition to the diet has a dramatic negative impact on larval growth dynamics (Figure S3B) (Erkosar et al., 2015). Yet, it only marginally affects *Lp^{WJL}* maintenance in the niche: even though niche titer is significantly lower at D12 in the presence of PIC, the beneficial effect of larval presence on bacterial maintenance is still observed (compare “Food matrix” and “Niche + Proteases Inhibitor” conditions in Figure S3C). Thus, processing of dietary starch and proteins by *Drosophila* larvae does not seem to be strictly required to maintain *Lp^{WJL}* on the diet in the long run.

Next, we reasoned that the diet is fortified with metabolites or nutrients of larval origin that can sustain the long-term mainte-

nance of *Lp^{WJL}* cells. Consistently, supplementing axenic diets with GF larvae homogenates promoted long-term maintenance of *Lp^{WJL}* (Figure 7A). In addition, supplementing diets with heat-treated GF larvae gut homogenates recapitulates this effect (Figure 7B). Thus, one or multiple non-enzymatic compound(s) of intestinal origin are required for *Lp^{WJL}* maintenance. To further refine our analyses, we fortified diets with larval intestinal excreta. To do so, we bathed larvae overnight in PBS to purge them from their intestinal content (Figures 7C and S3D–S3F). Fortifying diets with intestinal excreta collected from fed or starved larvae favors *Lp^{WJL}* long-term maintenance on the diet (Figures 7D and S3D–S3F). As a control, a solution collected after bathing dead larvae overnight in PBS failed to promote bacterial maintenance (Figure S3G).

Collectively our observations indicate that the intestinal excreta of larvae are sufficient to sustain bacterial maintenance, and that this effect is not explained by the supply of non-assimilated dietary nutrients contained in larval feces. In addition, heat-treating intestinal excreta only slightly reduces their ability to sustain bacterial presence in the niche (Figure S3H), indicating again that this beneficial effect does not rely on the supply of larval digestive capabilities. Therefore, we postulated that one or multiple compounds, which we refer to as “maintenance factors,” are shed by larval intestines and fortify the axenic diet leading to long-term maintenance of *Lp^{WJL}* in the niche.

The Effect of *Drosophila* Intestinal Excreta on *L. plantarum* Long-Term Maintenance Is Mediated by Multiple Maintenance Factors, Including N-Acetylglucosamine

To further characterize these maintenance factors, we performed a metabolite profiling of live or dead larva excreta (Table S3). We focused on compounds enriched in the excreta of live larvae, and further rationalized our candidate approach by selecting families of compounds that may influence the long-term maintenance of *Lp^{WJL}* (Figure S4A). To determine if one or more of these compounds sustains *Lp^{WJL}* long-term maintenance, we supplemented poor yeast diet (PYD) with the respective purified compounds, and scored bacterial maintenance. Supplementing diets with derivatives of purine metabolism does not improve

Figure 6. Presence of *Drosophila* Larvae Spares Essential Nutrients and Fortifies the Diet Ensuring *L. plantarum* Growth and Maintenance

(A) Quantification of niche (red dots) and food matrix (black dots) bacterial loads along time. Niches and food matrixes were processed at D2, D4, D8, and D12 post-inoculation/larval addition for bacterial load quantification. Asterisks just above the dot plots represent statistically significant differences between substrate (black asterisks) or niche (red asterisks) bacterial load at a given time point, and the bacterial load of respective substrate or niche at D2 post-inoculation. Asterisks above horizontal bars represent statistically significant differences between niche and substrate bacterial load at the same time point.

(B–E) Graphs representing the relative levels of metabolites in the diet incubated for 3 days with *Lp^{WJL}* compared with axenic diet (GF). Open circles represent the GF samples, black closed circles the *Lp^{WJL}* inoculated samples. Metabolites not detected in one condition (samples falling below the compound’s detection threshold) are marked with ND (not detected). Asterisks illustrate statistically significant difference between conditions.

(F and G) Effect of food matrix pre-incubation with bacteria, larvae, or bacteria + larva on bacterial titer evolution after re-inoculation. (F) Experimental setup. As parallel controls, pools of $n = 3$ food matrixes pre-incubated with PBS, bacteria, larva, and bacteria + larva were re-inoculated with PBS after aseptic larva removal and heat treatment, and incubated for 11 days at 25°C before crushing and plating on MRS agar plates. No colony was found on MRS agar plates, confirming efficient bacterial inactivation by the heat treatment. These controls are not illustrated in the scheme of the experimental setup for the sake of clarity. (G) Quantification of food matrix bacterial load evolution after pre-incubation with PBS, bacteria, larvae or larvae + bacteria. Food matrixes were processed at D5, D7, and D11 post re-inoculation for bacterial load quantification. Black dots illustrate bacterial loads for PBS pre-incubated food matrixes, purple dots for food matrixes pre-incubated with bacteria, blue dots for food matrixes pre-incubated with GF larva, and red dots for food matrixes pre-incubated with both larva and bacteria. Vertical interrupted lines delineate values obtained for the different conditions at the same day. Asterisks illustrate statistically significant differences with the samples of food matrixes pre-incubated with PBS at the same day.

(H–K) Graphs representing the relative levels of metabolites in the niches incubated for 3 days with *Lp^{WJL}* compared with axenic niches (GF). Open circles represent the GF samples, black closed circles the *Lp^{WJL}*-inoculated samples. Asterisks illustrate statistically significant differences between conditions. Asterisks above horizontal bars illustrate statistical significance between conditions: **0.001 < $p < 0.01$, * $p < 0.05$, ns, not significant ($p > 0.1$).

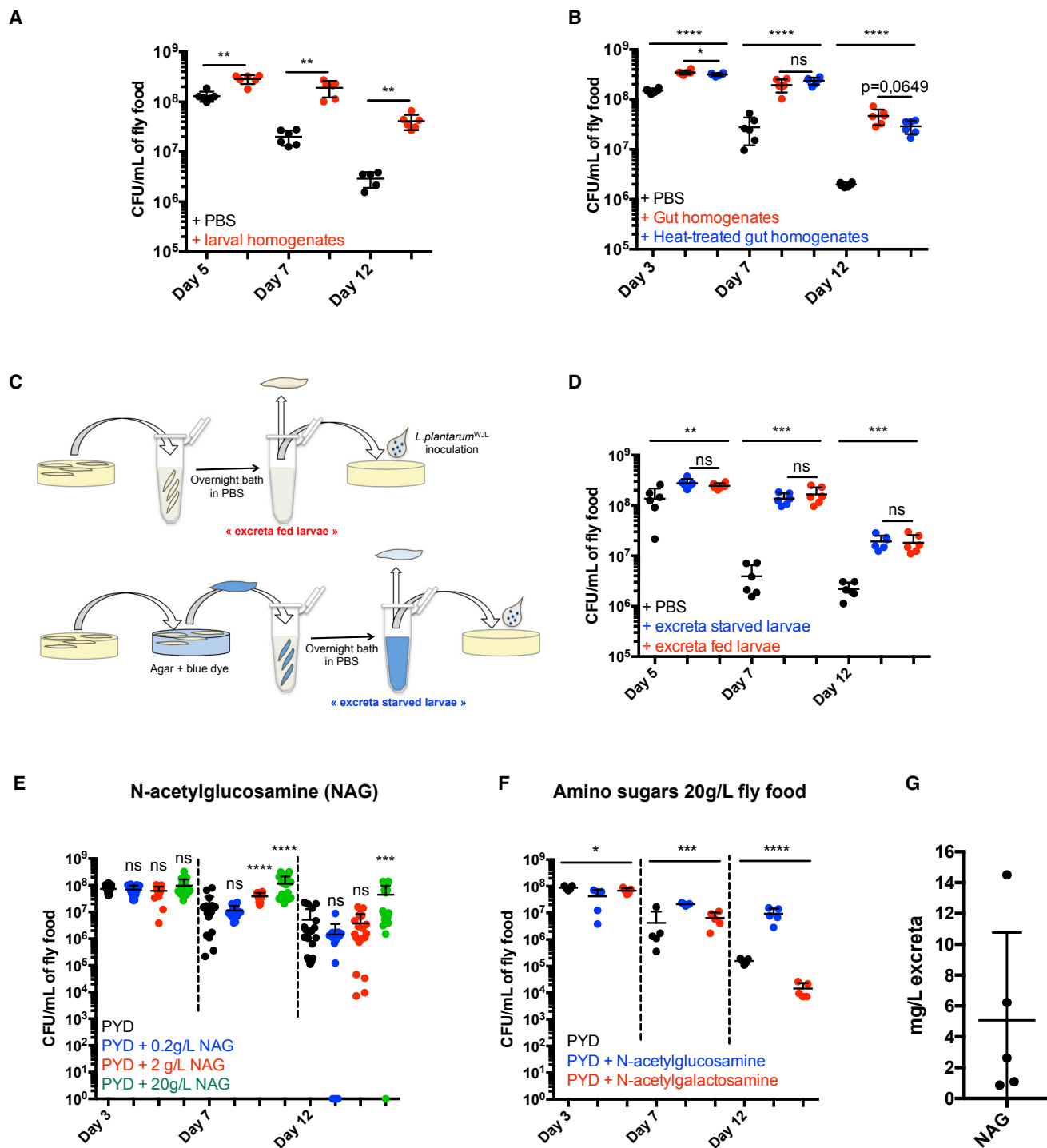


Figure 7. *Drosophila* Intestinal Excreta and N-Acetyl-Glucosamine Maintains *L. plantarum* in the Niche

(A) Evolution of food matrix bacterial load over time after bacteria co-inoculation with PBS (black dots) or heat-treated larval homogenates (red dots).

(B) Evolution of food matrix bacterial load over time after bacteria co-inoculation with PBS (black dots), gut homogenates (red dots), or heat-treated gut homogenates (blue dots).

(C and D) Evolution of food matrix bacterial load over time after bacteria co-inoculation with larval excreta. (C) Experimental setup. For controls and more detailed information, see Figure S3 and the STAR Methods. (D) Evolution of food matrix bacterial load after bacteria co-inoculation with larval excreta collected from fed larvae (red dots) or from starved larvae (blue dots).

(E) Evolution of food matrix bacterial load over time, on substrate supplemented with various concentrations of N-acetyl-glucosamine (NAG). NAG was added at concentrations of 0.2 (blue), 2 (red), and 20 g/L (green) fly food.

(legend continued on next page)

maintenance of Lp^{WJL} over time (Figure S4B). The same observation is made for tryptophan derivatives (Figure S4C), xanthurenate even hastening bacterial titers decrease over time (Figure S4C, right panel). Next, we tested N-acetylated amino acids and formylmethionine in individual supplementations (Figure S4D). Most supplementations do not influence Lp^{WJL} titers over time, with the exceptions of N-acetyl-asparagine, -glutamine, -glutamate, -arginine, and -glycine. N-Acetylasparagine seems deleterious to the bacterial maintenance, while N-acetylglutamine and N-acetylglutamate, have a slight beneficial effect at D7 (lost at D12). In addition, N-acetylarginine and N-acetylglycine have a slight beneficial effect on bacterial titer at D12. We wondered whether supplying greater quantities of these four N-acetylated amino acids would amplify their beneficial effect on bacterial persistence. We therefore supplemented diets with 20 times more N-acetylglutamine, -glutamate, -arginine, and -glycine (Figure S4E). In this setting, we did not detect any beneficial effect of these compounds on the maintenance of Lp^{WJL} over time. Taken together, these results establish that N-acetyl amino acids do not significantly impact bacterial persistence. Finally, we tested N-acetylated amino sugars supplementation. Our metabolic analysis was not able to distinguish between NAG and N-acetyl-galactosamine (Figure S4A). We thus supplemented PYD with these two N-acetylated amino sugars independently and checked their effect on bacterial persistence (Figures 7E and 7F). We found that NAG supplementation promotes bacterial persistence in a dose-dependent manner (Figures 7E and 7F). This effect is specific to this amino sugar, as supplementation with N-acetyl-galactosamine is ineffective (Figure 7F). We next checked if larval excreta indeed contains free NAG, and in which quantity. To this end, we submitted the excreta to high-performance anion-exchange chromatography with pulsed amperometric detection (Figures S4F, S4G, and 7G). Free NAG was detected in the excreta of starved GF larvae, with an average concentration of 5 mg/L (Figure 7G). This concentration is 400–4,000 times lower than the one sufficient to promote bacterial persistence in our NAG supplementations assays (Figures 7E and 7F). Altogether, our results demonstrate that among all the candidate maintenance factors identified and tested, NAG is the only factor, which on its own is able to sustain bacterial persistence. However, it does so when supplemented in excess in the diet as compared with the concentration found the excreta. Adding NAG alone in a “physiological” concentration range is not sufficient to recapitulate the effect of the excreta. Thus, we posit that the maintenance effect of larval excreta is due to a complex blend of factors, including NAG, acting together to ensure bacterial long-term bacteria persistence.

DISCUSSION

The use of animal models in an integrative research framework has recently gained traction to study the interactions between

microbiota and animal physiology (Leulier et al., 2017). Within this framework, the *Drosophila* model offers unique advantages to shed light on fundamental concepts and characterize the mechanisms involved in animal-commensal bacteria interactions (Erkosar et al., 2013; Lee and Brey, 2013; Ma et al., 2015; Strigini and Leulier, 2016). Until now, the exact mode of association between *Drosophila* and its commensal microbes remain unclear.

Our work demonstrates that there is no long-term bacterial residency in the larval gut: ingestion of axenic food can wipe all traces of symbionts. Therefore, *Drosophila/Lp^{WJL}* association is transient by nature. The larva itself renders the delicate balance of the association more precarious as it actively kills its commensals. This may appear paradoxical, as constant association with live Lp^{WJL} is required to grant a maximum growth benefit to the larvae, but this paradox may reflect a strategy employed by *Drosophila* to preserve its own fitness. In the wild, *Drosophila* larvae feed on rotting fruits and ingest a large variety of microbes, including potential pathogens, over which they must keep a strict control. The *Drosophila* intestine possesses a defensive antimicrobial arsenal, which includes the production of antimicrobial peptides and reactive oxygen species by enterocytes (Buchon et al., 2013a). The copper cells likely belong to this arsenal: indeed, their ablation in *Drosophila* adults carrying a diverse microbiota leads to premature aging and reduced lifespan, probably due to microbiota dysbiosis (Li et al., 2016). Therefore, the acidic pH of the copper cells region should more be seen as a selective defense mechanism against environmental micro-organisms sensitive to low pH, rather than a major part of the digestive process, as acid-less larvae grew normally in conditions where environmental microbes are strictly controlled. In this respect, it is noteworthy that the dominant families of *Drosophila* commensal bacteria are acid-generating bacteria such as Acetobacteraceae and Lactobacillaceae, which tolerate low pH. For these reasons, we do not consider *Drosophila* as a *bona fide* “host” for its symbionts, but rather as a “partner,” conveying and seeding its commensals into the entire nutritional niche, whether it is a rotting fruit in the wild or a food vial in the laboratory. This strategy allows *Drosophila* to get the most out of its association with its symbiotic bacteria at the lowest cost: while keeping a strict control over ingested microbes, it maintains the stability of its association with commensals through the continuous cycles of excretion, seeding of live bacteria, bacterial proliferation on the food, and re-ingestion.

A direct and constant association with live bacteria is required for maximal larval growth gain. Therefore, live bacteria probably elicit a specific response while transiting through the larval gut. In a previous study, we demonstrated that Lp^{WJL} induces the transcription of a set of intestinal peptidases, thus maximizing amino acid uptake and sustaining the activity of the nutrient-sensitive TOR signaling pathway (Erkosar et al., 2015; Storelli et al.,

(F) Evolution of food matrix bacterial load on substrate supplemented with the amino sugars NAG (blue dot) and N-acetyl-galactosamine (red dots). Amino sugars were supplied independently at a concentration of 20 g/L in the fly food. As controls, bacteria were incubated on PYD (black dots).

(G) Quantification of NAG in the excreta of starved larvae by high-performance anion-exchange chromatography with pulsed amperometric detection.

* $p < 0.05$, ** $0.001 < p < 0.01$, *** $0.0001 < p < 0.001$, **** $p < 0.0001$. ns, not significant ($p > 0.1$).

Asterisks above horizontal bars illustrate statistical significance between conditions: **** $p < 0.0001$, *** $0.0001 < p < 0.001$, ** $0.001 < p < 0.01$, * $p < 0.05$, ns, not significant ($p > 0.1$). The exact p value is indicated when approaching statistical significance ($0.05 < p < 0.1$).

2011). Combining our previous and current findings, we propose a model whereby the continuous flow of ingested live *Lp*^{WJL} cells maintains constant peptidases activation, which favors optimal digestion of dietary proteins and amino acid uptake along larval development. This process would then sustain TOR pathway activity and higher larval growth rate. Consistent with this model, forced and continuous transcriptional activation of intestinal peptidases in GF animals partly recapitulates the effect of *Lp*^{WJL} on larval growth (Erkosar et al., 2015). The questions remain as to how bacteria sustain peptidases activation and why living bacteria are strictly required. We showed that peptidase activation in presence of *Lp*^{WJL} relies on the sensing of bacterial cell wall components (Erkosar et al., 2015; Matos et al., 2017). We propose that the constant release of cell wall fragments by live bacteria play a role in the transcriptional activation of these digestive enzymes, and in sustaining growth rates.

The advantages of *Drosophila/Lp*^{WJL} symbiosis may seem, at first sight, biased toward the animal partner. Even though a great fraction of ingested bacteria get killed while transiting through the larval gut, symbiosis asserts an overall beneficial effect for symbionts. In addition to spreading their commensals in the niche, larvae also ensure their long-term maintenance on the substrate. When alone in the food matrix, *Lp*^{WJL} cells rapidly consume essential nutrients until exhaustion, after which their titer drops. In contrast, upon symbiosis, *Lp*^{WJL} titer remains high for a longer period of time. We demonstrate that larvae excrete a complex blend of metabolites, among which NAG, supporting the long-term persistence of *Lp*^{WJL} in the shared habitat. We refer to these metabolites as “maintenance factors” and posit that they act as nutrients for symbionts, which could compensate for the exhaustion of nutritional resources in the substrate and subsequently delay population decay in the niche. Yet, the full complement of factors secreted by larvae required for bacterial maintenance, as well as their mode of action, remain elusive.

Drosophila/Lp^{WJL} symbiosis is facultative by nature. Both partners can exist without each other and symbiosis can be suddenly broken by the ingestion of axenic food (in the lab) or microbes incapable of coping with low pH. In this context, we propose that the flexibility of facultative nutritional mutualism contributes to the ecological success of species with nomadic lifestyles, and therefore changing and often scanty dietary sources. We can postulate that, in order to adopt such lifestyle, nomadic organisms must be able to adapt to various and fluctuating environments without relying on a fixed symbiotic relationship. *L. plantarum* is a highly versatile bacterial species, notably thanks to its vast metabolic repertoire (Martino et al., 2016). The flexible nature of its symbiosis with *Drosophila* (and probably other animals) may have helped retain this potential: keeping extensive metabolic capabilities would preserve *Lp*'s aptitude to thrive in a variety of niches, with and without its animal partner. On the other hand, *Drosophila* larvae would benefit from *Lp*'s ability to efficiently and rapidly colonize the shared niche, especially when excreted in minute amounts. The same reasoning is applicable to *Drosophila*: larvae feed on a variety of fruits, whose microbial composition and nutritional content can change upon maturation and decay. Consequently, *Drosophila* larvae can experience varying nutritional and microbial conditions depending on where and when eggs have been laid. Therefore, it is

advantageous for the larvae not to strictly rely on specific symbionts' functionalities to survive fluctuating dietary conditions. In support of this idea, *Lp* (and probably other commensals) potentiates existing functions in *Drosophila* physiology to accelerate larval development on a poor diet, i.e., by enhancing larval gut peptidase activity (Erkosar et al., 2015; Matos et al., 2017). Therefore, *Drosophila/Lp* symbiosis represents a facultative nutritional mutualism paradigm that may apply to the symbioses between bacterial and animal species with nomadic lifestyles and changing dietary environments.

While a lot of attention has been dedicated to the taxonomic classification of symbiotic bacteria that modulate the physiology of their animal partner, or to the bacterial mechanisms granting physiological benefits to the host, little is known regarding the animal factors that impact bacterial fitness and that are potentially implicated in the perpetuation of animal-bacteria symbiosis. Exploring both sides of symbioses is necessary to gain a more comprehensive understanding of the interaction. A vast number of studies agree on the fact that dysbiosis and impoverishment of the microbiota by disease, diet, or antibiotic treatment are a threat to health (Blaser, 2016; Mondot et al., 2013; Sonnenburg et al., 2016). A more complete understanding of the mechanism of host/bacteria symbioses, and notably the animal factors favoring the growth and persistence of functionally important commensal phyla, would help in designing innovative dietary or prebiotic interventions aimed at maintaining or restoring symbiotic homeostasis. Using a model animal-commensal association upon chronic undernutrition, we now reveal that the animal partner farms its commensals with the secretion of maintenance factors that allow the perpetuation of their association. In parallel, symbionts are required to optimize extraction of dietary nutrients and sustain growth despite chronic undernutrition. Knowing that the phenomenon of commensal-mediated growth promotion is conserved in mammals (Schwarzer et al., 2016), our study paves the way to identify the evolutionary-conserved animal factors required to maintain symbiosis.

STAR★METHODS

Detailed methods are provided in the online version of this paper and include the following:

- KEY RESOURCES TABLE
- CONTACT FOR REAGENT AND RESOURCE SHARING
- EXPERIMENTAL MODEL AND SUBJECT DETAILS
 - *Drosophila* Stocks and Rearing
 - Fly Diets Used in This Study
 - Bacteria Culture and Association with Larvae
 - Sex and Developmental Stage of *Drosophila* Larvae
- METHOD DETAILS
 - Standard Monoassociation in Petri Dishes
 - Monoassociation/Inoculation in Microtubes
 - Delayed Monoassociation
 - Bacterial Load Quantification
 - Larval Longitudinal Length Measurement
 - Larvae Transfer on Axenic Substrates
 - Diet Preincubation with Bacteria
 - Diet Preincubation and Larval Growth Gain

- Diet Preincubation and Bacterial Persistence
- Bacteria and Larval Homogenate Coinoculation
- Bacteria and Larval Excreta Coinoculation
- Spectrometric Measurements
- Metabolite Profiling of Diets and Niches
- Metabolite Profiling of Excreta
- N-acetyl-Glucosamine Quantification
- *L. plantarum*^{WJL} Fluorescent Strains
- Bromophenol Blue and Fluorescent Imaging
- Immunofluorescence
- Live/dead Bacterial Stains
- Transmission Electron Microscopy
- Information Related to Experimental Design
- **QUANTIFICATION AND STATISTICAL ANALYSIS**
- **DATA AND SOFTWARE AVAILABILITY**

SUPPLEMENTAL INFORMATION

Supplemental Information includes four figures and three tables and can be found with this article online at <https://doi.org/10.1016/j.cmet.2017.11.011>.

ACKNOWLEDGMENTS

The authors would like to thank Dali Ma for editing of the manuscript, the Arthro-Tools and PLATIM platforms of the SFR Biosciences (UMS3444/US8) for providing *Drosophila* and imaging facilities, Christelle Boulé and Annie Rivoire from the Centre Technologique des Microstructures attached to the Faculty of Sciences and Technologies of the University Claude Bernard Lyon 1 for TEM, Bruno Lemaître and the Bloomington Stock Centre for fly lines, and the Developmental Studies Hybridoma Bank and Mikio Furuse for antibodies. G.S. and R.M. were funded by fellowships from the "Fondation pour la Recherche Médicale" (FDT20140930923 for G.S. and SFP20140129318 for R.M.). This work was funded by an ERC starting grant (FP7/2007-2013-N°309704). The F.L. lab is supported by the Finovi Foundation and the EMBO Young Investigator Program.

AUTHOR CONTRIBUTIONS

F.L. supervised the work. G.S. and F.L. designed the experiments with input from M. Strigini. G.S., M. Strigini, M. Schwarzer, T.G., and L.B. performed the experiments. R.M. generated the fluorescent bacterial strains. C.D. provided key reagents. G.S., M. Strigini, T.G., and F.L. analyzed the results. F.L. and G.S. wrote the paper with input from M. Strigini.

DECLARATION OF INTERESTS

These authors have no competing interests to declare.

Received: February 27, 2017

Revised: October 9, 2017

Accepted: November 22, 2017

Published: December 28, 2017

REFERENCES

- Baer, R., Bankier, A.T., Biggin, M.D., Deininger, P.L., Farrell, P.J., Gibson, T.J., Hatfull, G., Hudson, G.S., Satchwell, S.C., Seguin, C., et al. (1984). DNA sequence and expression of the B95-8 Epstein-Barr virus genome. *Nature* **310**, 207–211.
- Blaser, M.J. (2016). Antibiotic use and its consequences for the normal microbiome. *Science* **352**, 544–545.
- Blum, J.E., Fischer, C.N., Miles, J., and Handelsman, J. (2013). Frequent replenishment sustains the beneficial microbiome of *Drosophila melanogaster*. *MBio* **4**, e00860–13.
- Broderick, N.A., Buchon, N., and Lemaître, B. (2014). Microbiota-induced changes in *Drosophila melanogaster* host gene expression and gut morphology. *MBio* **5**, e01117–14.
- Buchon, N., Broderick, N.A., and Lemaître, B. (2013a). Gut homeostasis in a microbial world: insights from *Drosophila melanogaster*. *Nat. Rev. Microbiol.* **11**, 615–626.
- Buchon, N., Osman, D., David, F.P., Fang, H.Y., Boquete, J.P., Deplancke, B., and Lemaître, B. (2013b). Morphological and molecular characterization of adult midgut compartmentalization in *Drosophila*. *Cell Rep.* **3**, 1725–1738.
- Chaston, J.M., Newell, P.D., and Douglas, A.E. (2014). Metagenome-wide association of microbial determinants of host phenotype in *Drosophila melanogaster*. *MBio* **5**, e01631–14.
- Chng, W.B., Bou Sleiman, M.S., Schupfer, F., and Lemaître, B. (2014). Transforming growth factor beta/activin signaling functions as a sugar-sensing feedback loop to regulate digestive enzyme expression. *Cell Rep.* **9**, 336–348.
- Collins, S.M., Surette, M., and Bercik, P. (2012). The interplay between the intestinal microbiota and the brain. *Nat. Rev. Microbiol.* **10**, 735–742.
- Douglas, A.E. (2010). *The Symbiotic Habit* (Princeton University Press).
- Dubreuil, R.R. (2004). Copper cells and stomach acid secretion in the *Drosophila* midgut. *Int. J. Biochem. Cell Biol.* **36**, 745–752.
- Erkosar, B., Storelli, G., Defaye, A., and Leulier, F. (2013). Host-intestinal microbiota mutualism: "learning on the fly". *Cell Host Microbe* **13**, 8–14.
- Erkosar, B., Storelli, G., Mitchell, M., Bozonnet, L., Bozonnet, N., and Leulier, F. (2015). Pathogen virulence impedes mutualist-mediated enhancement of host juvenile growth via inhibition of protein digestion. *Cell Host Microbe* **18**, 445–455.
- Flint, H.J., Scott, K.P., Duncan, S.H., Louis, P., and Forano, E. (2012). Microbial degradation of complex carbohydrates in the gut. *Gut Microbes* **3**, 289–306.
- Gilbert, J.A., and Neufeld, J.D. (2014). Life in a world without microbes. *PLoS Biol.* **12**, e1002020.
- Hickey, D.A., Benkel, B.F., Abukashawa, S., and Haus, S. (1988). DNA rearrangement causes multiple changes in gene expression at the amylase locus in *Drosophila melanogaster*. *Biochem. Genet.* **26**, 757–768.
- Hooper, L.V., Midtvedt, T., and Gordon, J.I. (2002). How host-microbial interactions shape the nutrient environment of the mammalian intestine. *Annu. Rev. Nutr.* **22**, 283–307.
- Hoppler, S., and Bienz, M. (1994). Specification of a single cell type by a *Drosophila* homeotic gene. *Cell* **76**, 689–702.
- Huang, J.H., and Douglas, A.E. (2015). Consumption of dietary sugar by gut bacteria determines *Drosophila* lipid content. *Biol. Lett.* **11**, 20150469.
- Lee, W.J., and Brey, P.T. (2013). How microbiomes influence metazoan development: insights from history and *Drosophila* modeling of gut-microbe interactions. *Annu. Rev. Cell Dev. Biol.* **29**, 571–592.
- Lemaître, B., and Miguel-Aliaga, I. (2013). The digestive tract of *Drosophila melanogaster*. *Annu. Rev. Genet.* **47**, 377–404.
- Leulier, F., MacNeil, L.T., Lee, W.J., Rawls, J.F., Cani, P.D., Schwarzer, M., Zhao, L., and Simpson, S.J. (2017). Integrative physiology: at the crossroads of nutrition, microbiota, animal physiology and human health. *Cell Metab.* **25**, 522–534.
- Li, H., Qi, Y., and Jasper, H. (2016). Preventing age-related decline of gut compartmentalization limits microbiota dysbiosis and extends lifespan. *Cell Host Microbe* **19**, 240–253.
- Ma, D., Storelli, G., Mitchell, M., and Leulier, F. (2015). Studying host-microbiota mutualism in *Drosophila*: harnessing the power of gnotobiotic flies. *Biomed. J.* **38**, 285–293.
- Martino, M.E., Bayjanov, J.R., Caffrey, B.E., Wels, M., Joncour, P., Hughes, S., Gillet, B., Kleerebezem, M., van Hijum, S.A., and Leulier, F. (2016). Nomadic lifestyle of *Lactobacillus plantarum* revealed by comparative genomics of 54 strains isolated from different habitats. *Environ. Microbiol.* **18**, 4974–4989.
- Matos, R.C., Gervais, H., Joncour, P., Schwarzer, M., Gillet, B., Martino, M.E., Courtin, P., Hughes, S., Chapot-Chartier, M.-P., and Leulier, F. (2017). D-Alanine esterification of teichoic acids contributes to *Lactobacillus plantarum* mediated intestinal peptidase expression and *Drosophila* growth

- promotion upon chronic undernutrition. *Nat. Microbiol.* <https://doi.org/10.1038/s41564-017-0038-x>.
- McFall-Ngai, M., Hadfield, M.G., Bosch, T.C., Carey, H.V., Domazet-Lošo, T., Douglas, A.E., Dubilier, N., Eberl, G., Fukami, T., Gilbert, S.F., et al. (2013). Animals in a bacterial world, a new imperative for the life sciences. *Proc. Natl. Acad. Sci. USA* **110**, 3229–3236.
- Mondot, S., de Wouters, T., Dore, J., and Lepage, P. (2013). The human gut microbiome and its dysfunctions. *Dig. Dis.* **31**, 278–285.
- Mushegian, A.A., and Ebert, D. (2016). Rethinking "mutualism" in diverse host-symbiont communities. *Bioessays* **38**, 100–108.
- Nicholson, J.K., Holmes, E., Kinross, J., Burcelin, R., Gibson, G., Jia, W., and Pettersson, S. (2012). Host-gut microbiota metabolic interactions. *Science* **336**, 1262–1267.
- Overend, G., Luo, Y., Henderson, L., Douglas, A.E., Davies, S.A., and Dow, J.A. (2016). Molecular mechanism and functional significance of acid generation in the *Drosophila* midgut. *Sci. Rep.* **6**, 27242.
- Phillips, M.D., and Thomas, G.H. (2006). Brush border spectrin is required for early endosome recycling in *Drosophila*. *J. Cell Sci.* **119**, 1361–1370.
- Ryu, J.H., Kim, S.H., Lee, H.Y., Bai, J.Y., Nam, Y.D., Bae, J.W., Lee, D.G., Shin, S.C., Ha, E.M., and Lee, W.J. (2008). Innate immune homeostasis by the homeobox gene caudal and commensal-gut mutualism in *Drosophila*. *Science* **319**, 777–782.
- Schneider, C.A., Rasband, W.S., and Eliceiri, K.W. (2012). NIH Image to ImageJ: 25 years of image analysis. *Nat. Methods* **9**, 671–675.
- Schwarzer, M., Makki, K., Storelli, G., Machuca-Gayet, I., Srutkova, D., Hermanova, P., Martino, M.E., Balmund, S., Hudcovic, T., Heddi, A., et al. (2016). *Lactobacillus plantarum* strain maintains growth of infant mice during chronic undernutrition. *Science* **351**, 854–857.
- Shanbhag, S., and Tripathi, S. (2009). Epithelial ultrastructure and cellular mechanisms of acid and base transport in the *Drosophila* midgut. *J. Exp. Biol.* **212**, 1731–1744.
- Sommer, F., and Backhed, F. (2013). The gut microbiota – masters of host development and physiology. *Nat. Rev. Microbiol.* **11**, 227–238.
- Sonnenburg, E.D., Smits, S.A., Tikhonov, M., Higginbottom, S.K., Wingreen, N.S., and Sonnenburg, J.L. (2016). Diet-induced extinctions in the gut microbiota compound over generations. *Nature* **529**, 212–215.
- Storelli, G., Defaye, A., Erkosar, B., Hols, P., Royet, J., and Leulier, F. (2011). *Lactobacillus plantarum* promotes *Drosophila* systemic growth by modulating hormonal signals through TOR dependent nutrient sensing. *Cell Metab.* **14**, 403–414.
- Storey, J.D., and Tibshirani, R. (2003). Statistical significance for genomewide studies. *Proc. Natl. Acad. Sci. USA* **100**, 9440–9445.
- Strand, M., and Micchelli, C.A. (2011). Quiescent gastric stem cells maintain the adult *Drosophila* stomach. *Proc. Natl. Acad. Sci. USA* **108**, 17696–17701.
- Strigini, M., and Leulier, F. (2016). The role of the microbial environment in *Drosophila* post-embryonic development. *Dev. Comp. Immunol.* **64**, 39–52.
- Wilson, A.C., Ashton, P.D., Calevro, F., Charles, H., Colella, S., Febvay, G., Jander, G., Kushlan, P.F., Macdonald, S.J., Schwartz, J.F., et al. (2010). Genomic insight into the amino acid relations of the pea aphid, *Acyrtosiphon pisum*, with its symbiotic bacterium *Buchnera aphidicola*. *Insect Mol. Biol.* **19** (Suppl 2), 249–258.

STAR★METHODS

KEY RESOURCES TABLE

REAGENT or RESOURCE	SOURCE	IDENTIFIER
Antibodies		
2B10 mouse monoclonal anti-Cut antibody	Developmental Studies Hybridoma Bank	RRID: AB_528186
Rabbit anti-Ssk antibody	Mikio Furuse (Kobe University Graduate School of Medicine)	N/A
Bacterial and Virus Strains		
<i>E. coli</i> : TG1 <i>supE hsd5h thi</i> (Δ lac-proAB) F' (<i>traD36 proAB-lacZ</i> Δ M15)	Baer et al., 1984	N/A
<i>L. plantarum</i> : Lp ^{WJL}	Ryu et al., 2008	N/A
<i>L. plantarum</i> : Lp ^{WJL} -GFP (<i>L. plantarum</i> ^{WJL} carrying pMEC276)	This paper	N/A
<i>L. plantarum</i> : Lp ^{WJL} -mCherry (<i>L. plantarum</i> ^{WJL} carrying pMEC275)	This paper	N/A
Chemicals, Peptides, and Recombinant Proteins		
Inactivated Dried Yeast	Bio Springer	Springaline BA95/0-PW
Cornmeal	Westhove	Farigel maize H1
Agar	VWR	#20768.361
Methylparaben Sodium Salt	MERCK	ref. #106756
Propionic Acid	CARLO ERBA	cref. #409553
Bromophenol Blue sodium salt	Sigma-Aldrich	B5525-5G
Erioglaucine Disodium salt	Sigma-Aldrich	861146-5G
Protease Inhibitor Cocktail	Sigma-Aldrich	P2714
Man, Rogosa and Sharpe (MRS) Broth Medium	Difco	ref. #288110
Man, Rogosa and Sharpe (MRS) Agar Medium	Difco	ref. #288210
N-Acetyl Glucosamine	Sigma-Aldrich	A8625
N-Acetyl Galactosamine	Carl Roth	4114.2
Hypoxanthine	Sigma-Aldrich	H9377
Xanthine	Sigma-Aldrich	X7375-10G
Orotate	Sigma-Aldrich	O2750-10G
Kynurenate	Sigma-Aldrich	K3375-250MG
Tryptophan	Carl Roth	1739.2
Xanthurenate	Sigma-Aldrich	D120804-1G
N-Acetyls erine	Sigma-Aldrich	A2638-1G
N-Acetylvaline	Sigma-Aldrich	8.14599.0050
N-Acetylglutamine	Sigma-Aldrich	A9125-25G
N-Acetylglutamate	Sigma-Aldrich	855642-25G
N-Acetylasparagine	Sigma-Aldrich	441554-1G
N-Acetylglycine	Sigma-Aldrich	A16300-5G
N-Acetylarginine	Sigma-Aldrich	A3133-5G
N-Acetylalanine	Sigma-Aldrich	A4625-1G
N-Acetylhistamine	Sigma-Aldrich	858897-1G
N-Formylmethionine	Sigma-Aldrich	F3377-1G
Critical Commercial Assays		
LIVE/DEAD BacLight Bacterial Viability Kit	Invitrogen	L7007
Deposited Data		
Metabolomic Dataset of Diet +/- <i>L. plantarum</i> ^{WJL}	This paper	Table S1
Metabolomic Dataset of Niche +/- <i>L. plantarum</i> ^{WJL}	This paper	Table S2
Metabolomic Dataset of Live/dead Larvae Excreta	This paper	Table S3

(Continued on next page)

Continued		
REAGENT or RESOURCE	SOURCE	IDENTIFIER
Experimental Models: Organisms/Strains		
<i>D. melanogaster</i> ; <i>y,w</i> (reference strain for this work)		N/A
<i>D. melanogaster</i> : A142::GFP	Buchon et al., 2013b	N/A
<i>D. melanogaster</i> : <i>mex-GAL4</i> (X chromosome insertion)	Phillips and Thomas, 2006	N/A
<i>D. melanogaster</i> : UAS- <i>lab-IR</i>	Bloomington Drosophila Stock Center	26753
<i>y</i> [1] <i>v</i> [1]; <i>P</i> [<i>y</i> + <i>t</i> 7.7] <i>v</i> [+ <i>t</i> 1.8]= <i>TRiP</i> .JF02317}attP2/TM3, <i>Sb</i> [1]		
<i>D. melanogaster</i> : <i>amy</i> ^{null} (deletion of the amylase locus)	Hickey et al., 1988 ; Chng et al., 2014	N/A
Recombinant DNA		
<i>pNZ8148</i> plasmid: Cm ^r , <i>Lactococcus lactis</i> <i>pSH71</i> replicon	MoBiTech	VS-ELV00200-01
<i>pMEC275</i> plasmid: <i>pNZ8148</i> carrying <i>mCherry</i> cDNA codon-optimized for <i>L. plantarum</i> fused to the <i>L. plantarum Pldh</i> constitutive promoter (<i>lactate dehydrogenase</i>)	C.D., unpublished data	N/A
<i>pMEC276</i> plasmid: <i>pNZ8148</i> carrying <i>GFP</i> cDNA codon-optimized for <i>L. plantarum</i> fused to the <i>L. plantarum Pldh</i> constitutive promoter (<i>lactate dehydrogenase</i>)	C.D., unpublished data	N/A
<i>L. plantarum</i> codon-optimized <i>mCherry</i> and <i>GFP</i> genes	Eurogentec (Belgium)	N/A
Software and Algorithms		
ImageJ	NIH Image	https://imagej.net/ImageJ
MetaMorph Microscopy Automation & Image Analysis Software	Molecular devices, USA	N/A
EnspireManager software	PerkinElmer	Ref# 2300-0000
Leica application suite (LAS)	Leica	N/A
Scan 1200 Automatic HD colony counter and Software	Intersciences	Ref. 437 000

CONTACT FOR REAGENT AND RESOURCE SHARING

Further information and requests for resources and reagents should be directed to and will be fulfilled by the Lead Contact, François Leulier (francois.leulier@ens-lyon.fr).

EXPERIMENTAL MODEL AND SUBJECT DETAILS

Drosophila Stocks and Rearing

A detailed list of fly strains and genotypes used for these studies are provided in the [Key Resources Table](#). *Drosophila* stocks are routinely kept at 25°C with 12/12 hrs dark/light cycles (lights on at 1 pm) on a Rich Yeast Diet (RYD) containing 50g/L inactivated yeast. Poor Yeast Diet (PYD) is obtained by reducing the amount of inactivated yeast to 6g/L. Experiments were performed using standard RYD, modified RYD or PYD poured in 55mm petri dishes (≈ 7mL of diet) or 1.5mL microtubes (≈ 100μL of diet). Fresh food was prepared weekly to avoid desiccation, and no yeast paste was added to the medium. Germ Free stocks of different fly strains were established by bleaching and cultivating embryos on fresh RYD supplemented with a cocktail of four antibiotics (RYD-ATB, see below) for at least one generation, and then maintained on RYD-ATB. Axenicity was routinely tested by plating animal lysates on nutrient agar plates. *Drosophila y,w* flies were used as the reference strain in this work.

Fly Diets Used in This Study

Rich Yeast Diet (RYD): 50g inactivated dried yeast, 80g cornmeal, 7.2g Agar, 5.2g methylparaben sodium salt, 4 mL 99% propionic acid for 1 litre.

RYD+ATB: Same composition as RYD but Ampicillin, Kanamycin and Tetracyclin were added at 50μg/mL final concentration and Erythromycin at 15μg/mL final concentration just before pouring fly food.

RYD+Bromophenol Blue (RYD-BB). Same composition as RYD, BB stock solution was added just before pouring fly food to obtain a final concentration of 0.5% v/v. BB stock solution was obtained by dissolving Bromophenol Blue sodium salt in water at a concentration of 5% w/v. Diet used for taking pictures shown on [Figures 1D, 1E, and S1](#).

Poor Yeast Diet (PYD): 6g inactivated dried yeast, 80g cornmeal, 7.2g Agar, 5.2g methylparaben sodium salt, 4 mL 99% propionic acid for 1 litre.

PYD-ATB: Same composition as PYD but Ampicillin, Kanamycin and Tetracyclin were added at 50μg/ml final concentration and Erythromycin at 15μg/ml final concentration just before pouring fly food.

PYD-BB: Same composition as PYD, BB was added just before pouring fly food at the final concentration of 0.05% v/v. The concentration is lower than in RYD-BB to avoid deleterious effects of high BB concentration on both larval growth and bacterial proliferation. Reduced BB concentration was not adequate for taking pictures but sufficient for visual discrimination of the midgut acid zone and subsequent dissections. Diet used in [Figures 1F and 1H](#).

PYD-Erioglaucine Blue (PYD-EB). Same composition as PYD, Erioglaucine disodium salt powder was directly added to fly food just before pouring at the final concentration of 0.8% w/v. Diet used in [Figures 2A, 7C, 7D, and S3D–S3H](#).

PYD + Protease inhibitors: Protease Inhibitor Cocktail or “PIC” (prepared according to the manufacturer’s guidelines) was added just before pouring fly food at the final concentration of 10% v/v. The control diets (“PYD”) used in the same experiments were obtained by adding water (10% v/v) to PYD just before pouring. Diet used in [Figures S3B and S3C](#).

PYD + N-acetyl-Glucosamine (NAG). Fly food is prepared by mixing 6g of inactive dried yeast, 80g of cornmeal, 7.2g of agar, 5.2g of methylparaben sodium salt, 4 mL of 99% propionic acid in 800 mL water. After cooking and before solidification, 40mL of fly food are mixed with 10mL of a solution of N-acetyl-Glucosamine (prepared from a stock solution at 100g NAG/L sterile water) in a 50mL tube. Fly food is then mixed vigorously by vortexing, and then poured in microtubes.

Fly food was poured in petri dishes (diameter=55mm; fly food volume \approx 7ml) to grow larvae used for imaging, larval longitudinal length analysis and larval/gut/gut sections bacterial load. Fly food was poured in 1.5ml microtubes (fly food volume=100 μ l) for diet or niche bacterial load and metabolites profiling. After being poured in microtubes, the flyfood is cut in two after solidification with a sterile Pasteur pipette. This helps homogenous repartition of the inoculum and enhances larval survival at the time of inoculation. Otherwise, the inoculum forms a meniscus on the top of the food, in which young larvae will drown.

Bacteria Culture and Association with Larvae

Lactobacillus plantarum^{WJL} (referred to as *Lp*^{WJL}) is a bacterial strain isolated from adult *Drosophila* midgut ([Ryu et al., 2008](#)). *Lp*^{WJL} was cultivated in Man, Rogosa and Sharpe (MRS) broth medium over night at 37°C without shaking. Precise inoculation and manipulation procedures for each type of experiment are described in more details in “[Method Details](#)”. Briefly, *Lp*^{WJL} inoculation of 55mm petri dishes containing fly food are performed as follows: bacterial cultures are centrifuged and supernatant discarded (for more details about bacterial and centrifugation steps, please see ([Erkosar et al., 2015](#))). Bacterial pellet is then suspended in 1X PBS to have a final OD=0.5, and 300 μ L are inoculated onto the diet (“1X” inoculum, \approx 7 \times 10⁷ CFUs corresponding to \approx 10⁷ CFUs.mL⁻¹ of fly food). Inoculum is homogeneously spread on the food surface, the substrate being previously seeded with 40 freshly laid *Drosophila* eggs. For other inoculum concentrations, the final OD in PBS is adjusted to keep the inoculation volume constant. For Germ Free controls, an equal volume of sterile PBS is inoculated. For inoculation in microtubes containing fly food, bacteria suspensions at OD=5 in PBS and a volume of 3 μ l (\approx 7 \times 10⁶ CFUs corresponding to \approx 7.10⁷ CFUs.mL⁻¹ of fly food) are used as inocula. For inoculation of heat-killed bacteria, the bacterial pellet is suspended in PBS and the bacterial solution is incubated at 60°C for 4 hr. The heat-treated bacteria solution is plated in parallel on MRS agar to check efficient killing. We also plate larval homogenates on MRS agar to validate larval axenicity at the end of the experiments (for Germ Free controls and larvae inoculated with heat-killed bacteria).

Sex and Developmental Stage of *Drosophila* Larvae

For the majority of our experiments, we used early third instar *Drosophila* larvae, unless explicitly written in the figure legends and in the text. The larvae used in these experiments were randomly selected, without distinction between males and females.

METHOD DETAILS

Standard Monoassociation in Petri Dishes

Axenic adults are put overnight in breeding cages to lay eggs on axenic PYD. Fresh axenic embryos are collected the next morning and seeded by pools of 40 on 55mm petri dishes containing fly food. Bacterial resuspensions (see above) or PBS is then spread homogeneously on the substrate and the eggs. Petri dishes are sealed with parafilm and incubated at 25°C until larvae collection.

Monoassociation/Inoculation in Microtubes

This inoculation procedure was followed for niche or diet bacterial load quantification and metabolites profiling ([Figure 6](#)). For niche bacterial load and metabolite profiling, axenic parents are put overnight in breeding cages to lay eggs on axenic PYD. PYD is collected the morning after, flies are removed and eggs incubated an additional day at 25°C to let the larvae hatch. Substrate is then flushed with sterile PBS for larvae collection. Pools of 5 larvae (1DAEL, mostly first instar larvae) are gently sampled by pipetting and deposited at the surface of fly food contained in 1.5mL microtubes. Extra water is then carefully pipetted out from the microtube without removing larvae. Finally, microtubes containing larvae are inoculated with bacterial suspension (see above) and incubated at 25°C. For diet bacterial load quantification and diet metabolite profiling, the fly food contained in 1.5ml microtubes was inoculated with bacterial suspension in the absence of larvae and incubated at 25°C.

Delayed Monoassociation

This procedure was followed for [Figures 5E and 5F](#). Axenic adults are put overnight in breeding cages to lay eggs on PYD. Fresh axenic embryos are collected the morning after and seeded by pools of 40 on 55mm petri dishes containing fly food. PBS is spread homogeneously on the substrate and eggs, and petri dishes are incubated at 25°C until bacterial inoculation. At Day 1, 3 or 5 after egg

laying, bacterial suspension is applied on substrate and larvae, and petri dishes are left at 25°C until larvae collection. Controls for this experiment are larvae inoculated following the standard procedure in 55mm petri dishes.

Bacterial Load Quantification

Larval bacterial loads quantification: larvae are collected from the nutritive substrate and surface-sterilized with a 15 seconds bath in 70% EtOH under manual agitation and rinsed in sterile water. Guts or gut portions are then dissected in PBS if needed. For whole gut samples, portions from the proventriculus (included) and to approximately the 1st half of the hindgut (malpighian tubules removed) are kept. Larvae or dissected guts/gut portions are deposited individually or by pools in 1.5mL microtubes containing 0.75-1mm glass microbeads and 500 μ L of PBS. For niche (diet+larvae) and diet bacterial load quantification, 0.75-1mm glass microbeads and 500 μ L PBS are deposited directly onto PYD (+/- larva(e)) contained in microtubes. In all cases, samples are homogenized with the Precellys 24 tissue homogenizer (Bertin Technologies). Lysates dilutions (in PBS) are plated on MRS agar using the Easyspiral automatic plater (Intersciences). MRS agar plates are then incubated for 24 hr at 37°C. The bacterial concentration in initial homogenates is deduced from CFU count on MRS agar plates, using the automatic colony counter Scan1200 (Intersciences) and its accompanying software.

Larval Longitudinal Length Measurement

Drosophila larvae (pools of $n \geq 20$ animals) are collected, washed in water, killed with a short microwave pulse (900W for 15 sec), transferred on a microscopy slide, and mounted in water. They are pictured with a Leica stereomicroscope M205FA. Individual larval longitudinal length is then quantified using ImageJ software (Schneider et al., 2012).

Larvae Transfer on Axenic Substrates

This procedure was followed for Figures 2A, 3, 5C, and 5D. Figure 2A: pools of 7DAEL *y,w* monoassociated larvae reared on PYD are picked out of the food and washed with a 30 seconds bath in sterile water to get rid of contaminated food remnants on their cuticle. Larvae are then transferred in 55mm petri dishes containing axenic PYD-EB. 2 hr post transfer, larvae with entire blue guts coloration (confirming the ingestion of fresh axenic food and the transit of preceding contaminated alimentary bolus) are collected for bacterial load quantification or washed in water before a second transfer on axenic non-colored PYD. 4 hr after the initial transfer, larvae showing no visible trace of blue dye in their guts (confirming the ingestion of fresh non-colored food) are collected for bacterial load quantification or washed in water before a third and last transfer on axenic PYD-EB. 7 hr after the initial transfer; larvae with blue guts are collected for final bacterial load quantification.

Figures 3A–3F: After being reared on PYD, 7DAEL monoassociated larvae (from different genotypes) are picked out from the food and washed with a 30 seconds bath in sterile water to get rid of contaminated food remnants on their cuticle. Larvae are then transferred individually in 1.5ml microtubes containing axenic PYD. The niche (diet+larva), the substrate alone, or larva alone are then processed for bacterial load quantification.

Figure 3G: Axenic PYD was inoculated with 10^4 CFU/mL of *Lp*^{WJL}, which is approximately the quantity of bacteria found in the food matrix 4 hr post transfer of monoassociated *mex>* larvae (Figure 3F). We inoculated bacteria alone on food matrixes, or in presence of a single *y,w mex>* or *mex>lab-IR* GF larva. We then scored bacterial proliferation after a 20 hr incubation period. Differences (if any) relative to “bacteria alone” controls could be attributable to the presence of larvae. Differences (if any) between larva-containing samples would be attributable to differences in the physiology of larvae of these three different genotypes.

Figures 5C and 5D: *y,w* monoassociated larvae reared on PYD are picked out of the food at different timings post inoculation, surface-sterilized with a 30 seconds bath in 70% Ethanol under agitation and rinsed in sterile water. Surface-sterilized larvae are then transferred by pools of 40 in 55mm petri dishes containing PYD-ATB and incubated at 25°C before collection and measure at 7DAEL.

Diet Preincubation with Bacteria

This procedure was followed for Figures 5A and 5B. 55mm petri dishes containing PYD are inoculated with OD=0.5 and V=300 μ l of bacterial suspension or PBS (for controls). Petri dishes are then sealed with parafilm and incubated for a total of 14 days at 25°C. Bacteria killing is performed at different timings during the incubation. At t=0 (straight after inoculation, for controls (PBS inoculated) and “t=0 HK *Lp*^{WJL}”, at t=7 days, and at t=14 days post-inoculation. Bacteria inactivation is obtained by incubating petri dishes at 60°C for 4 hr before putting them back at 25°C.

Diet Preincubation and Larval Growth Gain

We preincubated diet with bacteria and check the effect on larval growth gain. As controls, axenic embryos are seeded on PBS preincubated substrates (diets originally inoculated with PBS, heat-treated at t=0 and incubated for 14 days at 25°C). They are then inoculated with PBS or OD=0.5, V=300 μ l of bacterial suspension (“Germ Free” and “+ *Lp*^{WJL}” larvae). For the other experimental conditions, axenic embryos are seeded on substrates pre-incubated with bacteria (“t=0, t=7 and t=14 days HK *Lp*^{WJL}”) and inoculated with PBS. Larvae are then incubated on their different substrates for 7 days at 25°C until collection and length measurement. In parallel, we plate larval homogenates on MRS agar (at the time of collection) to confirm the axenicity of larvae reared on diets pre-incubated with bacteria.

Diet Preincubation and Bacterial Persistence

We preincubated diet with bacteria, larvae, or bacteria and larvae and checked the effect on bacterial persistence (Figures 6F and 6G). Microtubes containing 100 μL of PYD are inoculated, in presence or absence of one 1st instar larvae, with OD=5 and V=3 μL of bacterial suspension or PBS. Microtubes are then incubated 7 days at 25°C. After incubation, larvae (when present) are aseptically removed manually, and all microtubes are heat-treated for 4 hr at 60°C for bacteria killing. Microtubes are then allowed to cool down at room temperature before reinoculation with OD=5 and V=3 μL of bacterial suspension, and are incubated at 25°C. The evolution of the bacterial titre over time is followed using the procedures detailed below. As contamination controls, pools of n=3 microtubes containing PYD inoculated with *Lp*^{WJL} or with larvae + *Lp*^{WJL} are incubated for 7 days at 25°C before larval removal and heat-treatment. After cool-down, the microtubes are reinoculated with V=3 μL of PBS and incubated for 11 days at 25°C before crushing and plating undiluted homogenates on MRS agar plates. Absence of colonies on MRS agar plates guarantees the efficiency of heat treatment for bacterial elimination and the absence of parallel contaminations due to handling procedures.

Bacteria and Larval Homogenate Coinoculation

We co-inoculated bacteria with larval homogenates and checked the effect on bacterial persistence (Figures 7A and 7B). For the collection of larval and gut homogenates, Germ Free *y,w* embryos are seeded on RYD-ATB and incubated at 25°C. Larvae are collected at 3 days of age, and crushed in 500 μL PBS by pools of 5. For gut homogenates, pools of 5 aseptically dissected guts are crushed in 500 μL PBS (for further details about homogenization, see above “Bacterial load quantification”). 30 μL of larval and gut homogenates are then co-inoculated “as is” or after heat-treatment at 70°C for 10 min (to disrupt enzymatic activities) with a bacterial suspension of OD=5 and V=3 μL in microtubes containing 100 μL of PYD. The evolution of the bacterial titre on the diet is monitored using the protocol detailed below. As contamination controls, pools of n=3 microtubes containing PYD are inoculated with 30 μL of larvae or gut homogenates and 3 μL of PBS. These microtubes are incubated for 12 days at 25°C before crushing and plating of undiluted homogenates on MRS agar plates. Absence of colonies on MRS agar plates guarantees the absence of parallel contaminations due to handling procedures.

Bacteria and Larval Excreta Coinoculation

We checked the effect of bacterial co-inoculation with larval excreta on bacterial persistence. For the collection of excreta from fed larvae, Germ Free *y,w* embryos are seeded on RYD-ATB and incubated at 25°C. Burrowing feeding larvae are collected at 3 days of age, rinsed 3 times in PBS to remove the food that could stay attached to the cuticle, and bathed by pools of n=10 larvae in 500 μL PBS. They are then incubated in PBS overnight at 25°C in 2mL horizontally disposed Eppendorf tubes. Larvae are then aseptically removed and the PBS used for the bath is kept “as is,” or submitted to heat-treatment (70°C for 10 min) to disrupt enzymatic activities (“heat-treated larval excreta”). Of the PBS used for the bath, 30 μL are co-inoculated with a bacterial suspension (OD=5, V=3 μL , corresponding to $\approx 7 \times 10^6$ CFUs) in microtubes containing 100 μL of PYD, and the evolution of the bacterial titer over time is followed using the protocols detailed below. As contamination controls, pools of n=3 microtubes containing PYD are inoculated with 30 μL of PBS containing larval excreta (heat-treated or not) plus 3 μL of PBS. These microtubes are incubated for 12 days at 25°C before crushing and plating undiluted homogenates on MRS agar plates. Absence of colonies on MRS agar plates guarantees the absence of parallel contaminations due to handling procedures.

To determine the contribution of the alimentary bolus (contained in the gut lumen) to the effect of larval excreta on bacterial persistence, larvae are reared on RYD + ATB for 3 days, and transferred on a non-nutritious agar matrix supplemented with Erioglaucine Blue (at the final concentration of 0.8% w/v) for about 8 hr. Full blue gut coloration confirms the ingestion of non-nutritious agar and the excretion of previous alimentary bolus (Figure S3D, left panel). Larvae efficiently purged (and thus with guts fully colored in blue) are picked and bathed in PBS. Larvae are then aseptically removed, and the PBS remains tainted in blue (Figure S3F, left panel), providing proof of the release of the intestinal contents in the bath. The PBS containing excreta from starved larvae is co-inoculated with bacteria following the same protocols as described above. In parallel, to test if the effect of larval excreta on bacterial persistence is due to cuticle contaminants or compounds that could be released by animals dying from drowning, we collected larvae purged of their alimentary bolus (see above), rinsed them in water, and killed them with a 10 seconds microwave pulse. We then bathed dead animals overnight in PBS and aseptically removed them the day after, as described above. We co-inoculated “dead larvae excreta” with bacteria and followed bacterial titre over time (Figure S3G).

Spectrometric Measurements

We performed spectrometric measurements of larval homogenates and larvae excreta after feeding them RYD supplemented with Erioglaucine Blue (Figures S3D and S3F). Embryos are seeded on RYD supplemented with Erioglaucine Blue (final concentration 0.8% w/v), and at D3AEL, pools of n=5 feeding larvae (with guts fully colored in blue) are collected, rinsed 3 times in PBS to remove dyed food that could stay attached to the external cuticle, and homogenized in PBS following the protocol detailed previously (for further details about homogenization, see above “Bacterial load quantification”). Lysates are then spun at 14,000 rpm on a tabletop centrifuge for 20 min to pellet tissue debris, and 200 μL of the resulting supernatant transferred to a 96-well plate. Absorbance of the homogenates is read at 625 nm. For blank measurements, equivalent lysates were prepared from animals fed RYD without blue dye. A sample's net absorbance is calculated by subtracting the mean blank value to the sample's absorbance obtained with an EnSpire Multimode Plate Reader (PerkinElmer) and its accompanying software EnSpireManager. The same protocol (centrifugation and then measurement) is followed for spectrometric measurement of larval excreta.

Metabolite Profiling of Diets and Niches

Microtubes containing axenic PYD are inoculated with a bacterial suspension or with PBS in presence or absence of $n=5$ freshly hatched larvae, and incubated for 3 days at 25°C. Microtubes are then snap-frozen in liquid nitrogen and stored at -80°C before sending to Metabolon Inc. (www.metabolon.com). For our experiments, 5 biological replicates per condition were generated. Samples are then extracted and prepared for analysis using Metabolon's standard solvent extraction method. The extracted samples are split into equal parts for analysis with GC/MS and LC/MS/MS. Compounds are identified by comparison to library entries of purified standards or recurrent unknown entities.

Metabolite Profiling of Excreta

To collect excreta, we slightly modified the protocol shown in Figure 7C. Notably, erioglaucline blue is added to food instead of agar. We didn't want the excreta to contain high quantities of blue dye post starvation, as this may have a deleterious impact on subsequent analyses. In summary, larvae are reared on RYD + ATB + Erioglaucline Blue (at the final concentration of 0.8% w/v) for 3 days, and transferred to a colour-less, non-nutritious, agar matrix. After a few hours, absence of blue gut coloration confirms the ingestion of non-nutritious agar and the excretion of previous alimentary bolus. Larvae efficiently purged (and thus with color-less guts) are picked and bathed in PBS. "Control excreta" is generated by killing larvae straight after starvation with a short microwave pulse, and infusing them overnight in PBS. Dead and live larvae were then aseptically removed, and the PBS containing excreta was snap-frozen in liquid nitrogen and stored at -80°C before sending to Metabolon Inc. (www.metabolon.com). Metabolite profiling is then performed as described in the paragraph above.

N-acetyl-Glucosamine Quantification

We quantified N-acetyl-Glucosamine (NAG) in the excreta of starved larvae. For this experiment, the excreta are collected as described in the paragraph above, snap-frozen in liquid nitrogen, and stored at -80°C prior to analysis. Samples are then thawed and diluted ten times before being submitted to High-Performance Anion-Exchange Chromatography with Pulsed Amperometric Detection (HPAE-PAD). Prior to samples analyses, we used pure NAG (Sigma-Aldrich) to determine its retention time post-injection and generate standard curves (Figures S4F and S4G).

L. plantarum^{WJL} Fluorescent Strains

Bacterial strains and plasmids used to construct the fluorescent strains are listed in the Key Resources Table. The *L. plantarum* codon-optimized mCherry and GFP genes were synthesized by Eurogentec (Belgium). Both fragments are cloned into pNZ8148 under the control of Pldh (*L. plantarum* constitutive promoter for lactate dehydrogenase). The two resulting constructs are subsequently transformed into *Lp*^{WJL} by electroporation and named *Lp*^{WJL}-GFP and *Lp*^{WJL}-mCherry. The strains are grown at 37°C in MRS medium supplemented with 10 μg/mL of chloramphenicol. We noticed that when incubated at 25°C on PYD containing 10 μg/mL chloramphenicol, *Lp*^{WJL}-GFP and *Lp*^{WJL}-mCherry have a marked tendency to lose their plasmids after a few days, maybe due to the instability of the antibiotic. To circumvent this aspect and for imaging purposes, specific association procedures have been followed. Axenic embryos are seeded on PYD and associated with fluorescent *Lp*^{WJL} according to standard association protocol (see above). At 6 days of age, larvae are re-inoculated with a fresh fluorescent bacteria inoculum of OD=1.5 and V=300 μL. Larvae are then dissected the day after, and gut imaged as described below.

Bromophenol Blue and Fluorescent Imaging

Gut lumen coloration with bromophenol blue (BB): pools of 40 axenic embryos from *y,w*, *mex*-GAL4, UAS-*lab*-IR and *mex*>*lab*-IR genotypes were seeded on RYD-BB diet. Larvae were harvested at the age of 2 or 3 days AEL and dissected. Dissected guts were mounted between slide and coverslip in 80% glycerol/PBS and imaged using LEICA M205 FA stereomicroscope and Leica application suite software.

Immunofluorescence

Pre-wandering mid third instar larvae of the relevant genotypes (*A142::GFP*; *mex*-GAL4>*lab* RNAi or *mex*-GAL4>) were dissected, fixed, and stained according to standard procedures. Briefly, larvae were dissected in ice-cold PBS, fixed for 20 min in PBS-4% formaldehyde, washed in PBS-0.1% TritonX-100 (PBX1), incubated with primary antibodies in PBX1 overnight at 4°C, washed in PBX1, incubated with secondary antibodies and/or DAPI, washed in PBX1, rinsed in PBS, mounted in 80% glycerol-1X PBS. All steps were performed at room temperature (RT) unless otherwise noted. Antibodies: 2B10 mouse monoclonal anti-Cut antibody (1:100) from the Developmental Studies Hybridoma Bank; rabbit anti-Ssk antibody (1:1000), a kind gift of Mikio Furuse (Kobe University Graduate School of Medicine). Mounted guts were observed using a LSM780 confocal microscope (Zeiss, Jena, Germany).

Larvae associated with fluorescent bacteria: Larvae (genotypes: *y,w* or *A142::GFP*) associated with fluorescent *Lp*^{WJL} strains (*Lp*^{WJL}-GFP or *Lp*^{WJL}-mCherry) were dissected and fixed as described above. Alternatively, dissected but unfixed samples were directly placed in a drop of PBS on a Lysine-coated microscope coverslip, the PBS confined in a circle drawn with Super PAP PEN (Electron Microscopy Sciences, Japan). The coverslip was then mounted on a microscope slide, sided by spacers, covered with a wider coverslip and observed at the confocal microscope. For Figures S2A and S2B, dissected and unfixed guts were viewed

at a MF205 stereomicroscope (Leica, Germany) equipped with Leica LAS AF software for image capturing. For Figures 2B, 2C, S2C, and S2D pictures were acquired using a LSM780 confocal microscope (Zeiss, Jena, Germany). Identical parameters of acquisition were applied between the different genotypes.

Live/dead Bacterial Stains

7 days old *yw* and *mex>lab-IR* larvae were transferred on 6g/L yeast extract diet inoculated with *L. plantarum*^{WJL}. We used yeast extract instead of inactive dried yeast to avoid strong background stains due to dead yeast cells in food bolus. Larvae were surface-sterilized with a 30 seconds bath in 70% EtOH under agitation, rinsed in sterile water and their intestines were dissected in a drop of 0.9% NaCl on a microscopic slide. The intestinal cell layer was dilacerated in areas anterior and posterior to the acidic region in order to expose the peritrophic membrane containing food bolus and bacteria. Samples were stained with LIVE/DEAD BacLight Bacterial Viability Kit (Invitrogen), mounted under coverslip and observed under immersion with Leica DM6000 microscope (Leica, Germany). Images were taken by MetaMorph Microscopy Automation & Image Analysis Software (Molecular devices, USA).

Transmission Electron Microscopy

Guts from *Lp*^{WJL}-monoassociated *y,w* larvae (6DAEL) were dissected in ice-cold PBS. Samples were fixed in a mixture of 2% glutaraldehyde in cacodylate buffer 0.075 M pH= 6.9 for 2 hr at RT, embedded in 2% agar and rinsed 3 times in cacodylate buffer. They were post-fixed in 1% Osmium tetroxide, dehydrated in a graded series of ethanol, and embedded in Epon. Sections of 65 nm were cut at a Leica UC7 ultramicrotome, contrasted with uranyl acetate and lead citrate, and observed under a Philips CM120 Transmission Electron Microscope at 80 kV. Image acquisition relied on Digital Micrograph software.

Information Related to Experimental Design

Blinding was not used in the course of our study. No data or subjects were excluded from our analyses.

QUANTIFICATION AND STATISTICAL ANALYSIS

Data representation and statistical analysis were performed using Graphpad PRISM 6 software (www.graphpad.com). For metabolite profiling, The False Detection Rate (FDR) for a given compound is estimated using the q-value (Storey and Tibshirani, 2003). We performed Student's t test with Welch correction to determine if differences in metabolites levels between two conditions are statistically significant. For all the other pairwise comparisons throughout our study, we performed Mann Whitney's test. We applied Kruskal Wallis test to perform statistical analyses of multiple ($n > 2$) conditions. No particular method was used to determine whether the data met assumptions of the statistical approach.

Information about the nature and graphical representation of main figures' data:

Figure 1

(A-C, F and H) The single dots represent mean individual CFU counts calculated from pools of $n=5$ animals or $n=5$ gut portions. The horizontal bar in the dot plot represents the mean value calculated from the set of samples. Whiskers represent upper standard deviation. (B) The single dots represent mean individual CFU counts and mean larval longitudinal length. The mean individual CFU counts were calculated from $n=3$ samples of $n=5$ larvae, the mean larval longitudinal length from a pool of $n > 60$ individual larval measurements. Asterisks illustrate statistical significance between conditions: **: $0.001 < p < 0.01$, *: $p < 0.05$. ns = not significant ($p > 0.05$).

Figure 2

(A) Each dot represents quantification from a single larva. The horizontal line in the dot plot represents mean value. Whiskers represent upper standard deviation. Asterisks represent a statistically significant difference with the initial bacterial burden ($t=0hr$): ***: $0.0001 < p < 0.001$, **: $0.001 < p < 0.01$, *: $p < 0.05$.

Figure 3

(A-F) Each dot represents quantification from a single larva, food matrix or niche. The horizontal line in the dot plot represents the mean value. Whiskers represent upper standard deviation. Asterisks illustrate statistical significance between conditions: **: $0.001 < p < 0.01$, *: $p < 0.05$. ns = not significant ($p > 0.1$). The p value is indicated when approaching statistical significance ($0.05 < p < 0.1$).

Figure 4

(A-C) Each single dot represents an individual larval measurement; the horizontal bar in the dot plot represents the mean value obtained from the pool of individual larval measurements. The whiskers represent the standard deviation. Asterisks illustrate statistical significance between conditions: ****: $p < 0.0001$, *: $p < 0.05$. ns = not significant ($p > 0.1$).

Figure 5

(B, D and F) Each single dot represents an individual larval measurement; the horizontal bar in the dot plot represents the mean value obtained from the pool of individual larval measurements. The whiskers represent the standard deviation. Asterisks illustrate statistical significance between conditions: ****: $p < 0.0001$, *: $p < 0.05$. ns = not significant ($p > 0.1$).

Figure 6

(A, G) Each dot represents a single substrate or niche quantification. The horizontal line in the dot plot represents the mean value. Whiskers represent upper standard deviation. To plot all data points on a log scale, the value 1 has been attributed to samples with no detectable CFU and have been marked "ND" (Not Detected). (B-E, H-K): Each single dot represents the level of a given metabolite in

one of the $n=5$ samples. The horizontal bar in the dot plot represents the mean value obtained from the pool of $n=5$ samples. The whiskers represent the standard deviation. Metabolites not detected in one condition (samples falling below the compound's detection threshold) are marked with ND (not detected). If a metabolite was not detected in GF but detected in Lp^{WJL} inoculated samples, the compound "relative" level was arbitrarily represented by plotting the values obtained after dividing Lp^{WJL} inoculated samples values by the theoretical detection threshold value of this metabolite.

Figure 7

(A,B, D, E and F): Each dot represents quantification from a single food matrix. The horizontal line in the dot plot represents the mean value. Whiskers represent standard deviation. Mann Whitney's test was applied to perform pairwise statistical analyses between conditions. For grouped analysis, significant difference in the distribution of samples at the same date was assayed using Kruskal Wallis test. Asterisks above horizontal bars illustrate statistical significance between conditions: ****: $p<0.0001$, ***: $0.0001<p<0.001$, **: $0.001<p<0.01$, *: $p<0.05$. ns = not significant ($p>0.1$). The exact p value is indicated when approaching statistical significance ($0.05<p<0.1$). (G) Each dot represents the quantification from a single sample. The horizontal line in the dot plot represents the mean value.

DATA AND SOFTWARE AVAILABILITY

Metabolomic datasets are available within the [Supplemental Information](#) as [Tables S1](#), [S2](#), and [S3](#).

Annex III:

How commensal microbes shape the physiology of
Drosophila melanogaster

Review published in Curr Opin Insect Sci 2020 41, 92-99.



ELSEVIER



How commensal microbes shape the physiology of *Drosophila melanogaster*

Theodore Grenier and François Leulier

The interactions between animals and their commensal microbes profoundly influence the host's physiology. In the last decade, *Drosophila melanogaster* has been extensively used as a model to study host-commensal microbes interactions. Here, we review the most recent advances in this field. We focus on studies that extend our understanding of the molecular mechanisms underlying the effects of commensal microbes on *Drosophila*'s development and lifespan. We emphasize how commensal microbes influence nutrition and the intestinal epithelium homeostasis; how they elicit immune tolerance mechanisms and how these physiological processes are interconnected. Finally, we discuss the importance of diets and microbial strains and show how they can be confounding factors of microbe mediated host phenotypes.

Address

Univ Lyon, Institut de Génomique Fonctionnelle de Lyon, Ecole Normale Supérieure de Lyon, Université Claude Bernard Lyon 1, CNRS UMR5242, 46, allée d'Italie, 69007, Lyon, France

Corresponding author: Leulier, François (francois.leulier@ens-lyon.fr)

Current Opinion in Insect Science 2020, 41:92–99

This review comes from a themed issue on **Molecular physiology section**

Edited by **Spencer T Behmer** and **Heiko Vogel**

For a complete overview see the [Issue](#) and the [Editorial](#)

Available online 14th August 2020

<https://doi.org/10.1016/j.cois.2020.08.002>

2214-5745/© 2020 Elsevier Inc. All rights reserved.

Introduction

The gut microbiota comprises all the micro-organisms present in the intestine of an animal. In the early 2000s, culture-independent studies coupled to the advances of genome sequencing began to unravel the complexity of the human gut microbiota. In the following years, studies established that the human gut microbiota composition is associated to a wide spectrum of human pathologies, and play an important role in human biology [1]. The implications of the gut microbiota for its host's immunity, metabolism and physiology has been established in animal models through gnotobiotic experiments [2]. They involve generation of Germ-Free (GF) animals, and re-colonization with defined communities of microbes, allowing direct testing of how microbes impact their host.

Drosophila melanogaster (hereafter referred to as *Drosophila*), a traditional animal model to study host–pathogen interactions, is now increasingly exploited to study host–microbiota interactions. *Drosophila* provides many advantages to study the action of commensal microbes: its microbiota is composed of culturable, extra-cellular aerotolerant bacteria, some of which can be genetically engineered, as well as yeasts and fungi that are largely under explored (we deliberately exclude endosymbionts from this definition). Furthermore, compared to other classical animal models, gnotobiotic flies are relatively easy and cost-effective to generate and maintain in large quantities (Box 1). Finally, decades of research using the *Drosophila* model have yielded a vast panel of genetic tools that facilitates deep mechanistical studies. An important difference with the Mammalian gut microbiota is that commensal bacteria from lab-reared flies do not colonize the *Drosophila* adult [3] or larval gut [4]. Instead, they proliferate on the food and transit with it through the gut. They therefore form a transient microbiota. On the contrary, certain isolates from wild flies can stably colonize the crop of adults [5,6]. Some commensal bacteria from wild flies can therefore form a resident microbiota. Importantly, both resident and transient microbes can influence the physiology of *Drosophila*. Therefore, we believe that association of *Drosophila* with resident or transient commensals is a relevant and valid model to study the microbial influence on host physiology [7].

The use of *Drosophila* as a model for host–microbiota research has been recently extensively reviewed [8]. Here, we review the most recent literature with the focus on the question: how do *Drosophila*'s commensal microbes affect host physiology? We summarize the evidence on the mechanisms underlying the effects of commensal microbes on their host's post-embryonic development and lifespan. Because these mechanisms often involve signaling through immunity pathways, we also review recent findings about how commensal microbes interact with *Drosophila*'s immune system.

Of note, many recent studies focus on the influence of commensal bacteria on adult fly behavior, such as locomotion [9,10], feeding [11,12], social interactions [10,13] and egg-laying [14]. These are important advances but will not be covered in this review.

Commensal microbes and post-embryonic development

Acceleration of *Drosophila* larval development in the presence of commensals was first described almost ten

Box 1 How to study the influence of commensals on *Drosophila* physiology?

Gnotobiotic animals are organisms associated with only a defined and controlled set of microorganisms. In contrast to mice, gnotobiotic *Drosophila* are easy to generate and maintain [54]. One of the widely used protocols consists in dechorionation of embryos with bleach, sterilizing with ethanol, washing in sterile water and transferring to fly food supplemented with a cocktail of broad-range antibiotics to avoid environmental contamination. The Germ-Free (GF) stock can then be maintained on antibiotics for a few months (not more as antibiotics are not neutral to the host). Importantly, the antibiotic cocktail should allow elimination of intracellular symbionts (Tetracyclin to remove *Wolbachia* for example). GF flies can be transferred to the experimental medium, which should not contain antibiotics, to be compared to GF flies associated with a controlled set of microbes. Many studies to date have been focusing on one bacterial species or strain, and thus compare GF condition to mono-association. However, recent work has started tackling the importance of bacterial diversity through poly-associations [55–58].

Gnotobiotic *Drosophila* can be used to investigate the interaction between the microbiota and the host genotype. It is tempting, when a *Drosophila* strain of a given genotype harbors a microbiota that is different from that of another strain, to conclude that the given genotype affects the gut microbiota. However, this conclusion risks to be hasty: two strains of *Drosophila* can harbor different commensals due to different history of having been exposed to different environments, not because of genetic differences. To determine whether the host genotype is responsible for a shift in microbiota composition, one should thus generate GF stocks for both genotypes, associate them with the same controlled microbiota, and follow the evolution of this microbiota over time. Because rearing gnotobiotic *Drosophila* is neither technically challenging nor expensive, our opinion is that studies focusing on the effects of microbiota on *Drosophila* physiology should adopt these standards.

years ago [15,16]. These two studies first demonstrated diminished nutrient sensing-related hormonal signals and developmental delays in GF larvae compared to conventionally reared (CR) larvae. The growth-promoting effect of the microbiota can be recapitulated by mono-association of GF larvae with bacterial strains from the genera *Acetobacter* and *Lactobacillus*. Importantly, the growth-promoting effect of these commensal bacteria is especially marked in nutrient scarcity: microbes do not impact larval growth when larvae are fed a rich diet (Figure 1a). This observation defines an important link between nutrition and commensal microbes.

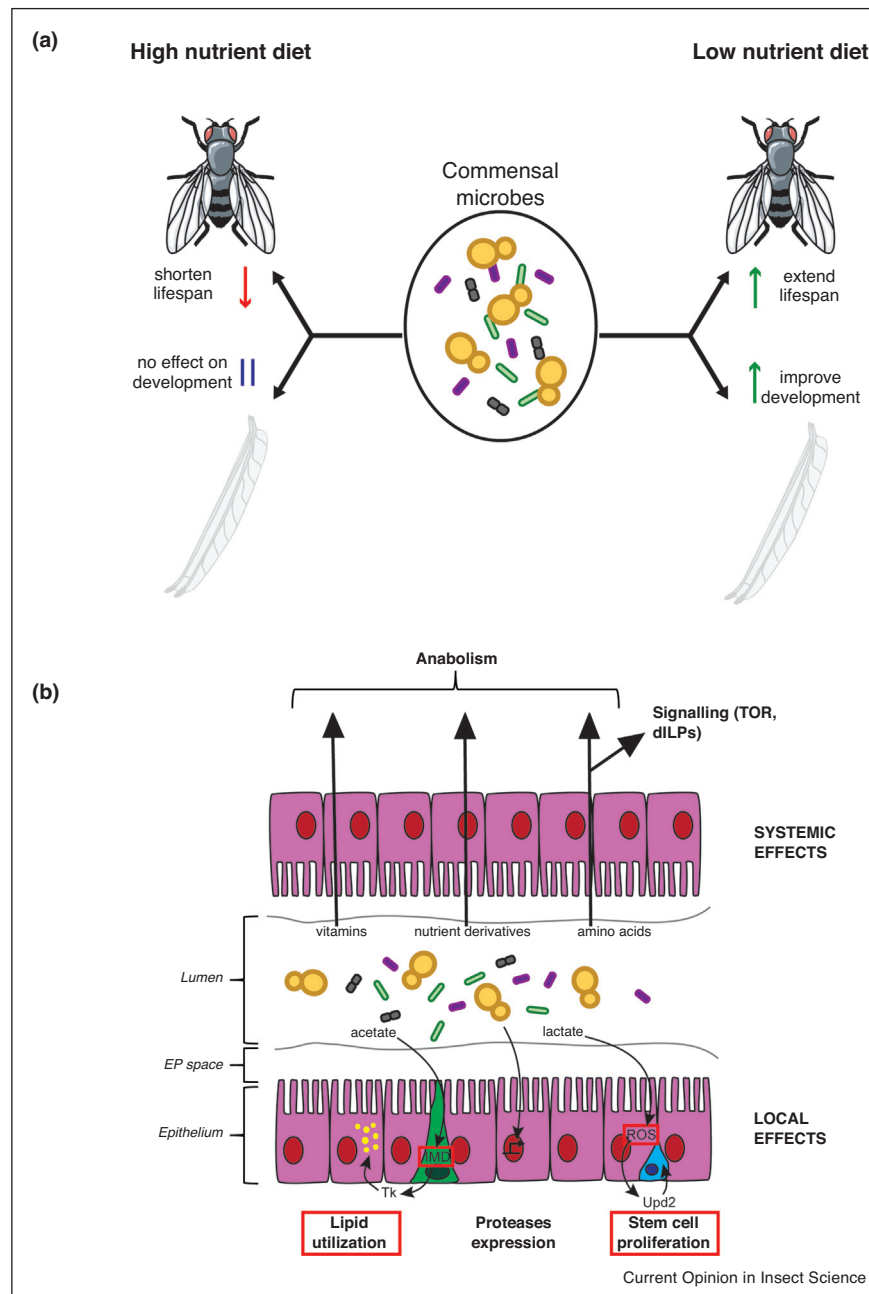
Commensal microbes promote host growth by several mechanisms (Figure 1b). First of all, they improve the host's nutrition by different means. First, *Drosophila* larvae can use the biomass of inert microbes as a source of additional nutrients, especially under nutrient-scarce conditions [4,17]. Secondly, live microbes can improve amino acid absorption by increasing the host's intestinal peptidases activity [18,19]. Finally, commensal microbes actively produce and release essential nutrients that are missing or sparse in the diet. Holidic diets (HDs, i.e. synthetic media composed of chemically pure nutrients) are powerful tools to test the importance of a specific

nutrient on larval development [20]. By removing components from the HD recipe, one can determine the nutrients essential to the developing GF larva, and whether commensal microbes can compensate for the absence or scarcity of such nutrient. Using this strategy, Saninno *et al.* established that *Acetobacter pomorum* and *Acetobacter tropicalis* strains can provide thiamine (vitamin B1) to the *Drosophila* larva [21]. This approach was recently deployed in a more systematic manner: Consuegra *et al.* removed each individual component of the HD one after another, and assessed whether the impact on larval growth due to each drop-out could be compensated by growth-promoting strains of either *A. pomorum* or *Lactobacillus plantarum* (now reclassified as *Lactiplantibacillus plantarum* [22]), two bacteria frequently found in the wild and in laboratory fly stocks. Both bacteria can provide specific essential nutrients to *Drosophila* larvae depending on their biosynthetic capacities. Importantly, commensal microbes may also provide precursors or derivatives of the missing essential nutrients, rather than the nutrient itself [23]. In line with this notion, increased production of *N*-acetylated amino acids by variants of *L. plantarum* obtained through experimental evolution improves larval growth upon nutrient scarcity [24].

In addition to their contribution to host nutrition, commensals influence the development of their host through the action of Reactive Oxygen Species (ROS). While *Drosophila* is under nutritional stress, *L. plantarum* reduces the phenotypic variation in certain developmental traits attributed to cryptic genetic variation by buffering transcriptional variation in developmental genes [25]. As a result, larvae associated with *L. plantarum* vary less in size than GF larvae and adult flies emerging from these *L. plantarum*-associated larvae show less developmental traits abnormalities, such as wing patterning defects. The mechanism of this buffering effect remains elusive, but it can be inhibited by the anti-oxidant *N*-Acetyl Cystein. Moreover, association with *L. plantarum* triggers ROS production in the gut, which leads to increased number of Adult Midgut Precursors (AMPs), the stem cells in the larval gut that give rise to the adult midgut during metamorphosis [26*]. AMPs themselves are in a reducing micro-environment (the 'ROS-sheltered zone'). *L. plantarum* triggers production of ROS in enterocytes, which then secrete the cytokine Unpaired2 (Upd2) that transduces the signal to the AMPs. The authors of this study did not provide detailed information about the impact of this mechanism on larval development, yet they show that *upd2* knock-down in the larval enterocytes leads to reduced adult weight [26*].

Finally, Kamareddine *et al.* reported that acetate produced by commensal bacteria from the *Acetobacter* genus can stimulate the Immune Deficiency (IMD) pathway in a subpopulation of gut cells: the entero-endocrine cells (EE cells) expressing the neuropeptide tachykinin (Tk).

Figure 1



Effects of commensal microbes on *Drosophila* physiology.

(a) Effect of commensal microbes on adult lifespan (top) and larval development (bottom) fed a high nutrient diet (left) or low nutrient diet (right). **(b)** Mechanisms underlying the effects of commensal microbes. Lumen: lumen of the midgut, containing commensal microbes. EP space: ectoperitrophic space between the peritrophic membrane (in grey) and the epithelium. Epithelium: midgut epithelium composed of enterocytes (in pink), enteroendocrine cells (in green) and stem cells (in blue). IMD: Immune Deficient Pathway. ROS: Reactive Oxygen Species. Tk: Tachykinin. Upd2: Unpaired2. Mechanisms that interact with the immune system are framed in red.

We used images from Servier Medical Art, licensed under a Creative Commons Attribution 3.0 Unported License <https://smart.servier.com/>.

Activation of the IMD pathway through PGRP-LC in EE cells leads to mobilization of lipid resources in the nearby enterocytes via Tk paracrine signaling, and ultimately to growth promotion. It remains unclear how acetate activates

PGRP-LC and the IMD pathway in EE cells and how this leads to growth promotion, but this work shows that local signaling of microbial metabolites can have systemic consequences on the host's development [27**].

Commensal microbes and adult lifespan

How commensal microbes influence *Drosophila* lifespan has long been subjected to controversy. Some studies show decreased lifespan in GF flies compared to their CR counterparts [17,28] whereas other studies report the opposite [29,30^{••},31–34]. Interestingly, work from W. Ja's group showed that the influence on *Drosophila* lifespan by a commensal yeast (*Issatchenkia orientalis*) is diet-dependent: *I. orientalis* improves lifespan on a low yeast diet (0,1% yeast extract) [17,35] but reduces lifespan on a high-yeast diet (5% yeast extract) [31]. These observations suggest that the discrepancies among previous studies may be attributed to the nutritional value of the diet (Figure 1a). This issue is common in the field of *Drosophila*-commensal microbes interactions. Of note, discrepancies among studies may as well be attributed to microbial strain-specificity: two strains of the same microbial species can have different effects on their host's physiology. We illustrate these two potential confounding factors, *Drosophila* diet and strain-specificity, with the example of mating preference (Box 2).

Commensal microbes influence *Drosophila* lifespan either positively or negatively by various mechanisms (Figure 1b). On a low-yeast diet, microbial biomass may act as a source of nutrients, especially amino acids, which would compensate for the low nutrient content of the diet and therefore extend lifespan in microbe-associated flies [17,35]. On a high-yeast diet, how commensal microbes reduce lifespan is less clear. This observation seems to depend on the overall quantity of microbes in the gut, which increases as flies age [32], and with the composition of the microbiota [33]. Indeed, treatment of developing larvae with the oxidant *tert*-butyl hydroperoxide (tBH) increases adult lifespan through the loss of *Acetobacter* strains, without affecting other microbiota members such as Lactobacilli [33]. Fan *et al.* suggest that microbe-mediated decrease in lifespan is associated to gut aging. They report that commensal-mediated stimulation of stem cell proliferation in the gut causes hyperplasia, leading to dysfunction of the gut, which reduces lifespan [36]. Accordingly, Iatsenko *et al.* recently reported how a commensal microbe causes hyperplasia in the aging *Drosophila* gut [30^{••}]. *L. plantarum* produces lactate, which can be oxidized to pyruvate in the enterocytes, a reaction accompanied by the reduction of NAD⁺ into NADH. NADH then serves as a substrate for the enzyme Nox to generate ROS, a well-established trigger of intestinal stem cells (ISCs) proliferation [37]. In aging flies, increased amounts of *L. plantarum* in the gut thus leads to ISCs over proliferation, gut hyperplasia and shortening of lifespan. The increase in bacterial loads in the gut of the aging flies has been associated to gut immune senescence, which leads to a weakening of the immune response to both pathogenic and commensal microbes [38]. Similar to Iatsenko *et al.*, Fast *et al.* showed that CR *Drosophila* show reduced lifespan and increased ISCs

Box 2 Diet and microbial strains as confounding factors: the example of mating preference

Because the microbiota of *Drosophila* mostly resides in the fly food, the diet is a central element shaping microbiota composition and therefore greatly affects the outcome of an experiment. One good example is the controversy between a 2010 study and a 2018 study on the topic of mating preference [59–64]. In 2010, Sharon *et al.* from the Rosenberg group demonstrated that flies show mating preference towards flies raised on the same diet [64]. Mating preference was abolished by antibiotic treatment, but restored by association with a *L. plantarum* strain, showing the involvement of commensal microbes. In 2017, Leftwich *et al.* failed to reproduce these results: the same strains of *Drosophila* raised on the same diets do not show mating preference [61]. Antibiotic treatment followed by association with *L. plantarum* did not induce mating preference either. Rosenberg *et al.* replied that the two studies were actually not performed in the same conditions, because before the experiments, flies may not have had the same microbiota [63]. Especially, they pointed the importance of methyparaben (mp), a fungicide used as conservative in fly food, as a confounding factor: Leftwich *et al.* used higher amounts of mp than Sharon *et al.* Independent studies [62,65] reported that the growth of most *Drosophila* commensal bacteria (but not *L. plantarum*) is inhibited by mp at the concentration used by Leftwich *et al.* Of note, variations in the initial microbiota does not explain why Leftwich *et al.* failed to reproduce the effect of *L. plantarum* on mating behavior after antibiotic treatment. The reason may be strain-specificity: two strains of the same species may have distinct effects on the host. More studies are therefore needed to confirm or infirm Sharon *et al.*'s results. This controversy illustrates well the point made in Box 1: because two different labs work with different diets to maintain their stocks, it is very likely that their flies are associated with different strains of commensals even if they originate from the same stock. We believe a good practice in the field would be either to work with standardized consortia of commensals, or to systematically compare different isolates to test for strain specificity of the reported phenotype. Research groups should thus share not only fly lines and media, but also microbial strains.

proliferation compared to their GF counterparts. However, mono-association with *L. plantarum* reduced proliferation of ISCs compared to GF and CR animals [29]. Whether *L. plantarum* increases or decreases ISCs proliferation in the gut may depend on the dietary conditions or on the strain used (see Box 2), but in both cases it seems that the outcome is shortened lifespan.

Chemical interventions with either rapamycin or metformin have been shown to increase lifespan in animal models, including *Drosophila*. Because these drugs are administered in the food, they can directly affect the microbiota. Studies have thus investigated whether their effect on lifespan may be mediated by their action on commensal microbes. Treatment with rapamycin increases lifespan of both CR and GF *Drosophila* [39], which shows that the effect of rapamycin on lifespan is independent of the microbiota. On the contrary, studies on the nematode *Caenorhabditis elegans* have shown that the metformin effects on lifespan requires the presence and the metabolic activity of commensal microbes. Recently, a four-way host–microbe–drug–nutrient screen performed with *C. elegans* and its commensal *Escherichia*

coli [40] demonstrated that: (1) metformin increases expression of the regulator Crp in *E. coli* (2) Crp activation changes the carbon metabolism of *E. coli*, leading especially to production of agmatine, a metabolic derivative of arginine (3) agmatine supplementation to worms extends their lifespan. The authors report that this mechanism might be conserved in *Drosophila* as metformin extends *Drosophila* lifespan through the action of *E. coli* Crp and the agmatine molecule alone can slightly extend flies' lifespan [40]. Further studies are needed to confirm this in fly models associated with conventional commensals.

Commensal microbes and immune signaling

One central feature of *Drosophila*'s immune system is its ability to directly sense bacterial cell wall components (peptidoglycans) through Peptidoglycan Recognition Proteins (PGRP-LC, PGRP-LE and PGRP-SA) and activate two canonical immune pathways: Toll and IMD [41]. Infection by pathogenic bacteria triggers a systemic activation of these pathways and elicit a strong immune response, whereas association with commensal bacteria does not [41]. Such immune tolerance to commensal bacteria primarily occurs in the intestine and relies at least partly on the regulation of peptidoglycan sensing and signaling through the IMD pathway by additional members of the PGRP family [41]. PGRP-SC1/2 [42,43] and PGRP-LB [44^{*}] mediate *Drosophila* immune tolerance mechanisms in the intestine. Recently, Iatsenko *et al.* established that PGRP-SD, another PGRP family member that enhances peptidoglycan mediated activation of the IMD pathway [45], stimulates the expression of PGRP-LB and PGRP-SCs in the intestine in response to the microbiota and therefore contributes to establishing intestinal immune tolerance to commensal bacteria [30^{**}].

Drosophila immunity genes strongly interact with the effects of commensal microbes on lifespan and development. *PGRP-SD* mutants exhibit overproliferation of commensal bacteria in the intestines, intestinal dysplasia and reduced lifespan [30^{**}]. These findings reinforce the notion that the intestinal immune tolerance mechanisms to commensal bacteria are critical to maintain intestinal homeostasis and lifespan. Moreover, signaling through immune pathways contributes to the acceleration of larval development by commensal microbes via the activity or sensing of different microbial cues: acetate [15,27^{**}], peptidoglycans [18], or additional molecular motifs in the bacterial cell walls [19]. Another important facet of the *Drosophila* intestinal immune system is the production of ROS by enterocytes as antimicrobial effectors and signaling molecules triggering intestinal repair. Both pathogens [46,47] and commensal microbes [26^{*},30^{**}] trigger intestinal ROS production, albeit to different levels and by different enzymes. In addition, infection by the pathogen *Erwinia carotovora* triggers increase lipid utilization by the enterocytes [46], a phenomenon also

recently identified in response to commensal bacteria [27^{**}]. Therefore, similar mechanisms (microbial cues sensing and IMD signaling, ROS production, lipid utilization) are engaged in response to pathogens or commensal microbes, but with different outcomes.

This raises the question of how the host may distinguish between infection by a pathogen and association with commensal microbes. In the fly gut, both pathogens and commensals release peptidoglycans. Immune pathways may be sensitive to the quantity of peptidoglycans: over proliferation of pathogens may lead to high amounts of peptidoglycans, triggering an immune response, whereas commensal microbes produce lower amounts of peptidoglycans, allowing tolerance. The localization of the peptidoglycans (in the gut lumen or in the hemolymph) may also be of importance: accumulation of microbiota-derived peptidoglycans in the hemolymph is precluded by active filtering by nephrocytes, which prevents systemic immune response against the microbiota [48]. Cell-type specific response in the gut may help to distinguish commensal microbes and pathogens: for example, IMD pathway activation in enterocytes leads to immune response, whereas IMD pathway activation in EE cells causes lipid utilization in enterocytes and improved anabolic growth [27^{**}]. This suggests that EE cells may be specialized in sensing the microbiota [49]. Finally, the *Drosophila* immune system can recognize metabolites that are specific to pathogens, and absent from commensals. Uracil, which is only produced by opportunistic pathogens as a by-product of quorum-sensing [50^{**}] triggers a Duox-dependant release of ROS through Hedgehog-induced signaling upon infection [51,52].

Conclusion

Here we have summarized recent findings depicting how commensal microbes modulate *Drosophila*'s post-embryonic development and lifespan (Figure 1a), as well as some of the mechanisms underlying the outcome (Figure 1b). The impact of commensals on development and lifespan depends strongly on the nutrient content of the diet, which can now be analyzed using an online tool, the *Drosophila* Dietary Composition Calculator [53]: on a nutrient poor diet, commensal microbes accelerate development and extend lifespan, whereas on a nutrient rich diet, they have little effect on development and shorten lifespan. At the cellular level, a parallel can be drawn between the effects of commensal microbes on lifespan and on development. Indeed, in both processes, commensal microbes stimulate the proliferation of progenitor cells: AMPs in larvae [26^{*}] and ISCs in adults [30^{**}] by triggering ROS production. Similarly, nutrient sensing pathways (TOR and insulin receptor signaling) can be activated by commensal microbes at both stages through the provision or increased absorption of nutrients [17,23]. This leads to both faster development and faster aging. Hence, commensal microbes seem to favor a 'live fast, die

young' host lifestyle [33]. We posit that this lifestyle is overall beneficial to the flies' fitness: in nature, the selection pressure on fast development must be strong, because it allows earlier reproduction. On the contrary, the selection pressure on a long lifespan must be weak, as fecundity sharply decreases with age and flies may often die prematurely due to predation or infections.

Sensing the commensal microbes by the immune system is also paramount to trigger and regulate beneficial host responses to commensal microbes. The influence of commensal microbes on *Drosophila* physiology therefore relies on intricate nutritional, metabolic and immune inputs. Dissecting these intertwined mechanisms constitute an exciting perspective to the study of the functional consequences of *Drosophila*-commensal microbes interactions. Because nutrient sensing, metabolic and immune pathways are evolutionary conserved, such mechanisms will provide general hypotheses to test in other animals.

Conflict of interest statement

Nothing declared.

Acknowledgements

Research in F.L.'s lab is supported by the 'Fondation pour la Recherche Médicale' (« Equipe FRM DEQ20180339196) and the Scientific Breakthrough Project 'Microbehave' from the Université de Lyon. T.G. is funded by a Ph.D fellowship from ENS de Lyon.

References and recommended reading

Papers of particular interest, published within the period of review, have been highlighted as:

- of special interest
- of outstanding interest

1. Gilbert JA, Blaser MJ, Caporaso JG, Jansson JK, Lynch SV, Knight R: **Current understanding of the human microbiome.** *Nat Med* 2018, **24**:392-400 <http://dx.doi.org/10.1038/nm.4517>.
2. Leulier F, MacNeil LT, Lee W, Rawls JF, Cani PD, Schwarzer M, Zhao L, Simpson SJ: **Integrative physiology: at the crossroads of nutrition, microbiota, animal physiology, and human health.** *Cell Metab* 2017, **25**:522-534 <http://dx.doi.org/10.1016/j.cmet.2017.02.001>.
3. Blum JE, Fischer CN, Miles J, Handelsman J: **Frequent replenishment sustains the beneficial microbiome of *Drosophila melanogaster*.** *mBio* 2013, **4** <http://dx.doi.org/10.1128/mBio.00860-13> e00860-00813.
4. Storelli G, Strigini M, Grenier T, Bozonnet L, Schwarzer M, Daniel C, Matos R, Leulier F: ***Drosophila* perpetuates nutritional mutualism by promoting the fitness of its intestinal symbiont *Lactobacillus plantarum*.** *Cell Metab* 2018, **27**:362-377.e8 <http://dx.doi.org/10.1016/j.cmet.2017.11.011>.
5. Obadia B, Güvener ZT, Zhang V, Ceja-Navarro JA, Brodie EL, Ja WW, Ludington WB: **Probabilistic invasion underlies natural gut microbiome stability.** *Curr Biol* 2017, **27**:1999-2006.e8 <http://dx.doi.org/10.1016/j.cub.2017.05.034>.
6. Pais IS, Valente RS, Sporniak M, Teixeira L: ***Drosophila melanogaster* establishes a species-specific mutualistic interaction with stable gut-colonizing bacteria.** *PLoS Biol* 2018, **16** <http://dx.doi.org/10.1371/journal.pbio.2005710>.
- Pais *et al.* isolate strains of commensals from wild flies that stably colonize the adult crop and persist inside the host.
7. Ma D, Leulier F: **The importance of being persistent: the first true resident gut symbiont in *Drosophila*.** *PLoS Biol* 2018, **16**: e2006945 <http://dx.doi.org/10.1371/journal.pbio.2006945>.
8. Douglas AE: **The *Drosophila* model for microbiome research.** *Lab Anim (NY)* 2018, **47**:157-164 <http://dx.doi.org/10.1038/s41684-018-0065-0>.
9. Schretter CE, Vielmetter J, Bartos I, Marka Z, Marka S, Argade S, Mazmanian SK: **A gut microbial factor modulates locomotor behaviour in *Drosophila*.** *Nature* 2018, **563**:402 <http://dx.doi.org/10.1038/s41586-018-0634-9>.
10. Selkrig J, Mohammad F, Ng SH, Chua JY, Tumkaya T, Ho J, Chiang YN, Rieger D, Pettersson S, Helfrich-Förster C *et al.*: **The *Drosophila* microbiome has a limited influence on sleep, activity, and courtship behaviors.** *Sci Rep* 2018, **8** <http://dx.doi.org/10.1038/s41598-018-28764-5>.
11. Leitão-Gonçalves R, Carvalho-Santos Z, Francisco AP, Fioreze GT, Anjos M, Baltazar C, Elias AP, Itskov PM, Piper MDW, Ribeiro C: **Commensal bacteria and essential amino acids control food choice behavior and reproduction.** *PLoS Biol* 2017, **15** <http://dx.doi.org/10.1371/journal.pbio.2000862>.
12. Qiao H, Keesey IW, Hansson BS, Knaden M: **Gut microbiota affects development and olfactory behavior in *Drosophila melanogaster*.** *J Exp Biol* 2019, **222** <http://dx.doi.org/10.1242/jeb.192500>.
13. Chen K, Luan X, Liu Q, Wang J, Chang X, Snijders AM, Mao J-H, Secombe J, Dan Z, Chen J-H *et al.*: ***Drosophila* histone demethylase KDM5 regulates social behavior through immune control and gut microbiota maintenance.** *Cell Host Microbe* 2019, **25**:537-552.e8 <http://dx.doi.org/10.1016/j.chom.2019.02.003>.
14. Kurz CL, Charroux B, Chaduli D, Viallat-Lieutaud A, Royet J: **Peptidoglycan sensing by octopaminergic neurons modulates *Drosophila* oviposition.** *eLife* 2017, **6**:e21937 <http://dx.doi.org/10.7554/eLife.21937>.
15. Shin SC, Kim S-H, You H, Kim B, Kim AC, Lee K-A, Yoon J-H, Ryu J-H, Lee W-J: ***Drosophila* microbiome modulates host developmental and metabolic homeostasis via insulin signaling.** *Science* 2011, **334**:670-674 <http://dx.doi.org/10.1126/science.1212782>.
16. Storelli G, Defaye A, Erkosar B, Hols P, Royet J, Leulier F: ***Lactobacillus plantarum* promotes *Drosophila* systemic growth by modulating hormonal signals through TOR-dependent nutrient sensing.** *Cell Metab* 2011, **14**:403-414 <http://dx.doi.org/10.1016/j.cmet.2011.07.012>.
17. Keebaugh ES, Yamada R, Obadia B, Ludington WB, Ja WW: **Microbial quantity impacts *Drosophila* nutrition, development, and lifespan.** *iScience* 2018, **4**:247-259 <http://dx.doi.org/10.1016/j.isci.2018.06.004>.
18. Erkosar B, Storelli G, Mitchell M, Bozonnet L, Bozonnet N, Leulier F: **Pathogen virulence impedes mutualist-mediated enhancement of host juvenile growth via inhibition of protein digestion.** *Cell Host Microbe* 2015, **18**:445-455 <http://dx.doi.org/10.1016/j.chom.2015.09.001>.
19. Matos RC, Schwarzer M, Gervais H, Courtin P, Joncour P, Gillet B, Ma D, Bulteau A-L, Martino ME, Hughes S *et al.*: **D-alanylation of teichoic acids contributes to *Lactobacillus plantarum*-mediated *Drosophila* growth during chronic undernutrition.** *Nat Microbiol* 2017, **2**:1635-1647 <http://dx.doi.org/10.1038/s41564-017-0038-x>.
20. Piper MD: **Using artificial diets to understand the nutritional physiology of *Drosophila melanogaster*.** *Curr Opin Insect Sci* 2017, **23**:104-111 <http://dx.doi.org/10.1016/j.cois.2017.07.014>.
21. Sannino DR, Dobson AJ, Edwards K, Angert ER, Buchon N: **The *Drosophila melanogaster* gut microbiota provisions thiamine to its host.** *mBio* 2018, **9** <http://dx.doi.org/10.1128/mBio.00155-18> e00155-e00118.
22. Zheng J, Wittouck S, Salvetti E, Franz CMAP, Harris HMB, Mattarelli P, O'Toole PW, Pot B, Vandamme P, Walter J *et al.*: **A taxonomic note on the genus *Lactobacillus*: description of 23 novel genera, emended description of the genus *Lactobacillus* beijerinck 1901, and union of *Lactobacillaceae***

- and *Leuconostocaceae*. *Int J Syst Evol Microbiol* 2020, **70**(4) <http://dx.doi.org/10.1099/ijsem.0.004107>.
23. Consuegra J, Grenier T, Baa-Puyoulet P, Rahioui I, Akherraz H, Gervais H, Parisot N, da Silva P, Charles H, Calevro F, Leulier F: **Drosophila-associated bacteria differentially shape the nutritional requirements of their host during juvenile growth.** *PLoS Biol* 2020, **18**:e3000681 <http://dx.doi.org/10.1371/journal.pbio.3000681>.
 24. Martino ME, Joncour P, Leenay R, Gervais H, Shah M, Hughes S, Gillet B, Beisel C, Leulier F: **Bacterial adaptation to the host's diet is a key evolutionary force shaping *Drosophila-Lactobacillus* symbiosis.** *Cell Host Microbe* 2018, **24**:109-119.e6 <http://dx.doi.org/10.1016/j.chom.2018.06.001>.
 25. Ma D, Bou-Sleiman M, Joncour P, Indelicato C-E, Frochoux M, Braman V, Litovchenko M, Storelli G, Deplancke B, Leulier F: **Commensal gut bacteria buffer the impact of host genetic variants on *Drosophila* developmental traits under nutritional stress.** *iScience* 2019, **19**:436-447 <http://dx.doi.org/10.1016/j.isci.2019.07.048>.
 26. Reedy AR, Luo L, Neish AS, Jones RM: **Commensal microbiota-induced redox signaling activates proliferative signals in the intestinal stem cell microenvironment.** *Development* 2019, **146** <http://dx.doi.org/10.1242/dev.171520>.
 - Reedy *et al.* show that *L. plantarum* triggers ROS production in enterocytes, but not in stem cells. The signal is then transduced to the stem cells through Upd2.
 27. Kamareddine L, Robins WP, Berkey CD, Mekalanos JJ, ●● Watnick PI: **The *Drosophila* immune deficiency pathway modulates enteroendocrine function and host metabolism.** *Cell Metab* 2018, **28**:449-462.e5 <http://dx.doi.org/10.1016/j.cmet.2018.05.026>.
 - Kamareddine *et al.* show that acetate produced by commensals can activate the IMD pathway in enteroendocrine cells, which leads to lipid mobilization in neighboring enterocytes and increases systemic growth.
 28. Brummel T, Ching A, Seroude L, Simon AF, Benzer S: ***Drosophila* lifespan enhancement by exogenous bacteria.** *PNAS* 2004, **101**:12974-12979 <http://dx.doi.org/10.1073/pnas.0405207101>.
 29. Fast D, Duggal A, Foley E: **Monoassociation with *Lactobacillus plantarum* disrupts intestinal homeostasis in adult *Drosophila melanogaster*.** *mBio* 2018, **9** <http://dx.doi.org/10.1128/mBio.01114-18>.
 30. Iatsenko I, Boquete J-P, Lemaitre B: **Microbiota-derived lactate ●● activates production of reactive oxygen species by the intestinal NADPH oxidase Nox and shortens *Drosophila* lifespan.** *Immunity* 2018, **49**:929-942.e5 <http://dx.doi.org/10.1016/j.immuni.2018.09.017>.
 - Iatsenko *et al.* show that lactate produced by the commensal *Lactobacillus plantarum* can trigger ROS production in enterocytes. Moreover, they identify a novel role of PGRP-SD in commensal tolerance.
 31. Keebaugh ES, Yamada R, Ja WW: **The nutritional environment influences the impact of microbes on *Drosophila melanogaster* life span.** *mBio* 2019, **10** <http://dx.doi.org/10.1128/mBio.00885-19>.
 32. Lee H-Y, Lee S-H, Lee J-H, Lee W-J, Min K-J: **The role of commensal microbes in the lifespan of *Drosophila melanogaster*.** *Aging (Albany NY)* 2019, **11**:4611-4640 <http://dx.doi.org/10.18632/aging.102073>.
 33. Obata F, Fons CO, Gould AP: **Early-life exposure to low-dose oxidants can increase longevity via microbiome remodelling in *Drosophila*.** *Nat Commun* 2018, **9**:975 <http://dx.doi.org/10.1038/s41467-018-03070-w>.
 34. Resnik-Docampo M, Sauer V, Schinaman JM, Clark RI, Walker DW, Jones DL: **Keeping it tight: the relationship between bacterial dysbiosis, septate junctions, and the intestinal barrier in *Drosophila*.** *Fly (Austin)* 2018, **12**:34-40 <http://dx.doi.org/10.1080/19336934.2018.1441651>.
 35. Yamada R, Deshpande SA, Bruce KD, Mak EM, Ja WW: **Microbes promote amino acid harvest to rescue undernutrition in *Drosophila*.** *Cell Rep* 2015, **10**:865-872 <http://dx.doi.org/10.1016/j.celrep.2015.01.018>.
 36. Fan X, Gaur U, Yang M: **Intestinal homeostasis and longevity: *Drosophila* gut feeling.** *Adv Exp Med Biol* 2018, **1086**:157-168 http://dx.doi.org/10.1007/978-981-13-1117-8_10.
 37. Jones RM, Luo L, Ardita CS, Richardson AN, Kwon YM, Mercante JW, Alam A, Gates CL, Wu H, Swanson PA *et al.*: **Symbiotic lactobacilli stimulate gut epithelial proliferation via Nox-mediated generation of reactive oxygen species.** *EMBO J* 2013, **32**:3017-3028 <http://dx.doi.org/10.1038/emboj.2013.224>.
 38. Min K-J, Tatar M: **Unraveling the molecular mechanism of immunosenescence in *Drosophila*.** *Int J Mol Sci* 2018, **19** <http://dx.doi.org/10.3390/ijms19092472>.
 39. Schinaman JM, Rana A, Ja WW, Clark RI, Walker DW: **Rapamycin modulates tissue aging and lifespan independently of the gut microbiota in *Drosophila*.** *Sci Rep* 2019, **9**:7824 <http://dx.doi.org/10.1038/s41598-019-44106-5>.
 40. Pryor R, Norvaisas P, Marinos G, Best L, Thingholm LB, Quintaneiro LM, De Haes W, Esser D, Waschina S, Lujan C *et al.*: **Host-microbe-drug-nutrient screen identifies bacterial effectors of metformin therapy.** *Cell* 2019, **178**:1299-1312.e29 <http://dx.doi.org/10.1016/j.cell.2019.08.003>.
 41. Capo F, Charroux B, Royet J: **Bacteria sensing mechanisms in *Drosophila* gut: local and systemic consequences.** *Dev Comp Immunol* 2016, **64**:11-21 <http://dx.doi.org/10.1016/j.dci.2016.01.001>.
 42. Guo L, Karpac J, Tran SL, Jasper H: **PGRP-SC2 promotes gut immune homeostasis to limit commensal dysbiosis and extend lifespan.** *Cell* 2014, **156**:109-122 <http://dx.doi.org/10.1016/j.cell.2013.12.018>.
 43. Paredes JC, Welchman DP, Poidevin M, Lemaitre B: **Negative regulation by amidase PGRPs shapes the *Drosophila* antibacterial response and protects the fly from innocuous infection.** *Immunity* 2011, **35**:770-779 <http://dx.doi.org/10.1016/j.immuni.2011.09.018>.
 44. Charroux B, Capo F, Kurz CL, Peslier S, Chaduli D, Viallat-Lieutaud A, Royet J: **Cytosolic and secreted peptidoglycan-degrading enzymes in *Drosophila* respectively control local and systemic immune responses to microbiota.** *Cell Host Microbe* 2018, **23**:215-228.e4 <http://dx.doi.org/10.1016/j.chom.2017.12.007>.
 - Charroux *et al.* discover a new function for the PGRP-LB locus: cytosolic PGRP-LB in enterocytes prevent peptidoglycans produced by commensals from reaching the hemolymph and activating a systemic immune response.
 45. Iatsenko I, Kondo S, Mengin-Lecreux D, Lemaitre B: **PGRP-SD, an extracellular pattern-recognition receptor, enhances peptidoglycan-mediated activation of the *Drosophila* IMD pathway.** *Immunity* 2016, **45**:1013-1023 <http://dx.doi.org/10.1016/j.immuni.2016.10.029>.
 46. Lee K-A, Cho K-C, Kim B, Jang I-H, Nam K, Kwon YE, Kim M, Hyeon DY, Hwang D, Seol J-H, Lee W-J: **Inflammation-modulated metabolic reprogramming is required for DUOX-dependent gut immunity in *Drosophila*.** *Cell Host Microbe* 2018, **23**:338-352.e5 <http://dx.doi.org/10.1016/j.chom.2018.01.011>.
 47. You H, Lee WJ, Lee W-J: **Homeostasis between gut-associated microorganisms and the immune system in *Drosophila*.** *Curr Opin Immunol* 2014, **30**:48-53 <http://dx.doi.org/10.1016/j.coi.2014.06.006>.
 48. Troha K, Nagy P, Pivovar A, Lazzaro BP, Hartley PS, Buchon N: **Nephrocytes remove microbiota-derived peptidoglycan from systemic circulation to maintain immune homeostasis.** *Immunity* 2019, **51**:625-637.e3 <http://dx.doi.org/10.1016/j.immuni.2019.08.020>.
 49. Watnick PI, Jugder B-E: **Microbial control of intestinal homeostasis via enteroendocrine cell innate immune signaling.** *Trends Microbiol* 2020, **28**:141-149 <http://dx.doi.org/10.1016/j.tim.2019.09.005>.
 50. Kim E-K, Lee K-A, Hyeon DY, Kyung M, Jun K-Y, Seo SH, ●● Hwang D, Kwon Y, Lee W-J: **Bacterial nucleoside catabolism controls quorum sensing and commensal-to-pathogen transition in the *Drosophila* gut.** *Cell Host Microbe* 2020, **27**:345-357.e6 <http://dx.doi.org/10.1016/j.chom.2020.01.025>.

Kim *et al.* show that opportunistic pathogens, but not commensals, produce uracil as a byproduct of quorum-sensing. Uracil production is necessary and sufficient to make the transition from opportunistic pathogen to commensal.

51. Lee K-A, Kim B, Bhin J, Kim DH, You H, Kim E-K, Kim S-H, Ryu J-H, Hwang D, Lee W-J: **Bacterial uracil modulates Drosophila DUOX-dependent gut immunity via hedgehog-induced signaling endosomes.** *Cell Host Microbe* 2015, **17**:191-204 <http://dx.doi.org/10.1016/j.chom.2014.12.012>.
52. Lee K-A, Kim S-H, Kim E-K, Ha E-M, You H, Kim B, Kim M-J, Kwon Y, Ryu J-H, Lee W-J: **Bacterial-derived uracil as a modulator of mucosal immunity and gut-microbe homeostasis in Drosophila.** *Cell* 2013, **153**:797-811 <http://dx.doi.org/10.1016/j.cell.2013.04.009>.
53. Lesperance DNA, Broderick NA: **Meta-analysis of diets used in Drosophila microbiome research and introduction of the Drosophila dietary composition calculator (DDCC).** *G3 (Bethesda)* 2020, **10**:2207-2211 <http://dx.doi.org/10.1534/g3.120.401235>.
54. Kietz C, Pollari V, Meinander A: **Generating germ-free Drosophila to study gut-microbe interactions: protocol to rear Drosophila under axenic conditions.** *Curr Protoc Toxicol* 2018, **77**:e52 <http://dx.doi.org/10.1002/cptx.52>.
55. Aranda-Díaz A, Obadia B, Dodge R, Thomsen T, Hallberg ZF, Güvener ZT, Ludington WB, Huang KC: **Bacterial interspecies interactions modulate pH-mediated antibiotic tolerance.** *eLife* 2020, **9** <http://dx.doi.org/10.7554/eLife.51493>.
56. Consuegra J, Grenier T, Akherraz H, Rahioui I, Gervais H, da Silva P, Leulier F: **Metabolic cooperation among commensal bacteria supports Drosophila juvenile growth under nutritional stress.** *iScience* 2020, **23**:101232 <http://dx.doi.org/10.1016/j.isci.2020.101232>.
57. Gould AL, Zhang V, Lamberti L, Jones EW, Obadia B, Korasidis N, Gavryushkin A, Carlson JM, Beerenwinkel N, Ludington WB: **Microbiome interactions shape host fitness.** *Proc Natl Acad Sci U S A* 2018, **115**:E11951-E11960 <http://dx.doi.org/10.1073/pnas.1809349115>.
58. Walters AW, Hughes RC, Call TB, Walker CJ, Wilcox H, Petersen SC, Rudman SM, Newell PD, Douglas AE, Schmidt PS, Chaston JM: **The microbiota influences the Drosophila melanogaster life history strategy.** *Mol Ecol* 2019, **29**(3):639-653 <http://dx.doi.org/10.1111/mec.15344>.
59. Leftwich PT, Clarke NVE, Hutchings MI, Chapman T: **Reply to Obadia et al.: effect of methyl paraben on host-microbiota interactions in Drosophila melanogaster.** *PNAS* 2018, **115**:E4549-E4550 <http://dx.doi.org/10.1073/pnas.1805499115>.
60. Leftwich PT, Clarke NVE, Hutchings MI, Chapman T: **Reply to Rosenberg et al.: diet, gut bacteria, and assortative mating in Drosophila melanogaster.** *PNAS* 2018, **115**:E2154-E2155 <http://dx.doi.org/10.1073/pnas.1721804115>.
61. Leftwich PT, Clarke NVE, Hutchings MI, Chapman T: **Gut microbiomes and reproductive isolation in Drosophila.** *PNAS* 2017, **114**:12767-12772 <http://dx.doi.org/10.1073/pnas.1708345114>.
62. Obadia B, Keebaugh ES, Yamada R, Ludington WB, Ja WW: **Diet influences host-microbiota associations in Drosophila.** *PNAS* 2018, **115**:E4547-E4548 <http://dx.doi.org/10.1073/pnas.1804948115>.
63. Rosenberg E, Zilber-Rosenberg I, Sharon G, Segal D: **Diet-induced mating preference in Drosophila.** *PNAS* 2018, **115**:E2153 <http://dx.doi.org/10.1073/pnas.1721527115>.
64. Sharon G, Segal D, Ringo JM, Hefetz A, Zilber-Rosenberg I, Rosenberg E: **Commensal bacteria play a role in mating preference of Drosophila melanogaster.** *PNAS* 2010, **107**:20051-20056 <http://dx.doi.org/10.1073/pnas.1009906107>.
65. Téfit MA, Gillet B, Joncour P, Hughes S, Leulier F: **Stable association of a Drosophila-derived microbiota with its animal partner and the nutritional environment throughout a fly population's life cycle.** *J Insect Physiol* 2018, **106**:2-12 <http://dx.doi.org/10.1016/j.jinsphys.2017.09.003>.